Submitted dissertation

for

obtaining the doctoral degree

of the

Combined Faculty of Mathematics, Engineering and Natural Sciences

of the

Ruprecht-Karls-University

Heidelberg

Presented by

M.Sc. Micha Tobias Rosenkranz

born in: Neuwied, Germany

Oral examination: 03.03.2023

Old but gold:

The *Plasmodium falciparum* merozoite surface protein 1 is still a promising blood stage vaccine candidate

Referees: Prof. Dr. Michael Lanzer

Prof. Dr. Faith Osier

DECLARATION

I hereby declare that this thesis is my own work and has not been submitted for examination or award of degree in any other institution of learning. I also declare that the experiments for the presented work were conducted using the indicated resources between September 2019 and December 2022 in the laboratories of Prof. Faith Osier and the Malaria Clinical Trial Unit (MCTU) at the parasitology unit of the centre of infectious diseases at the Ruprecht-Karls University in Heidelberg.

Heidelberg, 03. 12. 2022.

Micha Tobias Rosenkranz

PUBLICATION LIST

The figures of my dissertation have been taken partially from my submitted or prepared manuscript with modifications and have been originally created by myself.

Rosenkranz, M., I.N. Nkumama, S. Kraker, M. Blickling, K. Mwai, D. Odera, J. Tuju, K. Fürle, R. Frank, E. Chepsat, M.C. Kapulu, and F.H.A. Osier. 2022. Full-length merozoite surface protein 1 of Plasmodium falciparum is a major target of protective immunity following controlled human malaria infections. *medRxiv* 2022.2010.2012.22280947. (Chapter 4.1)

Manuscript in preparation

Rosenkranz, M., K. Fürle, J. Hibbert, A. Ulmer, A. Ali, J. Kehrer, N. Osswald, K. Chavdarova, M. Winter, T. Giese, A. Aschenbrenner, E. Böhnlein, M. Lanzer, R. Thomson Luque. 2022. Multifucntional IgG/IgM antibodies and cellular cytotoxicity are elicited by the full-length MSP1 “SumayaVac1” malaria vaccine in a phase 1a clinical trial. (Chapter 4.2)

ACKNOWLEDGEMENTS

I would like to express my deep and sincere gratitude to Prof. Faith H.A. Osier and Prof. Michael Lanzer for giving me the great opportunity to work in their labs on this fascinating project. I am very grateful for their supervision, the intellectual discussions as well as their mentorship during this PhD project.

I would like to deeply thank Dr. Richard Thomson Luque for his unwavering enthusiasm, intellectual and technical support as well as having great discussions during our seminars or beer hours during the weekends.

I am very grateful to Miriam Griesheimer and Sandra Niebel, for their administrative support, patience and encouragement during my PhD project.

I would like to thank all former members of Prof. Faith Osier's group for their unwavering support. Dr. James Tuju, Rinter Kimanthi, and Emily Chepsat, I thank you for your help setting up the protein expression system. A hearty thanks to Dr. Irene Nkumama for her assistance in statistical analysis, intellectual discussions as well as being a mentor and a true friend. I am very grateful to Kristin Fürle for technical assistance, her calm presence and fun times in and outside of the lab. I would like to thank Dennis Odera for teaching me the Ab-NK assay and great karaoke nights. I would also like to give special thanks to Marie Blickling and Sara Kraker for their meaningful contribution to this project during their master's internship and thesis. I deeply want to thank Dr. Ken Mwai for helping me with the statistical analysis.

I wish to show my appreciation to my colleagues in the malaria clinical trial unit, past and present. Dr. Arin Ali for her patience and guidance to ensure high quality standards of my laboratory work. A special thanks to Julia Hibbert, Marina Buck, Anne Ulmer and Max Winter for the great atmosphere in the lab, for interesting discussions, joyful coffee breaks as well as being good friends.

A special thank you to the whole parasitology unit; AG Lanzer, Ag Frischknecht, AG Ingham, AG Kilian, AG Ganter and AG Guizetti for intellectual discussions during the department seminars.

I wish to acknowledge the Heidelberg Biosciences International Graduate School (HBIGS), especially Dr. Rolf Lutz, Martina Galvan and Sandra Marini for their support and career advice.

I am deeply thankful to the members of the AG Voegtle; Dr. Cansu Kücükköse, Dr. Carlotta Peselj, Maria Gala and Jacky Wilhelm for the best possible lunchbreaks, unforgettable night outs and for being fantastic friends.

I want to thank all study participants in Kenya and Germany. This work would have not been possible without you.

I am very thankful to everyone who donated blood for my experiments. Without you, most of the functional assays would have been impossible.

Finally, I would like to deeply thank my whole family and friends for their love, support, encouragement and prayers. To my mum Manuela, my dad Thomas, my brother Daniel and my grandparents Margret and Wolfgang. Thank you for always believing and encouraging me to never give up. I am incredibly grateful to my fiancée Selina Dimmer for supporting me and standing by my side through the good and the bad times.

STATEMENT OF CONTRIBUTION

Dr. Ken Mwai contributed to the analysis of the epitope mapping data and generated the functions specific thresholds.

Dr. Irene Nkumama provided the merozoite ELISA data and contributed to the analysis of the CHMI study.

M.Sc. Marie Blickling and M.Sc. Sara Kraker helped with the expression and functional characterization of recombinant merozoite antigens.

Dr. Richard Thomson Luque and Kristin Fürle performed the C3b and C5-C9 complement fixation assays and helped with the functional assays.

Kristin Fürle, B.Sc. Natascha Oßwald and B.Sc. Kalina Chavdarova purified IgM from human sera.

B.Sc. Max Winter established the purification of $MSP1_{FL}$-specific antibodies in our lab.

DEDICATION

I dedicate this work to my brother Daniel. Thank you for being my closest friend!

SUMMARY

Despite the global efforts, malaria is still a serious public health concern with approximately 241 million cases and 627000 deaths globally in 2020 (WHO report 2021) with the majority of deaths occurring in young children living in Sub-Saharan Africa. This underscores the urgent need of highly effective and durable malaria vaccines which are not yet available.

The *Plasmodium falciparum* merozoite surface protein 1 (MSP1) is the most abundant surface antigen of merozoites and has long been considered as a key antigen for naturally acquired immunity (NAI) and a promising blood stage vaccine candidate for malaria; however, sero-epidemiological studies and clinical trials in humans could not confirm protective effects of anti-MSP1 immune responses. Notably, previous studies focussed only on small fragments of the whole protein, particularly the conserved C-terminal subunit and might therefore have missed important B and T cell epitopes that are relevant for a protective immune response.

Using samples from a controlled human malaria infection study in semi-immune Kenyan adults (CHMI-SIKA), I showed that pre-challenge antibodies target conserved epitopes distributed across the full-length MSP1 ($MSP1_{FL}$) protein and induced a range of distinct Fc-mediated effector functions: complement fixation (AbC'), opsonic phagocytosis (OPA), respiratory burst of neutrophils (ADRB), degranulation and IFNγ expression of natural killer cells (Ab-NK) that were significantly associated with protection from malaria. Notably, the breadth of effector functions was the strongest correlate of protection. The magnitude of effector functions of antibodies directed against $MSP1_{FL}$ was the strongest compared to other merozoite antigens highlighting $MSP1_{FL}$ as a major driver of anti-merozoite immune responses.

Furthermore, I showed that vaccination of malaria-naïve adults from Germany with $MSP1_{FL}$ formulated with the GLA-SE adjuvant (SumayaVac1) elicited highly functional IgG and IgM that exert the same range of Fc-mediated effector functions that were observed for CHMI volunteers. Notably, functions reached similar or even higher levels to that of semi-immune Kenyan adults and remained over baseline levels even 6 months after immunization. Functional antibodies from protected CHMI volunteers as well as vaccinees preferably targeted the C-terminal p42 as well as the N-terminal p83 subunit which has never been included in previous MSP1-based vaccines.

My study suggests that full-length MSP1 is an important target of naturally acquired and vaccine-induced functional antibodies which might be strong contributors to protection from

malaria. An upcoming phase Ib study with SumayaVac1 is currently under development and expected to be tested in malaria-exposed adults in Tanzania followed by CHMI.

ZUSAMMENFASSUNG

Trotz der weltweiten Bemühungen bleibt Malaria ein großes Problem für die öffentliche Gesundheit, denn ungefähr 241 Millionen Infektionen und 627 000 Todesfälle wurden weltweit im Jahr 2020 (WHO-Bericht 2021) registriert, wobei die Mehrheit der Todesfälle bei jungen Kindern in Afrika südlich der Sahara auftrat. Dies unterstreicht den dringenden Bedarf an hochwirksamen und langlebigen Malaria-Impfstoffen, die jedoch noch nicht verfügbar sind.

Das *Plasmodium falciparum* Merozoiten-Oberflächenprotein 1 (MSP1) ist das am häufigsten vorkommende Oberflächenantigen auf Merozoiten und gilt seit langem als ein Schlüsselantigen für die natürlich erworbene Immunität und als vielversprechender Impfstoffkandidat gegen das Blutstadium der Malaria. Sero-epidemiologische und klinische Studien am Menschen konnten jedoch bisher keine schützenden Wirkungen von MSP1-basierten Immunantworten bestätigen. Bemerkenswerterweise konzentrierten sich frühere Studien nur auf kleine Fragmente des gesamten Proteins, insbesondere die konservierte C-terminale Untereinheit. Möglicherweise wurden deshalb wichtige B und T Zell Epitope nicht beachtet, die jedoch für eine schützende Immunantwort relevant sein könnten.

Unter Verwendung von Proben aus einer kontrollierten humanen Malaria-Infektionsstudie in semi-immunen erwachsenen Kenianern konnte ich zeigen, dass Prä-Challenge-Antikörper an konservierte Epitope binden, die über das gesamte MSP1 Protein verteilt sind. Außerdem fand ich heraus, dass Antikörper gegen das vollständige MSP1 Protein einige antikörperabhängige Effektorfunktionen auslösen. Darunter waren Komplementfixierung (AbC‘), Phagozytose (OPA), respiratorischer burst von neutrophilen Granulocyten (ADRB) sowie Degranulation und die Produktion von IFNγ von natürlichen Killerzellen (Ab-NK), die signifikant mit dem Schutz vor Malaria korrelierten. Es gelang mir aufzuzeigen, dass ein breites Spektrum an antikörperabhängigen Effektorfunktionen das stärkste Korrelat für Schutz darstellte. Das Ausmaß der Antikörperaktivitäten, die gegen das vollständige MSP1 Protein gerichtet waren, war im Vergleich zu anderen Merozoiten-Antigenen am stärksten. Diese Ergebnisse zeigen, dass MSP1 tatsächlich eine wichtige Rolle für wirksame Immunantworten gegen Merozoiten spielt.

Darüber hinaus habe ich gezeigt, dass die Impfung von Malaria-naiven gesunden Erwachsenen aus Deutschland mit dem ganzen MSP1 Protein, zugesetzt mit dem Adjuvant GLA-SE (SumayaVac1), hochfunktionelles IgG und IgM induzierte. Die Bandbreite der Funktionen war die gleiche, die bei Freiwilligen der Malaria-Infektionsstudie beobachtet wurden. Außerdem stellte ich fest, dass die Stärke der induzierten Effektorfunktionen von

geimpften Probanden ähnliche oder sogar höhere Werte erreichte als bei semi-immunen Kenianern. Darüber hinaus blieb die Aktivität sogar sechs Monate nach der Immunisierung über den Ausgangswerten. Interessanterweise richteten sich die funktionalen Antikörper von geschützten semi-immunen Kenianern sowie von deutschen geimpften Probanden vorzugsweise sowohl auf die C-terminale p42 als auch auf die N-terminale p83-Untereinheit, die in keinem der früheren MSP1-basierten Impfstoffe enthalten war.

Meine Studie legt nahe, dass das vollständige MSP1 Molekül besondere Beachtung in Bezug auf natürlich erworbene und induzierte funktionelle Antikörper verdient und damit zum effektiven Schutz vor Malaria beitragen könnte. Eine Phase-Ib-Studie mit SumayaVac1 befindet sich derzeit in der Entwicklung und soll an Malaria-exponierten Erwachsenen in Tansania getestet werden, gefolgt von kontrollierter Malaria-Infektion.

TABLE OF CONTENTS

LIST OF FIGURES

LIST OF TABLES

LIST OF ABBREVIATIONS

Abbreviation	Full name
µg	Micro gram
µl	Micro liter
AbC’	Antibody-dependent complement fixation
Ab-NK	Antibody-dependent natural killer cell activity
ACTs	Artemisinin-based combination therapies
ADCI	Antibody-dependent cellular inhibition
ADRB	Antibody-dependent respiratory burst
AE1	Anion exchanger 1
aHR	Adjusted hazard ratio
AMA1	Apical membrane antigen 1
AQ	Amodiaquine
ART	Artemisinin
BSA	Bovine serum albumin
BSV	Blood stage vaccine
ChAd	Chimpanzee adenovirus
CHKV	Chikungunya virus
CHMI	Controlled human malaria infection
CHMI-SIKA	Controlled Human Malaria Infection of Semi-Immune Kenyan Adults
CM	Cerebral malaria
COVID-19	Coronavirus disease 2019
CPS	Chemoprophylaxis with sporozoites
CQ	Chloroquine
CSP	Circumsporozoite protein
cyRPA	Cysteine-rich protective antigen
DBL	Duffy binding-like
ddH_2O	Double distilled water

DENV	Dengue virus
DFHR	Dihydrofolate reductase
DHA	Dihydroartemisinin
DHPS	Dihydropteroate synthase
DHOD	Dihydroorotate dehydrogenase
dl	Deci liter
DNA	Deoxyribonucleic acid
dsx	Doublesex gene
DVI	Direct venous inoculation
EBAs	Erythrocyte binding antigens
EGF	Epidermal growth factor
EIR	Entomological inoculation rate
EPCR	Endothelial Protein C receptor
F	Febrile CHMI volunteers
Fab	Fragment antigen-binding
FACS	Fluorescence-activated cell sorting
FBS	Fetal bovine serum
Fc	Fragment crystallizable region
FcRn	Neonatal Fc receptor
FcRs	Fc receptors
GAP	Genetically attenuated parasites
GIA	Growth inhibition assay
GLA-SE	Glucopyranosyl lipid adjuvant stable emulsion
GNP	German-naïve plasma pool
GPI	Glycophosphatidylinositol
GST	Gluthathione S-transferase
CPS	Chemoprophylaxis and sporozoite vaccination
DiCo	Diversity covering
GLURP	Glutamine-rich protein
GYP	Glycophorin

h	Hour
HBsAG	HBV surface antigen
HEPES	4-(2-hydroxyethyl)-1-piperazineethanesulfonic acid
HRP-II	Histidine-rich protein II
HTS	High throughput sampler
ICAM1	Intracellular adhesion molecule 1
iEs	Infected erythrocytes
IFNγ	Interferon gamma
Ig	Immunoglobin
IMC	Inner membrane complex
IRS	Indoor residual spraying
ITNs	Insecticide-treated nets
K13	Kelch 13
KEMRI	Kenya Medical Research Institute
LDH	Lactate dehydrogenase
LLITNs	Long-lasting insecticide-treated nets
mAb	Monoclonal antibody
MAC	Membrane attack complex
MBL	Mannose-binding lectin
MHC	Major histocompatibility complex
MIG	Purified human IgG from Malawian adults
min	Minute
ml	Milli liter
mM	Milli molar
MSP	Merozoite surface protein
$MSP1_{FL}$	Full-length merozoite surface protein1
MSRP4	Merozoite surface protein 7-related protein 4
MVA	Modified Vaccinia Ankara
NAI	Naturally acquired immunity
NF	Non-febrile CHMI volunteers

NK	Natural killer
NT	Non-treated CHMI volunteers
OD	Optical density
OPA	Opsonic phagocytosis assay/activity
OPD	O-phenylenediamine dihdydrochloride
PART	Presumptive anti-relapse therapy
PBMCs	Peripheral blood mononuclear cells
PBO	Piperonyl butoxide
PBS	Phosphate-buffered saline
PCR	Polymerase chain reaction
PEV	Pre-erythrocytic vaccines
PFA	Paraformaldehyde
P.f.	*Plasmodium falciparum*
PfCRT	*Plasmodium falciparum* CQ-resistant transporter
PfEMP1	*Plasmodium falciparum* erythrocyte membrane protein-1
PHIS	Polled hyperimmune serum from Kenyan adults
PMN	Polymorphonuclear cells
PTEX150	*Plasmodium* translocon of exported protein 150
PQ	Primaquine
PV	Parasitophorous vacuole
qPCR	Quantitative polymerase chain reaction
RAMA	Rhoptry.associated membrane antigen
RAS	Radiation-attenuated sporozoites
RBC	Red blood cell
RDTs	Rapid diagnosis tests
RHs	Reticulocyte-binding-like homologues
Ripr	RH5 interacting protein
RLU	Relative light units
ROS	Reactive oxygen species
RPI	Relative phagocytosis index

RPMI	Roswell park memorial institute medium
rRNA	Ribosomal ribonucleic acid
SA	Sialic acid
SMFA	Standard membrane feeding assay
SUB	Subtilisin-like protease
T	Treated CHMI volunteers
TBV	Transmission blocking vaccines
TNFα	Tumour necrosis factor alpha
TRAP	Thrombospondin-related adhesion protein
v/v	Volume to volume
VLP	Virus-like particle
w/v	Weight to volume
WBC	White blood cells
WHO	World Health Organisation
WSV	Whole sporozoite vaccines

1.0 INTRODUCTION

1.1 Malaria

1.1.1 The global burden of malaria

Although global malaria control strategies resulted in the decline of malaria deaths by 38% from 2000 to 2019 (WHO report 2020), the World Health Organisation (WHO) reported 241 million estimated malaria cases and 627,000 deaths in 2020 which represents an increase of 5% and 12%, respectively, compared to 2019. This was attributed to malaria service disruptions during the COVID-19 pandemic (WHO report 2021). The majority of the malaria burden is carried by subtropical and tropical regions, especially in sub-Saharan Africa that account for 93% of the global malaria cases. The most vulnerable group are children under the age of 5 accounting for 77% of deaths in 2020.

Malaria imposes high direct economic costs estimated to be US$ 3.3 billion in 2020 paid by governments in malaria endemic countries and international partners (WHO report 2021); however, current funding is only covering half of the amount that is required to meet the milestones of the Global Technical Strategy for malaria (GTS).

1.1.2 Malaria parasites

Malaria is caused by obligate intracellular protozoan parasites of the phylum Apicomplexa and genus *Plasmodium*. There are approximately 250 *Plasmodium* species known to infect vertebrates such as birds, reptiles and mammals (Faust and Dobson, 2015) while only 5 species are reported to infect humans that are: *P. falciparum*, *P. vivax*, *P. ovale*, *P. malariae* and *P. knowlesi*. *Plasmodium falciparum* is the most common species in sub-Saharan Africa and is accounted for approximately 90% of the world's malaria mortality (WHO report 2021). Although, significantly less virulent, *Plasmodium vivax* is the most widely distributed species outside of Africa comprising for 68% of malaria cases in the region of the Americas, 36% in South-East-Asia and 18.1% in the Eastern Mediterranean regions (WHO report 2021).

1.1.3 Malaria vectors

Mosquitos that serve as vectors for *Plasmodium* parasites are of the genus *Anopheles*; however, of the 465 formally named *Anopheles* species, approximately 70 are known to

transmit *Plasmodium* parasites to humans (Hay et al., 2010). Only female *Anopheles* mosquitos that commonly feed on humans, are susceptible to the parasite and have a sufficient life-span to ensure parasite development (Cohuet et al., 2009), are able to transmit *Plasmodium* parasites to humans. The major anopheline vectors for malaria in the African region are of the *Anopheles gambiae* complex including *An. gambiae*, *An. Arabiensis* and *An. coluzzi*, (Gillies and De Meillon, 1968; Harbach, 2004).

1.1.4 The *Plasmodium falciparum* lifecycle

Plasmodium spp. that cause infections in humans have a complex live cycle involving both a mosquito vector that functions as definitive host and a human as an intermediate vertebrate host. Infection is initiated during a blood meal of a parasite-infected female anopheline mosquito, where a small number (10-100) of free-moving parasite stages (Beier et al., 1991; Medica and Sinnis, 2005), called sporozoites are injected into the dermis (Sidjanski and Vanderberg, 1997) where they can move for up to an hour. During this pre-erythrocytic phase, the sporozoites migrate through the dermis through gliding motility (Amino et al., 2007; Vanderberg and Frevert, 2004) and either stay within the skin or enter the blood or lymphatic vessels.

Once sporozoites enter the blood stream, they are passively transported and reach the liver sinusoid. Sporozoites cross the sinusoidal barrier by traversal of Kupffer cells, i.e., liver macrophages (Baer et al., 2007), followed by several hepatocytes before a final one is infected resulting in the formation of a parasitophorous vacuole (PV) (Lingelbach and Joiner, 1998; Mota et al., 2001). Sporozoites within the PV differentiate into liver schizonts which undergo asexual replication (schizogony) leading to the formation of thousands of merozoites. The newly-formed merozoites are packed and released in membranous structures, i.e., merosomes (Sturm et al., 2006; Tarun et al., 2006) and eventually enter the blood stream.

In the blood, merozoites can survive for a few minutes (Boyle et al., 2013) before they rapidly invade (<1 min) red blood cells (RBCs) (Gilson and Crabb, 2009) initiating the blood stage of infection. Within the RBCs, merozoites develop through ring stages, trophozoites and schizonts that undergo asexual replication (erythrocytic schizogony) leading to the formation of approximately 8-32 daughter merozoites over the course of 48h (Garg et al., 2015). The rupture of schizonts results in the release of daughter merozoites into the blood stream which starts another cycle of invasion and replication. Clinical manifestation of malaria occurs during the blood stage of infection (Trampuz et al., 2003).

Instead of undergoing schizogony, some asexual stages differentiate into male or female gametocytes which mature from stage I to stage V gametocytes for 7-10 days in the bone marrow and spleen (Hawking et al., 1971). Mature gametocytes are then eventually released into the blood stream and can be transmitted to a female *Anopheles* mosquito during a blood meal. Several environmental stimuli within the midgut of the mosquito including change in temperature and pH as well as presence of the metabolite xanthurenic acid induce gametogenesis (Arai et al., 2001; Billker et al., 2000; Sinden and Croll, 1975) resulting in the formation of female macro gametes and 8 flagellated male microgametes. Gametes unite in the lumen of the midgut which gives rise to a zygote that quickly undergoes meiosis followed by differentiation into an ookinete. This actively moving stage traverses the midgut epithelium and transforms into an oocyst which remains attached to the basal lamina. By multiple rounds of DNA replication, a sporoblast is generated within the oocyst (Gerald et al., 2011) that undergoes schizogony which leads to formation of several thousand crescent shaped sporozoites (Rosenberg and Rungsiwongse, 1991). The actively moving sporozoites egress from the oocysts and float in the hemolymph until they attach to the salivary glands. After attachment, sporozoites invade the salivary glands from where they can be transmitted to a new human host during a blood meal (**Fig. 1.1**)

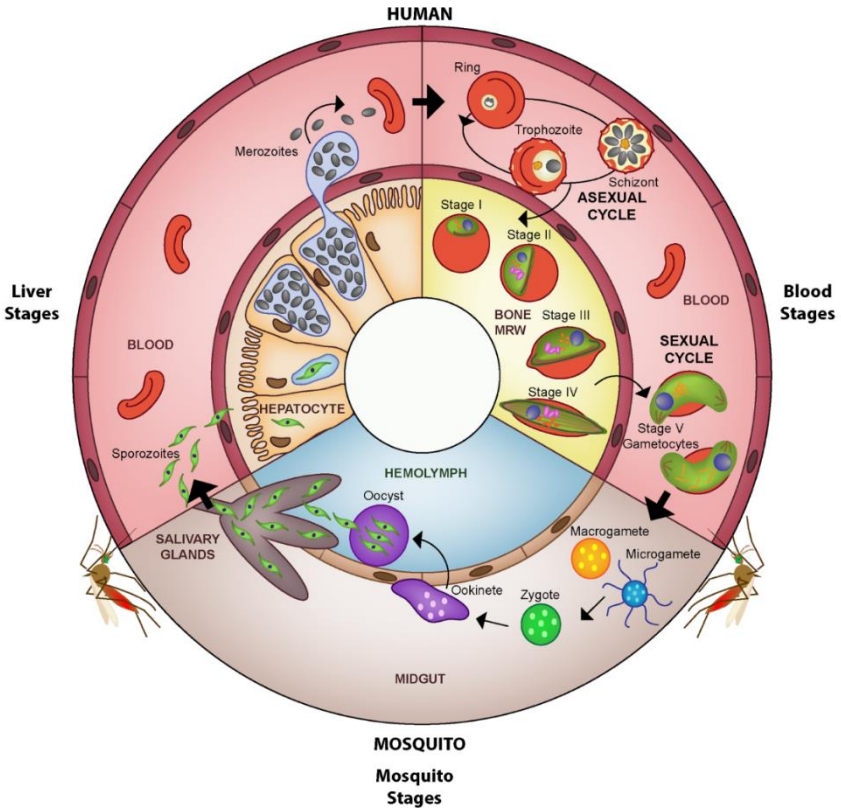

Figure 1.1: Illustration of the *Plasmodium falciparum* lifecycle.
The figure was adopted from Nilsson et al., 2015

1.1.5 Merozoite invasion

Plasmodium falciparum merozoites are released into the blood stream after the burst of schizonts at the end of each erythrocytic cycle. Merozoites have an ovoid shape, of approximately 1.5 µm in diameter and are covered by a surface coat that contains a range of surface proteins that are either tethered to the plasma membrane via a glycophosphatidylinositol (GPI)-anchor, transmembrane domains or associations to other surface proteins at the periphery. At the apical tip of the merozoite, special secretory organelles are located, namely micronemes, rhoptries and dense granules that contain a range of proteins involved in invasion (Beeson et al., 2016; Blackman and Bannister, 2001).

Merozoites can invade RBCs in distinct pathways which are broadly classified as sialic acid (SA)-dependent and SA-independent-pathway. Micronemal proteins from the erythrocyte binding antigens (EBA) family such as EBA175, EBA140, EBA181 are involved in the SA-dependent invasion pathway by interacting with SA residues of glycophorin A (GYPA), C (GYPC) and yet unknown receptors, respectively, on the surface of erythrocytes (Ord et al., 2012). This interaction can be prevented by treatment with neuraminidase which removes SA residues from glycophorins and thus inhibits SA-dependent invasion (Maier et al., 2003). The alternative SA-independent pathway involves rhoptry-secreted proteins of the reticulocyte-binding-like homologues (RHs) family including, RH2a, RH2b, RH3, RH4 and RH5; however, so far only receptors for RH4 (complement factor 1; Tham et al., 2010) and RH5 (Basigin; Crosnier et al 2011) are known.

Merozoite invasion is a complex process that involves several steps. First, merozoites attach initially to the erythrocyte which is largely mediated by GPI-anchored merozoite surface proteins (MSPs), followed by stronger either SA-dependent or independent receptor-ligand interactions initiated by members of EBA or RH family, respectively. The merozoite then reorients with the apical tip facing the membrane of the RBC. Following reorientation, RH5 associated with RH5 interacting protein (Ripr) and cysteine-rich protective antigen (CyRPA) (Volz et al., 2016) at the apical tip, binds to basigin on the RBC leading to pore formation on the erythrocyte membrane (Weiss et al., 2015). The micronemal apical membrane antigen 1 (AMA1) at the surface of the merozoite then binds the secreted rhoptry neck protein RON2 promoting the formation of a tight junction (Riglar et al., 2011; Tonkin et al., 2011). The activation of the ‘glideosome’, an actin-myosin motor complex connected to membrane-spanning surface proteins and the inner membrane complex (IMC) of the merozoite, generates a forward thrust pulling the merozoite inside the RBC. During this process a range of merozoite surface proteins such as MSP1 and AMA1 are shed from the merozoite surface mediated by membrane-associated subtilisin-like protease PfSUB2 (‘sheddase’) catalysed cleavage

(Blackman et al., 1991; Howell et al., 2003; Riglar et al., 2011). During the invasion process a parasitophorous vacuole is created, sealed and encapsulates the parasite (Lingelbach and Joiner, 1998) (**Fig. 1.2**).

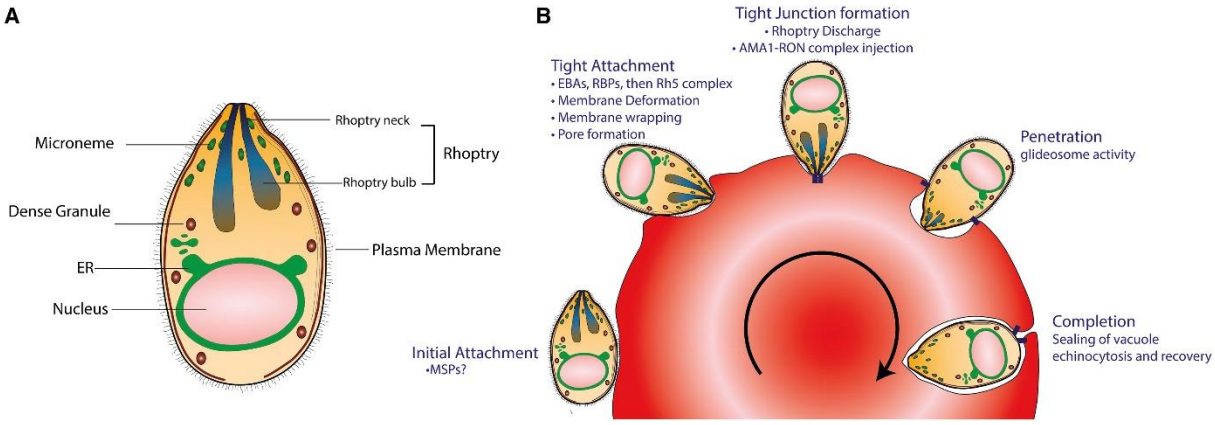

Figure 1.2: Invasion of *Plasmodium falciparum* merozoites.
(**A**) Illustration of the merozoite morphology and organization. (**B**) Illustration of the sequential invasion process. The figure was adopted from Cowman et al., 2017

1.2 Malaria epidemiology

1.2.1 Geographical distribution

Malaria is endemic in regions of Sub-Saharan Africa, South-America, South-East Asia and the Mediterranean. Malaria transmission is not uniform, since it depends on several climate-based conditions such as vegetation, temperature, humidity and rainfall (Castro, 2017). Temperature has been considered as a primary environmental factor for mosquito development. The intensity of malaria transmission is commonly estimated by the entomological inoculation rate (EIR) that is based on the number of infectious mosquito bites per person over a fixed period of time.

1.2.2 Clinical symptoms and pathophysiological factors

The clinical features of acute malaria are manifested during the blood stage of infection which can be highly variable and include fever, chills, headache, vomiting, rigors and muscle aches usually occurring 10-15 days post infection (Trampuz et al., 2003). These ‘mild’ malaria symptoms mimic other diseases such as flu which often leads to misdiagnosis and wrong treatment. When malaria is not treated, severe symptoms that affect multiple organs can occur including, cerebral malaria (CM), anemia (haemoglobin < 7g/dl), renal impairment, hypoglycaemia, metabolic acidosis and respiratory distress (Trampuz et al., 2003). The most

vulnerable group of severe malaria are young children in areas with high malaria transmission but also travellers that lack pre-existing anti-malarial immunity.

Several pathophysiological factors have been proposed for severe malaria including loss of RBCs, cytoadherence and pro-inflammatory responses. Cytoadherence to the endothelium of infected erythrocytes (iEs) and subsequent sequestration in vital organs such as the brain, heart or lungs, leads to mechanical microvascular obstruction and undersupply of oxygen. Cytoadherence of iEs is predominantly mediated by members of *var*-genes encoded *Plasmodium falciparum* erythrocyte membrane protein1 (PfEMP1) family located at the knobs of iEs (Kraemer and Smith, 2006). Variants of PfEMP1 can bind to several endothelial receptors including intracellular adhesion molecule 1 (ICAM1), CD36 or the Endothelial Protein C receptor (EPCR) (Miller et al., 2002). Furthermore, the release of excessive levels of pro-inflammatory cytokines such as tumour necrosis factor alpha TNFα or interferon gamma (IFNγ) have been linked to severe malaria (Angulo and Fresno, 2002).

1.2.3 Diagnosis of malaria

Malaria remains a serious public health concern and effective and rapid diagnosis is critical to reduce severe and life-threatening complications of the disease. Since the clinical manifestations of malaria are non-specific and sometimes similar to other febrile diseases, clinical diagnosis is challenging. The gold standard for malaria diagnosis is microscopical examination of Giemsa stained blood smears. This involves thick-smears for parasite screening and thin smears for species identification. The attractivity of this method is attributed to its low cost, simplicity and ability to identify parasite species as well as densities; however, since the sensitivity and specificity of this method is highly dependent on the quality of smears, reagents and expertise of the analyst, the average detection limit of parasites is approximately 50-100 *P.f.*/µl (Payne, 1988); therefore, the detection of low parasite densities is challenging. Moreover, microscopy is laborious and requires well-trained experts as well as electricity which is limited in remote areas (Ohrt et al., 2002).

The use of rapid diagnosis tests (RDTs) overcomes the limitations of microscopic diagnostics, since the performance is user-friendly, quick, cheap and independent of laboratory equipment. All RDTs detect specific *Plasmodium*-specific antigens, eg. histidine-rich protein II (HRP-II) or lactate dehydrogenase (LDH) in the blood of the patient with overall good specificity (Endeshaw et al., 2008; Kyabayinze et al., 2008; Ratsimbasoa et al., 2008); however, some studies using HRP-II-based RDTs reported false-negative results due to deletion of the HRP-II gene in some *Plasmodium falciparum* isolates (Koita et al., 2012; Kozycki et al., 2017). False-positive results for HRP-II-based RDTs have also been reported since HRP-II persists in the

blood for weeks after a cleared infection (Biswas et al., 2005; Grandesso et al., 2016; Kiemde et al., 2017). Additional limitations of RDTs are the moderate sensitivities (>100 *P.f.*/µl) which raises concern about their use in regions with low malaria transmission intensity (Ranadive et al., 2017) as well as inadequate storage or transport conditions (temperature, humidity) which reduce RDT performance (Chiodini et al., 2007).

Molecular diagnosis methods, especially the use of polymerase chain reaction (PCR)-based techniques overcome the sensitivity issues of microscopy and RDTs and have been shown to reliably detect low parasite densities (1-5 *P.f.*/µl), mixed infections (Morassin et al., 2002) and can be scaled up for examination of large sample sets (Swan et al., 2005). Despite the advantages of PCR-based diagnostic methods over conventional microscopy and RDTs, high costs, the required expertise and laboratory complexity makes it impractical for routine diagnostics in remote clinics.

1.2.4 Treatment of malaria

Antimalarial drugs are important measures to control parasite density and clinical manifestation of malaria. Furthermore, they limit the development of sexual stages and thus reduce parasite transmission (Gosling et al., 2011). The principal targets of antimalarials are blood stages, particularly trophozoites and schizonts that cause clinical symptoms of malaria. Antimalarials can be chemically classified as antifolates, 8-aminoquinolin, naphthoquinone, 4-aminoquinolines, amino alcohols, antibiotics and endoperoxides (**Tab. 1.1**) (Haldar et al., 2018).

1.2.4.1 Antimalarials: mode of action and resistance

Antifolates used for malaria treatment either target dihydropteroate synthase (DHPS), class I antifolates (pyrimethamine and proguanil) or dihydrofolate reductase (DFHR), class II antifolates (sulfadoxine) thereby inhibiting synthesis of folate which is essential for DNA synthesis (Hyde, 2005). Resistance to antifolates is conferred by point mutations of DHPS and DFHR genes (Hyde, 1990; Peterson et al., 1990; Peterson et al., 1988; Sibley et al., 2001).

The 8-aminoquinoline analogue primaquine (PQ) is used as a gametocytocidal drug against *P. falciparum* disrupting transmission and prevents malaria relapses by killing *P. vivax* and *P.ovale* hypnozoites in the liver (presumptive anti-relapse therapy; PART). The exact mode of action of primaquine is not clear but a recent study suggests that administration with PQ generates high levels of H_2O_2 in the bone marrow and liver which is detrimental to liver stages (Camarda et al., 2019); however, patients with glucose-6-phosphate dehydrogenase (G6PD)

deficiency must not take primaquine since it can cause hemolytic anemia (Bolchoz et al., 2001). Therefore, screening for G6PD deficiency is critical before PART or chemoprophylaxis to primaquine. Failure of PQ leading to increased *P. vivax* relapses has been linked to polymorphisms in cytochrome P-450 2D6, a key enzyme involved in the formation of the active metabolites of PQ (Silvino et al., 2016). *Plasmodium* vivax strains with resistance to PQ have been reported; however, the mechanism of resistance is not understood (Thomas et al., 2016).

Atovaquone, a substituted 2-hydroxy-naphthoquinone, resembles ubiquinone (coenzyme Q) involved in the electron transport chain of *Plasmodium* mitochondria for aerobic respiration. Atovaquone inhibits the transport of electrons by binding to cytochrome bc1 (Complex III) (Fry and Pudney, 1992) which consequently inhibits the mitochondrial dihydroorotate dehydrogenase (DHOD) that is required for the synthesis of pyrimidine for DNA synthesis leading to parasite death (Baggish and Hill, 2002). Resistance to atovaquone is associated by specific mutations in cytochrome b (Akhoon et al., 2014; Goodman et al., 2016).

The 4-aminoquinolines are the oldest antimalarials and include chloroquine (CQ), amodiaquine (AQ), piperaquine and pyronaridine. The mode of action of 4-aminoquinolines lies in prevention of the parasite's detoxification of free heme to hemozoin which is generated by the consumption of haemoglobin from the erythrocyte. Due to the high use of CQ in the past, the prevalence of resistant *Plasmodium falciparum* isolates is high (Alam et al., 2017; Mwai et al., 2009). Resistance to CQ is conferred by a single point mutation, K76T of the *P. falciparum* CQ-resistant transporter (*pfcrt*) that causes an efflux of CQ from the parasitophorous vacuole (Djimdé et al., 2001).

Amino alcohols, including quinine, mefloquine, lumefantrine and halofantrine have been developed to treat malaria. The mode of action as well as the targets of amino alcohols are not known but may inhibit the detoxification of heme.

Several antibiotics, drugs with antibacterial properties, are used as antimalarials for example clindamycin, doxycycline or tetracycline. Most of those drugs impair protein biosynthesis in the apicoplast of the parasite which makes them highly specific (Gaillard et al., 2016); however,

mutations in the apicoplast-encoded 23S rRNA are associated with resistance (Blasco et al., 2017).

Table 1.1: List of antimalarial drugs and markers of resistance.

Chemical class	Common name	Targeted parasite stage	Genetic marker for drug resistance	
			Plasmodium falciparum	***Plasmodium vivax***
Sesquiterpene lactone endoperoxides	Artemisinin	All parasite stages	pfkelch13	Unknown
	Artesunate	All parasite stages	pfkelch13	Unknown
	Artemether	All parasite stages	pfkelch13	Unknown
	Dihydroartemisinin	All parasite stages	pfkelch13	Unknown
4-Aminoquinolines	Chloroquine	Trophozoite and schizont	pfcrt	pvmdr1
	Amodiaquine	Trophozoite and schizont	pfcrt, pfmdr1	Unknown
	Piperaquine*	Trophozoite and schizont	pfplm2	Unknown
	Pyronaridine	Ring,trophozoite and schizont	pfcrt	Unknown
	Naphthoquine	Trophozoite and schizont	Unknown	Unknown
Amino alcohols	Quinine	Trophozoite and stages I to III gametocytes	pfcrt, pfmdr1	Unknown
	Mefloquine	Trophozoite and schizont	pfmdr1	pvmdr1
	Lumefantrine	Trophozoite and schizont	pfcrt, pfmdr1	Unknown
	Halofantrine	Trophozoite and schizont	pfcrt, pfmdr1	Unknown
8-Aminoquinoline	Primaquine	Gametocyte and liver schizont	Unknown	Unknown
Antifolates	Pyrimethamine	Blood and liver schizont and oocysts	pfdhfr	pvdhfr
	Sulfadoxine	Blood and liver schizont	pfdhps	pvdhps
	Proguanil	Blood and liver schizont and gametocytes	pfdhfr	Unknown
Naphthoquinone	Atovaquone	Blood and liver schizont and gametocytes	pfcytb	Unknown
Antibiotics	Clindamycin	Blood stages	Apicoplast target	Unknown
	Doxycycline	Blood stages	Apicoplast target	Unknown
	Tetracycline	Blood stages	Apicoplast target	Unknown

The table was adopted and modified from Haldar et al.,2018. *Pf Plasmodium falciparum, Pv Plasmodium vivax*, *crt* chloroquine-resistance transporter, *cytb* cytochrome b, *dhfr* dihydrofolate reductase, *dhps* dihydropteroate synthase, *mdr1* multidrug resistance protein, and *plm2*- plasmepsin 2.

Artemisinin (ART) and its derivatives are endoperoxidases that induce cellular damage to the parasite. It has been shown that the clinically relevant form dihydroartemisinin (DHA) causes protein damage by alkylation (Tilley et al., 2016) and accumulation of damaged proteins by inhibition of proteasome function which in turn leads to cell death (Bridgford et al., 2018). Unlike other antimalarials that only effectively destroy late stages, ART has been proven to also target ring stages (Xie et al., 2016). Parasite isolates showing resistance to ART emerged as shown by a prolonged clearance rate of parasites (Fairhurst and Dondorp, 2016). Resistance to ART is associated with mutations in the Kelch-like protein K13 gene. Although the precise mode of action of K13-mediated resistance to ART is not fully known evidence suggests a role in the

cellular stress response by reducing the ubiquitinoylation of proteins (Dogovski et al., 2015; Mbengue et al., 2015).

1.2.4.2 Combination therapies and future of antimalarials

A major reason for the high severity and mortality of malaria are existing and emerging resistances to antimalarial drugs (White, 2004). The use of antimalarial drug combination (combination therapies) can overcome resistance. Artemisinin-based combination therapies (ACTs) composed of a rapidly acting artemisinin derivative and a partner drug to confer sustained activity, are generally regarded as the best combination therapies due to their high and broad antimalarial activity (Nosten and White, 2007).

However, parasite resistance to ACTs have been reported in Cambodia (Dondorp et al., 2009) and other countries of the Greater Mekong Region in South-East Asia (Ashley et al., 2014; Tun et al., 2015). The development of new antimalarial drugs or combination therapies that are broadly active at single-dose with novel modes of action is therefore crucial to significantly delay the occurrence and spread of resistance (Belete, 2020). New antimalarials are currently being developed and evaluated in preclinical and clinical studies (MMV report 2021). An understanding of the mechanisms and targets of antimalarials as well as resistance can help to develop more efficient next-generation antimalarials.

1.2.5 Control strategies for *P. falciparum* malaria

Malaria control strategies are the cornerstones to prevent infections and morbidity and could eventually lead to eradication of the disease. Due to high adaptivity of the parasite and the anopheline mosquitos, malaria control is challenging yet achievable since 12 countries were certified by the WHO to be malaria free after 2000, including China and El Salvador in 2021 (WHO report 2021). Importantly, several control measures are necessary to progress towards a reduction of malaria cases and mortality by 90% until 2030 set by the WHO and its partners (WHO GTS 2015)

1.2.5.1 Vector control

The control of malaria vectors is one of the most important strategies to reduce malaria infections. Several vector-interventions have been adapted to the behaviour of anopheline mosquitos and successfully implemented. Insecticide-treated nets (ITNs) and notably long-lasting insecticide-treated nets (LLITNs) on the one hand provide a physical barrier between the human host and the mosquito vector thereby preventing infectious bites. On the other hand,

insecticides (mostly pyrethroids) on or incorporated into the fibre of the nets, kill the mosquito (Lengeler, 2004).

Moreover, indoor residual spraying (IRS) of insecticides onto walls or surfaces effectively kills resting mosquitos. The main classes of insecticides used for IRS are organochlorines, pyrethroids, organophosphates, carbamates and neonicotinoids (Tangena et al., 2020). The combined use of ITNs with IRS has been shown to effectively reduce malaria transmission in some malaria endemic regions (Fullman et al., 2013; Hamel et al., 2011; Kleinschmidt et al., 2009). Both ITNs and IRS target the imago in households while larval source management controls water bodies for the presence of larval or pupal stages and in consequence reduces the number of imagos in the environment. These measures include habitat modification/manipulation by drainage, filling and flushing as well as inducing larvicide through the application of synthetic or biological insecticides (Lobo et al., 2018).

The use of spatial repellents which disrupts the host-seeking behaviour of mosquitos have also been effective in reducing malaria transmission in Indonesia (Syafruddin et al., 2020) and will soon be tested in Kenya (Ochomo et al., 2022).

Although the coverage of IRS and INTs/LLITNs increased between 2000 to 2022 the percentage of available malaria prevention measures is still low for some malaria endemic countries (WHO report 2021). Furthermore, the spread of mosquito resistance to pyrethroids have limited the effectivity of ITNs/LLITNs (Churcher et al., 2016; Ngongang-Yipmo et al., 2022) which highlights the need for new types of bed nets that do not rely on pyrethroids alone. Recent studies in areas with high insecticide resistance have shown that a combination of pyrethroids with piperonyl butoxide (PBO) in INTs showed sustained reduction of infectious bites and survival of mosquitos compared to standard pyrethroid nets (Gleave et al., 2021; Martin et al., 2021).

1.2.5.2 Chemoprevention

The use of preventive chemotherapy has been suggested by the WHO in order to prevent malaria infections and mortality of highly vulnerable groups such as young children under 5 years of age and pregnant women (WHO 2012). Large-scale use of preventive chemotherapy in areas with seasonal malaria has resulted in a significantly decrease of clinical malaria cases (Baba et al., 2020; Cairns et al., 2021; Coldiron et al., 2017); however, the effectiveness of preventive chemotherapy needs to be carefully monitored due to the potential of emerging resistances as a result of mass administration of antimalarials (Desai et al., 2016; Griffin et al., 2010).

1.2.5.3 Novel control strategies

Biotechnological vector control

Vector control is currently the most effective tool to reduce the global malaria burden; however, due to the increasing resistance against insecticides, the development and implementation of new approaches and technologies is urgent.

Wolbachia is an intracellular endosymbiotic α-proteobacterium that is estimated to live in >76% of arthropods including mosquitos (Hertig and Wolbach, 1924; Hilgenboecker et al., 2008; Jeyaprakash and Hoy, 2000). *Wolbachia* bacteria have direct fitness benefits for their hosts by providing nutrients (Brownlie et al., 2009), supporting oogenesis (Dedeine et al., 2001) and protection from viral or parasitic infections. For example, the presence of specific *Wolbachia* strains in transfected *Aedes agypti* mosquitos caused interference with viruses such as dengue virus (DENV) and chikungunya virus (CHKV) (Bian et al., 2010; Moreira et al., 2009). *Wolbachia*-based biocontrol of *Plasmodium* falciparum has gained a lot of attention since presence of native *Wolbachia* interfered with parasite infections in *Anopheles* mosquitos (Gomes et al., 2017; Shaw et al., 2016); however, the prevalence and transmission of *Wolbachia* in the malaria vector are significantly lower compared to *Aedes* mosquitos (Hughes et al., 2011). Despite the promising observations in the field, further research is needed to increase the spread of *Plasmodium*-interfering *Wolbachia* strains to disrupt malaria transmission.

Genetically modified mosquitos generated by genome editing are currently under development and highly promising for the disruption of malaria transmission. Importantly, the genetic modifications need to spread in the mosquito populations and should not be outcompeted by wildtype genes. Gene drive technology overcomes this limitation and results in super-Mendelian spread of specific genes within the mosquito population resulting in self-sustained suppression of parasite transmission (Gantz et al., 2015) or quick collapse of the entire mosquito population (Hammond et al., 2016); however, nuclease-resistant mosquitos that stopped the spread of the drive, have already been identified in laboratory experiments (Hammond et al., 2017). Mosquito resistance was overcome by targeting the *doublesex* gene (*dsx*) which is essential for sex differentiation of *Anopheles gambiae* and resulted in a quick crash of mosquito populations (Kyrou et al., 2018). Despite the potential of gene drive technology for vector control, major concerns about the safety and control of the gene drive once released into the environment remain and should be thoroughly addressed and evaluated in future research (Collins, 2018).

Human antibodies to treat or prevent malaria

Passive transfer experiments demonstrated that immunoglobins isolated from malaria-exposed adults were responsible for the fall of blood stage parasitemia and resolution of clinical symptoms in several studies in Africa and Asia (Cohen et al., 1961; Sabchareon et al., 1991). Monoclonal antibodies (mAbs) for prophylaxis or therapeutic use have furthermore several advantages over other small-molecule drugs due to their high affinity and specificity.

Although many monoclonal antibodies (mAbs) with antimalarial activity have been isolated from semi-immune or vaccinated humans (Julien and Wardemann, 2019) only a few have been tested in clinical trials. A recently conducted phase I trial with a mAb directed against the pre-erythrocytic circumsporozoite protein (CSP) (CIS43LS) was safe and showed 100% protection of malaria-naïve adults following CHMI (Gaudinski et al., 2021); however, due to the COVID-19 pandemic only 9 volunteers participated in that study. Similarly, another anti-CSP mAb was tested in humans (L9LS) that showed even stronger activity at lower concentrations in animal models (Wang et al., 2020). Notably, L9LS achieved 88% protective efficacy in a recently conducted phase I clinical trial followed by CHMI (Wu et al., 2022). Despite the promising results in first-in-human trials, major challenges such as high production costs or resistance to mAbs might limit large-scale passive immunotherapy.

1.3 Immunity to malaria

1.3.1 Naturally acquired immunity (NAI)

The first evidences of naturally acquired immunity (NAI) were reported in 1900 by Robert Koch using cross-sectional blood smears from individuals living in malaria endemic regions with different transmission intensities (Doolan et al., 2009). On the one hand, he observed uniform distribution of parasite densities among all-age groups in Sukabumi, West Java, an area of low malaria transmission intensity. On the other hand, parasite densities were distributed age-dependently in Ambarawa, Central Java, an area of high endemicity. He concluded that protection from malaria required uninterrupted and repeated exposure to malaria parasites (Doolan et al., 2009).

Numerous epidemiological studies support these early observations showing that malaria-naïve individuals as well as young children in endemic areas almost always develop clinical malaria symptoms upon *Plasmodium* infections due to the lack of an effective anti-malarial immune response (Doolan et al., 2009). In contrast, adults who live in areas of

high transmission are frequently re-infected with *Plasmodium falciparum*, can control parasitaemias, rarely succumbing to clinical disease (Marsh and Kinyanjui, 2006). Immunity to malaria is acquired stepwise with age and repeated parasite exposure and first involves quickly acquired 'anti-disease immunity' resulting in control of malaria

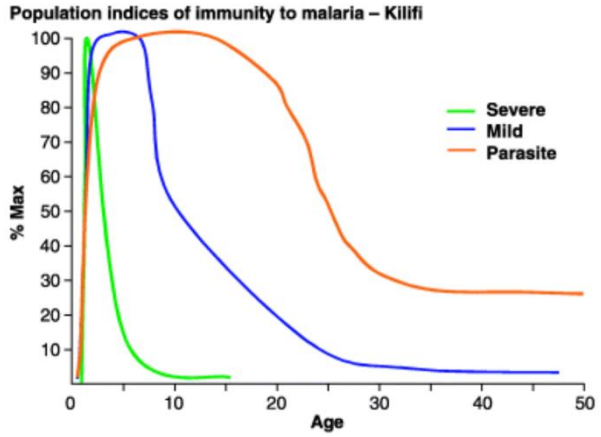

Figure 1.3: Population indices of immunity to malaria.
Representative prevalence of malaria symptoms (mild, severe) and asymptomatic infections dependent on age shown for a population in Kilifi, Kenya. The data is shown in relation to the maximum prevalence of mild, severe and asymptomatic infections recorded. The figure was adopted from Marsh and Kinyanjui 2006.

symptoms and reduced morbidity. This is followed by the relatively slowly acquired 'anti-parasite immunity' resulting into controlling of peripheral blood stage densities but is never sterilizing (Doolan et al., 2009; Langhorne et al., 2008; Marsh and Kinyanjui, 2006) (**Fig. 1.3**). Importantly, naturally acquired immunity can be lost due to cessation of exposure to *Plasmodium* parasites as seen in transmigrants moving away from areas with high malaria transmission (Färnert et al., 2015) or the effective use of malaria control measures (Trape et al., 2011).

1.3.2 Humoral immunity

1.3.2.1 Passive transfer of antibodies

Passive transfer studies have unequivocally demonstrated the role of antibodies for NAI to malaria. Purified gamma-globulins (IgG) from semi-immune adults living in The Gambia, West Africa were transferred to 12 children between 4 months and 2.5 years of age suffering from *P. falciparum* infections. Treatment resulted in significant declines of peripheral blood stage parasitemia and alleviation of symptoms compared to children who either received IgG from non-exposed adults, IgG-free serum from semi-immune adults or remained untreated (Cohen et al., 1961). This was supported by another study showing that purified IgG from Nigerian adults transferred to 6 children with acute *P. falciparum* infections resulted in significant drops of blood stage parasitemia and clinical symptoms (Edozien et al., 1962).

Cross-reactive effects of naturally acquired antibodies was demonstrated by the transfer of purified IgG from adults living at the Cote d'Ivoire, West Africa to eight Thai patients suffering from infections with recrudescent *P. falciparum* parasites. Similar to previous passive transfer studies, purified IgG from semi-immunes helped to clear parasites and symptoms (Sabchareon et al., 1991) suggesting strain-transcending activities of anti-malarial antibodies. After the decline of anti-malarial IgG in plasma, parasitemia increased steadily but recrudescent parasites remained susceptible to the same IgG pool (Sabchareon et al., 1991) indicating lack of selection pressure. In those studies, purified IgG from semi-immune adults failed to reduce the number of gametocytes suggesting that naturally acquired antibodies predominantly target other blood stages.

1.3.2.2 Maternal antibodies

Although young children under 5 years of age are the most vulnerable group of *Plasmodium falciparum* infections and severe clinical disease, newborns and young infants younger than 6 months of age rarely show symptomatic malaria and low parasite densities (Mwaniki et al., 2010; Riley et al., 2001; Sehgal et al., 1989; Snow et al., 1998; Wagner et al., 1998). Although this level of protection might be attributed to several immunological and physiological mechanisms, the presence of maternal antibodies has been inversely associated with risk for clinical malaria and blood stage parasitemia (Murungi et al., 2017). The transfer of maternal IgG from the mother to the foetus occurs transplacentally via binding to the neonatal Fc-receptor (FcRn) (Simister, 2003). After birth, maternal IgA is transferred from breast milk to the newborn and has been associated with reduced growth of parasites *in vitro* (Kassim et al., 2000).

1.3.2.3 Antibody targets and functions

Although early passive transfer experiments demonstrated that antibodies play an important role in NAI, the targets and mechanisms that result in a protective immune response are still not fully known. Sequence analysis of the *Plasmodium falciparum* parasite genome revealed more than 5300 genes (Gardner et al., 2002) that might encode for a range of proteins targeted by antibodies. Several studies demonstrated that antibodies bind to a range of antigens covering all stages of *Plasmodium falciparum* (Crompton et al., 2010; Dantzler et al., 2019; Dent et al., 2015; Obiero et al., 2019) and responses against many antigens have been associated with protection from malaria in independent cohort studies (Dent et al., 2015; Osier et al., 2014b; Proietti et al., 2020; Richards et al., 2013). Moreover, there is increasing evidence that antibody responses against several antigens are stronger correlates of protection than

reactivity against single antigens (Garcia-Senosiain et al., 2020; Osier et al., 2008; Richards et al., 2013). Antibodies can induce a range of anti-parasitic functions that target pre-erythrocytic as well as erythrocytic stages of the *Plasmodium falciparum* lifecycle that are explained below (**Fig. 1.4**).

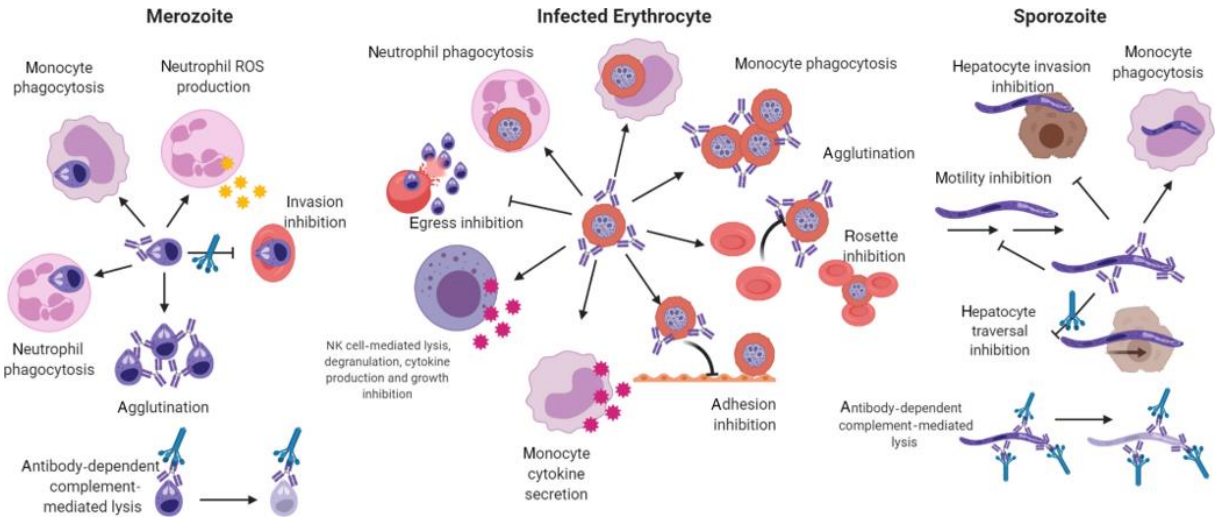

Figure 1.4: Functions of anti-malaria antibodies in the human host.
Antibodies target different stages of *Plasmodium* in the human host including sporozoites, merozoites and infected erythrocytes. Antiparasitic mechanisms are induced via the Fab or Fc part of antibodies. The figure was adopted from Aitken et al., 2020.

Invasion/Growth inhibition

Antibodies can directly prevent the invasion of host cells via Fab-mediated inhibition of receptor-ligand interactions, protein maturation or complex formation. Antibodies targeting sporozoites via binding to CSP have been demonstrated to reduce parasite gliding motility (Barry et al., 2018; de Korne et al., 2022), traversal through the sinusoidal cell layer (Behet et al., 2014) and finally hepatocyte invasion (Seder et al., 2013). Neutralizing monoclonal antibodies against sporozoites bind to NANP repeats at the central repeat region (Imkeller et al., 2018; Oyen et al., 2017; Triller et al., 2017) and the unique NPDP peptide followed by NVDP repeats at the junctional region of CSP (Kisalu et al., 2018; Wang et al., 2020).

Antibodies against the merozoite stage block invasion of erythrocytes by binding to several antigens including MSP1 (Woehlbier et al., 2006), AMA1 (Harris et al., 2005), EBA175 (Chitnis et al., 2015) and RH5 (Douglas et al., 2015; Douglas et al., 2011) measured by the standard growth inhibition assay (GIA). Notably, neutralizing anti-RH5 antibodies show the strongest levels of growth inhibition among other vaccine candidates tested so far (Douglas et al., 2019; Douglas et al., 2015; Douglas et al., 2011). While some antibodies against RH5 block the interaction with basigin disrupting erythrocyte invasion, other antibodies slowed down the

invasion process by binding to other RH5 epitopes but were non-neutralizing. These antibodies are thought to act synergistically with antibodies to other merozoite antigens such as AMA1 (Alanine et al., 2019).

Although the GIA is still the most widely used functional assay to evaluate blood stage malaria vaccine candidates, there is conflicting data about the association of neutralizing antibodies with protection from malaria (Duncan et al., 2012).

Antibodies to infected erythrocytes such as trophozoites and schizonts have shown to prevent sequestration to the endothelium by blocking interactions of *Plasmodium* antigens such as PfEMP1 with endothelial surface receptors (Chan et al., 2014; Olsen et al., 2018; Turner et al., 2015). Furthermore, antibodies can prevent rosette formation (Carlson et al., 1990), promote merozoite agglutination (Green et al., 1981) and prevent schizont rupture (Raj et al., 2014) which limits blood stage parasitemia and clinical symptoms of malaria.

Antibodies against antigens of sexual blood stages including Pfs230 and Pfs48/45 of immature gametocytes, have demonstrated strong transmission blocking activity (Stone et al., 2018). Moreover, antibodies against Pfs47 of female gametes (Canepa et al., 2018) or Pfs25 on zygotes and ookinetes (Wu et al., 2008) have been shown to strongly impair parasite transmission.

Antibody-dependent complement fixation (AbC')

Complement is part of the innate immune system and encompasses soluble and membrane-bound effector proteins that activate each other in an enzyme-triggered cascade resulting in pathogen opsonization and lysis via the formation of a membrane attack complex (MAC) (Merle et al., 2015). Complement gets activated via three distinct pathways. First, the classical complement pathway involves the complement factor C1q of the C1 complex that binds to the Fc-part of opsonizing antibodies. Second, the mannose-binding lectin pathway involves the C1q-like mannose-binding lectin (MBL) which binds to mannose on the pathogen's cell surface. Finally, the alternative pathway which is activated by deposition of spontaneously processed complement factors. Each pathway results in the activation of a C3 convertase that further activates other complement factors by enzymatic cleavage.

Cytophilic IgG (IgG1 and IgG3) and IgM are strong activators of the classical complement cascade which targets sporozoites (Behet et al., 2018; Kurtovic et al., 2018) and merozoites (Boyle et al., 2019; Boyle et al., 2015). Naturally acquired antibodies directed against NANP repeats of CSP strongly reduced hepatocyte traversal and viability of sporozoites in a complement-dependent manner (Kurtovic et al., 2018). Furthermore, immunization of

volunteers under chemoprophylaxis with sporozoites (CPS) elicited IgG and IgM that both resulted in decreased cell traversal, hepatocyte invasion and sporozoite death via complement-mediated membrane damage (Behet et al., 2018).

Naturally acquired (Boyle et al., 2015; Reiling et al., 2019) as well as vaccine-induced antibodies (Blank et al., 2020; Feng et al., 2018) against merozoites have been shown to activate the classical complement cascade. Antibodies against the p19 subunit of MSP1 as well as MSP2 in the presence of complement abbreviated merozoite invasion (Boyle et al., 2015); however, this was not observed with antibodies against full-length MSP1 (Blank et al., 2020). Furthermore, antibody-dependent complement fixation (AbC') was highly correlated with protection from malaria in children living in Papua New Guinea (Boyle et al., 2015) and AbC' was a stronger correlate compared to GIA (Reiling et al., 2019). Several merozoite antigens are targeted by opsonizing antibodies with AbC' activity including well-known antigens such as MSP1-p19 and AMA1 and less-well studied antigens such as BA140RIII-V, MSP7, RALP1, GAMA, PfRH2 and MSPDBL1. Notably, a combination of responses to 3-6 selected antigens has been shown to be the strongest correlate of protection accounting for an approximate protective efficacy of >95% (Reiling et al., 2019).

Opsonic phagocytosis activity (OPA)

Antibodies against *Plasmodium falciparum* sporozoites promote their phagocytosis by engaging FcγRs on phagocytes including monocytes, neutrophils (Feng et al., 2021) and the monocytic cell line THP1 (Steel et al., 2017). Recent data suggests that net-phagocytosis activity against sporozoites is dominated by neutrophils whereas monocytes play only a minor role (Feng et al., 2022; Feng et al., 2021). All regions of CSP are targets of naturally acquired opsonising antibodies that induce neutrophil phagocytosis by FcγRIIa and FcγRIII engagement, particularly the N-terminus (Feng et al., 2021). Furthermore, the level of opsonic phagocytosis activity of naturally acquired antibodies is age-dependent with young children showing lower magnitudes of sporozoite phagocytosis compared to adults living in endemic areas (Feng et al., 2021). Antibodies from children vaccinated with RTS,S induced only modest levels of neutrophil and monocyte OPA activity and waned over time which corresponds to the moderate protective efficacy of the vaccine in phase III clinical trials (Feng et al., 2022).

Opsonization of merozoites by cytophilic antibodies promotes their phagocytosis shown by early and more recent sero-epidemiological studies (Hill et al., 2013; Khusmith and Druilhe, 1982; Khusmith et al., 1982; Osier et al., 2014a). Phagocytosis of merozoites by THP1 cells was highly correlated with protection from clinical malaria and high blood stage parasitemia in

children living in Papua New Guinea (Hill et al., 2013) and Kenya (Osier et al., 2014a). Moreover, phagocytosis activity increased with age and was boosted upon reinfection (Osier et al., 2014a). Merozoite phagocytosis resulted in monocyte activation and promoted release of the pro-inflammatory cytokine tumour necrosis factor alpha (TNFα) (Osier et al., 2014a) which is known to play an important role in anti-malarial immunity (Muniz-Junqueira et al., 2001).

Neutrophils are also involved in merozoite phagocytosis which is enhanced in the presence of antibodies from malaria-exposed individuals and pro-inflammatory cytokines (Kumaratilake and Ferrante, 2000). A recent study demonstrated that monocyte-mediated phagocytosis of antibody-bound merozoites occurs at low antibody concentrations via FcγRIIa engagement, whereas high antibody concentrations activate neutrophils via FcγRIIa and FcγRIIIB more effectively (Garcia-Senosiain et al., 2021). Several merozoite antigens have been identified as targets of antibodies with OPA activity including MSP1-p19, MSP2, MSP3, Glutamine-rich protein (GLURP) and RH2 (Kana et al., 2019; Osier et al., 2014a). Notably, phagocytosis activity against a spectrum of those antigens was highly associated with reduced odds of clinical malaria in children living in Ghana (Kana et al., 2019).

Naturally acquired antibodies also promote phagocytosis of infected erythrocytes by monocytes including young rings (Musasia et al., 2022) and mature blood stages (Ataíde et al., 2010; Chan et al., 2012) which was associated with protection from malaria (Chan et al., 2019; Musasia et al., 2022). Surface-proteomic approaches identified a list of merozoite antigens present on the surface of ring stages, including EBA175 and -140 that might be involved in antibody-dependent phagocytosis activity of rings (Musasia et al., 2022). Vaccine-induced and naturally acquired antibodies against PfEMP1 resulted in phagocytosis of late blood stages (Chan et al., 2012; Ghumra et al., 2011; Quintana et al., 2016). Phagocytosis against gametes by both monocytes and neutrophils have been reported; however, no transmission-reducing effect was observed (Healer et al., 1999) suggesting that phagocytosis of sexual stages does not play a major role in blocking transmission in mosquitos

Antibody-dependent cellular inhibition (ADCI)

Besides phagocytosis of merozoites or infected erythrocytes, monocytes inhibit parasite growth *in vitro* by the release of soluble mediators, predominantly the pro-inflammatory cytokine TNFα upon antibody binding to infected erythrocytes via FCγRIIa and FcγRIII (Bouharoun-Tayoun et al., 1995; Tiendrebeogo et al., 2015). Notably, this antibody-dependent cellular inhibition (ADCI) activity increased with age and was significantly associated with

reduced risk of febrile malaria in Ghanaian children (Tiendrebeogo et al., 2015). ADCI activity has been reported to be strain transcending (Bouharoun-Tayoun et al., 1995) suggesting that conserved antigens are targeted; however, antibodies against MSP1 block 2 induced only variant-specific ADCI activity due to the highly polymorphic nature of the protein (Galamo et al., 2009). Other merozoite proteins have been identified as targets of vaccine-induced antibodies with ADCI activity including MSP2 (McCarthy et al., 2011), MSP3 (Druilhe et al., 2005) and GLURP (Jepsen et al., 2013).

Antibody-dependent respiratory burst (ADRB)

Naturally acquired (Jäschke et al., 2017; Joos et al., 2010) and vaccine-induced (Blank et al., 2020) antibodies which opsonize merozoites bind to FCγRII on neutrophils triggering respiratory burst and release of reactive oxygen species (ROS) measured by the antibody-dependent respiratory burst (ADRB) assay (Kapelski et al., 2014). Early studies have demonstrated that ROS is detrimental to growth of blood stages (Allison and Eugui, 1983; Clark and Hunt, 1983; Golenser et al., 1992) and neutrophil ADRB activity was highly correlated with protection from malaria in Senegalese villagers (Joos et al., 2010). However, only a combination of GIA and ADRB was associated with reduced odds of clinical malaria in young Kenyan children while individual activities were not (Murungi et al., 2016). Several merozoite surface proteins have been identified as targets of antibodies with ADRB activity that are MSP1-p83 (Jäschke et al., 2017), MSP1-p19 (Joos et al., 2015), MSP5 (Perraut et al., 2014) and MSP2 (Rosenkranz 2018, Master thesis).

ADRB activity against sporozoites has been recently demonstrated in children vaccinated with RTS,S (Feng et al., 2022); however, its contribution to sporozoite killing remains yet to be assessed.

Antibody-dependent natural-killer cell (Ab-NK) activity

Although the role of natural killer (NK) cells for immunity against infectious diseases has been mostly limited to viral infections, there is increasing evidence that NK cells contribute to immunity against malaria in an antibody-dependent manner (Wolf et al., 2017).

It was shown that naturally acquired antibodies against infected erythrocytes activate NK cells via binding to FcγRIII which resulted in degranulation and production of pro-inflammatory cytokines such as IFNγ and TNFα (Arora et al., 2018). This activation resulted in rapid lysis of infected erythrocytes and reduced parasite growth *in vitro* in a process known as antibody-dependent natural killer cell (Ab-NK) activity or antibody-dependent cellular cytotoxicity

(ADCC). Notably, antibodies against PfEMP1 and RIFINs on the surface of blood stages activated NK cells which resulted in selective killing of parasites without destroying uninfected RBCs (Arora et al., 2018).

Recently it was shown that naturally acquired antibodies against *Plasmodium falciparum* merozoites activate NK cells promoting Ab-NK activity measured by IFNγ and the presence of the degranulation marker CD107 (Odera et al., 2021). Ab-NK activity increased with age and correlated with lower risk of clinical malaria in a longitudinal cohort of children and control of parasitemia following CHMI in adults living in Kenya (Odera et al., 2021). Furthermore, antibodies with Ab-NK activity targeted several merozoite antigens such as AMA1, MSP3 and others. The net-activity of NK cells increased with the combination of antigen-specific responses which was highly correlated with activity against whole merozoites (Odera et al., 2021).

Naturally acquired antibodies from Kenyan adults as well as vaccine-induced antibodies from children collected 3 months after immunization with RTS,S bound FcγRIII on NK cells which promoted Ab-NK activity against sporozoites (Feng et al., 2022; Feng et al., 2021). Similar to responses against merozoites, Ab-NK activity against sporozoites was dependent on the antibody-concentrations with high antibody amounts inducing higher levels of NK cell degranulation (Feng et al., 2022).

1.3.3 T cell-mediated immunity

Besides of antibodies, T cell-mediated immune responses are critical for limiting parasitemia and severity of clinical symptoms of malaria and involves several subsets of αβ and γδ T cells.

The presentation of foreign antigens via MHC-II on antigen presenting cells (APC) such as dendritic cells or macrophages activates $CD4^+$ T cells that differentiate into functionally divers subsets in the presence of cytokines.

The presence of T helper cells 1 (T_H1 cells) is a common immune signature in *Plasmodium* infections (Kurup et al., 2019). Although the precise mechanisms behind a T_H1-mediated anti-malarial immune response is still not completely understood, they produce and secrete the pro-inflammatory cytokine IFNγ which activates macrophages promoting parasite phagocytosis (Bastos et al., 2002) or production of nitric oxide (NO) (Blanchette et al., 2003; Jaramillo et al., 2003) which was associated with malaria tolerance in semi-immune individuals (Boutlis et al., 2003). T_H1 cells have also been shown be involved in class-switch recombination in mature B cells in response to *Plasmodium* infections (Su and Stevenson, 2000) and activation of NK cells via secretion of IL-2 (Horowitz et al., 2010). Furthermore, T_H1 cells might

contribute to immunity against pre-erythrocytic stages. IFNγ secretion of central-memory T_H1 cells of RTS,S-vaccinated adults, upon stimulation with CSP, was associated with protection from malaria (Reece et al., 2004).

T_H2 cells are rare during *Plasmodium* infections (Perez-Mazliah and Langhorne, 2014) and primarily secrete IL-4 which stimulates antibody class switching in B cells (Shimoda et al., 1996). Furthermore, the presence of IL-4 was highly associated with serum-antibody levels of naturally-exposed individuals against blood stage antigens (Troye-Blomberg et al., 1990). However, IL-4 deficient mice could clear parasite infections similarly to wildtype mice indicating that IL-4-secreting T_H2 cells might play a minor role in anti-malarial immunity (von der Weid et al., 1994).

T follicular helper cells (T_{FH}) are localized at the germinal centres in secondary lymphoid organs and play a major role in B cell activation promoting their differentiation into antibody-secreting long-lived plasma cells or memory B cells. Interleukin 17-producing T helper (T_H17) cells have been demonstrated to recruit neutrophils (Sandquist and Kolls, 2018) and expand during *Plasmodium vivax* infections (Bueno et al., 2012). IL-10-expressing $CD4^+$ T regulatory 1 (T_{reg}) cells have been linked to dampen inflammation limiting clinical manifestations of malaria. High levels of IL-10 were associated with high blood stage parasitemia (Luty et al., 2000; Othoro et al., 1999) and protection from severe anemia in children (Kurtzhals et al., 1998; Othoro et al., 1999).

Cytotoxic $CD8^+$ T cells take a critical role in pre-erythrocytic immunity against liver-stages (Cockburn et al., 2013). They get activated via recognition of foreign peptides presented in MHC class I molecules on hepatocytes and other liver resident cells (Chakravarty et al., 2007). While the precise mechanisms of T cell-mediated killing of infected hepatocytes is not fully understood, secretion of IFNγ is suggested to be critical (Ferreira et al., 1986; Imai et al., 2010; Mellouk et al., 1987). IFNγ promotes the production of NO in hepatocytes which is detrimental to liver stages (Seguin et al., 1994). The presence of $CD8^+$ T cells was correlated with protection in individuals immunized with thrombospondin-related adhesion protein (TRAP) via vector-delivery (Ewer et al., 2013).

Although the unconventional γδ T cells represent only approximately 4% of T lymphocytes, their role in immunity against malaria is increasingly recognized. They express the γ and δ chains of the T cell receptor (TCR) and are activated by phosphorylated antigens (Behr et al., 1996; Guenot et al., 2015). γδ T cells expand upon acute malaria infection (Ho et al., 1994; Roussilhon et al., 1990) and release cytokines which was associated with protection against *Plasmodium* reinfections in children (D'Ombrain et al., 2008; Jagannathan et al., 2017). It was

recently demonstrated that γδ T cells could contribute to a protective anti-malarial immune response by TCR independent ADCC activity via binding to opsonizing antibodies bound to infected erythrocytes (Farrington et al., 2020).

1.4 Malaria vaccines

Although rigorous efforts have been made, the burden of malaria remains high suggesting that measures currently available are not sufficient enough to control the disease. Vaccines are the cornerstones of modern medicine and have saved millions of lives worldwide (Amanna and Slifka, 2020). Since it is known that humans can acquire protective immunity against malaria, the development of highly active and durable malaria vaccines has been considered as a milestone to combat and eventually eradicate the disease. Since 2000, more than 240 clinical trials against *P. falciparum* malaria have been launched (https://clinicaltrials.gov/ct2/about-site/history) including pre-erythrocytic vaccines, blood stage vaccines and transmission-blocking vaccines (**Tab. 1.2**).

1.4.1 Pre-erythrocytic vaccines

Pre-erythrocytic vaccines (PEV) are directed against sporozoites and liver stages which do not cause clinical manifestations of malaria and aim to prevent infection. PEV can be further classified as whole sporozoite vaccines (WSV) or subunit vaccines. PEVs need to confer sterile protection to avoid blood stage parasitemia and thus clinical symptoms which is a major bottleneck of those vaccines.

1.4.1.1 Whole sporozoite vaccines (WSV)

Protective effects of WSV have already been demonstrated by Clyde and colleagues in the early 1970s. Immunization with thousands of radio-attenuated *Plasmodium falciparum* sporozoites via infectious mosquito bites, conferred sterile protection in humans following homologues and heterologous sporozoite challenge (Clyde, 1975; Clyde et al., 1973) but failed to protect from challenge with infected erythrocytes (Clyde et al., 1973); however, immunization via infectious mosquito bites is not applicable for mass vaccination. The manufacturing of aseptic, purified and cryopreserved sporozoites of the NF54 strain (PfSPZ) under GMP compliance by the biotech company Sanaria® has overcome those major obstacles (Hoffman et al., 2010). Since this platform is available, different classes of WSV are developed including sporozoites attenuated via radiation or genetic modification or live-non-attenuated sporozoites under chemoprophylaxis.

Radiation-attenuated sporozoites (RAS)

Immunization with cryopreserved irradiated sporozoites (PfSPZ vaccine) via direct intravenous inoculation has been shown to elicit 100% sterile protection in malaria-naïve adults following homologous sporozoite challenge (Seder et al., 2013) over a 12 months period (Ishizuka et al., 2016); however, the level of protection was highly dependent on the dosage and time of controlled human malaria infection. Notably, vaccination with PfSPZ elicited protection against homologues challenge in 70% of malaria-naïve volunteers while only 10% of vaccinees were protected following heterologous challenge 24 weeks after the last immunization (Epstein et al., 2017). Furthermore, protection against natural exposure was only 29% throughout the transmission season in Mali (Sissoko et al., 2017). This data showed that the PfSPZ vaccine confers higher levels and longer lasting homologues protection compared to heterologous protection. However, a recent study in malaria-naïve adults reported similar protective efficacies of 78% against homologues and heterologous challenge upon immunization with an improved dose regimen of 9×10^5 PfSPZ on days 1, 8, and 29 (Mordmüller et al., 2022). The efficacy of this dose regimen is currently being assessed in Malian children (NCT04940130).

Genetically attenuated parasites (GAP)

Several genes of *P. falciparum* parasites have been identified to be essential for the development within hepatocytes (Kaiser et al., 2004). Genetically attenuated parasites (GAP) that harbour mutations in specific genes resulting in arrest at different steps of liver stage development have been characterized. Several GAPs have shown promising results in mouse models (Goswami et al., 2020; van Schaijk et al., 2014; VanBuskirk et al., 2009) and were tested for protective efficacy in humans. The first GAP tested in a phase I clinical trial was based on knockouts of Pfb9 and slarp (PfSPZ-GA1 vaccine) (van Schaijk et al., 2014) and although no breakthrough infections were detected, the overall protective efficacy of this vaccine after CHMI was small (sterile protection in 3 out of 25 volunteers) (Roestenberg et al., 2020). Recently a triple knockout GAP with deletions in P52, P36, and SAP1 was tested for protective efficacy against CHMI via infectious mosquito bites in malaria-naïve volunteers. The vaccine was safe, immunogenic and protected half of the volunteers from blood stage parasitemia (Murphy et al., 2022). Moreover, 1 out of the 6 protected vaccinees remained parasite free after a second CHMI (Murphy et al., 2022).

Chemoprophylaxis and sporozoite vaccination

Immunization with live sporozoites under chemoprophylaxis allows completion of the pre-erythrocytic cycle and release of merozoites into the blood stream. The parasites are subsequently killed by an antimalarial compound preventing the development of blood stage parasitemia and thus clinical disease (Bijker et al., 2015). The advantage of this approach is the development of potent anti-liver stage immunity as well as antibody-mediated immunity against merozoites (Marques-da-Silva et al., 2020). A phase I with chemoprophylaxis and sporozoite vaccination (CPS) using chloroquine (PfSPZ-CVac) resulted in sterile protection of all malaria-naïve volunteers against homologous (Mordmüller et al., 2017) and heterologous challenge (Mwakingwe-Omari et al., 2021); however, immunization with PfSPZ-CVac of malaria-exposed individuals in Mali conferred only 33% protection which was statistically non-significant (Coulibaly et al., 2022).

1.4.1.2 Subunit vaccines

The circumsporozoite protein (CSP) is the most abundant surface protein of *Plasmodium* sporozoites and has been the focus of pre-erythrocytic subunit vaccines. The RTS,S vaccine which is the most advanced anti-malaria vaccine to date, is a virus-like particle (VLP) which contains the central repeat and C-terminal region of CSP fused to hepatitis B surface antigen (HBsAG) in order to display the immunogen on the surface. Together with the oil-in-water emulsion AS01 it has been tested in a large phase III trial in all age groups of seven African countries (Burkina Faso, Gabon, Ghana, Kenya, Malawi, Mozambique and Tanzania). Four immunizations of the vaccine reduced clinical malaria cases in young children 5-17 months of age by approximately 36% and 29% in young infants and children 6-12 years of age, respectively, during a four-year follow-up. Notably, protective efficacy waned significantly over time (RTS Partnership, 2015). Despite its limitations, the WHO recommended the use of RTS,S for pilot implementation in Malawi, Ghana and Kenya to assess its feasibility of administration, efficacy in real-life settings and safety in routine use (clinicaltrials.gov ID NCT03806465). After review of the Malaria Vaccine Implementation Programme (MVIP) in 2021, the WHO recommended the use of RTS,S/AS01 vaccine in young children living moderate to high malaria transmission areas (WHO 2022).

The R21 vaccine is another CSP-based subunit vaccine that aims to improve the moderate protective efficacy of RTS,S. In this approach, VPLs contain only CSP-HBsAG fusion proteins and lack unfused HBsAG leading to a higher frequency of CSP presented on the VPL surface (Collins et al., 2017). After promising results in pre-clinical studies, R21 formulated with the saponin-based adjuvant Matrix-M (R21/MM) was tested in a phase IIb trial in Burkina Faso. Indeed, the vaccine conferred 77% protective efficacy in young children aged 5-17 months

over 6 months (Datoo et al., 2021) after receiving three doses. A booster dose administered one year after the primary immunization, prolonged the protective effects for an additional 6 months (Datoo et al., 2022). Although these results are highly encouraging, the trials were conducted in an area with seasonal malaria transmission and thus might only explain protective efficacy for 6 months and one year, respectively. More and larger clinical trials are needed to confirm this.

Pre-erythrocytic subunit vaccines targeting other sporozoite surface antigens such as TRAP have been tested in clinical trials; however, protective efficacy of this vaccine is overall disappointing (Ewer et al., 2013; Mensah et al., 2016; Tiono et al., 2018).

1.4.2 Blood stage vaccines

Blood stage vaccines (BSV) aim to limit disease severity by targeting the asexual blood stages, primarily merozoites, of the parasite which cause clinical manifestation of malaria. Major challenges of BSVs are I) the short time of merozoite invasion (<1 min), II) antigenic polymorphisms which elicit strain-specific antibody responses limiting protective efficacies across parasite strains, III) redundant invasion pathways and IV) the large number of merozoites that are released from liver and blood schizonts.

1.4.2.1 Subunit vaccines

Several blood stage subunit vaccines that target-specific proteins of merozoites have been evaluated in clinical trials. Notably, those proteins have been considered as essential and play a key role in merozoite invasion including AMA1, MSP1, MSP2, MSP3 and EBA175 (Beeson et al., 2016); however, outcomes of those clinical trials are overall disappointing. The vaccine candidates AMA1 and MSP1 failed to confer protection from clinical malaria in children living in malaria endemic regions presumably due to strain-specific antibody responses (Ogutu et al., 2009; Thera et al., 2011). Additionally, an MSP3-based vaccine provided only moderate protection which was short-lived (Sirima et al., 2011). In order to overcome strain-specific responses, BSVs that include multiple allelic variants of the same antigen have been developed and evaluated in phase I clinical trials. This included MSP2-C1 (MSP2 3D7 and FC27) or AMA1 Diversity Covering (DiCo) which induced antibody responses against multiple parasite strains (McCarthy et al., 2011; Sirima et al., 2017).

A promising vaccine candidate that is essential for merozoite invasion and shows high degree of sequence conservation is RH5 (Volz et al., 2016). Pre-clinical studies demonstrated protection of monkeys from homologous and heterologous challenge by the induction of strain-

transcending neutralizing antibodies (Douglas et al., 2015; Douglas et al., 2011). However, protection of monkeys required high titres (approximately 200µg/ml) of anti-RH5 antibodies which was not achieved by vaccination of malaria-naïve adults (Payne et al., 2017).

Combinations of distinct antigens have been assessed for protective efficacy such as the GMZ2 vaccine composed of MSP3 fused to GLURP. Despite showing immunogenicity in malaria-naïve adults (Esen et al., 2009), malaria-exposed adults (Mordmüller et al., 2010) and children (Bélard et al., 2011), the vaccine conferred only 20% protection from clinical disease in a large phase IIb study in children 3-4 years of age and 6% in children 1-2 years of age (Sirima et al., 2016).

1.4.2.2 Whole blood stage vaccines

The use of attenuated blood stages as vaccines has been considered as an alternative approach to subunit vaccines since a multitude of antigens are presented to the immune system. Pre-clinical studies with chemically attenuated blood stages demonstrated T cell-dependent protective immunity against homologous and heterologous challenge in mice (Raja et al., 2016) and the first study in humans was safe, well tolerated and induced strain-transcending cellular responses but failed to elicit antibodies (Stanisic et al., 2018). Parasites lacking the knob-associated histidine-rich protein (KAHRP) were recently tested as a genetically attenuated blood stage vaccine in malaria-naïve adults. The vaccine was safe at low doses but significant breakthrough infections were detected when high doses of parasites were administered (Webster et al., 2021) which underscores the safety concerns of whole-blood stage vaccines.

1.4.3 Transmission blocking vaccines

Transmission blocking vaccines (TBV) incorporate antigens that induce immune responses preventing the transmission of parasites by mosquitos. TBVs mainly target surface antigens expressed on gametocytes (Pfs230 and Pfs48/45) and zygotes after fertilization (Pfs25 and Pfs2) (Delves et al., 2018). Pre-clinical studies have demonstrated that immunization with those antigens induced inhibitory antibodies that blocked transmission in mosquitos using the standard membrane feeding assay (SMFA) (Kapulu et al., 2015; Menon et al., 2018). Moreover, increased transmission blocking activity of antibodies against Pfs230 has been demonstrated in the presence of complement (Read et al., 1994). Pfs25 has been considered as the leading TBV candidate since it induced the strongest levels of transmission blocking activity among the other candidates tested (Kapulu et al., 2015; Menon et al., 2018).

A clinical trial with Pfs25 formulated with Montanide ISA 51 was poorly immunogenic and resulted in systemic adverse events (Wu et al., 2008). When formulated with Allohydrogel the vaccine was safe, well-tolerated and induced antibodies that blocked transmission in malaria-naïve adults; however, 4 immunization were required and activity waned over time (Talaat et al., 2016). Notably, the vaccine failed to induce antibodies with blocking activity in malaria-exposed individuals (Sagara et al., 2018). Preclinical and clinical studies suggest that combinations of Pfs25 with other antigens such as Pfs230 might enhance immunogenicity (Duffy and Kaslow, 1997; Healy et al., 2021). However, when comparing the transmission blocking activity of those two vaccine candidates, Pfs230 was much more potent compared to Pfs25 (50%-90% versus <50%) (Healy et al., 2021).

The development of vaccines against Pfs48/45 has been hampered by production of high-quality proteins; however, the use of bioinformatical approaches resulted in the production of highly stable Pfs48/45. Pre-clinical studies of this protein in mice demonstrated significantly higher magnitudes of antibodies with transmission blocking activity compared to immunizations with the native protein (McLeod et al., 2022).Challenges of transmission blocking vaccines are

Table 1.2: Current malaria vaccine candidates in pre-clinical and clinical trails

Vaccine candidate	Immunogen type	Current status
Pre-erythrocytic stage (anti-infection)		
RTS,S	Subunit	Phase IV
R21	Subunit	Phase I/II
Full-length CSP	Subunit	Phase I
PfSPZ vaccine	Whole sporozoite (radiation attenuation)	Phase II
Chemoprophylaxis vaccination (CVAc)	Whole sporozoite (chemical attenuation)	Phase II
Genetically attenuated parasites (GAP) vaccines	Whole sporozoite (genetic attenuation)	Phase I
Blood stage (anti-disease)		
PfRH5	Subunit	Phase I
Full-length MSP1	Subunit	Phase I
AMA1-RON2	Subunit	Preclinical
PfSEA-1	Subunit	Preclinical
PfGARP	Subunit	Preclinical
Chemically attenuated parasite (CAP) vaccines	Whole blood stage parasite	Phase I
VAR2CSA	Subunit	Phase I
PvDBP (*Plasmodium vivax*)	Subunit	Phase I
Mosquito stage (Transmission blocking)		
Pfs25	Subunit	Phase I
Pfs230	Subunit	Phase II
Pfs48/45	Subunit	Preclinical
Pvs230 (*Plasmodium vivax*)	Subunit	Preclinical

The table was adopted and modified from Duffy and Gorres 2020

the high coverage required for herd immunity, and the maintenance of functional antibodies over time. Moreover, since TBVs do not directly protect the vaccinee from infection and clinical disease, combinations with pre-erythrocytic or erythrocytic vaccines could provide additional protective effects.

1.5 Merozoite surface protein1 (MSP1)

1.5.1 MSP1 sequence

Merozoite surface protein 1 (MSP) is the most abundant surface protein of *Plasmodium* merozoites (Gilson et al., 2006) and has been identified in all human-infectious *Plasmodium* species (Birkenmeyer et al., 2010; Carlton et al., 2008). MSP1 is encoded by its gene on chromosome 9 and expressed in mature schizonts of the liver (Szarfman et al., 1988; Tarun et al., 2008) and the blood (Bozdech et al., 2003). Based on the degree of amino acid sequence conservation, MSP1 has been sectioned into 17 blocks (Tanabe et al., 1987). Although some domains are conserved (block 1,3, 5,12,17) and others highly oligomorphic (block 2 and 4), the overall sequence of MSP1 has been considered as dimorphic (block 6-11, 13-16), since all MSP1 variants can be classified into one of the two main but distinct allelic forms, namely K1 or MAD20 (Tanabe et al., 1987) that have been isolated from Papa New Guinea and Thailand, respectively (**Fig. 1.5**).

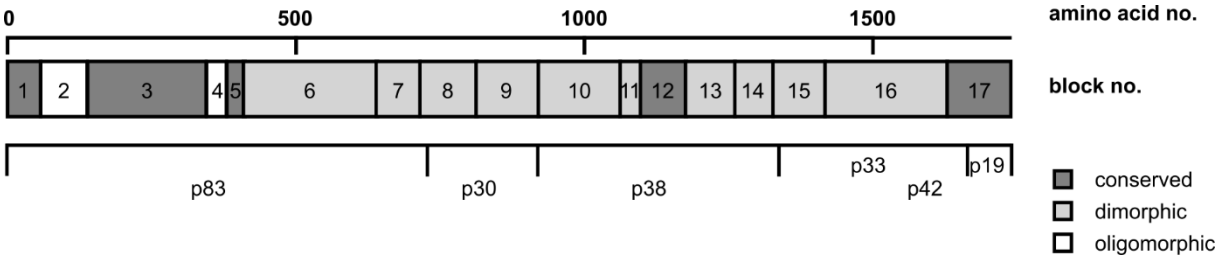

Figure 1.5: Illustration of the primary amino acid sequence of MSP1.
MSP1 is expressed as a precursor consisting of 17 blocks with different levels of conservation. During maturation, the protein is processed in 4 subunits (p83, p30, p38 and p42).

1.5.2 MSP1 complex and maturation

Full-length MSP1 ($MSP1_{FL}$) is expressed as an approximately 190 kDa precursor. Similar to other merozoite surface proteins, MSP1 is not glycosylated (Berhe et al., 2000) except for the addition of a GPI-anchor at the C-terminus that tethers the protein to the parasite surface. Prior to egress of merozoites, the MSP1 precursor is naturally cleaved by a serine protease called subtilisin-like protease 1 (PfSUB1) that has been released from exonemes into the lumen of the parasitophorous vacuole (Blackman et al., 1998; Koussis et al., 2009). PfSUB1 cleaves

MSP1 at conserved processing sites (Blackman et al., 1991; Cooper and Bujard, 1992; Koussis et al., 2009; Stafford et al., 1994) which consequently results into the formation of four subunits named accordingly to their approximate size: p83, p30, p38 and p42. The subunits remain non-covalently attached to each other and form a complex on the merozoite surface (Holder et al., 1987; McBride and Heidrich, 1987).

Before invasion of erythrocytes, the macromolecular complex gets processed a second time. The integral-membrane serine-protease PfSUB2 which has been discharged from micronemes cleaves the MSP1 complex at the p33/19 processing site which eventually results into shedding of the majority of the complex while only the small C-terminal p19 subunit remains anchored to the merozoite surface and gets internalized during invasion (Blackman and Holder, 1992; Blackman et al., 1991) (**Fig. 1.6**).

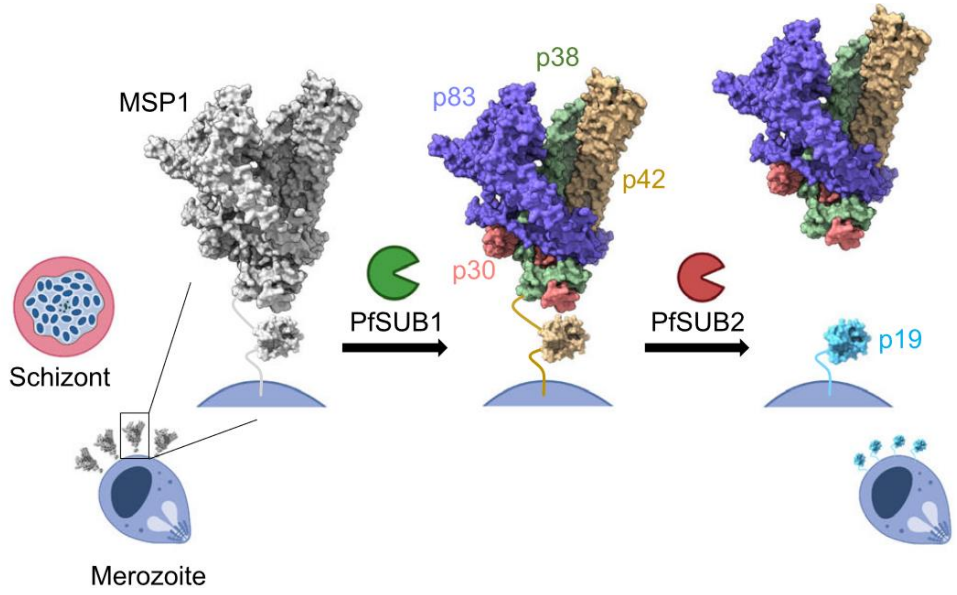

Figure 1.6: Maturation and processing of MSP1.
MSP1 is expressed as a large precursor (grey) in late stage schizonts which is tethered to the merozoite surface via a GPI-anchor. Before egress, MSP1 gets cleaved by the serine protease PfSUB1 resulting into 4 subunits (p83, p30, p38 and p42) that remain non-covalently attached. During invasion, PfSUB2 cleaves the MSP1 complex resulting into shedding of the p83, p30, p38 and p33 subunit while p19 remains attached to the merozoite surface and is carried into the erythrocyte. The figure was adopted from Patel et al., 2022.

1.5.3 MSP1 structure

The structural information of MSP1 has primarily focussed on the C-terminal p19 subunit due to the flexibility of the N-terminal domain and the size of the full-length protein which hampered the production of high-quality crystals of $MSP1_{FL}$. Early NMR spectroscopy and X-ray, analysis revealed the presence of two epidermal growth factor (EGF)-like domains within p19 (Chitarra

et al., 1999; Morgan et al., 1999; Pizarro et al., 2003). All studies identified highly conserved disulphide-bonds that connect and stabilize the two EGF domains which partially explains the high sequence homology of p19 among *Plasmodium* species. Another study investigated the interactions of the primary processing subunits with each other showing that the integral p30 domain interacts with all subunits, while N-terminal p83 associates only with p30 (Kauth et al., 2003). Furthermore, it was shown that p38 and C-terminal p42 interact with p30 and with each other (Kauth et al., 2003). More recently, structural analysis of full-length MSP1 revealed a high degree of intrinsic flexibility especially in the N-terminal wing domain of p83 (Dijkman et al., 2021) which is suggested to support interactions with other merozoite proteins (Kauth et al., 2003). Moreover, it was shown that MSP1 persists in a monomer-dimer equilibrium (**Fig. 1.7**) that was dependent on the presence of spectrin proteins of erythrocytes (Dijkman et al., 2021) which supports previous observations of MSP1 dimerization in cross-linking studies of detergent resistant schizonts (Sanders et al., 2007).

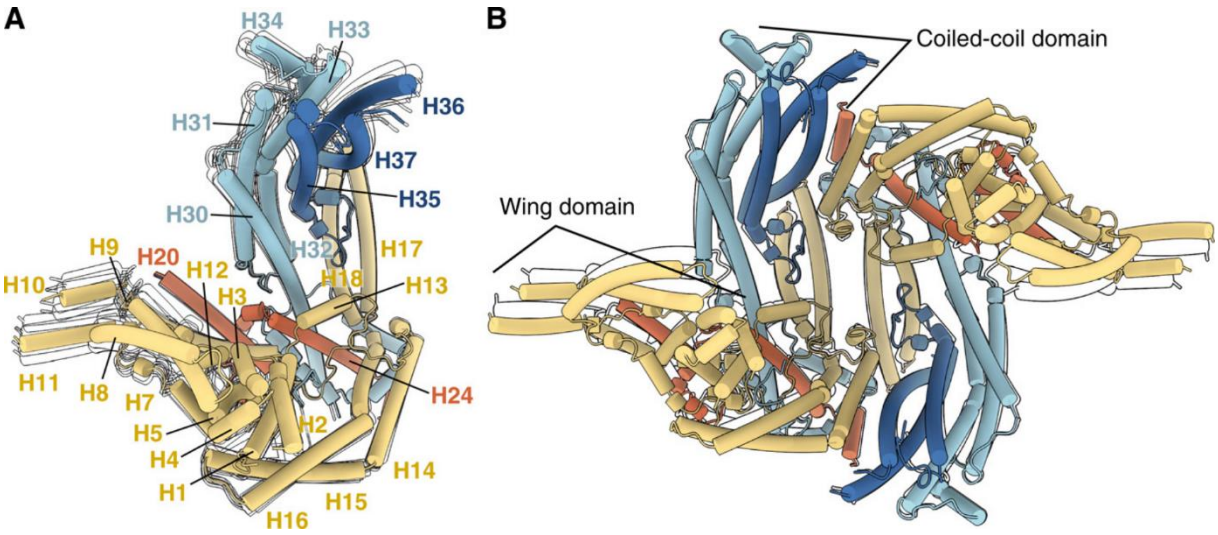

Figure 1.7: Conformation of MSP1.
(**A**) monomeric form and (**B**) dimeric form of $MSP1_{FL}$. The p83 subunit is highlighted in yellow, p30 in orange, p38 in light blue and p42 in dark blue. H, α-helices. The figure was adopted from Dijkman et al., 2021.

1.5.4 MSP1 function

Although MSP1 has been extensively studied, the precise mechanisms of the protein are still not fully known. Gene targeting studies have shown that full-length MSP1 was refractory to deletion which suggests that the protein is essential for the parasite development and survival (Combe et al., 2009; Drew et al., 2004; O'Donnell et al., 2001). Several interaction partners of MSP1 have been identified, including several peripheral merozoite surface proteins (MSP3, 6, 7 and 9) and other members of the MSP3 family, i.e., MSPDBL1 and MSPDBL2, that harbour

the cysteine-rich Duffy binding-like (DBL) domain. Both MSPDBL1 and MSPDBL2 have been shown to interact with the surface of erythrocytes via their DBL domain (Hodder et al., 2012; Lin et al., 2014; Wickramarachchi et al., 2009) which suggests a role of those proteins in merozoite invasion; however, their receptors have not yet been identified. Interestingly the individual peripheral surface proteins associate with MSP1 independently leading to formation of several macromolecular complexes (Lin et al., 2016). Of these, MSP1-complexes with either MSP6, MSPDBL1 and MSPDBL2 associate with the erythrocyte surface (Lin et al., 2016). Together this shows that MSP1 works as an anchoring platform for other peripheral merozoite surface proteins which is critical for the initial contact with the host cell and thus merozoite invasion. MSP1 also interacts with surface receptors of erythrocytes on its own such as glycophorin A (GYPA) (Baldwin et al., 2015), heparin-like molecules (Boyle et al., 2010) and band 3, also known as anion exchanger 1 (AE1) (Goel et al., 2003; Li et al., 2004) which has been shown to be essential for invasion (Baldwin et al., 2015).

Furthermore, there is increasing evidence that MSP1 plays also a critical role in merozoite egress. The primary processing by PfSUB1 modifies the structure of the MSP1 complex promoting MSP1 binding to heparin and spectrin of the erythrocyte cytoskeleton (Das et al., 2015). This interaction is proposed to cause internal shear forces that promote rupture of the erythrocyte membrane leading to merozoite release (Das et al., 2015). This activity is highly dependent on the proteolytical modification of MSP1 by PfSUB1 as demonstrated by defects in egress of MSP1 mutants refractory to PfSUB1 processing (Child et al., 2010; Das et al., 2015; Yeoh et al., 2007).

1.5.5 Immunity to MSP1

1.5.5.1 Humoral immunity

The role of antibodies against MSP1 for naturally acquired immunity has been debated for a long time but sero-epidemiological evidence is still conflicting. Numerous studies have demonstrated that antibody responses against specific regions of MSP1 are associated with protection from malaria such as the polymorphic block 2 within the N-terminal p83 domain (Cavanagh et al., 2004; Conway et al., 2000; Polley et al., 2003) as well as the conserved C-terminal p19 subunit (al-Yaman et al., 1996; Branch et al., 1998; Egan et al., 1996; Perraut et al., 2005; Stanisic et al., 2009); however, other studies could not confirm those results (Dodoo et al., 1999; Nebie et al., 2008; Osier et al., 2008). Moreover, a systematic review of those cohort studies revealed that only antibody responses against p19 were correlated with protection (Fowkes et al., 2010).

Despite the conflicting data, several immunological studies have shown that MSP1 might be targeted by the immune system in several ways. First, multiple epitopes distributed across the whole MSP1 complex have been shown to induce antibodies that inhibit parasite invasion and growth *in vitro* including regions within p19 (Blackman et al., 1990; Egan et al., 1996; O'Donnell et al., 2001; Woehlbier et al., 2006), p83 (Lin et al., 2016; Woehlbier et al., 2006) as well as central p38 and p30 (Woehlbier et al., 2006). Some of those neutralizing antibodies interfered with processing of MSP1 (Das et al., 2015; Guevara Patiño et al., 1997) and complex formation with other peripheral merozoite surface proteins (Lin et al., 2016) which suggests that neutralizing antibodies can on the one hand block receptor-ligand interactions and on the other hand interfere with MSP1 maturation.

Apart from Fab-mediated neutralization, antibodies directed against p19 have been demonstrated to induce a range of Fc-mediated effector functions including complement fixation (AbC') (Boyle et al., 2015; Reiling et al., 2019), opsonic phagocytosis (OPA) activity of monocytes (Kana et al., 2019) and respiratory burst of neutrophils (ADRB) (Joos et al., 2015). The p19-specific AbC' and OPA activity was significantly associated with a reduced risk from malaria in independent cohort studies (Kana et al., 2019; Reiling et al., 2019). Additionally, antibodies against p83 elicited strong antibody-dependent respiratory burst (ADRB) activity (Jäschke et al., 2017) and reduced parasite growth by ADCI (Galamo et al., 2009).

1.5.5.2 Cellular immunity

Since MSP1 is also expressed at late liver stages (Szarfman et al., 1988; Tarun et al., 2008), studies have shown that MSP1 is a target of cellular, particular $CD4^+$ and $CD8^+$, immune responses. Immunization of mice with p42 delivered via the AdHu5-MVA system induced $CD4^+$ and $CD8^+$ responses that resulted in enhanced survival following sporozoite challenge in part due to secretion of the effector cytokine IFNγ (Draper et al., 2009).

Moreover, mass spectrometry identified several epitopes for the HLA haplotype A0201 within full-length MSP1 that could promote a $CD8^+$ response (Carralot et al., 2008; Jäschke 2017, PhD thesis) in humans. Notably, IFNγ secretion of T cells in response to MSP1 peptides in humans living in malaria endemic regions increased with age (Chelimo et al., 2011; Chelimo et al., 2003) and was associated with reduced parasitemia (Bowman et al., 2016) and a prolonged time of malaria (re)infections (Moormann et al., 2013).

1.5.6 MSP1 as a vaccine candidate

MSP1 has been considered as a blood stage vaccine candidate for many years and pre-clinical immunization experiments in animals have demonstrated protective but variable efficacies. Immunization of mice with either full-length MSP1 from parasite extracts or recombinant C-terminal p19/p42 proteins resulted in protection from homologues challenge with *P.yoelii* (Daly and Long, 1995; Hirunpetcharat et al., 1997; Holder and Freeman, 1981; Rénia et al., 1997; Tian et al., 1997). Similarly, immunization with native full-length MSP1 isolated from parasite cultures resulted in complete protection from malaria challenge in *Aotus* and *Saimiri* monkeys (Etlinger et al., 1991; Perrin et al., 1984; Siddiqui et al., 1987) while vaccinations with subunits mediated only partial protection (Cavanagh et al., 2014; Etlinger et al., 1991; Herrera et al., 1990; Kumar et al., 1995).

Clinical trials in humans focused on the C-terminal p19 or p42 subunits (**Tab. 1.3**); however, most of them were eliminated after phase I trials due to the lack of safety (Keitel et al., 1999), low immunogenicity (Chitnis et al., 2015), lack of neutralizing antibodies (Chitnis et al., 2015; Malkin et al., 2007) or unknown reasons (Ellis et al., 2010; Ellis et al., 2012). Three MSP1-based vaccines were tested in phase II clinical trials. Despite showing promising results phase I trials, immunization with the Combination B vaccine (Genton et al., 2000; Saul et al., 1999) comprised of N-terminal MSP1 block 3, full length 3D7 MSP2 and parts of ring infected erythrocyte surface antigen (RESA) induced strain-specific immunity (Genton et al., 2002). The FMP1 vaccine based on p42 of the 3D7 strain, was highly immunogenic in malaria-naïve adults (Ockenhouse et al., 2006) and malaria-exposed adults (Stoute et al., 2007; Thera et al., 2006) and children (Withers et al., 2006) but failed to confer protection from clinical disease in Kenyan children (Ogutu et al., 2009). The delivery of MSP1 fragments including p42 (Sheehy et al., 2011) together with AMA1 using the ChAd63-MVA delivery approach induced strong T cell responses but no neutralizing antibodies and failed to protect malaria- naïve adults after CHMI (Sheehy et al., 2012). Although the lack of efficacy of MSP1-based vaccines is not completely understood, strain-specific responses as well as the lack of functional antibodies are considered as major causes responsible for vaccine failure (Beeson et al., 2016).

Recently, a phase Ia trial in malaria-naïve adults with full-length MSP1 (3D7 strain) formulated with the GLA-SE adjuvant (SumayaVac1) was safe and induced high levels of cross-reactive antibodies that fixed the first component of the classical complement cascade (C1q) and induced respiratory burst of neutrophils (Blank et al., 2020). Furthermore, immunization could recall T cell memory response measured by IFNγ secretion.

Table 1.3: List of clinical trials with MSP1-based vaccines.

Vaccine	Constructs	Phase	Population	Dosage	Outcome	Ref.
Combination-B	Block 3 of KI MSP1 (KI), full-length MSP2 (3D7), 70% of RESA (FCQ-27)	I	Malaria-naive adults, Australia	4 µg of each antigen (2x) (n=12) 13.3.µg of each antigen (2x) (n=12) 50 µg of each antigen+20 µg boost (n=12)	No antigenic competition, Weak antibody responses, Cellular immune responses	1
Combination-B	Block 3 of KI MSP1 (KI), full-length MSP2 (3D7), 70% of RESA (FCQ-27)	I	Malaria-exposed adults, PNG (18-50 yr.)	15 µg of each antigen (2x) (n=10)	Cellular immune responses, only antibody responses against MSP1	2
Combination-B	Block 3 of KI MSP1 (KI), full-length MSP2 (3D7), 70% of RESA (FCQ-27)	II	Malaria-naive adults, USA (39-61 yr. and 19-27 yr.)	13 µg of each antigeng (2x) (n=8) 13 µg of each antigen (2x and 2 weeks after group 1) (n=9)	Low antibody responses, Strong T-cell responses, No GIA activity	3
Combination-B	Block 3 of KI MSP1, full length 3D7 MSP2, 70%I of FCQ-27 RESA	I-II	Malaria-exposed children, PNG (5-9yr)	15 µg of antigens (2x) (n=30) w. treatment 15 µg of antigens (2x) (n=30) w.o treatment	62% reduced parasite densities, Lower prevalence of 3D7 parasites, but more FC27 parasites %	4
p19	p19 (3D7 or FVO) fused to Tetanus toxoid epitopes	Ia	Malaria-naive adults, USA (18-45 yr)	20 µg (n=16), 200 µg (n=24)	Hyper sensitivity reactions, Poorly immunogenic	5
p42	3D7 or FVO of p42 external domain of p42	I	Malaria-naive adults, USA (18-48 yr.)	5 µg (FVO, n=10 3D7; n=10), 20 µg (FVO, n=10; 3D7, n=10), 80 µg (FVO, n=10; 3D7, n=10)	High sero-conversion, Cross-reactivity of antibodies, Strongest response against p19, Antibodies against parasites (IFA), little GIA activity	6
FMP1	p42 (3D7)	I	Malaria-exposed adults, Kenya	50 µg (3x) (n=20)	Immunization boosted baseline titers	7
FMP1	p42 (3D7)	I	Malaria-naive adults, (18-55 yr)	10 µg (3x) (n= 5), 25 µg (3x) (n=5) 50 µg (3x) (n=5)	Anti-p42 titers increased with dose, Higher reactivity against homologues MSP1, Low cellular immune responses, Moderate GIA activity	8
FMP1	p42 (3D7)	I	Malaria-exposed children, Kenya (12-47 mo.)	10 µg (3x) (n= 30), 25 µg (3x) (n=30) 50 µg (3x) (n=30) cohorts	Anti-p42 titers above baseline, Antibody titers remained over basline, over 1 year	9

Vaccine	Constructs	Phase	Population	Dosage	Outcome	Ref.
FMP1	p42 (3D7)	I	Malaria-exposed adults, Mali (18-55 yr.)	50 µg (3x) (n=20)	Antibody titers against p42, Cross-reactive antibody responses	10
FMP1	p42 (3D7)	II	Malaria-exposed children, Kenya (12-47 mo.)	50 µg (3x) (n=195)	5.1% efficacy, high p42 titers but waned over time	11
ChAd63-MVA MSP1	MSP1 insert consisting of block 1,3,5,12 Wellcome p33 and p19 MAD20 p33, MAD20 p19	I	Malaria-naive adults, UK (19-30yr.)	$5x10^9$ viral particels CHAd63 (group1, N=6), 4 of group 1+5 $x10^8$ pfu MVA MSP1 $5x10^{10}$ viral particles ChAd63 (group2, n=10), 8 of group 2+$5x10^8$ pfu MVA MSP1	Strong T-cell responses, Cross-reactive antibodies, Antibodies against perasites (IFA), No GIA activity	12
ChAd63-MVA vaccines	ChAd63-MVA MSP1 AMA1 (3D7 and FVO), Fusion of ME and TRAP	II	Malaria-naive adults, UK (18-50 yr.)	Chad63 MSP1+MVA MSP1 (n=10), Chad63 AMA1+MVA AMA1 (n=9), ChAd63 MSP1+AMA1 with MVA MSP1+AMA1 (n=9), Chad63 MSP1+ME-TRAP with MVA MSP1+ME-TRAP (n=10) Mosquito bite challenge after immunization	High T-cell activtity, High sero-conversion, No GIA activity, No protection	13
MSP1-42-C1	p42 (FVO and 3D7 mix)	I	Malaria-naive adults, USA (18-50 yr.)	40 µg (3x) (n=15), 40 µg +CPG (3x) (n=15), 160 µg (n=15), 160 µg+CPG (n=15)	CPG enhanced antibody repsones, No dosing effect, Moderate GIA activity	14
BSAM2	p42 (3D7 and FVO) and AMA1	I	Malaria-naive adults, USA (18-50 yr.)	40 µg (3x) (n=15), 160 µg (3x) (n=15)	Antibody titers against AMA1 and p42, High GIA activity (FVO and 3D7)	15
JAIVAC-1	PfF2 and p19 (FVO)	I	Malaria-naive adults, India (18-45 yr.)	10 µg (n=10), 25 µg (n=10), 50 µg (n=10)	Responses against PfF2 titers, No responses against p19, Antibodies against parasites (IFA), Good GIA activity in CAMP strain	16
SumayaVAC1	Full-length MSP1 (3D7)	I	Malaria-naive adults, Germany (19-57 yr.)	50 µg (n=12) , 25 µg (n=6), 150 µg (n=6)	Long lasting cross-reactive antibodies, Antibodies against parasites (IFA), No GIA activity but ADRB and AbC' Cellular immune respons	17

Table summarizes the vaccine dosage, population, and outcomes of MSP1-based clinical trials. 1 Saul et al., 1999, 2 Genton et al., 2000, 3 Lawrence et al., 2000 ,4 Genton et al., 2002, 5 Keitel et al., 1999, 6 Malkin et al., 2007, 7 Stoute et al., 2005, 8 Ockenhouse et al., 2006, 9 Withers et al., 2006, 10 Thera et al., 2006, 11 Ogutu et al., 2009, 12 Sheehy et al., 2011, 13 Sheehy et al., 2012, 14 Ellis et al., 2010, 15 Ellis et al., 2012, 16 Chitnis et al., 2015, 17 Blank et al., 2020.

2.0 STUDY AIMS AND RATIONALE

2.1 Research question

Is the *Plasmodium falciparum* full-length merozoite surface protein 1 ($MSP1_{FL}$) a promising blood stage vaccine candidate?

2.2 Study hypothesis

$MSP1_{FL}$ is a key target of antibodies that induce a range of Fc-mediated effector functions that collectively contribute to a protective immune response against malaria.

2.3 Aim of the study

To characterize functional antibodies against $MSP1_{FL}$ that have been naturally acquired or induced by vaccination.

2.3.1 Specific aims

I. Determine the importance of antibody responses and Fc-mediated effector mechanisms against $MSP1_{FL}$ for protection from malaria in a Controlled Human Malaria Infection (CHMI) study.

II. Characterize functional activity of IgG and IgM from malaria-naïve adults who received the $MSP1_{Fl}$-based vaccine, SumayaVac1.

2.4 Rationale for the study

2.4.1 Why full-length MSP1?

MSP1 is the most abundant surface protein of *Plasmodium falciparum* merozoites (Gilson et al., 2006) and plays a critical role in the lifecycle of the parasite, including invasion and egress of red blood cells (RBCs) (Baldwin et al., 2015; Das et al., 2015; Goel et al., 2003). It has long been considered as a key target of protective immunity; however, sero-epidemiological studies as well as in-human vaccine trials have focussed on small subunits of MSP1 including the conserved C- terminus and the polymorphic block 2 of the N-terminus and therefore could have missed epitopes that might be relevant for a protective immune response (Cavanagh et al.,

2004; Fowkes et al., 2010; Malkin et al., 2007; Ogutu et al., 2009; Okech et al., 2004; Sheehy et al., 2012; Wilson et al., 2011).

2.4.2 Why antibody-mediated effector functions against MSP1?

Blood stage vaccine candidates, including MSP1, have mostly been evaluated for their ability to inhibit invasion and parasite replication *in vitro* measured by the growth inhibition assay (GIA) (Dutta et al., 2003; O'Donnell et al., 2001; Woehlbier et al., 2006). Notably, previous MSP1 based vaccines that failed to induce neutralizing antibodies did not progress beyond phase I clinical trials (Chitnis et al., 2015; Malkin et al., 2007); however, GIA activity has not been a accurate predictor of protection in studies on naturally acquired (Dent et al., 2008; Duncan et al., 2012; McCallum et al., 2008; Perraut et al., 2005) and vaccine-induced immunity (Laurens et al., 2017; Miura et al., 2008). Recent independent studies have shown that Fc-mediated effector mechanisms are strong correlates of protection from malaria including the recruitment of complement factors (Boyle et al., 2015), monocytes (Hill et al., 2013; Musasia et al., 2022; Osier et al., 2014a), neutrophils (Joos et al., 2010) and NK cells (Odera et al., 2021). Furthermore, we and others showed that Fc-mediated effector functions were even better correlates compared to neutralization (Nkumama et al., 2022; Reiling et al., 2019). When we investigated the whole set of Fc-mediated effector functions against merozoites we showed that the combination of functions was stronger correlated with protection than individual effector functions (Nkumama et al., 2022) supporting the concept that multifunctional antibodies contribute to a protective anti-malarial response. This suggests that previous vaccine trials as well as sero-epidemiological studies addressed the functional relevance of MSP1 sub-optimally.

2.4.3 Why study anti-MSP1 antibodies in semi-immune individuals?

Epidemiological observations have shown that humans acquire immunity with age and following repeated infections with *Plasmodium falciparum* parasites (Marsh and Kinyanjui, 2006). Consequently, adults are relatively well protected from severe malaria symptoms and can control parasite densities while young children are the most vulnerable group to severe malaria and mortality. We previously conducted a controlled human malaria infection (CHMI) study with adults that were recruited from areas with different malaria transmission intensities in Kenya and subsequently different levels of NAI. Serological analysis of the CHMI samples against >100 *P.f.* merozoite antigens using the KILchip microarray platform (Kamuyu et al., 2018) identified a list of antigens that might be important targets of NAI, including $MSP1_{FL}$ (Nkumama 2021, PhD thesis).

2.4.4 Why study anti-MSP1 antibodies in vaccinees?

Between 2017-2018, a human single-centre, randomized, double-blind, placebo and adjuvant-controlled, dose escalation phase Ia clinical trial with $MSP1_{FL}$ formulated with GLA-SE (SumayaVac1) was conducted in malaria-naïve adults from Germany. The vaccine was safe, well-tolerated and immunogenic (Blank et al., 2020).

3.0 MATERIALS AND METHODS

3.1 Materials

3.1.1 Laboratory equipment

Equipment	Source
Autoclave	Systec GmbH, Göttingen, Germany
Centrifuge, J2-MC	Beckmann, Krefeld, Germany
Centrifuge, Megafuge 16R	Heraeus Instruments, Hanau, Germany
Centrifuge, Pico 17	Heraeus Instruments, Hanau, Germany
Centrifuge, RC5B Plus	Sorvall, Schwerte, Germany
Centrifuge, 5425R	Eppendorf, Germany
Cytation™ 3 Cell Imaging Multi-Mode Reader	BioTek, Bad Friedrichshall, Germany
Electrophoresis Power Supply EV245	Sigma-Aldrich, MO, USA
FACS Canto II flow cytometer	Becton Dickinson, Heidelberg, Germany
Freezer -20 C° comfort	Liebherr International, Germany
Freezer -80 °C	Ewald GmbH, Biberbach an der Riss, Germany
Fridge	Thermo Fisher Scientific, Karlsruhe, Germany

Gel Electrophoresis System EasyPhor	Biozym, Hessisch Oldendorf, Germany
Heating block	VWR International GmbH, Darmstadt, Germany
Ice machine	AF30 Scotsman, Vernon Hills, IL, USA
Incubator CO2, BBD6620	Heraeus-Instruments, Hanau, Germany
Incubator, Cell Star cyptoperm 2	Heraeus Instruments, Hanau, Germany
Innova 4000 Incubator shaker	Fisher Scientific, Schwerte Germany
Laminar Flow Cell culture hood, Hera safe	Heraeus-Instruments, Hanau, Germany
Light microscope, Primo Star	Axiolab Zeiss, Jena, Germany
Liquid nitrogen tank	Taylor-Wharton, USA
MACS, Quadro	Miltenyi Biotec, USA
Magnetic Stirrer	VWR International GmbH, Darmstadt, Germany
Microplate Washer ELx405™ Select Deep-Well	BioTek, Bad Friedrichshall, Germany
Multi-channel pipettes (P10, P100 and P300)	Thermo Fisher Scientific, Karlsruhe, Germany
pH meter, Five Easy	Mettler-Toledo GmbH, Gießen, Germany
Pipette aid, Hirschmann Pipetus Akku	Hirschmann, Labortechnik, Eberstadt, Germany
Precision balance EG 2200-2NM	Kern EG, Balingen, Germany

Precision balance Quintix64-1S	Sartorius, Göttingen, Germany
Protein Electrophoresis system Mighty Small II	Hoefer, Inc., Holliston, MA, USA
Roll mixer RS-TR05	Phoenix Instrument, Garbsen Germany
Scanner, perfection V39	Epson, Meerbusch, Germany
Water bath AQUAline AL12	Lauda, Delran, USA
Vortex Genie 2	Scientific Industries, Bohemia, USA

3.1.2 Software programs

Software	**Source**
BD FACS Diva Version 11	Becton, Dickinson and Company (BD), USA
Biorender (Web-based illustrator)	Biorender.com
FlowJo version 10	FlowJo, Becton, Dickinson and Company (BD), USA
Gen 5 3.02	Thermo Fisher Scientific, Karlsruhe, Germany
GraphPad Prism version 8.0	GraphPad software, San Diego, USA
Microsoft office 365 Proplus	Microsoft corporation, Washington, USA
STATA version 15.1	StataCorp, Texas, USA

3.1.3 Consumables

Consumable	Source
Acrodisc 1.2µm pore size filter	Pall, Deutschland GmbH, Dreieich, Germany
Amicon Ultra Centrifugal Filters, 10kD	Merck Millipore GmbH, Schwalbach, Germany
BD Falcon Round bottom tubes 5 ml	Becton Dickinson, Heidelberg, Germany
Centrifugation tubes (14ml)	Greiner Bio-One, Frickenhausen, Germany
Cryotubes (1.5ml)	Thermo Fisher Scientific, MA, USA
Culture dishes	Greiner Bio-One, Frickenhausen, Germany
Disposable Pipette tps	Gilson, Heidelberg, Germany
Eppendorf (1.5ml, 2ml) tubes	Neolab, Heidelberg, Germany
Falcon (15ml and 50ml) tubes	Greiner Bio-One, Frickenhausen, Germany
Filter cap cell culture flasks (T25, T75 and T175)	Greiner Bio-One, Frickenhausen, Germany
Filters 0.2µm pore size	Grainer Bio-One, Frickenhausen, Germany
Filters Stericup® quick release (0.22µm)	Merck, Darmstadt, Germany
Haemocytometer	Neolab, Heidelberg, Germany
Heparin Vacutainers	Sarstedt, Germany

Immunolon 4HBX maxi-sorb 96-well ELISA plates	Thermo Fisher Scientific, MA, USA
Latex gloves	VWR International GmbH, Darmstadt, Germany
LS columns for MACS	Miltenyi Biotec GmbH, Germany
Microscope glass slides	Paul Marienfeld GmbH, Lauda, Germany
Opaque 96 well white LUMITRAC F-bottom plates	Greiner Bio-One, Frickenhausen, Germany
Pasteur pipettes, sterile & disposable	Roth, Karlsruhe, Germany
Polypropylene columns (5ml)	Qiagen, Hilden, Germany
Polystrene round-bottom tubes	Corning, Kaiserslautern, Germany
Reagent reservoirs	Sigma-Aldrich, Darmstadt, Germany
Serological pipettes (1ml, 2ml, 5ml, 10ml, 25ml and 50ml)	Greiner Bio-One, Frickenhausen, Germany
Sterile Erlenmeyer flask (125ml, 250ml and 500ml)	Corning, Kaiserslautern, Germany
Sterile U-bottom 96 well plates	Thermo Fisher Scientific, MA, USA
Sterile F-bottom 96 well plates	Grainer Bio-One, Frickenhausen, Germany
Sterile V-bottom 96 well plates	Grainer Bio-One, Frickenhausen, Germany
Syringes (10ml, 20ml and 50ml)	Greiner Bio-One, Frickenhausen, Germany

3.1.4 Chemicals and reagents

Chemical/reagent	Source
Absolute ethanol	VWR International GmbH, Darmstadt, Germany
Acetic acid	Merck, Darmstadt, Germany
Acrylamide (30%)	Roth, Karlsruhe, Germany
Agar Bacteriology grade	AppliChem, Darmstadt, Germany
AlbuMAX™ I	Thermo Fisher Scientific, MA, USA
Borate buffer	Polysciences, Inc., Hirschberg, Germany
Bovine Serum Albumin (BSA)	Sigma-Aldrich, Taufkrichen, Germany
Brefeldin A (BFA)	Sigma-Aldrich, Taufkirchen, Germany
Brilliant blue G250	Roth, Karlsruhe, Germany
Casein in PBS (1% w/v)	Thermo Fisher Scientific, MA, USA
Casein sodium salt from bovine milk	Sigma-Aldrich, Taufkirchen, Germany
CellFIX™	Becton Dickinson, Heidelberg, Germany
CNBr-activated Sepharose® 4B	Merck, Darmstadt, Germany
Compensation beads anti-mouse Ig, κ	Becton Dickinson, Heidelberg, Germany

Compensation beads negative control	Becton Dickinson, Heidelberg, Germany
Complement C1q, Human	Calbiochem, Germany
Cytochalasin D	Sigma-Aldrich, Taufkirchen, Germany
Dextran	Carl Roth, Karlsruhe, Germany
D-(+)Glucose	Sigma-Aldrich, Taufkirchen, Germany
Dimethyl sulfoxide (DMSO)	Thermo Fisher, MA, USA
Disodium hydrogen phosphate	AppliChem, Darmstadt, Germany
DL-1.4-Dithiothreitol (DTT)	Carl Roth, Kalrsruhe, Germany
Dolbecco's phosphate buffered saline	Merck, Darmstadt, Germany
EDTA disodium salt (0.1mol/l)	Thermo Fisher Scientific, Hampton, USA
Expi293™ Expression medium	Gibco, Bleiswijk, Netherlands
FACS Clean solution	Becton Dickinson, Heidelberg, Germany
FACSDiva™ CS&T research beads	Becton Dickinson, Heidelberg, Germany
FACS Flow solution	Becton Dickinson, Heidelberg, Germany
FACS Rinse solution	Becton Dickinson, Heidelberg, Germany
FACS Shutdown solution	Becton Dickinson, Heidelberg, Germany

Fetal Bovine Serum, heat inactivated	Invitrogen, Karlsruhe, Germany
Fluoresbrite™ Polychromatic red 1.0 microspheres	Polysciences, Inc., Hirschberg, Germany
Formaldehyde solution (36.5%-38% in H_2O)	Sigma, St. Louis, USA
Glycerol (99%)	Sigma-Aldrich, Taufkirchen, Germany
Histopaque®-1077	Sigma-Aldrich, Taufkirchen, Germany
Hanks' balanced salt solution	Thermo Fisher Scientific, MA, USA
Hydrochloric acid, 1M	Sigma-Aldrich, Taufkirchen, Germany
Hypoxanthin	Sigma-Aldrich, Taufkirchen, Germany
Immerson oil (518 C)	Waldeck GmbH & Co KG, Münster, Germany
Imidazole	Merck, Darmstadt, Germany
Ionomycin calcium salt	Sigma, Taufkirchen, Germany
Luria-Bertani (LB) broth	Sigma, Taufkirchen, Germany
Luminol	Sigma, Taufkirchen, Germany
Methanol	VWR International GmbH, Darmstadt, Germany
Monensin	Sigma, Taufkirchen, Germany
Nickel (II) chloride hexahydrate	Fluka analytical, Seelze, Germany

Ni-NTA agarose	Invitrogen, Karlsruhe, Germany
OPD peroxidase substrate tablets	Sigma, Taufkirchen, Germany
Opti-MEM® I medium	Gibco, Bleiswijk, Netherlands
Penicillin – Streptomycin (Pen/Strep)	Invitrogen, Karlsruhe, Germany
p-Nitrophenylphosphate (pNPP) tablets	Sigma Aldrich, UK
PermWash	Becton Dickinson, Heidelberg, Germany
Powdered milk	Roth, Karlsruhe, Germany
Potassium chloride	AppliChem, Darmstadt, Germany
Potassium dihydrogen phosphate	Roth, Karlsruhe, Germany
Quick start bovine serum albumin standard	Bio Rad, Hercules, USA
Quick start Bradford 1x dye reagent	Bio Rad, Hercules, USA
RPMI 1640-Medium	Gibco, Bleiswijk, Netherlands
SIGMA FAST OPD tablets	Sigma-Aldrich, Taufkirchen, Germany
SOC medium	Thermo Fisher Scientific, Waltham, USA
Sodium azide	Sigma-Aldrich, Taufkirchen, Germany
Sodium dihydrogen phosphate	Grüssing, Germany

Sodium hydroxide >98%	Roth, Karlsruhe, Germany
Sodium chloride	Sigma-Aldrich, Taufkirchen, Germany
TEMED	Carl Roth, Karlsruhe, Germany
Tween 20	Carl Roth, Karlsruhe, Germany

3.1.5 Antibodies and dyes

Antibodies/dyes	**Source**
CellTrace™ Far red	Invitrogen Carlsbad, USA
Donkey anti-human IgG-Fcγ -specific Alexafluor647 antibody	Jackson ImmunoResearch, UK
Goat anti-human IgM HRP conjugate antibody	Thermo Fisher Scientific, MA, USA
Human plasma from German adults	Bloodbank Heidelberg, Germany
Human plasma from Kenyan adults	KEMRI-Wellcome Trust Research Programme, Kenya
Mouse anti-human CD107a-PE antibody	Becton, Dickinson (BD), Germany
Mouse anti-human CD235a-APC antibody	Becton, Dickinson (BD), Germany
Mouse anti-human CD3-PE-Cy5 antibody	Becton, Dickinson (BD), Germany
Mouse anti-human CD56-APC antibody	Becton, Dickinson (BD), Germany

Mouse anti-human IFNγ-PE-Cy7 antibody	Becton, Dickinson (BD), Germany
HRP-conjugated sheep anti-human IgG1 antibody	The Binding Site GmbH, Germany
HRP-conjugated sheep anti-human IgG2 antibody	The Binding Site GmbH, Germany
HRP-conjugated sheep anti-human IgG3 antibody	The Binding Site GmbH, Germany
HRP-conjugated sheep anti-human IgG4 antibody	The Binding Site GmbH, Germany
Purified IgG from immunized German adults	Sumaya-Biotech, Heidelberg, Germany
Purified IgG from Kenyan adults (WHO)	NIBSC code: 10/198 (Bryan D, 2014)
Purified IgM from immunized German adults	Sumaya-Biotech, Heidelberg, Germany
Purified human IgG from Malawian adults (MIG)	KEMRI-Wellcome Trust Research Programm, Kenya
Rabbit anti-Human IgG-HRP	Agilent, CA, USA
Sheep anti-human C1q, HRP conjugate	Abcam, MA USA
SYBR green nucleic acid dye	Thermo Fisher, MA, USA
Trypan blue	Carl Roth, Karlsruhe
Viability dye, Live/dead-FITC stain antibody	Becton, Dickinson (BD), USA

3.1.6 Kits

Kits	Source
ExpiFectamine™ 293 Transfection kit	Gibco, Bleiswijk, Netherlands
Giemsa staining Ral DIFF-Quick kit	Ral Diagnostics, Sinsheim
MicroVue Complement iC3b EIA kit	Quidel, San Diego, USA
MicroVue Complement Sc5b-9 Plus EIA kit	San Diego, USA
NK cell negative isolation kit	Miltenyi Biotec, Aubum, USA
Pan monocyte isolation Kit	Miltenyi Biotec, Aubum, USA
Plasmid mini kit	Qiagen, Hilden, Germany
Plasmid midi kit	Qiagen, Hilden, Germany

3.1.7 Buffers, media and solutions

Buffer/Solution	Composition
<u>General use</u>	
10X Phosphate buffered saline (PBS)	1.4 M NaCl + 27 mM KCl + 100 mM Na_2HPO_4 + 18 mM K_2HPO_4, pH 7.4
1X PBS	100ml 10x PBS + 900ml distilled, deionised water (ddH_2O)

2% Paraformaldehyde (PFA)	2% (v/v) PFA in 1 x PBS

Plasmodium falciparum culture

culture medium	RPMI 1640 (500 ml) + 2mM L-Glutamine + 25 mM HEPES + 0.1 mM Hypoxanthine + 20 µg/ml Gentamycin + 0.25% (w/v) AlbuMax I
D-sorbitol solution	5% (w/v) D-sorbitol dissolved in ddH_2O
Freezing solution	56% (v/v) Glycerol + 3% (w/v) D-sorbitol + 0.65% (w/v) NaCl
Thawing solutions	12% (w/v) NaCl in ddH_2O 1.6% (w/v) NaCl in ddH_2O 0.9% (w/v) NaCl in ddH_2O + 0.2% (w/v) D-glucose in ddH_2O

Protein purification

5X Native purification buffer	250mM NaH_2PO_4 + 2.5M NaCl in ddH_2O, pH 8.0
1X Native purification buffer	100ml 5X native purification buffer + 400ml, in ddH_2O
Imidazole solution	3M Imidazole + 20mM sodium phosphate + 500mM NaCl in ddH_2O, pH 6.0
Native binding buffer	30ml 1 × native purification buffer + 100µl 3M Imidazole, pH 8.0
Native wash buffer	50ml 1 × native purification buffer + 335µl 3 M Imidazole, pH 8.0
Native elution buffer	13.75ml 1 × native purification buffer + 1.25ml 3M Imidazole, pH 8.0
Storage solution	0.02% NaN_3 in 1 × ddH_2O

SDS-PAGE

SDS gel (10%)	For one separating gel: 1.85ml 30% acrylamide + 1.25ml lower Tris buffer + 2.1ml ddH_2O + 10µl TEMED + 50µl 10% APS For one stacking gel: 330µl 30% acrylamide + 625µl upper Tris buffer+ 1.55ml H_2O + 5µl TEMED + 25µl 10% APS
10X SDS-PAGE running buffer	10g SDS + 30.3g Tris + 144.1g glycine in ddH_2O
4X SDS-PAGE sample buffer	8% SDS + 50% upper Tris buffer + 40% glycine + 0.08% bromphenol blue + 100 mM DTT in ddH_2O
Lower Tris	1.5 M Tris + 0.4% SDS in ddH_2O, pH 8.8
Upper Tris	0.5 M Tris + 0.4% SDS in ddH_2O, pH 6.8
Coomassie staining solution	250ml ethanol + 50ml acetic acid + 1.25g coomassie blue + 200ml ddH_2O
Destaining solution	100ml acetic acid + 200ml ethanol (96%) ad 1l ddH_2O

PfSUB1 cleavage assay

PfSUB1 buffer	50 mM Tris-HCl + 15 mM CaCl in ddH_2O pH 7.6

Antibody purification from Sera

Coupling buffer	100mM $NaHCO_3$ + 500mM NaCl in ddH_2O, pH 8.3

Quenching buffer	100mM Tris ddH_2O, pH 8.0
High pH wash buffer	100mM TRIS + 500mM NaCl in ddH_2O, pH 8.0
Low pH wash buffer	100mM NaOAc + 500mM NaCl in ddH_2O, pH 4.0
Elution buffer	0.1M Glycine in ddH_2O, pH 2.4

ELISA

Blocking buffer, depending on protocol	1% (w/v) Casein in PBS
	or 3% (w/v) skimmed milk in PBS + 0.05% Tween 20
Wash buffer	0.05% (v/v) Tween 20 in 1% PBS
Substrate solution	OPD Peroxidase substrate in ddH_2O
Stopping solution	1M Hydrochloric acid (HCl)

Opsonic phagocytosis activity (OPA) assay

FACS buffer	0.5% (w/v) BSA + 2mM EDTA + 1 × PBS
THP1/monocyte/ neutrophil culture medium	RPMI 1640 + 10mM HEPES + 2mM L-Glutamine + 1% (v/v) Penicillin-streptomycin (PenStrep) + 10% (v/v) Fetal bovine serum (FBS)

Antibody-dependent respiratory burst (ADRB) assay

Dextran solution	3% (w/v) dextran dissolved in 1 × PBS
Luminol solution	0.04mg/ml luminol dissolved in 1 × PBS
PMN buffer	0.1% (w/v) bovine serum albumin (BSA) + 1% (w/v) D -glucose + Hank's buffered salt solution (HBSS)
Lysis solution	0.2% (w/v) NaCl dissolved in ddH_2O
Lysis stop solution	1.6% (w/v) NaCl dissolved in ddH_2O

Ab-NK assay

NK cell media	RPMI 1640 medium (without HEPES) + 1% (v/v) PenStrep + 10% (v/v) FBS
Cellfix solution	1X Cellfix in ddH_2O
Permwash/Permeabilization buffer	1x Permwash in ddH_2O
FACS buffer	0.1% (w/v) BSA + 0.1% (v/v) Sodium azide (NaN_3) + 1X PBS

3.1.8 Organisms, cells and cell lines

Organisms/cells	**Source**
Human O^+ erythrocytes	Blood bank for Heidelberg University Hospital

Mammalian Expi293F cells	KEMRI-Wellcome Trust Research Programme, Kenya
One Shot™ TOP10 Chemically Competent *E. coli*	Invitrogen, Carlsbad, USA
Plasmodium falciparum 3D7 strain	KEMRI-Wellcome Trust Research Programme, Kenya
THP1 cell line	KEMRI-Wellcome Trust Research Programme, Kenya

3.1.9 Expression plasmids

Plasmid	**Source**
MSP1-bio	KEMRI-Wellcome Trust Research Programme, Kenya
MSP5-bio	KEMRI-Wellcome Trust Research Programme, Kenya
MSP11-bio	KEMRI-Wellcome Trust Research Programme, Kenya
MSPR4-bio	KEMRI-Wellcome Trust Research Programme, Kenya
PTEX-150-bio	KEMRI-Wellcome Trust Research Programme, Kenya
Pf3D7_1136200-bio	KEMRI-Wellcome Trust Research Programme, Kenya
Pf3D7_1401600-bio	KEMRI-Wellcome Trust Research Programme, Kenya
Pf3D7_1252300-bio	KEMRI-Wellcome Trust Research Programme, Kenya
Pf3D7_1345100-bio	KEMRI-Wellcome Trust Research Programme, Kenya

3.1.10 Recombinant proteins

Protein	Source
$MSP1_{FL}$ (full-length protein, 3D7 strain, *E. coli*)	BIOMEVA GmbH, Heidelberg, Germany
$MSP1_{FL}$-F (full-length protein, FCB1 strain, *E. coli*)	Prof. Michael Lanzer, Department of Infectious Diseases, Heidelberg, Germany
MSP1-p83 (3D7 strain, *E. coli*)	Prof. Michael Lanzer, Department of Infectious Diseases, Heidelberg, Germany
MSP1-p30 (3D7 strain, *E. coli*)	Prof. Michael Lanzer, Department of Infectious Diseases, Heidelberg, Germany
MSP1-p38 (3D7 strain, *E. coli*)	Prof. Michael Lanzer, Department of Infectious Diseases, Heidelberg, Germany
MSP1-p42 (3D7 strain, *E. coli*)	Prof. Michael Lanzer, Department of Infectious Diseases, Heidelberg, Germany

3.1.11 Protein markers

Protein marker	Source
Color Plus Protein Marker	New England Biolabs, MA, USA
Unstained Protein standard Broad Range 10-200 kDa	New England Biolabs, MA, USA

3.2 Study design and population

3.2.1 CHMI-SIKA study

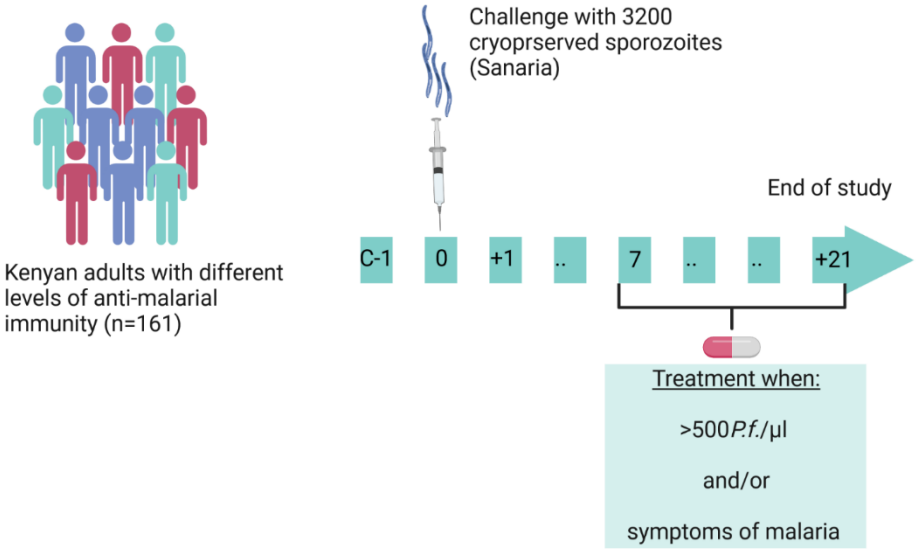

Figure 3.1: Illustration of the CHMI-SIKA study profile.
Healthy Kenyan adults (n=161) were recruited from three different regions within Kenya (Ahero, Kilifi north and Kilifi south) and challenged with viable cryopreserved sporozoites intravenously. Volunteers were monitored for blood stage parasitemia and malaria symptoms and treated with anti-malarial drugs when required. All volunteers were treated at day 21 post-challenge.

The Controlled Human Malaria Infection of Semi-Immune Kenyan Adults (CHMI-SIKA) study was performed to identify mechanisms and antibody targets that drive potent naturally acquired immunity against *Plasmodium falciparum* malaria. The study was unblinded, non-randomized and the design has been described previously (Kapulu et al., 2018). Briefly, healthy volunteers aged 18-45 years from Kenya with different antibody responses against crude schizont lysate were recruited to reflect different degrees of immunity against malaria. Volunteers who were parasite positive one day before challenge (C-1), HIV positive, pregnant, with sickle cell trait or used medications with antimalarial activity over the course of the study were excluded. A total of 161 volunteers were recruited from different malaria endemic regions in Kenya in three consecutive cohorts (2016, 2017, 2018): Ahero (high transmission intensity), Kilifi South (moderate transmission intensity), Kilifi North (low malaria transmission intensity.

A dose of 3200 cryopreserved *P. falciparum* NF54 sporozoites (Sanaria vaccine) was injected by direct venous inoculation (DVI). Venous blood was collected and monitored for blood stage parasitemia by quantitative real time PCR (qPCR) twice per day from day 7 (C+7) to day 14 (C+14), then once from day 15 (C+15) until day 21 (C+21) post challenge. If the endpoint criteria were met, the volunteers were treated with artemether-lumefantrine. Anti-malarial

treatment was given when blood stage parasite levels exceed 500 *P.f.*/µl or when volunteers exhibited clinical symptoms of malaria with detectable blood stage parasites. All volunteers were treated at day 21 post sporozoite challenge (**Fig. 3.1**).

Due to lumefantrine levels above the reported minimum inhibitory concentration in 12 volunteers and the presence of non-NF54 parasites in 7 volunteers, a total of 19 volunteers were excluded from the analysis. As a result, plasma samples from 142 volunteers collected one day before challenge (C-1) were used in this study.

3.2.2 Phase Ia clinical trial with SumayaVac1

A randomized, double-blind, placebo and adjuvant-controlled phase Ia dose-escalation study in malaria-naïve German adults (aged 19-57) was performed to test for the safety and immunogenicity of the full-length MSP1-based vaccine, SumayaVac1. The design of the study has been previously described (Blank et al., 2020). Briefly, 16 volunteers were grouped in two consecutive cohorts (**Fig. 3.2B**), with 12 receiving the vaccine and 2 receiving a placebo (0.9% NaCl) or adjuvant control (GLA-SE). In cohort 1, 12 volunteers received 50µg of the vaccine, while 6 volunteers each received the 25µg or the 150µg dosage of $MSP1_{FL}$. All vaccinees received at least 3 vaccinations (d0, d29, d58) and optionally a fourth vaccination at day 182 after unblinding (**Fig. 3.2A**). After each vaccination a safety protocol recording unsolicited adverse events and during the 6-month post-trial follow-up was created. The vaccine was safe, well-tolerated and induced high titres of functional cytophilic MSP1 antibodies (Blank et al., 2020).

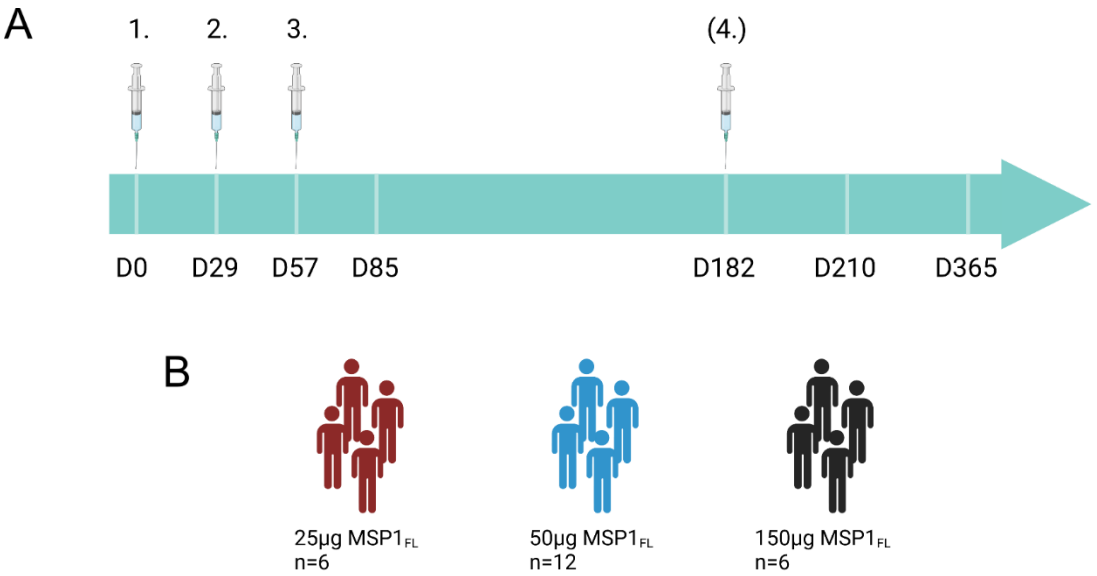

Figure 3.2: Illustration of the CHMI-SIKA study profile.
(**A**) Study participants were immunized with SumayaVac1 ($MSP1_{FL}$ with the adjuvant GLA-SE) at day 0, 29, 57 and optionally at day 182. (**B**) Volunteers received either 25µg, 50µg or 150 µg of SumayaVac1 at each immunization.

3.3 Laboratory methods

3.3.1 Parasite culture

3.3.1.1 Thawing and culturing

Plasmodium falciparum parasites (3D7 strain) were thawed in a water bath at 37°C and transferred into falcon tubes. After thawing, 1/5 volume of 12% NaCl solution was slowly added while gently mixing and incubated for 5 min at room temperature. After incubation, 9 × volume of 6% NaCl was added dropwise and incubated at room temperature for 5 min.

Afterwards, the parasite suspension was centrifuged at 800 × g for 4 min, the supernatant was discarded and the parasite pellet was carefully resuspended in 9 × volume of 0.9% NaCl. After centrifugation, the pellet was resuspended in 12ml complete parasite culture medium (500ml RPMI 1640 + 2mM L-Glutamine + 25mM HEPES with 0.1mM hypoxanthine, 0.25% AlbuMax I and 20µg/ml gentamycin), transferred into a cell culture flask, supplemented with O^+ red blood cells at 1-4% haematocrit and maintained in an incubator at an atmosphere of 5% CO2, 3 % O2, 92 % N2, 95% air humidity at 37 °C.

Parasitemia was determined by microscopy using the Giemsa staining Ral DIFF-Quick kit (Ral Diagnostics) according to manufacturer's instructions. Briefly, a thin smear on a glass slide was fixed in FIX-RAL 555 for 5 seconds, stained in EOSINE-RAL 555 and BLUE-RAL 555 for 5 seconds each. The slide was dried and parasites were counted under a microscope with 100 × magnification under oil immersion. Parasitemia was determined as: (number of infected RBCs) / (number total RBCs) × 100. Parasites were kept at 1-4% parasitemia by adding fresh erythrocytes.

3.3.1.2 Synchronisation with D-sorbitol

When the majority of parasites were ring stages, the parasite culture was transferred into a falcon tube, centrifuged at 800 × g for 4 min and the supernatant was discarded. The parasite pellet was then resuspended in sterile 5% D-sorbitol in water for 10 min at 37°C while shaking vigorously every 2-3 minutes to lyse late trophozoites and schizonts. After incubation, the culture was centrifuged at 800 × g for 4 min and the supernatant containing lysed late stages was removed. The pellet with ring stages was washed and finally resuspended in complete culture medium, transferred into a new culture flask and kept in the incubator.

3.3.1.3 Freezing of parasites

In order to freeze parasites, a culture containing high ring stage parasitemeas was transferred into falcon tubes, centrifuged at 800 × g for 4 min and the supernatant was removed. The pellet was resuspended dropwise in 1/3 volume of freezing solution (56% (v/v) Glycerol, 3% (w/v) D-Sorbitol and 0.65% (w/v) NaCl in ddH_2O) and incubated for 5 min at room temperature. Subsequently 4/3 volume of freezing solution was added dropwise while shaking and the parasite suspension was quickly transferred into cryotubes. Parasites were stored in liquid nitrogen.

3.3.2 Plasmid amplification

Plasmids encoding the codon optimized sequences for the expression of merozoite antigens were kindly provided from KEMRI-Wellcome Trust Research Programme, Kenya and are available on the plasmid respiratory Addgene (https://www.addgene.org). Chemically competent TOP10 *E. coli* cells (Invitrogen) were thawed on ice and 2µl of plasmid DNA were added to 25µl of competent cells and kept on ice for 30 min. Cells were heat-shocked at 42°C for 30 seconds in a water bath and recovered for 2 min on ice. Afterwards, 250µl SOC medium (Thermo Fisher) was added and cells were incubated for 1 h at 37°C before they were plated on LB-Agar plates supplemented with 100µg/ml ampicillin overnight at 37°C. The next day, colonies were picked, inoculated in 100ml LB-ampicillin broth and incubated overnight at 37°C at 180 rpm. Plasmids were extracted using the Plasmid midi kit (Qiagen) according to manufacturer's instructions.

3.3.3 Expression of recombinant merozoite antigens

EXP293F cells were stored at 1×10^7 cells/ml in cryotubes in liquid nitrogen. For culturing, cells were thawed rapidly in a water bath at 37°C before adding to 29ml of pre-warmed expi293 expression media in a 125ml Erlenmeyer shake flask with a vented cap. Cells were maintained at 5% CO_2 and 37°C shaking on an orbital shaker at 125 rpm. Cell counting and viability assessment was manually performed by trypan blue staining and light microscopy. When cells reached a density of 1×10^6 viable cells/ml at >90% viability, the culture was diluted to 0.3×10^6 viable cells/ml. Every 3-4 days, when cells reached a density of $3\text{-}5 \times 10^6$ viable cells/ml, cells were diluted to 0.3×10^6 viable cells/ml. For small scale transfection (30ml), 7.5×10^6 viable cells were added to 25.5ml of fresh pre-warmed expi293 expression medium. Transfection was scaled up to 60ml or 150ml depending on the expression level of the specific expression vector. For each transfection, 1mg of plasmid was used for each 1ml of transfection volume. For a 30ml transfection, 30mg of plasmid was diluted in 1.5ml Opti- Mem reduced

media and gently mixed. Next, 81ml of ExpiFectamine 293 reagent was diluted in 1.5ml of Opti-Mem reduced media, gently mixed and incubated for 5 min at room temperature. Afterwards, the two mixtures were combined and incubated for 20 min to allow complex formation. Thereafter, the ExpiFectamine 293/DNA complex was slowly added to the cells while gently swirling and the culture was incubated at 8% CO_2 and 37°C, shaking at 125 rpm. At 20 h post-transfection, 150ml of transfection enhancer 1 and 1.5ml of transfection enhancer 2 was added to get a final volume of 30ml. The culture flask was immediately returned to the shaking incubator for additional 4 days. Afterwards, the culture was centrifuged at 4000 × g for 5 min and the supernatant that contained the expressed recombinant protein was stored at 4°C.

3.3.4 Purification of secreted recombinant proteins

Hexa-histidine tagged proteins were purified using the Ni-NTA purification system. Prior to purification of recombinant proteins, 30µl of 1mM nickel chloride was added to the supernatant. Next 1ml of Ni-NTA agarose was washed with sterile distilled H_2O and equilibrated with binding buffer (50mM NaH_2PO_4, 0.5M NaCl, 10mM imidazole, pH.8.0). Thereafter, the Ni-NTA agarose was incubated with the supernatant for 1 h at room temperature while gently rotating. After incubation, the suspension was centrifuged at 800 × g for 2 min and the supernatant was removed and stored at 4°C for another round of purification. The Ni-NTA agarose was carefully placed in a purification column and washed 4 times with wash buffer (50mM NaH_2PO_4, 0.5M NaCl, 20mM imidazole, pH.8.0). After washing, the recombinant proteins were eluted in 1ml fractions using elution buffer (50mM NaH_2PO_4, 0.5M NaCl, 250mM imidazole, pH.8.0). The fractions were pooled and concentrated and using filter tubes. The concentration was measured by using the Quick start Bradford 1 × dye reagent (Bio Rad) according to manufacturer's instructions. Recombinant proteins were aliquoted and stored at -80°C for later use.

3.3.5 Polyacrylamide gel electrophoresis (SDS-Page)

Purity of expressed recombinant proteins was analysed by SDS-Page using 12% separation gels. After casting the gels. Samples containing 1-2mg of proteins were mixed with SDS-Page sample buffer (6×) containing DTT and denatured at 80°C for 10 min. After denaturation, 4µl of samples and 5µl of protein ladder were loaded onto the gel. The gel was run at 120V until the dye front migrated through the stacking gel, then the voltage was increased to 200V until the dye front reached the bottom of the separation gel. Afterwards, the gel was stained in Coomassie staining solution for 30 min while gently shaking. After staining, the gel was

incubated in destaining solution (20% (v/v) methanol, 10% (v/v) acetic acid) until the gel was visibly destained. The gel was imaged using a perfection V39 scanner (Epson).

3.3.6 PfSUB1 cleavage assay

Processing of $MSP1_{FL}$ (SumayaVac1) by PfSUB1 was performed according to a previously published protocol (Koussis et al., 2009) and was used to verify the stability of the $MSP1_{FL}$ batches that have been stored in the fridge for 4 years. Additionally, a reference batch of newly produced $MSP1_{FL}$ was used. Briefly, recombinant $MSP1_{FL}$ was reconstituted in PfSUB1 buffer (50mM Tris-HCl, 15 mM CaCl, pH 7.6) at 0.25mg/ml in a total volume of 350µl. Next, 5 units of recombinant PfSUB1 were added to the recombinant antigen, gently mixed and mixture was split to 5 aliquots of 60µl reaction volume each. A time course experiment was performed, letting the samples incubate for 0 min, 30 min, 1 h, 2 h and overnight at 37°C. After respective incubation, the samples were boiled at 80°C for 10 min, mixed with SDS sample buffer supplemented with DTT and separated using SDS-Page.

3.3.7 N-terminal Edman sequencing of MSP1 peptides after HPLC separation

N-terminal sequencing of MSP1 peptides after PfSUB1 cleavage was performed at the Proteome Factory for N-terminal Edman amino acid sequencing (Proteome Factory AG, berlin) according to the standardized operating procedure “AA-01-Edman, Edman-Sequencing”.

3.3.8 Indirect Enzyme-linked Immunosorbent Assay (ELISA)

3.3.8.1 IgG ELISA for optimal coating concentrations of recombinant merozoite antigens

A standard indirect ELISA was performed to assess immunogenicity of recombinant merozoite surface proteins. Recombinant proteins were serially diluted in phosphate buffered saline (PBS) to concentrations ranging from 30mg/ml to 0.01mg/ml and subsequently 50µl/well of the dilutions were coated onto Dynex4HBX Immunolon ELISA-plates overnight at 4°C. The next day, the plates were washed four times with 200µl/well in 1 × PBS containing 0.05% Tween 20 (PBST), then blocked with 200µl of 1% skimmed milk for 2 h at room temperature. After blocking, the plates were washed four times, followed by incubation with 50µl/well of plasma samples diluted in PBST (1:1000) for 2 h at room temperature. After incubation, unbound antibodies were removed by washing with PBST and 50µl/well of rabbit anti-human IgG horse radish peroxidase (HRP)-conjugated secondary antibodies (Agilent) diluted in blocking buffer (1:3000) were added and incubated for 1 h at room temperature. After washing, 50µl/well of

substrate solution (0.4mg/ml O-phenylenediamine (OPD), 0.4mg/ml urea hydrogen peroxide, and 0.05M phosphate-citrate, pH 5.0) was added and incubated at room temperature for 30 min protected from light. After incubation, 15µl/well of 1M hydrochloric acid (HCl) was added to stop the reaction and absorbance was read at 492nm using the BioTek Cytation 3 cell imaging multi-mode reader and Gen5 v3.02 software.

For validation of the assay, the following controls were included: 1) unopsonized recombinant antigen and 2) antigen opsonized with a pool of hyper immune sera from Kenyan adults (PHIS) or plasma samples from 5 malaria-naïve adults from Germany.

3.3.8.2 Recombinant antigen-based IgG, IgM and IgG subclass ELISA

Antibodies reactivity from CHMI-SIKA volunteers against recombinant merozoite antigens were measured using an ELISA protocol as described above with the following modifications: Recombinant antigens were diluted in PBS and 50µl/well at a concentration of 10mg/ml were coated onto Dynex4HBX Immunolon ELISA-plates overnight at 4°C. Plates were washed with PBST and incubated with 50µl of plasma samples at 1:1000 dilution. Bound antibodies were detected with HRP-conjugated secondary antibodies: rabbit anti-human IgG (Agilent), goat anti-human IgM (Thermo Fisher), and rabbit anti-human IgG1, 2,3 or 4 (The Binding Site), diluted at 1:3000 in 1% skimmed milk.

3.3.9 Mapping of linear B cell $MSP1_{FL}$ epitopes

The linear IgG epitope mapping of human plasma samples against $MSP1_{FL}$ was performed by PEPperPRINT GmbH, Heidelberg as previously described (Blank et al., 2020). The sequence of full-length MSP1 (3D7) (UniProt ID: Pf3D7_0930300) was elongated with GSGSGSG linkers at both ends to avoid truncated proteins. Subsequently, the modified amino acid sequence was converted into 15-mer amino acid peptides with a 14 amino acid overlap between the peptides. This resulted into 1,720 unique peptides that were printed in duplicates on the array that was framed by additional control peptides: HA (YPYDVPDYAG, 62 spots) and polio (KEVPALTAVETGAT, 62 spots). The chip was blocked with Rockland blocking buffer MB-070 for 30 min, followed by pre-staining with goat anti-human IgG (Fc) DyLight680 (0.1µg ml−1) and the monoclonal mouse anti-HA control antibody (12CA5) DyLight800 (0.5µg ml−1 in incubation buffer (washing buffer with 10% blocking buffer) for 45 min for controlling background signals. Next, other copies of the $MSP1_{FL}$ microarray were incubated with 40 human plasma samples from the CHMI study (1:1000 in incubation buffer) that were randomly selected for 16 h at 4°C while shaking at 140 rpm. After washing, secondary detection antibodies coupled to fluorophores were added and incubated for 45 min at room temperature.

Fluorescent signals were detected using an InnoScan 710-IR Microarray Scanner at scanning gains of 50/50 (red/green). Spot intensity quantification was based on 16-bit gray scale tiff files with higher dynamic range than the 24-bit colourized tiff files. Data analysis was performed with with PepSlide Analyzer. A maximum spot-to-spot deviation of 40% was tolerated, otherwise the intensity value was put manually to zero.

3.3.10 Antibody-dependent complement fixation (AbC') assay

3.3.10.1 C1q fixation

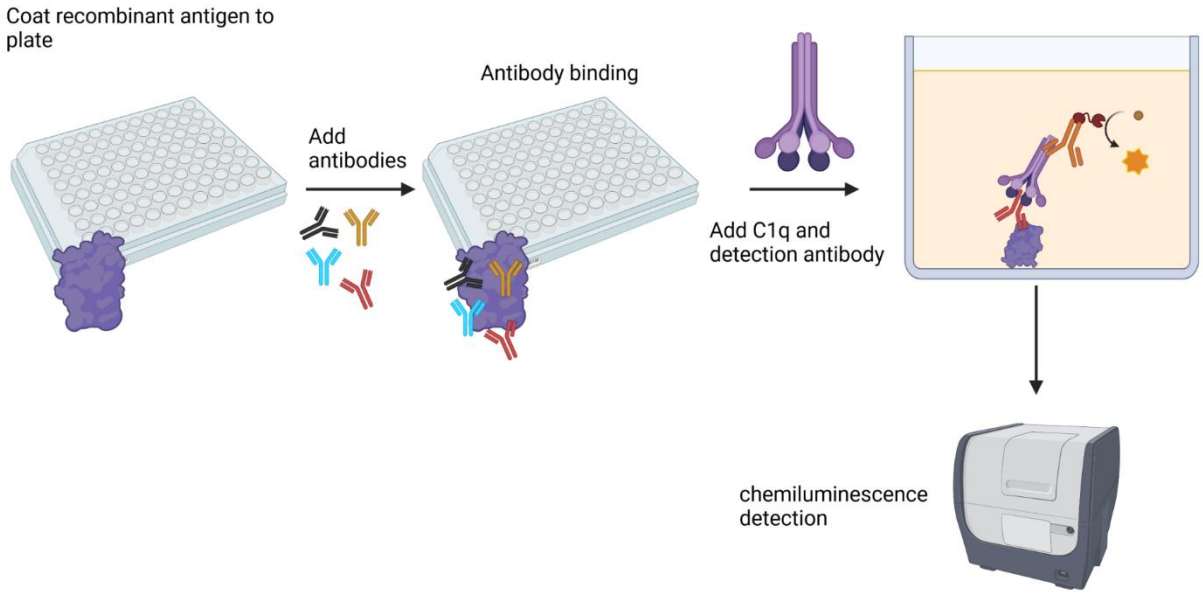

Figure 3.3: Illustration of the AbC' assay.
Recombinant antigen was immobilized on a 96 well plate and opsonized with test antibodies. Recombinant C1q was added and detected using anti-C1q secondary detection antibodies. Signal development was detected using BioTek Cytation 3 cell imaging multi-mode reader.

Fixation of C1q, the primary component of the classical complement pathway, was measured using a published protocol (Boyle et al., 2015; Reiling et al., 2019) as illustrated in **Figure 3.3**. Dynex4HBX Immunolon ELISA plates were coated with 50µl/well of recombinant proteins at 10mg/ml overnight at 4°C. The following day, plates were washed four times with 200µl/well PBST and blocked with 200µl/well of 1% Casein/PBS at 37°C for 2 h. After blocking, the plates were washed and 50µl/well of plasma samples (1:10), IgG (1mg/ml) or IgM (2mg/ml) in PBS were added for 2 h at 37°C.

Following incubation, the plates were washed four times to remove unbound antibodies. Next, 40µl/well of recombinant C1q (Abcam) at 10mg/ml diluted in 1% casein/PBS was added for 30 min at 37°C. Thereafter, the plates were washed and incubated with 50µl/well of sheep anti-human C1q HRP (Abcam) at a 1:100 dilution in 1% casein/PBS for 1 h at 37°C. After washing,

50µl/well of OPD solution was added and incubated for 45 min at room temperature before the reaction was stopped by adding 15µl of 1M HCl. The absorbance was read at 492nm using the BioTek Cytation 3 cell imaging multi-mode reader and Gen5 v3.02 software.

For validation of the assay, the following controls were included: 1) unopsonized recombinant antigen and 2) antigen opsonized with PHIS or plasma samples from 5 malaria-naïve adults from Germany. For assays using IgG samples, purified IgG from Kenyan adults (WHO reference standard, NIBSC code: 10/198) was used as a positive control.

3.3.10.2 C3b deposition

The C3b ELISA was similarly performed as the C1q fixation assay with recombinant antigens using the MicroVue Complement iC3b EIA kit (Quidel) by Dr. Richard Thomson and Kristin Fürle. Briefly, after incubation of $MSP1_{FL}$ coated plates with 50µl of either purified IgG (1mg/ml) or IgM (2mg/ml), 50µl/well of the C3b conjugate was added and incubated for 30 min at 37°C. Next, the plate was washed four times with PBST and incubated with 100µl/well substrate solution (substrate concentrate in substrate diluent, 1:20) for 30 min at room temperature in the dark. The reaction was stopped with 50µl/well stop solution (250mM oxalic acid) and the absorbance was read at 405nm using the BioTek Cytation 3 cell imaging multi-mode reader and Gen5 v3.02 software.

For assays using IgG samples, purified IgG from Kenyan adults (WHO reference standard, NIBSC code: 10/198) was used as a positive control.

3.3.10.3 C5b-9 deposition

The C3b ELISA was similarly performed as the C3 fixation assay with recombinant antigens using the MicroVue Complement Sc5b-9 Plus EIA kit (Quidel) by Dr. Richard Thomson and Kristin Fürle. Briefly, after incubation of $MSP1_{FL}$ coated plates with 50µl of either purified IgG (1mg/ml) or IgM (2mg/ml), 50µl/well of the SC5b-9 conjugate was added and incubated for 30 min at 37°C. After incubation, the plate was washed four times with PBST and incubated with 100µl/well substrate solution (peroxide substrate and 3,3',5,5'-tetramethylbenzidene (TMB)) for 15 min at room temperature in the dark. The reaction was stopped with 100µl/well stop solution (2M H_2SO_4) and the absorbance was read at 450nm using the BioTek Cytation 3 cell imaging multi-mode reader and Gen5 v3.02 software.

For assays using IgG samples, purified IgG from Kenyan adults (WHO reference standard, NIBSC code: 10/198) was used as a positive control.

3.3.11 Antibody-dependent respiratory burst (ADRB) assay

3.3.11.1 Isolation of neutrophils from healthy donors

Fresh whole blood, a volume of 50ml, from 2-3 individual healthy donors was collected in heparin vacutainer tubes. The blood was transferred into 50ml falcon tubes and mixed with hanks buffered saline solution (HBSS) in a 1:1 ratio, before it was carefully layered on top of 7ml Histopaque. The tubes were centrifuged at 600 × g for 15 min at 21°C with no break. The supernatant was carefully discarded and the neutrophil pellet was resuspended in HBSS in a 1:1 ratio and subsequently mixed with fresh sterile 3% Dextran/PBS solution at a 1:3 ratio, gently inverted and incubated for 1 h at room temperature. After incubation, the supernatant was collected and centrifuged at 500 × g for 7 min at 4°C. The cells were then resuspended in ice cold 0.2% NaCl for 30 seconds to lyse contaminating red blood cells followed by adding an equal volume of ice cold 1.6% NaCl to stop lysis. This was repeated to ensure sufficient lysis of RBCs. Cells were centrifuged at 500 × g for 7 min at 4°C, subsequently resuspended in polymorphonuclear buffer (0.1% BSA, 1% D-Glucose in HBSS) and counted using a hemocytometer. The concentration of viable neutrophils was adjusted to 10 x 10^6 cells/ml and kept on ice until use.

3.3.11.2 ADRB assay

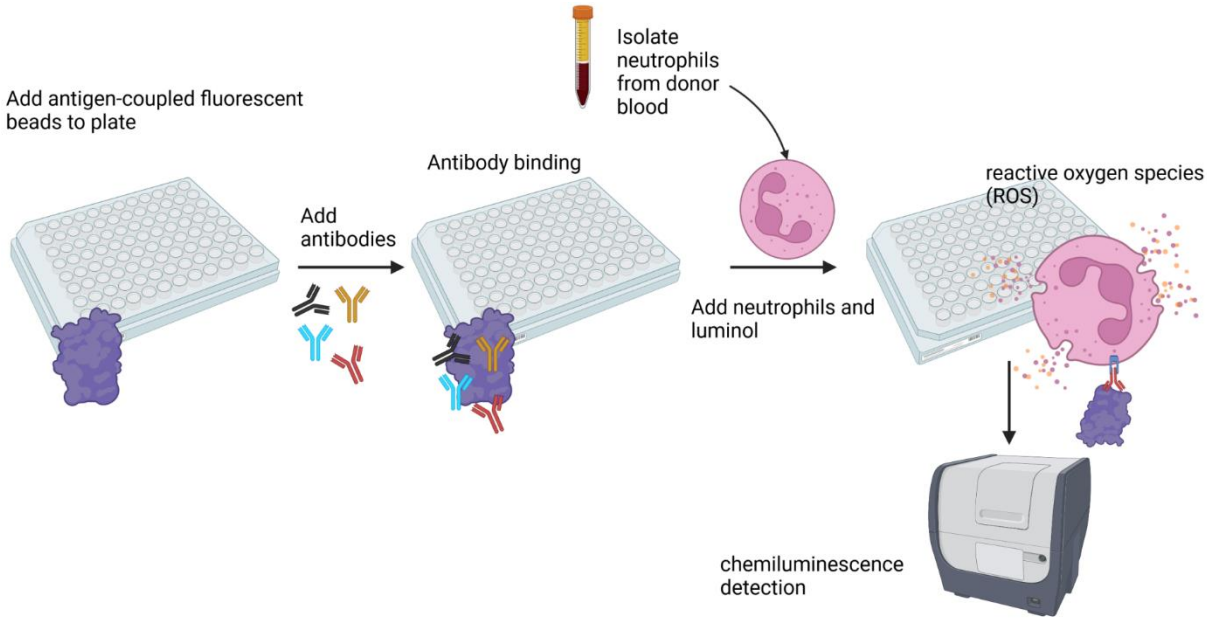

Figure 3.4: Illustration of the ADRB assay.
Recombinant antigen was immobilized on a 96 well plate and opsonized with test antibodies. Neutrophils were isolated from donor blood and added to the plate. Respiratory burst was detected by chemiluminescence.

The ADRB was performed as illustrated in **Figure 3.4**. Recombinant merozoite proteins were diluted in sterile PBS to 10mg/ml and 50µl/well were coated onto a 96-well LUMITRAC 200 white immunology plate overnight at 4°C. The following day, the plate was washed thrice with 200µl of sterile PBS and blocked with 200µl of sterile 1% casein/PBS for 1 h at 37°C. After blocking, the plate was washed thrice and incubated with 50µl/well of plasma samples (1:10), purified IgG (1mg/ml) or IgM (2mg/ml) diluted in PBS for 1 h at 37°C. Next, the plate was washed and 50µl/well of luminol at a concentration of 0.04mg/ml was added before adding 50µl/well of neutrophils. Chemiluminescence at 450nm was immediately read for every 2 min over a duration 1.5 h using the Biotek Synergy 4 plate reader and the Gen 5 acquisition software.

For validation of the assay the following controls were included: 1) unopsonized recombinant antigen and 2) antigen opsonized with PHIS or plasma samples from 5 malaria-naïve adults from Germany. For assays using IgG samples, purified IgG from Kenyan adults (WHO reference standard, NIBSC code: 10/198) was used as a positive control.

The relative light units (RLU) for each plasma sample were indexed against PHIS to reduce variability. The indexed RLU for each plasma sample was calculated as: (RLU of sample) / (RLU of PHIS) ×100.

3.3.12 Opsonic phagocytosis activity (OPA) assay

3.3.12.1 Culture of THP1 cells

The immortalized human monocyte like cell line THP1 was cultured as previously described (Osier et al., 2014a). Briefly, THP1 cells were maintained in THP1 medium (RPMI 1640 media with 2mM L-glutamine and 2mM HEPES supplemented with 10 fetal calf serum (FCS) and 1% Penicillin-streptomycin) in a humidified incubator at 5% CO_2 and 37°C. Cell density was assessed regularly using a hemocytometer and cells were maintained at 1×10^5 cells/ml to 1×10^6 cells/ml. Cells were only used until passage 7 and for the OPA, the concentration of THP1 cells was adjusted to 3.3×10^5 cells/ml.

3.3.12.2 Antigen-to bead coupling

A phagocytosis assay using antigen-coupled microsphere beads was used to determine the phagocytosis activity of antigen-specific antibodies. This assay was based on a published protocol (Kana et al., 2019) with modifications. Briefly, 1.5×10^9 polychromatic red microsphere beads (Polysciences) were resuspended in 1ml of borate buffer and centrifuged at 2000 × g for 7 min. Afterwards, the supernatant was carefully removed and the beads were washed

thrice in 1ml of borate buffer. After washing, the beads were resuspended in 1ml of borate buffer and 30mg of recombinant protein was added and incubated overnight at room temperature in the dark while rotating. The following day, the beads were centrifuged and supernatant with unbound antigen was carefully removed. Next, the beads were blocked thrice in 1ml borate buffer containing bovine serum albumin (BSA) at 10mg/ml for 30 min at room temperature while rotating. After blocking, the beads were stored in 1ml in PBS with 5% glycerol and 0.1% sodium azide at 4°C.

3.3.12.3 Bead OPA assay with THP1 cells

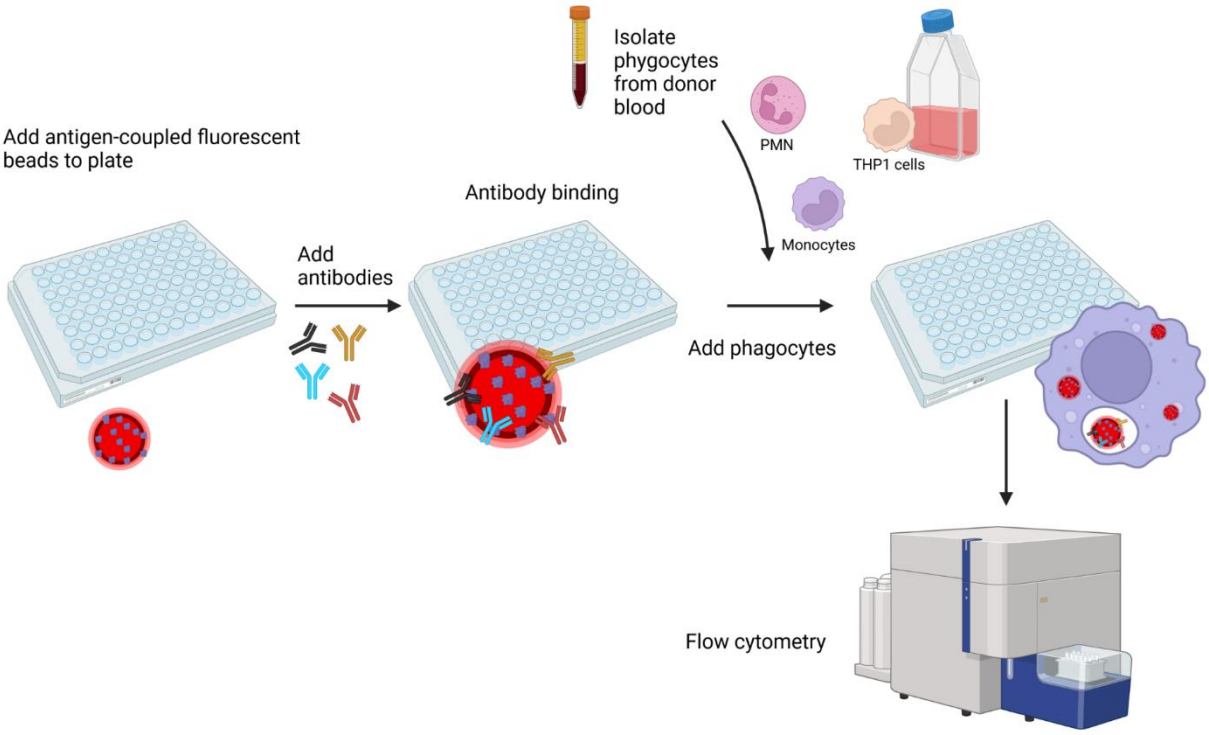

Figure 3.5: Illustration of the OPA assay.
Fluorescent beads were coupled with recombinant antigen, added to a 96 well plate and opsonized with test antibodies. Phagocytes (donor monocytes, donor neutrophils or THP1 cells) were added to the plate. Phagocytosis was measured by flow cytometry.

The OPA was performed as illustrated in **Figure 3.5**. Antigen-coupled beads were diluted in PBS to obtain 1.5 x 10^8 beads/ml. Next, 50µl containing 7.5 x 10^6 beads were added to each well of a 96-well U-bottomed plate followed by incubation with 50µl/well of heat-inactivated plasma samples (1:2000) or IgG (25µg/ml) for 1 h at 37°C. After incubation, the plate was centrifuged at 2000 × g for 7 min and washed thrice with 200µl/well PBS to remove unbound antibodies. Beads were resuspended in 50µl/well of THP1 medium and 50,000 THP1 cells in 150µl/well were added for 30 min at 37°C. Phagocytosis was arrested by centrifugation at 1200 rpm for 7 min at 4°C. Plates were washed thrice with 200µl/well of ice-cold FACS buffer (0.5%

BSA and 2mM EDTA in PBS) and subsequently fixed in 2% formaldehyde/PBS. Flow cytometry was used to quantify THP1 cells containing fluorescent beads in the PE channel on the BD FACS Canto II high-throughput system (HTS). Data analysis was performed using FlowJo V10.

For validation of the assay the following controls were included: 1) uncoupled beads 2) unopsonized antigen-coupled beads 3) antigen-coupled beads opsonized with PHIS or plasma samples from 5 malaria-naïve adults from Germany and 4) THP1 cells treated with the actin-polymerisation inhibitor cytochalasin D at 10mM for 1 h at 37°C. For assays using IgG samples, purified IgG from Kenyan adults (WHO reference standard, NIBSC code: 10/198) was used as a positive control.

Phagocytosis activity for each plasma sample was indexed against PHIS to reduce variability. The phagocytosis index was calculated as: (% of stained THP1 cells opsonized with samples) / (% of stained THP1 cells opsonized with PHIS) × 100.

3.3.12.4 Bead OPA assay with monocytes

The protocol for the bead OPA assay with monocytes was similar to the bead OPA assay protocol with THP1 cells above with the following modifications. Briefly, 25 ml of fresh blood from 2-3 healthy donors was collected in heparin tubes. Next, blood was transferred in 50 ml falcons, mixed with monocyte culture medium (RPMI 1640 media with 2mM L-glutamine supplemented with 10% FCS and 1% Penicillin-streptomycin) and carefully layered on top of 7ml Histopaque. After centrifugation at 1800 rpm for 10 min at 21°C with no break, the peripheral blood mononuclear cell (PBMC) layer was collected and washed in culture medium. The PBMCs were counted by trypan blue exclusion using a hemocytometer. Isolation of viable monocytes was performed using the Pan Monocyte Isolation Kit (Miltenyi Biotec) as per manufacturer's instructions. Briefly, the PBMC pellet was resuspended in 30µl resuspension buffer (0.5% bovine serum albumin (BSA), and 2 mM EDTA in PBS) per 10^7 cells. Afterwards, 10µl of biotin-conjugated monoclonal antibody-cocktail was added to 10^7 PBMCs and incubated for 5 min at 4°C. Next, 30µl of resuspension buffer was added followed by 10 min incubation with 20µl of anti-biotin microbeads at 4°C. The PBMCs were passed through LS columns placed on a precooled MidiMACS™ separator and unlabelled monocytes were collected in the flowthrough. Isolated monocytes were washed and resuspended in 1ml of ice-cold culture medium and counted by using a hemocytometer. The concentration of monocytes was adjusted to 3.3×10^5 cells/ml.

For the OPA assay, $MSP1_{FL}$ coupled microsphere beads were opsonized with human IgM samples (50µg/ml) and subsequently incubated with 50,000 monocytes/well. Flow cytometry was used to quantify monocytes containing fluorescent beads in the PE channel on the FACS Canto II high-throughput system (BD biosciences) and data analysis was performed using FlowJo V10.

3.3.12.5 Bead OPA assay with neutrophils

The protocol for the OPA assay with neutrophils was similar to the OPA assay protocol with THP1 cells above with the following modifications: Neutrophils were isolated from fresh human donor blood as described above and adjusted to a final concentration of 3.3×10^5 cells/ml in neutrophil culture medium (RPMI 1640 media with 2mM L-glutamine supplemented with 10% FCS and 1% Penicillin- streptomycin). $MSP1_{FL}$ coupled microsphere beads were opsonized with human IgG (25µg/ml) or IgM samples (50µg/ml) and subsequently incubated with 50,000 neutrophils/well. Flow cytometry was used to quantify neutrophils containing fluorescent beads in the PE channel on the FACS Canto II high-throughput system (BD biosciences) and data analysis was performed using FlowJo V10.

3.3.13 Antibody-dependent natural killer cell (Ab-NK) assay

3.3.13.1 Isolation of natural killer (NK) cells from healthy donors

Fresh whole blood, a volume of 50ml, from 2-3 individual healthy donors was collected in heparin vacutainer tubes. The blood was transferred into 50ml falcon tubes and mixed with NK cell medium (RPMI 1640 media with 2mM L-glutamine supplemented with 10% FCS and 1% Penicillin-streptomycin) in a 3:1 ratio, before it was carefully layered on top of 7ml Histopaque. Next, density gradient centrifugation was performed at 1800rpm for 10 min at 21°C with no break. After centrifugation, the PBMCs were collected and washed in NK cell medium and assessed for viability and cell density by trypan blue exclusion and a hemocytometer. The PBMCs were resuspended in ice-cold NK cell medium at a final concentration of 1×10^7 cells/ml. Isolation of viable NK cells from PBMCs was performed using the NK cell isolation kit (Miltenyi Biotec) as per manufacturer's instructions. Briefly, 1×10^7 PBMCs were incubated with 20µl of a biotin-conjugated monoclonal antibody cocktail for 30 min at 4°C followed by 30 min incubation with 40µl of microbeads. The PBMCs were passed through LS columns placed on a pre-cooled MidiMACS™ Separator and NK cells were collected in the flowthrough. Isolated NK cells were washed, resuspended in 1ml of ice-cold NK cell medium, counted by using a hemocytometer and adjusted to 0.25×10^6 NK cells/ml.

3.3.13.2 Ab-NK assay

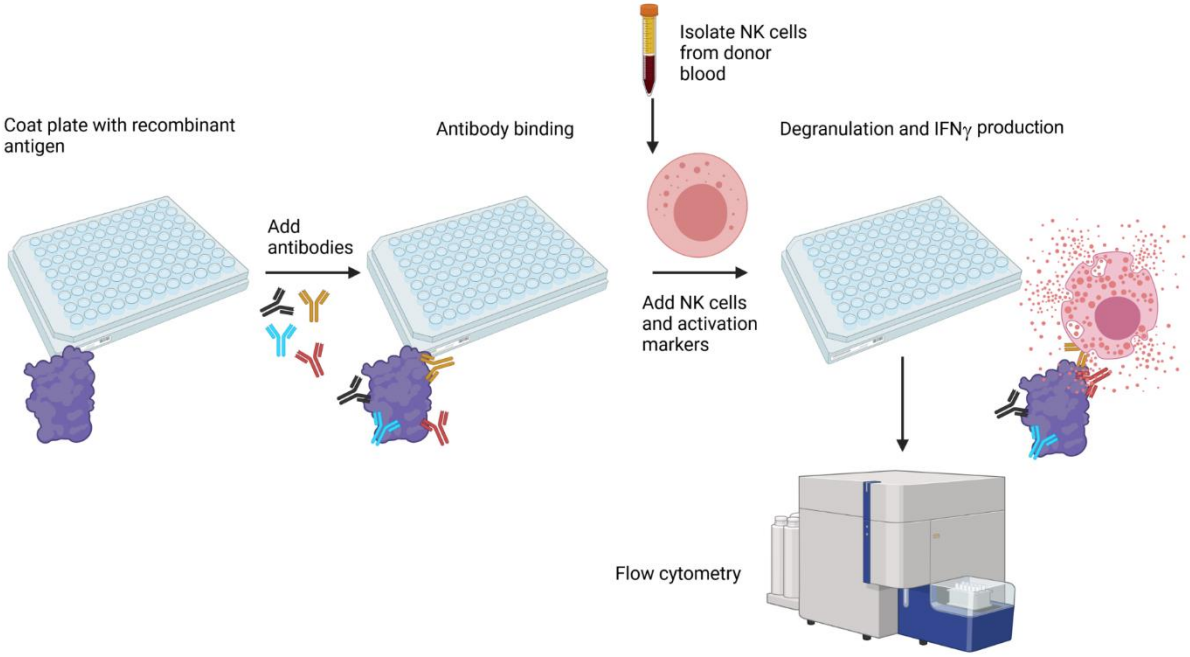

Figure 3.6: Illustration of the Ab-NK assay.
Recombinant antigen was immobilized on a 96 well plate and opsonized with test antibodies. NK cells were isolated from donor blood and added to the plate. Ab-NK activity (degranulation and IFNγ production) was measured by flow cytometry.

The Ab-NK assay was performed according to a previously published protocol (Odera et al., 2021) as illustrated in **Figure 3.6**. Recombinant $MSP1_{FL}$ was diluted in sterile PBS to 10mg/ml and 50µl/well were coated onto 96 well flat-bottomed culture plates overnight at 4°C. The next day, the plates were washed thrice with 200µl sterile PBS and blocked for 4 h with 1% Casein/PBS at 37°C. After blocking, the plates were washed and incubated with 50µl/well of diluted plasma samples (1:10), IgG (1mg/ml) or IgM (2mg/ml) in PBS for 4 h at 37°C. After incubation and washing, 200µl of a cocktail containing 5×10^4 freshly isolated NK cells, anti-human CD107a PE (BD biosciences, 1:70), brefeldin A (Sigma-Aldrich, 1:200) and monensin (Sigma, 1:200) was added into each well and incubated for 18 h in a humidified incubator at 37°C and 5% CO_2. PMA/ionomycin was used as a control for NK-cell stimulation. After incubation, NK cells were transferred into 96 well V-bottomed plates, centrifuged at 1500 rpm for 5 min at 4°C and washed with 150µl ice-cold FACS buffer (1% BSA, 0.1% sodium azide in PBS). Viability of NK cells was determined by staining with 10µl of fixable viability dye eFluor™520 (Thermo fisher) for 10 min at 4°C. Cell surface markers were stained with 20µl/well of an antibody cocktail of anti-CD56 APC (BD biosciences, 1:17) and anti-CD3 PE-Cy5 (BD biosciences, 1:33) for 30 min at 4°C in the dark. After staining, NK cells were washed with 150µl of ice-cold FACS buffer, fixed in 80µl/well of CELL fix (BD biosciences) for 10 min

at 4°C and subsequently permeabilized in 80µl/well of permeabilization buffer for 10 min at 4°C. Presence of intracellular IFNγ was assessed by staining with 30µl/well of anti-IFNγ PE-Cy7 (BD biosciences, 1:33) in permeabilization buffer for 1 h at 4°C in the dark. Afterwards, the cells were washed thrice with 150µl/well of permeabilization buffer to remove excess of antibodies and finally resuspended in 150µl for FACS buffer. Compensation controls included cells and beads unstained and stained with each fluorophore used in the experiment. Acquisition was done on the FACS Canto II high-throughput system (BD biosciences) and the data was analysed using FloJo V10.

For validation of the assay the following controls were included: 1) unopsonized recombinant antigens 2) antigens opsonized with PHIS and plasma samples from 5 malaria-naïve adults from Germany and 3) NK cells incubated with PMA/ionomycin. For assays using IgG samples, purified IgG from Kenyan adults (WHO reference standard, NIBSC code: 10/198) was used as a positive control.

NK cell activity (degranulation and IFNγ expression) for each plasma sample was indexed against PHIS to reduce variability. The degranulation/IFNγ index was calculated as: (% of NK cell degranulation / IFNγ of samples) / (% of NK cell degranulation / IFNγ production of PHIS) × 100.

3.3.14 Purification of $MSP1_{FL}$-specfic antibodies from sera

3.3.14.1 Coupling of $MSP1_{FL}$ to matrix

Prior to coupling, 2mg of lyophilized $MSP1_{FL}$ were dissolved in 10ml cold coupling buffer (100mM $NaHCO_3$, pH 8.3) and kept on ice. Next, 0.5g of CNBr-aktivated Sepharose® 4B (Cytiva) was added to 5ml activation buffer (1mM HCl). The swollen resin was washed ten times with 20ml of cold activation buffer on a sintered glass filter (porosity G3) to remove fragments of resin. The resin was washed again three times with 10ml coupling buffer and centrifuged at 6000 × g for 5 min. The supernatant was removed, the recombinant $MSP1_{FL}$ was added to the resin and incubated over night at 4°C while gently shaking. The next day, the antigen-coupled resin was centrifuged at 6000 × g for 5 min and washed three times with 5 × volume of coupling buffer to remove unbound protein. For blocking of non-reactive groups, the resin was incubated with 10ml quenching buffer (100mM TRIS-HCl, pH 8) for 2 h at room temperature. Afterwards, the supernatant was removed and the resin was washed with 3 cycles of washing steps using alternate low (100mM NaOAc, 500mM NaCl. pH 4) and high pH (100mM TRIS-HCl, 500mM NaCl, pH 8). Afterwards the resin was filled into chromatography columns.

3.3.14.2 Antibody binding and elution

A serum pool (30ml) from vaccinees collected at day 85 and rabbit sera receiving SumayaVac1 was filtered using a 0.2µm filter and split to 7ml aliquots. A serum aliquot was added onto the $MSP1_{FL}$ coupled resin per round of purification and incubated overnight at 4°C on a rotor. After incubation, the flowthrough was collected and the resin with bound antibodies was washed three times with cold PBS. Next, the $MSP1_{FL}$-specific antibodies were eluted in 10 × 1 ml steps using 0.1M glycine pH 2.4 and immediately neutralized with 30µl of 3M TRIS (pH 8.8) and 20µl of 5M NaCl. The collected eluates were pooled, concentrated using Ultracel columns and dialyzed against RPMI. The antibody concentration was determined by using the Cytation™ 3 Cell Imaging Multi-Mode Reader (Biotek).

3.3.15 *Plasmodium falciparum* growth inhibition assay (GIA)

3.3.15.1 Standard GIA

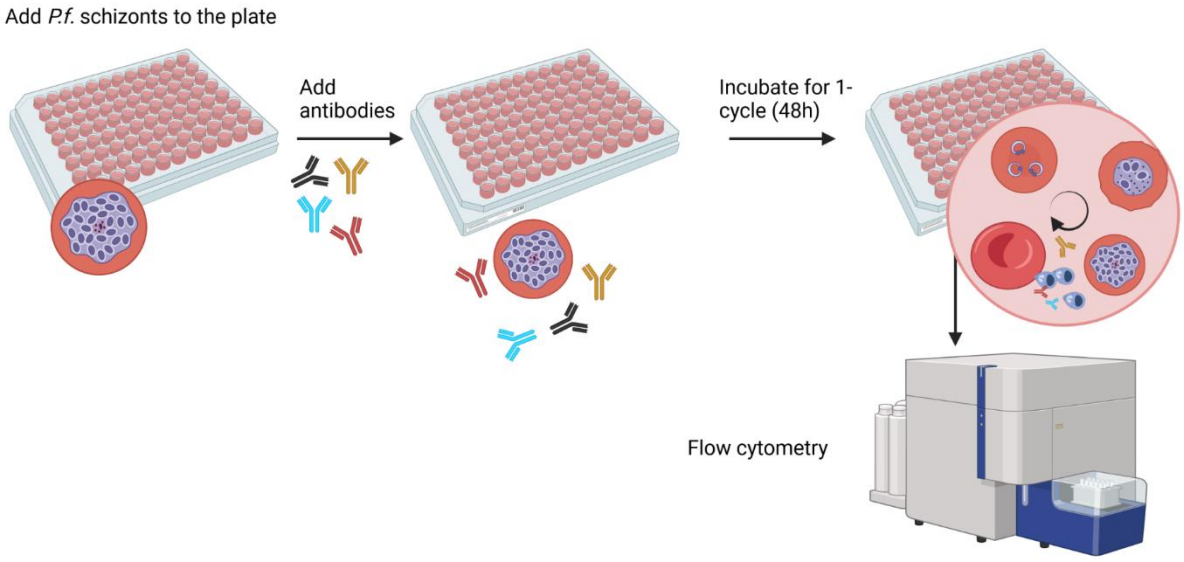

Figure 3.7: Illustration of the GIA.
Highly synchronous schizonts were co-cultured with test antibodies for 1 cycle (48h). Parasite DNA was stained and parasitaemia was determined by flow cytometry.

The GIA was performed as illustrated in **Figure 3.7**. A highly synchronous parasite culture (3D7) containing mostly mid-trophozoite stages were diluted with fresh red blood cells to prepare a parasite suspension of 0.5% parasitemia with 1% hematocrit using fresh complete culture medium. Next, 25µl/well of parasite culture was added in a 96-well U-bottomed plate and incubated with purified $MSP1_{FL}$ antibodies at concentrations ranging from 5mg/ml to 0.3mg/ml in duplicates for one replication cycle (48h). The final volume per well was 50µl. Rabbit antibodies against AMA1 were used as a positive whereas IgG from German adults

before $MSP1_{FL}$ immunization (D0) were used as negative controls. The outer wells of each plate were filled with 50µl of RPMI for humidification purposes. After one replication cycle, the plate was taken out of the incubator, centrifuged at 1800 rpm for 3 min and the supernatant was carefully discarded. Thereafter, the parasite DNA was stained with 100µl of 1 × SYBR Green and mouse anti-human CD235a APC (1:40, BD biosciences) in PBS in the dark for 30 min at room temperature. After incubation, the plate was centrifuged, washed with 200µl sterile PBS and fixed with 150µl of sterile 2% paraformaldehyde (PFA) at room temperature protected from light. The parasitemia was determined by flow cytometry using the HTS of a FACS Canto II (BD biosciences) and the data was analysed using FloJo V10. Growth inhibition was calculated as: Growth inhibition=100−(% parasitemia of test samples−% parasitemia of RBC) / (% parasitemia of parasite growth control−% parasitemia of RBC) × 100.

3.3.15.2 Modified GIA

To test for the potential growth inhibitory effect of cellular and soluble effectors in combination with anti-$MSP1_{FL}$ antibodies, freshly isolated white blood cells (WBC) diluted in human serum were added to the 50µl final GIA volume. Briefly, PBMCs and neutrophils were collected from 3 healthy malaria-naïve donors as described above, pooled and resuspended in cell culture medium (RPMI 1640 media with 2mM L-glutamine supplemented with 10% FCS and 1% Penicillin-streptomycin). The cells were counted using a hemocytometer and the WBC concentration was adjusted to 0.75 x 10^8 cells/ml in human O^+ serum. After adding 25µl/well of antibodies (5mg/ml) and 25µl/well of parasites in 96-well U-bottomed plates as described above, 5µl of WBC suspension (containing 3.8 x 10^5 WBC, to achieve a 1:100 WBC:RBC ratio) were added to each well in duplicates for one cycle of replication. The parasitemia was determined by flow cytometry as described above.

3.3.16 Statistical analysis

Mann-Whitney U test:

The nonparametric Mann-Whitney U test was performed in PRISM 9.3.1 (GraphPad) to to compare medians between CHMI volunteers that were either treated or non-treated and between IgG and IgM antibody levels.

Kruskal-Wallis H test with Dunn's multiple comparison test

The nonparametric Kruskal-Wallis test was performed in PRISM 9.3.1 (GraphPad) to compare the four clinical subgroups (febrile, non-febrile PCR+ and PCR-) followed by Dunn's test for multiple comparisons. The test was also used to compare the IgG mediated functional activities

of vaccinees that received different doses of SumayaVac1 and the fragment-specific effector functions.

Wilcoxon matched-pairs signed rank test

The Wilcoxon matched-pairs signed rank test was performed in PRISM 9.3.1 (GraphPad) to compare the magnitude of functional activities pre- and post-immunization with SumayaVac1. It was also used combined with Hommel correction to identify significantly different epitopes between treated and non-treated CHMI volunteers.

Threshold analysis

The maximally selected rank statistics analysis method in R was used to determine function specific-thresholds (Lausen and Schumacher, 1992; Musasia et al., 2022; Nkumama et al., 2022).

Correlations

Correlation between antibody levels and functions were determined by using Spearman's rank correlation in PRISM 9.3.1 (GraphPad).

Analysis of $MSP1_{FL}$-specific breadth of function

Breadth scores of functional activities were generated for every CHMI volunteer in STATA by categorizing functions as high (=1) or low (=0) based on function-specific thresholds. The sum of breadth scores for every volunteer was determined to generate the total breath score (Osier et al., 2008, Osier et al., 2014, Nkumama et al., 2022).

Survival analysis

The cox proportional hazards model was used to assess the breadth of function with time to treatment while adjusting for confounders (year of study and lumefantrine levels) in STATA. The Log rank sum test was used in PRISM 9.3.1 (GraphPad) to compare the Kaplan-Meier survival curves of volunteers with different breadth scores.

Friedmann test with Dunn's multiple comparisons test

The nonparametric Friedmann test followed by Dunn's multiple comparisons test was used to compare the levels of functional activity in vaccines at different timepoints during follow-up.

4.0 RESULTS

4.1 Full-length merozoite surface protein 1 of *Plasmodium falciparum* is a major target of protective immunity following controlled human malaria infection

4.1.1 Antibody responses against $MSP1_{FL}$

4.1.1.1 High seroprevalence of anti-$MSP1_{FL}$ antibodies in CHMI volunteers

I wanted to characterize the potential role of full-length MSP1 ($MSP1_{FL}$) in naturally acquired immunity to malaria. Therefore, I measured $MSP1_{FL}$ (3D7 strain, **Fig. 8.1**)-specific IgG, IgM and IgG subclass antibodies in plasma samples from CHMI volunteers (n=142) collected one day before challenge (C-1). The reactivity of sera collected from malaria-naïve adults from Germany (n=5) was used to determine the seropositivity cut-off (mean + 3 × standard deviations).

I found that the seroprevalence of anti-$MSP1_{FL}$ IgG was similar in treated and non-treated volunteers (95% versus 100%, respectively), while anti-$MSP1_{FL}$ IgM was more prevalent in non-treated compared to treated volunteers (69% versus 20%, respectively, **Fig. 4.1A**). For IgG subclasses I found that cytophilic IgG1 (82%:100%, treated versus non-treated) and IgG3 (86%:98%, treated versus non-treated) were more abundant compared to non-cytophilic IgG2 (16%-38%, treated versus non-treated) and IgG4 (25%:62%, treated versus non-treated) (**Fig. 4.1A**). When I investigated the anti-$MSP1_{FL}$ antibody profile within clinical subgroups (febrile, non-febrile, PCR+ and PCR-), I observed a trend for higher antibody prevalence with increasing ability to control malaria symptoms and blood stage parasitemia, since non-treated volunteers that were either PCR+ or PCR- tended to have a higher prevalence of anti-$MSP1_{FL}$ antibodies compared to those that were treated and either febrile or non-febrile. (**Fig. 4.1B**).

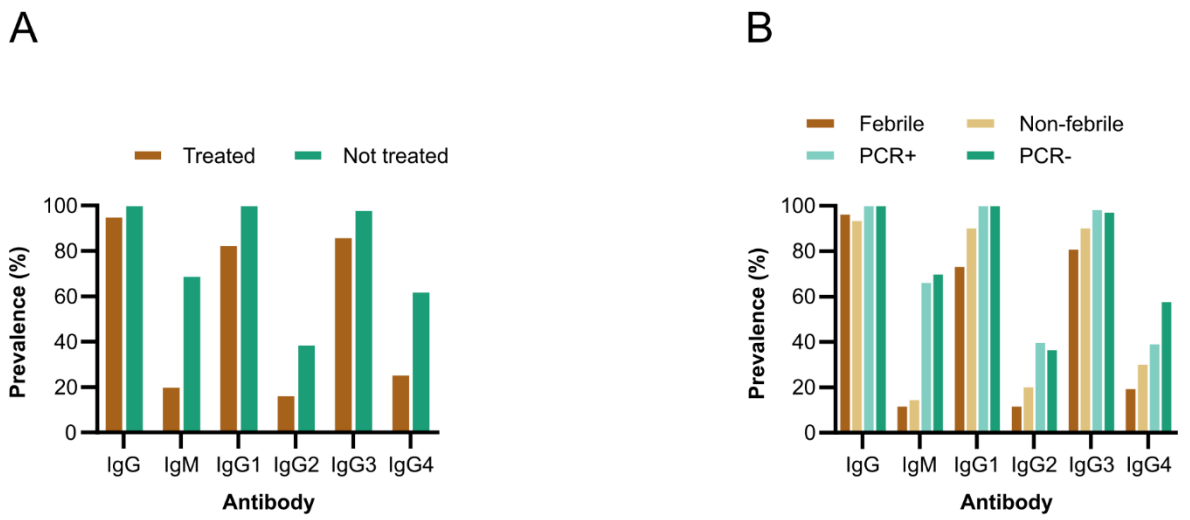

Figure 4.1 High prevalence of anti-MSP1$_{FL}$ antibodies in CHMI volunteers.
Seroprevalence of anti-MSP1$_{FL}$ IgG, IgM and IgG subclass 1-4 antibodies in (**A**) treated (n=56) versus non-treated volunteers (n=86) and in (**B**) subgroups based on parasite growth patterns, treated febrile (n=26), treated non-febrile (n=30), non-treated PCR+ (n=53) and non-treated PCR- (n=33) volunteers. Prevalence was determined by enzyme-linked immunosorbent assay (ELISA) based on the cut-off point for each antibody isotype or subclass which was calculated as the mean optical density (OD) plus three standard deviations of non-malaria-exposed sera from German adults (n=5).

Having shown that anti-MSP1$_{FL}$ antibodies are highly prevalent in CHMI volunteers, I next determined the magnitude of antibody responses. I found that the magnitude of anti-MSP1$_{FL}$ IgG and IgM were significantly higher in non-treated versus treated volunteers (p<0.0001, **Fig. 4.2A**). Within clinical subgroups, significantly higher levels of anti-MSP1$_{FL}$ IgG and IgM were detected for non-treated PCR+ and PCR- volunteers compared to treated febrile or non-febrile study participants. (p<0.0001-0.0014, **Fig. 4.2B**). Volunteers who developed clinical symptoms post sporozoite challenge tended to have the lowest level of anti-MSP1$_{FL}$. Interestingly, no significant difference in antibody levels between PCR- and PCR+ volunteers was observed.

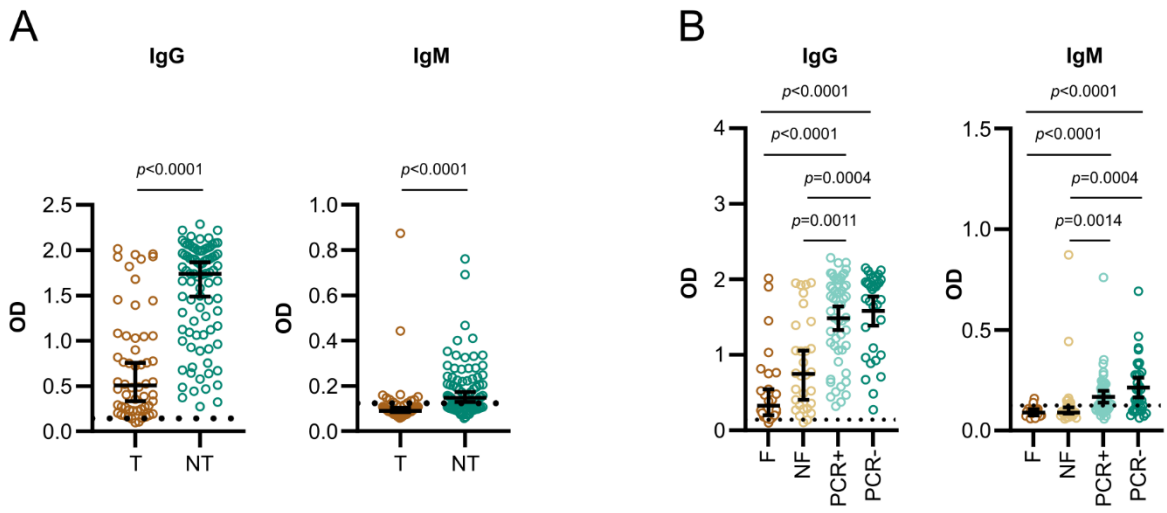

Figure 4.2: High magnitude of anti-MSP1$_{FL}$ IgG and IgM in non-treated volunteers.
Levels of anti-MSP1$_{FL}$ IgG, IgM antibodies measured by enzyme-linked immunosorbent assay (ELISA) in (**A**) treated (T, n=56) versus non-treated volunteers (NT, n=86) and in (**B**) subgroups based on parasite growth patterns, treated febrile (F, n=26), treated non-febrile (NF, n=30), non-treated PCR positive (PCR+, n=53) and non-treated PCR negative (PCR-, n=33) volunteers. Each data point represents antibody levels measured once with two technical replicates for one sample. The seropositivity cut-off value was calculated as the optical density (OD) of non-malaria-exposed sera from German adults (n=5) plus three standard deviations indicated as the dotted line. Error bars represent the median plus 95% confidence intervals. Statistical differences between treatment outcomes were calculated using Mann-Whitney test and between clinical subgroups using Kruskal-Wallis test followed by Dunn's multiple comparisons test.

When I subtyped the magnitude of the anti-MSP1$_{FL}$ IgG response, I observed that non-treated volunteers had significantly higher levels of IgG1,2,3 and 4 compared to treated volunteers (p<0.0001) similarly to the IgG and IgM response (**Fig. 4.3A**). Subgroup analysis showed again that PCR+ and PCR- volunteers had significantly higher antibody levels than those that were either febrile or non-febrile (p<0.0001-0.0213, **Fig. 4.3B**). Collectively, these results indicate that anti-MSP1$_{FL}$ antibodies might be important for naturally acquired immunity against malaria.

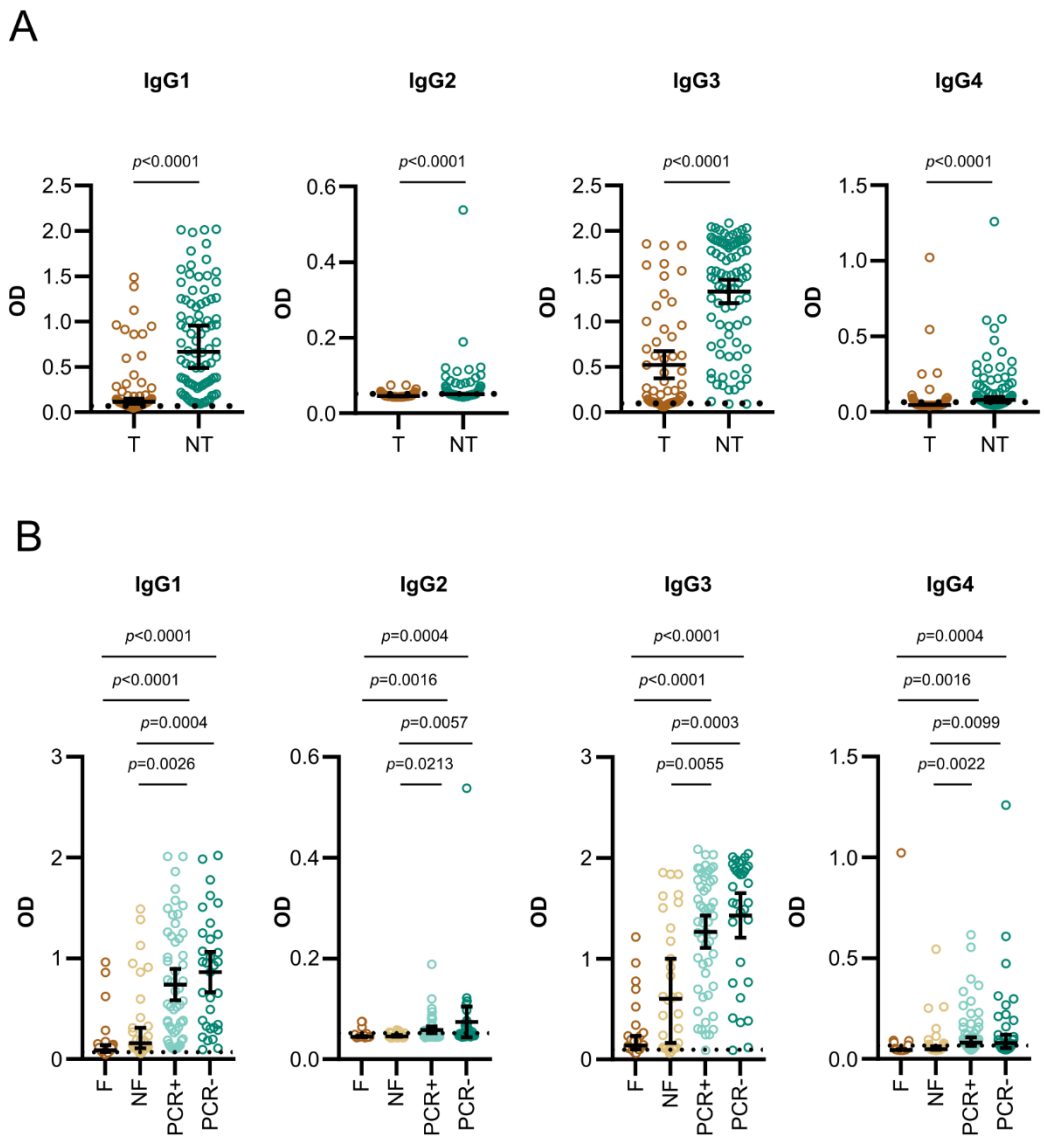

Figure 4.3: High magnitude of anti-MSP1$_{FL}$ IgG subclass antibodies in non-treated volunteers. Levels of anti-MSP1$_{FL}$ IgG subclass 1-4 antibodies measured by enzyme-linked immunosorbent assay (ELISA) in (**A**) treated (T, n=56) versus non-treated volunteers (NT, n=86) and in (**B**) subgroups based on parasite growth patterns, treated febrile (F, n=26), treated non-febrile (NF, n=30), non-treated PCR positive (PCR+, n=53) and non-treated PCR negative (PCR-, n=33) volunteers. Each data point represents antibody levels measured once with two technical replicates for one sample. The seropositivity cut-off value was calculated as the optical density (OD) of non-malaria-exposed sera from German adults (n=5) plus three standard deviations indicated as the dotted line. Error bars represent the median plus 95% confidence intervals. Statistical differences between treatment outcomes were calculated using Mann-Whitney test and between clinical subgroups using Kruskal Wallis test followed by Dunn's multiple comparisons test.

4.1.1.2 Levels of IgG and cytophilic antibody responses are higher compared to IgM and non-cytophilic antibodies

When I compared the levels of total IgG and IgM targeting MSP1$_{FL}$, I found that IgG levels were significantly higher (p<0.0001) than those of IgM (**Fig. 4.4A**). These findings highlight

that MSP1$_{FL}$ is predominantly targeted by IgG. Among the IgG subclasses, cytophilic anti-MSP1$_{FL}$ IgG1 and IgG3 levels significantly exceeded those from non-cytophilic IgG2 and IgG4 (p<0.0001) with IgG3 being the predominant IgG subclass (**Fig. 4.4B**); however, caution should be taken when comparing the antibody responses due to potential differences in sensitivities of secondary detection antibodies. These findings suggest that MSP1$_{FL}$ is predominantly targeted by cytophilic antibodies.

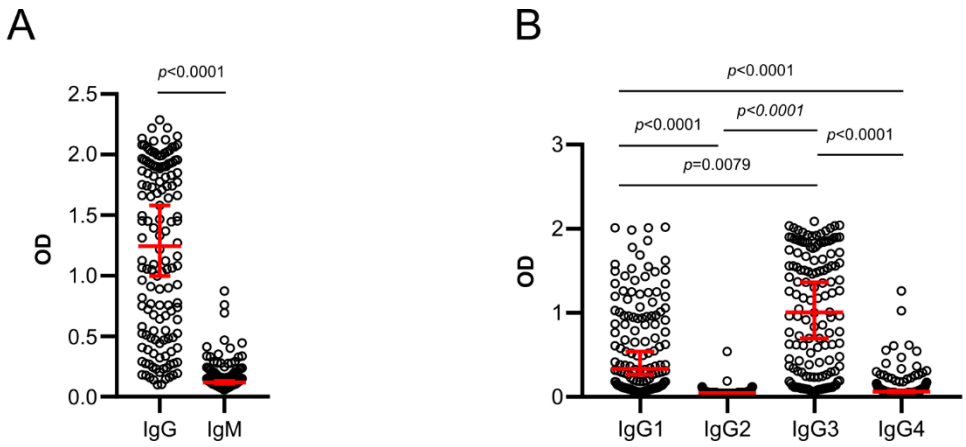

Figure 4.4: The levels of IgG and cytophilic antibody responses are higher compared to IgM and non-cytophilic antibodies.
Levels of (**A**) anti-MSP1$_{FL}$ IgG and IgM and (**B**) IgG subclass 1-4 antibodies in CHMI volunteers (n=142) tested in a single experiment. Each data point represents antibody levels measured once with two technical replicates for one sample. Error bars represent the median plus 95% confidence intervals. Statistical differences between IgG and IgM were calculated using Mann-Whitney test and between subclass 1-4 antibodies using Kruskal Wallis test followed by Dunn's multiple comparisons test.

4.1.1.3 Antibody responses against MSP1$_{FL}$ are correlated with responses against whole merozoites

I observed significant and positive correlations between IgG responses against MSP1$_{FL}$ and whole merozoites. The merozoite ELISA data was kindly provided by Dr. Irene Nkumama (Nkumama et al., 2022). As shown in **Figure 4.5**, I found strong correlations for cytophilic IgG1 (r=0.81, CI 0.75 to 0.86, p<0.0001) and IgG3 (r=0.82, 95% CI 0,76-0,87, p<0.0001) while only moderate correlations were found for non-cytophilic IgG2 (r=0.42, 95% CI 0.32-0.58, p<0.0001) and IgG4 (r=0.59, 95% CI 0.47-0.69, p<0.0001) These findings show that anti-MSP1$_{FL}$ antibodies are co-acquired alongside antibodies to other merozoite antigens and is in line with previous data from our group using the same samples (Musasia et al., 2022; Nkumama et al., 2022; Odera et al., 2021).

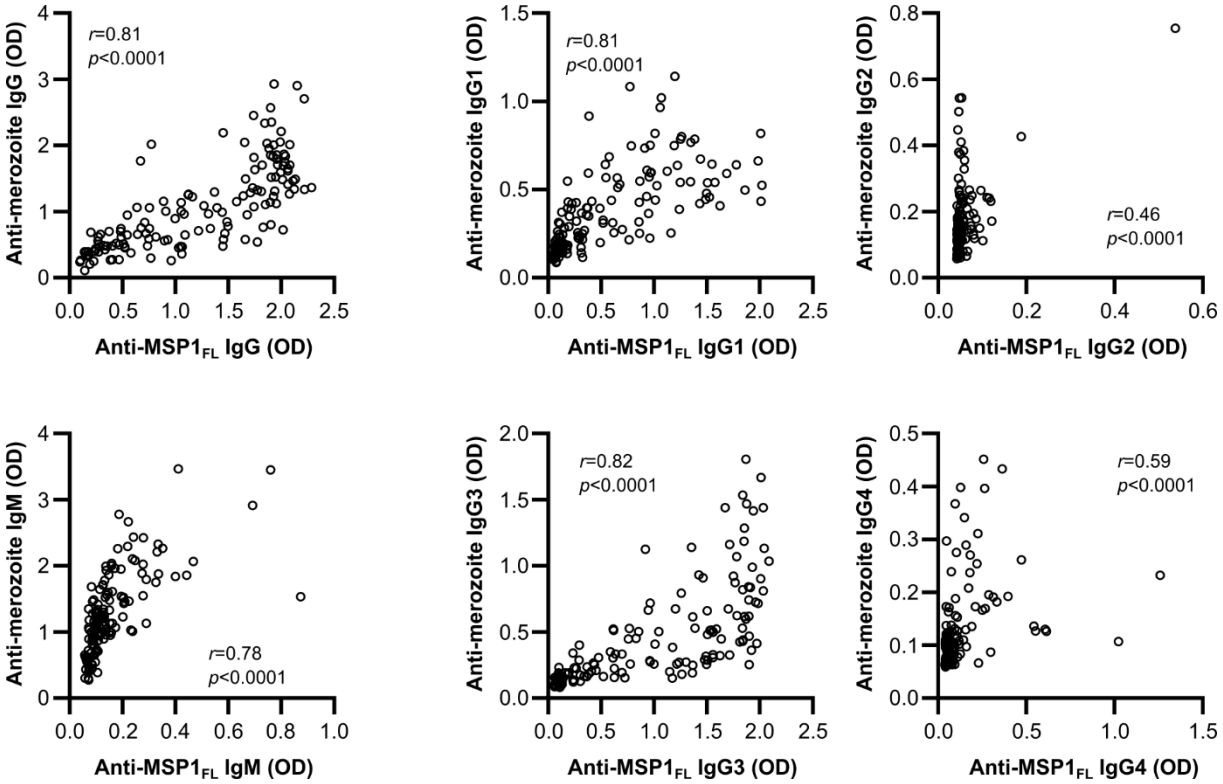

Figure 4.5: Levels of antibodies targeting $MSP1_{FL}$ are correlated with responses against merozoites.
Antibody reactivities against $MSP1_{FL}$ and merozoites (NF54 strain) were assessed by enzyme-linked immunosorbent assay (ELISA) in two single and independent experiments. Spearman's correlation of anti-$MSP1_{FL}$ and anti-merozoite IgG, IgM and IgG subclass 1-4 antibodies in CHMI volunteers (n=142). Each data point represents antibody levels measured once with two technical replicates for one sample. The merozoite ELISA data was produced and kindly provided by Dr. Irene Nkumama (Nkumama et al., 2022)

4.1.1.4 Low baseline anti-$MSP1_{FL}$ IgG is boosted upon challenge

I next wanted to determine the development of anti-$MSP1_{FL}$ IgG levels over the course of the CHMI study. Since plasma samples collected at all timepoints were only available from volunteers who were enrolled in the 2016 cohort, I was only able to determine the kinetics of anti-$MSP1_{FL}$ IgG in a subset of samples (n=36). Interestingly, anti-$MSP1_{FL}$ IgG levels did not change significantly following sporozoite challenge as observed in 21 days of follow-up (p=0.11, **Fig. 4.6A**); however, at C+35 (post study assessment), I observed that 83% (13/16) of treated volunteers developed significantly (p=0.0021) higher antibody levels which was only detectable for 39% (7/18) of non-treated volunteers (**Fig. 4.6B**). I observed the strongest boost of anti-$MSP1_{FL}$ IgG in individuals with low baseline antibody levels. However, since the CHMI study ended after 22 days post challenge, no information about *P. f.* infections that potentially occurred after the study and therefore could have boosted anti-$MSP1_{FL}$ IgG levels are available.

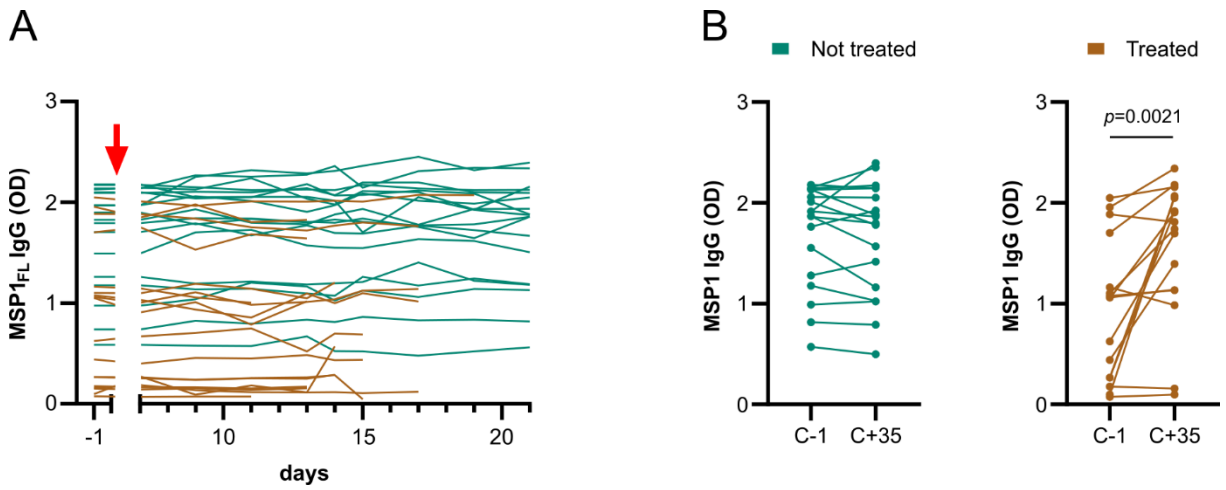

Figure 4.6: Levels of anti-MSP1$_{FL}$ IgG are boosted upon sporozoite challenge.
Kinetics of anti-MSP1$_{FL}$ IgG responses during the study in treated (n=16) and non-treated (n=16) volunteers from the 2016 cohort were measured by enzyme-linked immunosorbent assay (ELISA) in a single experiment. Each data point represents antibody levels measured once with two technical replicates for one sample. (**A**) Antibody levels were measured before (C-1) and after sporozoite challenge at specific timepoints (C+7, 9, 11, 13, 14, 15, 17, 19, 21). Statistical differences between timepoints were assessed using Kruskal-Wallis test. The arrow indicates the day of sporozoite challenge. (**B**) Pre-challenge (C-1) anti-MSP1$_{FL}$ antibody levels were compared to antibody levels post study assessment (C+35) in treated and non-treated volunteers. Statistical differences between timepoints were assessed using Wilcoxon matched-pairs signed rank test.

4.1.1.5 Anti-MSP1$_{FL}$ antibodies are cross-reactive

Overall, MSP1 variants can be categorized in two main allelic forms which are represented by the MAD20 and K1 variant (Tanabe et al., 1987). Since I previously measured antibody responses against MSP1$_{FL}$ from the 3D7 strain, I next tested whether antibodies were cross-reactive with MSP1$_{FL}$-F which represents the K1 variant. Interestingly, the correlation between both variants was high and significant (r=0.86, 95% CI 0.81-0.9, p<0.0001, **Fig. 4.7A**) and anti-MSP1$_{FL}$-F IgG levels from non-treated volunteers were significantly higher compared to treated volunteers (p<0.0001, **Fig. 4.7.B).** These results indicate that antibodies bind to conserved and/or dimorphic regions within the MSP1 molecule.

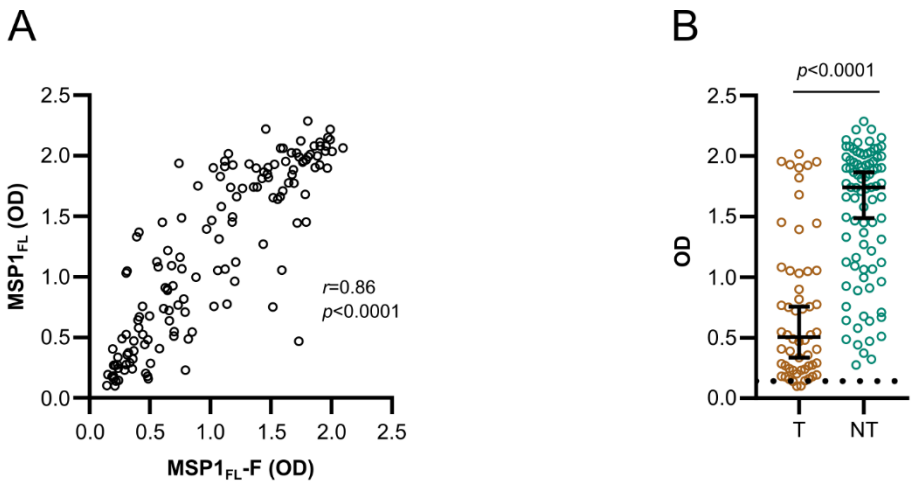

Figure 4.7: Anti-MSP1$_{FI}$ IgG is highly cross-reactive.
Antibody levels against the variant MSP1$_{FL}$-F in CHMI volunteers (n=142) was measured by enzyme-linked immunosorbent assay (ELISA). (**A**) Spearman's correlation of anti-MSP1$_{FL}$ (3D7 strain) with MSP1$_{FL}$-F (K1 strain) in CHMI volunteers (n=142). (**B**) IgG antibody levels against MSP1$_{FL}$-F were compared between treated (T, n=56) and non-treated volunteers (NT, n=86). Each data point represents antibody levels measured once with two technical replicates for one sample. The seropositivity cut-off value was calculated as the optical density (OD) of malaria-naïve plasma samples from German adults (n=5) plus three standard deviations indicated as the dotted line. Error bars represent the median plus 95% confidence intervals. Statistical differences between treatment outcomes were calculated using Mann-Whitney test.

4.1.2 Antibody responses against MSP1 subunits

4.1.2.1 Antibody prevalence and levels against subunits are high in non-treated volunteers

During its maturation, MSP1 is cleaved into 4 subunits (p83, p30, p38 and p42) that stay non-covalently attached. I wanted to determine if the antibody responses are preferentially directed against specific subunits. This was done by comparing the responses against the p83, p30, p38 and p42 subunits between non-treated and treated CHMI volunteers. As shown in **Figure 4.8**, all MSP1 subunits were targeted by antibodies and the seroprevalence was higher for non-treated volunteers compared to treated volunteers (**Fig. 4.8A**). This was evident for N-terminal p83 (61%:91%, treated versus non-treated), central p38 (23%:63%, treated versus non-treated) and C-terminal p42 (59%:67%, treated versus non-treated) while only 16% of the non-treated and 23% of the treated volunteers showed detectable antibody responses against the central p30 subunit.

Moreover, non-treated volunteers showed significantly higher antibody reactivity with p83, p38 and p42 (p<0.0001-0.0007, **Fig. 4.8B**) compared to treated individuals, while the differences for p30 were insignificant. Importantly to note, the negative controls showed stronger reactivities against p30 and p42 compared to p83 and p38 resulting higher background signals.

However, the immunogenicity profiles are in line with previous results from semi-immune adults living in Burkina Faso (Woehlbier et al., 2006).

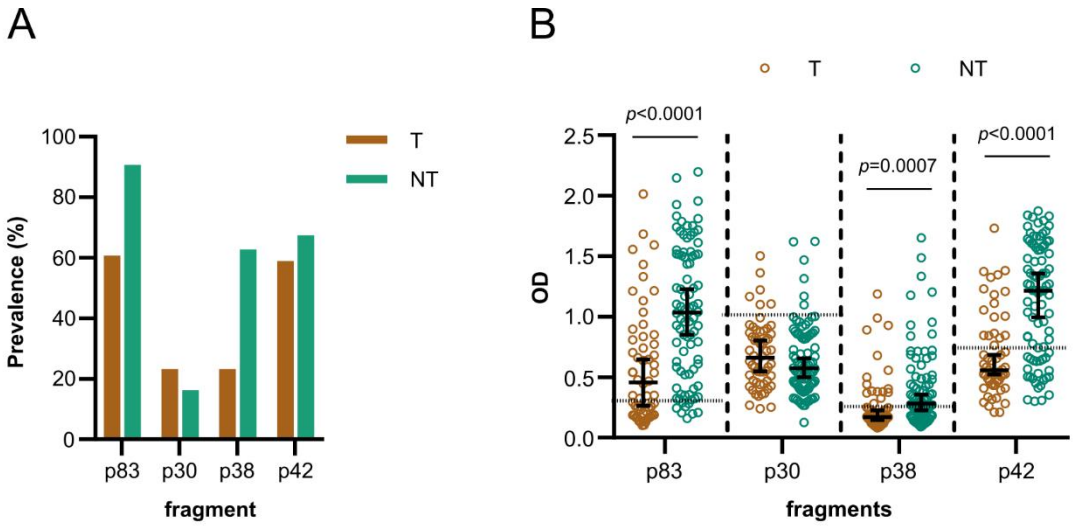

Figure 4.8: Antibody levels against MSP1 subunits are high in non-treated CHMI volunteers. Antibodies from treated (T, n=56) and non-treated (NT, n=86) volunteers specific for the subunits p83, p30, p38 and p42 were measured by enzyme-linked immunosorbent assay (ELISA) in a single experiment. (A) Seroprevalence of antibodies specific for subunits was determined based on the cut-off point for each subunit which was calculated as the mean optical density (OD) plus three standard deviations of sera from malaria-naïve German adults (n=5). (**B**) Magnitude of antibodies against subunits. Each data point represents antibody levels measured once with two technical replicates for one sample. The seropositivity cut-off specific for each subunit was determined by the reactivity of 5 malaria-naïve German adults (mean + 3 × standard deviation) and is indicated as the dotted line. Error bars represent the median plus 95% confidence intervals. Statistical differences between treatment outcomes were calculated using Mann-Whitney test.

4.1.2.2 Antibodies against MSP1 subunits fix complement and are higher in non-treated compared to treated volunteers

It was previously shown that the C-terminal domain of MPS1 (p19 and p42) is a target of complement fixing antibodies (Boyle et al., 2015; Reiling et al., 2019). To test if antibodies directed against the N-terminal or central regions could also fix complement, I performed a complement fixation assay (AbC') where I measured the fixation of the first complement factor C1q in an ELISA-based format. Therefore, 10 volunteers were randomly selected for each clinical subgroup (febrile, non-febrile, PCR+, PCR-) and the AbC' activity was compared between treated and non-treated volunteers.

Similar to the previously determined antibody reactivity, each subunit fixed complement which was significantly (p<0.0001-0.0214) higher for non-treated compared to treated volunteers (**Fig. 4.9**). Although the median level of C1q fixation was the highest for p42, I also observed the highest background for the C-terminal subunit. Although the sample size was small due to

the limited amount of antigen, this data shows that the whole MSP1 molecule is a target of complement fixing antibodies especially the N-terminus and C-terminus.

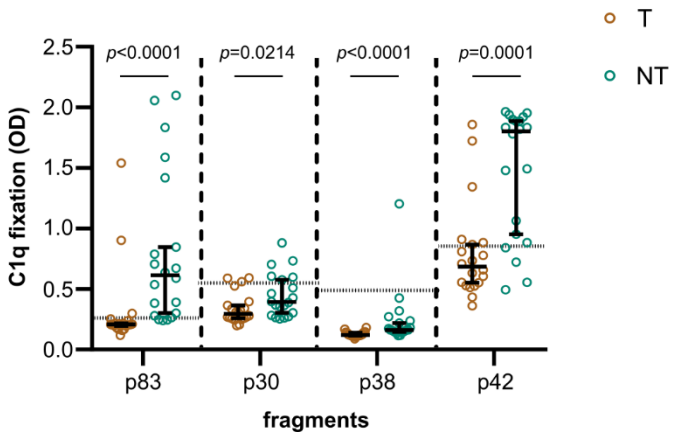

Figure 4.9: All subunits of MSP1 fix complement and the level of fixation is higher for non-treated volunteers.
Antibody-dependent complement fixation (AbC') of antibodies from treated (T, n=20) and non-treated (NT, n=20) volunteers specific for the subunits p83, p30, p38 and p42 were assessed in an ELISA-based format measuring the binding of the primary complement factor C1q to antigen-bound antibodies in a single experiment. The seropositivity cut-off specific for each subunit was determined by the AbC' activity of 5 malaria-naïve German adults (mean + 3 × standard deviation) and is indicated as the dotted line. Error bars represent the median plus 95% confidence intervals. Statistical differences between treatment outcomes were calculated using Mann-Whitney test.

4.1.3 Mapping of linear B cell epitopes

To get more detailed information about the IgG responses against $MSP1_{FL}$ a comparative high-resolution $MSP1_{FL}$ (3D7) peptide array was performed to determine the linear B cell repertoire of non-treated and treated CHMI volunteers. Therefore, 10 plasma samples from each of the four clinical subgroups (febrile, non-febrile, PCR+ and PCR-) were randomly selected and characterized for their linear epitope profile using an $MSP1_{FL}$ peptide array and an anti-IgG secondary detection antibody. Although the responses were heterogenic within the subgroups, I showed that sera from the volunteers recognized numerous epitopes distributed across the entire $MSP1_{FL}$ protein (**Fig. 4.10**). Strong responses were found for several volunteers in conserved (EEITTK, position 56-61, p83 and SPLKTLSEVSIQTE, position 1150-1163, p38) and dimorphic domains ($(TEE)_2$, position 747-754, p30).

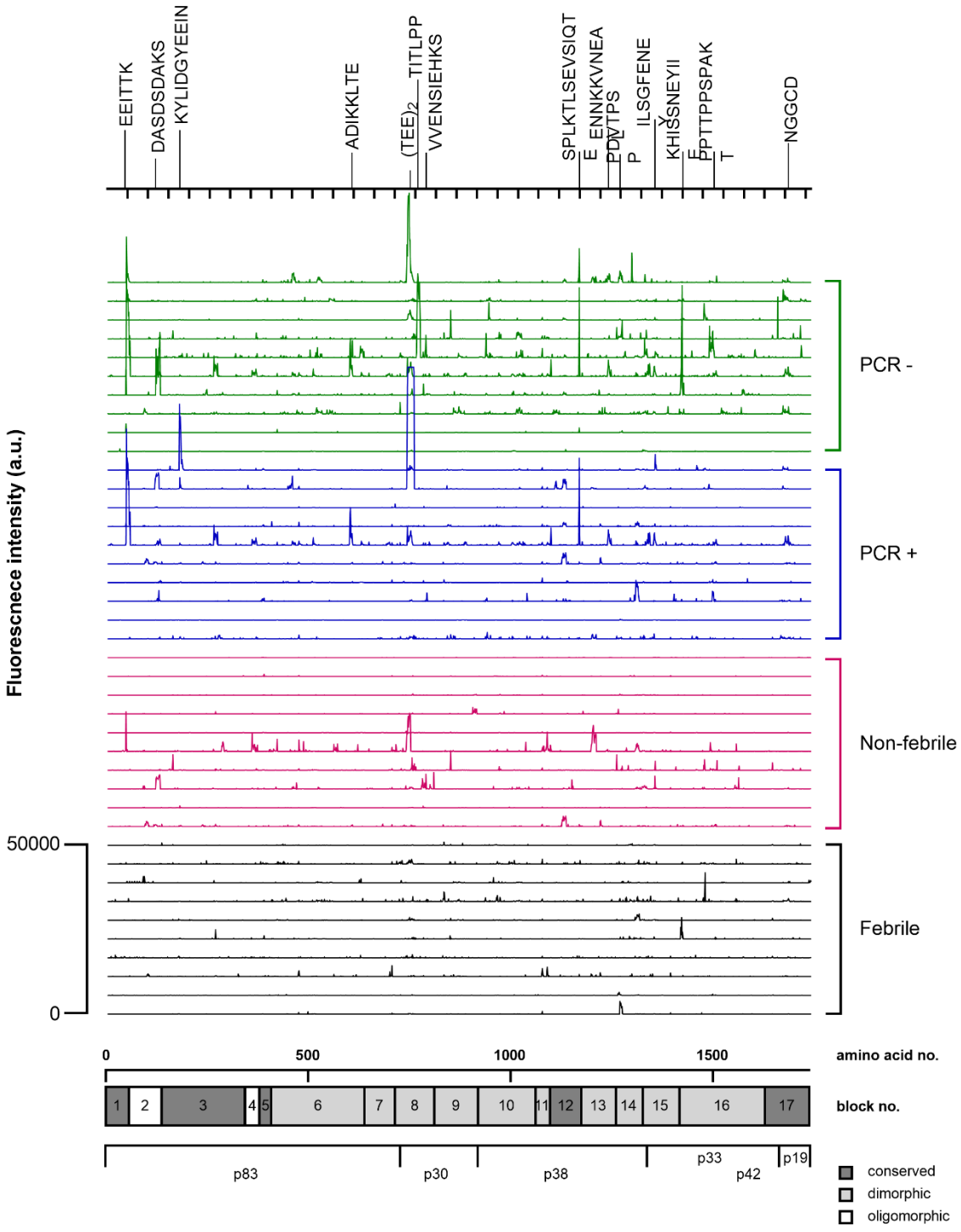

Figure 4.10: IgG from non-treated volunteers bind to epitopes across the whole MSP1 molecule. Mapping of linear B cell epitopes was done using a peptide microarray. The fluorescence intensity landscapes across the $MSP1_{FL}$ are shown for individuals of the four clinical subgroups based on parasite growth patterns: treated-febrile (n=10), treated non-febrile (n=10), non-treated PCR+ (n=10) and non-treated PCR- (n=10). Every line represents a sample. Relevant epitopes have been highlighted on top based on signal intensities. For orientation, a graphical representation of the primary structure of MSP1 is shown below the fluorescence intensity landscapes.

Although the antibody reactivity profiles were variable across the volunteers, non-treated PCR+ and PCR- showed significantly stronger responses to several conserved and dimorphic regions located within the N-terminal, central and C-terminal domains of MPS1 compared to treated volunteers (**Tab. 8.1**). Together these findings further highlight that anti-MSP1$_{FL}$ antibodies target epitopes distributed across the whole MSP1 molecule.

4.1.4 Antibody-mediated Fc effector functions

4.1.4.1 Establishment of the antigen-specific opsonic phagocytosis assay (OPA)

The antigen-specific OPA assay was adapted from a previously published protocol (Kana et al., 2019). Recombinant MSP1$_{FL}$ was coupled onto internally dyed microsphere beads and opsonized with a pool of hyper immune sera from Kenyan adults (PHIS), reference Malaria immune globulin from Malawian adults (MIG), sera from rabbits immunized with MSP1$_{FL}$ and a pool of sera from malaria-naïve German adults (GNP). Opsonized beads were incubated with THP1 cells and phagocytosis was assessed by flow cytometry (**Fig. 4.11**). Uncoupled or CD4-coupled beads were used as negative controls.

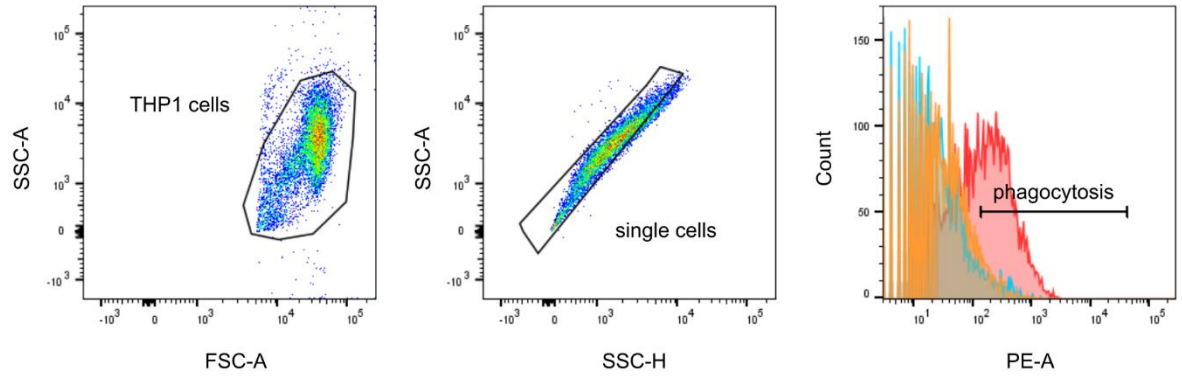

Figure 4.11: Phagocytosis of MSP1$_{FL}$-coupled beads by THP1 cells.
Representative flow cytometry plots showing the gating strategy and histogram overlay for phagocytosis in the THP1 monocytic cell line of MSP1$_{FL}$-coupled red fluorescent microsphere beads opsonized with a pool of hyper immune sera (PHIS) from Kenyan adults (red histogram), a pool of non-malaria-exposed sera from German adults (orange) and unopsonized beads (blue).

I found that, PHIS, MIG and anti-MSP1$_{FL}$ sera from rabbits induced phagocytosis of MSP1$_{FL}$-coupled beads while a negligible effect was observed for malaria-naïve sera or CD4-coupled and uncoupled beads showing that phagocytosis was antibody and antigen-specific (**Fig. 4.12A**).

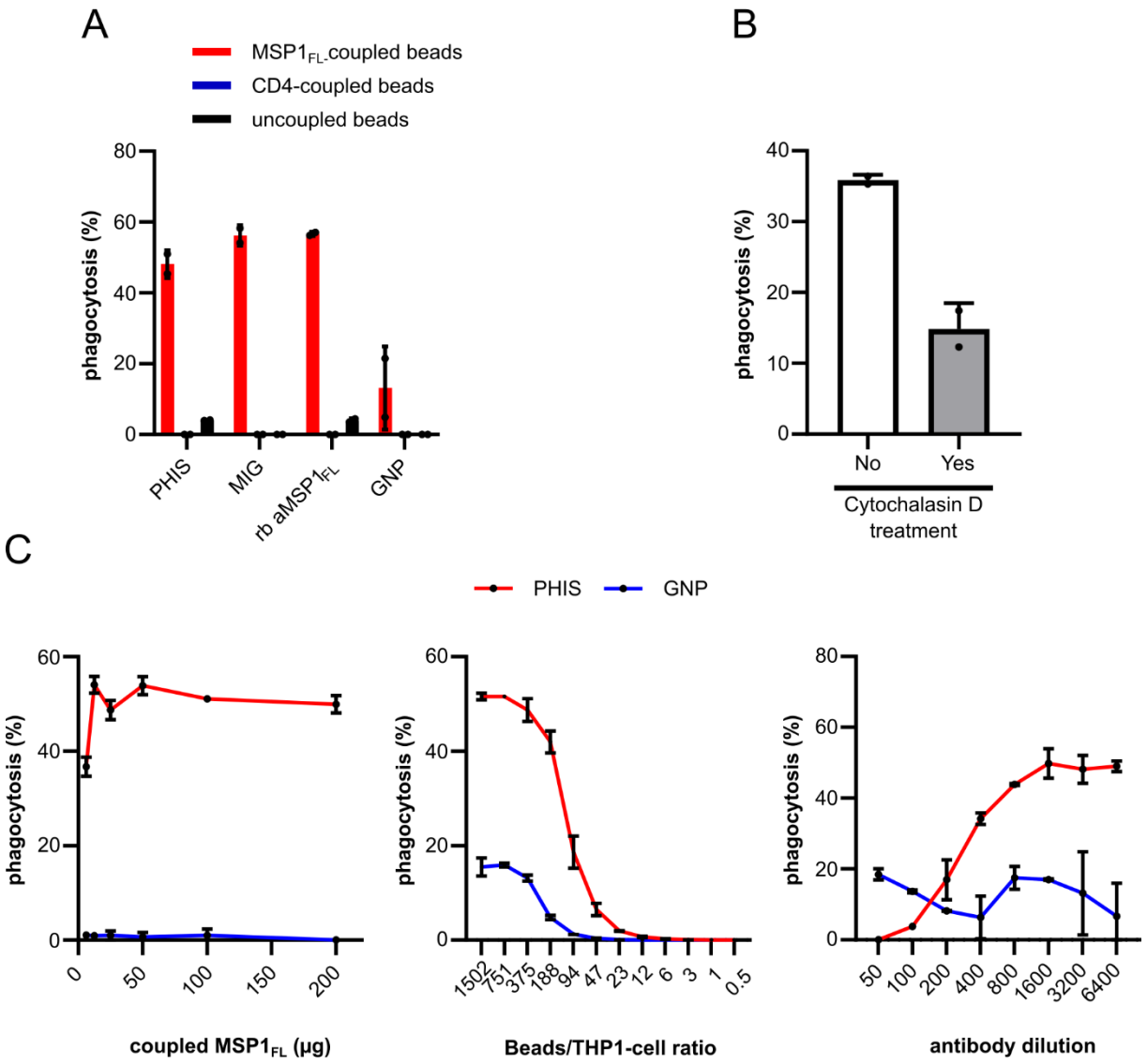

Figure 4.12: Optimization of the opsonic phagocytosis (OPA) assay with MSP1$_{FL}$-coupled beads. **(**A) Bar graphs showing percentage of phagocytosis activity using control antibodies and beads. MSP1$_{FL}$, CD4 and uncoupled beads were incubated with a pool of hyper immune sera from Kenyan adults (PHIS), purified malaria immune globulins (MIG), pooled sera from MSP1$_{FL}$ immunized rabbits (rb aMSP1$_{FL}$) or a pool of non-malaria-exposed sera from German adults (GNP). (**B**) Phagocytosis of PHIS-opsonized MSP1$_{FL}$-coated beads by THP1 cells that were either treated or not treated with cytochalasin D. (**C**) Phagocytosis of MSP1$_{FL}$- coupled beads in the presence of PHIS and GNP at different amounts of coupled MSP1$_{FL}$, Beads to THP1 cell ratio and antibody concentrations. Each data point represents phagocytosis activity measured once with two technical replicates for one sample. Error bars represent the mean plus standard deviations.

As expected, the presence of the actin polymerisation inhibitor cytochalasin D, reduced phagocytosis activity by 50% (**Fig. 4.12B**) showing that antigen-coupled beads are taken up by THP1 cells and did not stick onto the cell surface.

Phagocytosis was dependent on the amount of coupled antigen, bead to THP1 cell ratio and the antibody concentration (**Fig. 4.12C**). I used the optimized settings for the following OPA assays.

4.1.4.2 $MSP1_{FL}$-specific Fc-mediated effector functions are high in non-treated volunteers

I next wanted to assess whether anti-$MSP1_{FL}$ antibodies promote Fc-mediated effector mechanisms. Therefore, antigen-specific *in vitro* functional assays were utilized to study antibody-dependent complement fixation (AbC') by measuring the fixation of the complement factor C1q (Boyle et al., 2015, Reiling et al., 2019), opsonic phagocytosis activity (OPA) of $MSP1_{FL}$-coupled fluorescent beads, as surrogates of merozoites, by monocytes (Kana et al., 2019), antibody-dependant respiratory burst (ADRB) of neutrophils (Joos et al., 2015) and antibody-dependent natural killer cell (Ab-NK) activities (through the measurement of IFNγ and presence of the degranulation marker CD107a on NK cells) (Odera et al., 2021).

By comparing the anti-$MSP1_{FL}$-specific Fc-mediated effector functions between the different treatment outcomes of CHMI study, a higher prevalence of functional antibodies was observed across all 5 effector mechanisms for non-treated compared to treated volunteers (**Fig. 4.13A**). In line with that, a higher seroprevalence of functional antibodies was detected for non-treated PCR+ or PCR- compared to treated febrile or non-febrile volunteers (**Fig. 4.13B**).

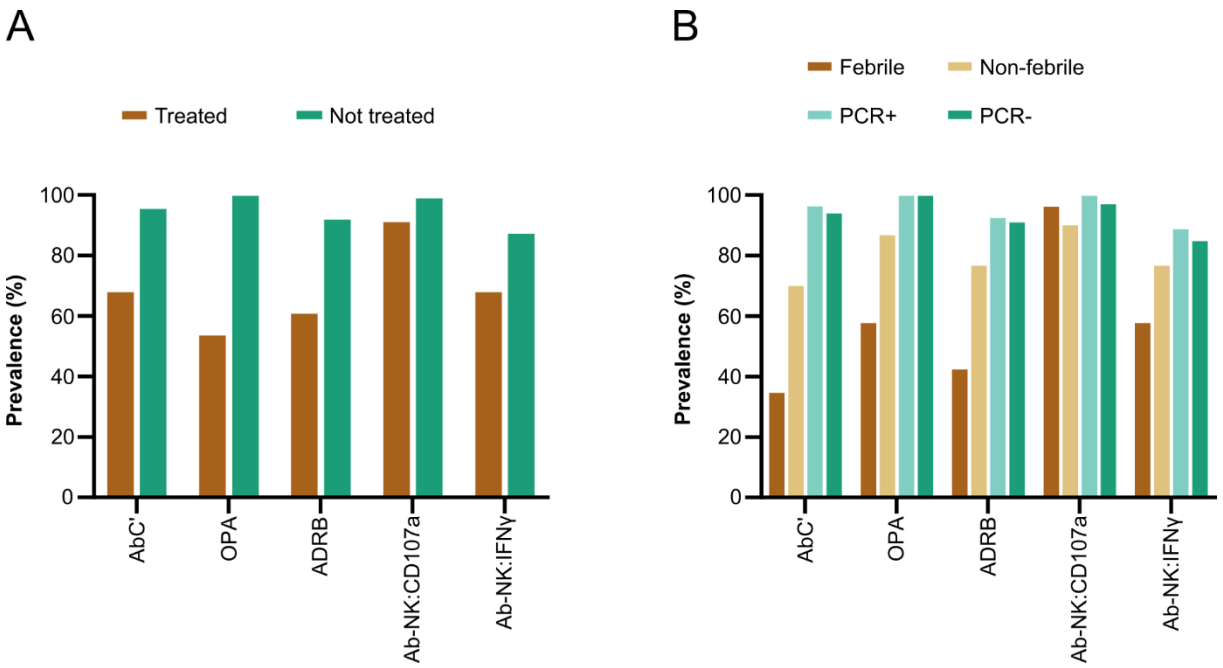

Figure 4.13: High prevalence of MSP1$_{FL}$-specific Fc-mediated effector functions in non-treated volunteers.
Prevalence of MSP1$_{FL}$specifc Fc-mediated effector functions in (**A**) treated (n=56) versus non-treated volunteers (n=86) and in (**B**) subgroups based on parasite growth patterns: treated febrile (F, n=26), treated non-febrile (NF, n=30), non-treated PCR positive (PCR+, n=53) and non-treated PCR negative (PCR-, n=33) volunteers. Prevalence was determined based on the cut-off point for each Fc-mediated effector function which was calculated as the mean functional activity plus three standard deviations of sera from malaria-naïve German adults (n=5). Antibody-dependent complement fixation (AbC') was measured in an ELISA-based format measuring the binding of the complement factor C1q to antigen-bound antibodies. Opsonic phagocytosis (OPA) activity of MSP1$_{FL}$-coupled beads by THP1 cells was measured by flow cytometry and indexed against the positive control (PHIS) to generate the relative phagocytosis index (RPI). Antibody-dependent respiratory burst (ADRB) of neutrophils was measured by detection of reactive oxygen species (ROS) by donor neutrophils using chemiluminescence and the results were indexed against PHIS to obtain the indexed relative light units (indexed RLU). Ab-NK activity (Ab-NK:CD107a and Ab-NK:IFNγ) by donor NK cells was measured by multiparameter flowcytometry and the results were indexed against PHIS.

Similarly, non-treated volunteers had significantly higher levels of all Fc-mediated effector functions compared to study participants who were treated (AbC'; p<0.0001, OPA; p<0.0001, ADRB; p<0.0001; Ab-NK:CD107a; p=0.0175, Ab-NK:IFNγ; p=0.0203, **Fig. 4.14A**). For the clinical subgroups, non-treated PCR+ and PCR- individuals had significantly higher levels of AbC', OPA and ADRB activity compared to treated febrile or non-febrile individuals while degranulation of NK cells (Ab-NK:CD107a) was only significantly different for non-treated PCR+/- compared to treated febrile individuals. No significant difference of IFNγ production of NK cells (Ab-NK:IFNγ) across clinical subgroups was observed (**Fig. 4.14B**).

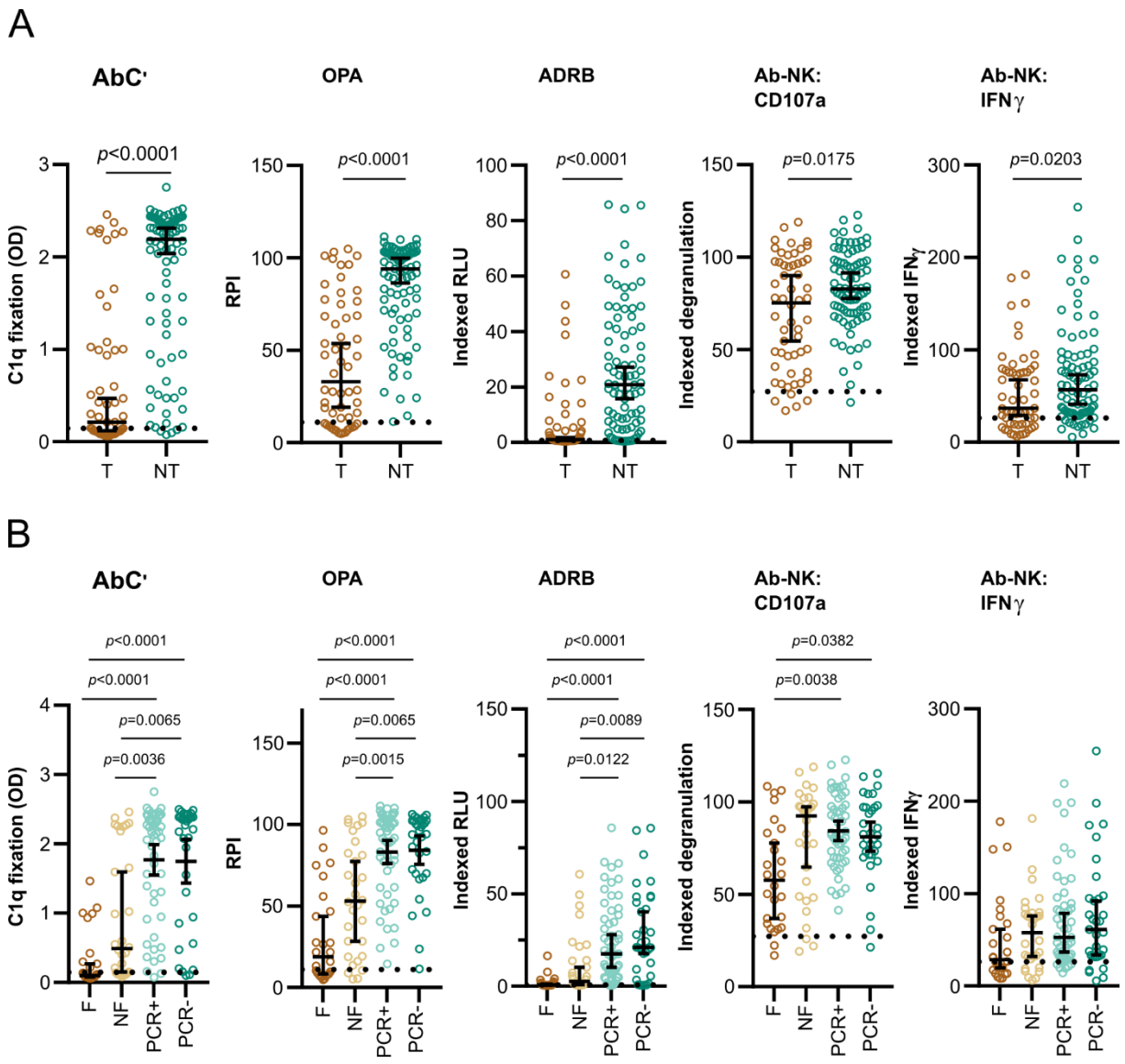

Figure 4.14: High magnitude of MSP1$_{FL}$-specific Fc-mediated effector functions in non-treated volunteers.

Levels of anti-MSP1$_{FL}$ Fc-mediated effector functions in (**A**) treated (T, n=56) versus non-treated volunteers (NT, n=86) and in (**B**) subgroups based on parasite growth patterns, treated febrile (F, n=26), treated non-febrile (NF, n=30), non-treated PCR positive (PCR+, n=53) and non-treated PCR negative (PCR-, n=33) volunteers. Antibody-dependent complement fixation (AbC') was measured in an ELISA-based format measuring the binding of the complement factor C1q to antigen-bound antibodies. Opsonic phagocytosis (OPA) activity of MSP1$_{FL}$-coupled beads by THP1 cells was measured by flow cytometry and indexed against the positive control (PHIS) to generate the relative phagocytosis index (RPI). Antibody-dependent respiratory burst (ADRB) of donor neutrophils was measured by detection of reactive oxygen species (ROS) using chemiluminescence and the results were indexed against PHIS to obtain the indexed relative light units (indexed RLU). Ab-NK activity (Ab-NK:CD107a and Ab-NK:IFNγ) by donor NK cells was measured by multiparameter flowcytometry and the results were indexed against PHIS. Each data point represents a specific Fc-function measured once with two technical replicates for one sample. The seropositivity cut-off value was calculated as the activity level of non-malaria-exposed sera from German adults (n=5) plus three standard deviations indicated as the dotted line. Error bars represent the median plus 95% confidence intervals. Statistical differences between treatment outcomes were calculated using Mann-Whitney test and between clinical subgroups using Kruskal-Wallis test followed by Dunn's multiple comparisons test.

4.1.4.3 MSP1$_{FL}$-specific Fc-mediated effector functions are highly correlated with each other and anti-MSP1$_{FL}$ antibody levels

The potential relationship between Fc-mediated effector functions of anti-MSP1$_{FL}$ antibodies and antibody levels was assessed and I observed high and significant correlations between anti-MSP1$_{FL}$ IgG and AbC' (r=0.83, 95% CI 0.77-0.88, p<0.0001), ADRB (r=0.91, 95% CI 0.88-0.94, p<0.0001) and OPA (r=0.89, 95% CI 0.85-0.92, p<0.0001) (**Fig. 4.15A**). However, I detected only moderate correlations for Ab-NK:CD107a (r=0.53, 95% CI 0.39-0.64, p<0.0001) and Ab-NK.IFNγ (r=0.54, 95% CI 0.41-0.65, p<0.0001) with IgG. Overall, correlations with IgM and effector functions were lower compared to IgG, with AbC' (r=0.58, 95% CI 0.46-0.69, p<0.0001), ADRB (r=0.60, 95% CI 0.48-0.70, p<0.0001) and OPA (r=0.55, 95% CI 0.42-0.66, p<0.0001), Ab-NK:CD107a (r=0.28, 95% CI 0.12-0.43, p<0.0001) and Ab-NK:IFNγ (r=0.30, 95% CI 0.14-0.45, p<0.0001). As expected, higher correlations were measured between cytophilic IgG1/IgG3 and functional activities than to non-cytophilic IgG2/IgG4 (r=0.43-0.90 versus 0.29-0.66, respectively).

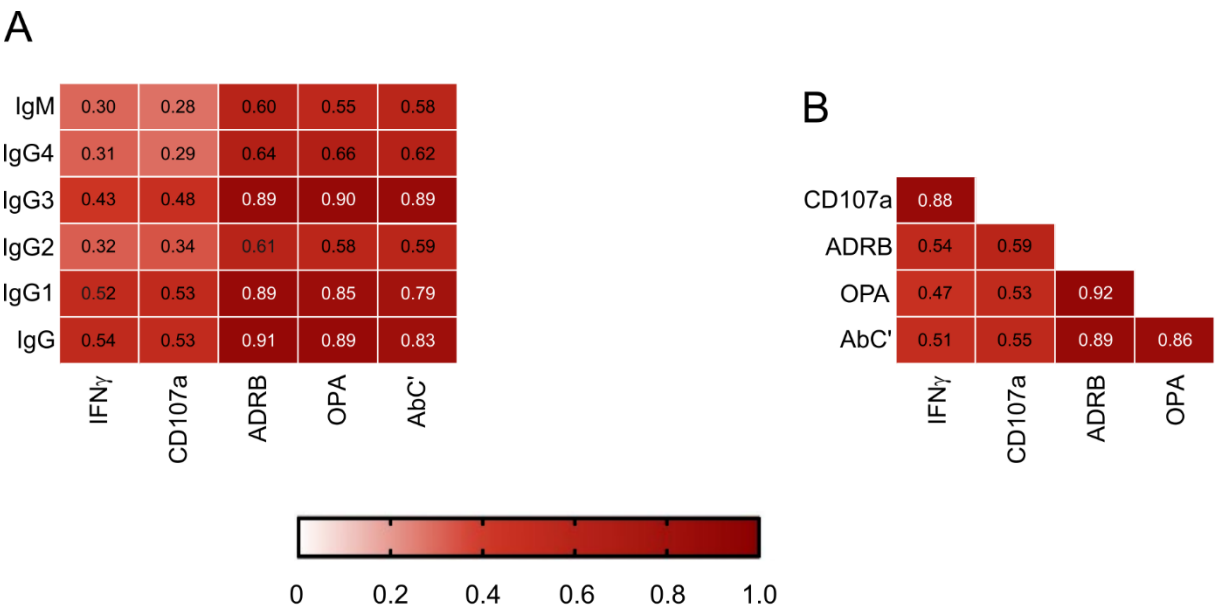

Figure 4.15: MSP1$_{FL}$-specific functional activities are correlated with each other and antibody levels.
Heatmaps with correlation matrix showing significant (p<0.0001) spearman rank correlation coefficients of (**A**) antibody levels with Fc-mediated effector functions and (**B**) effector functions with each other for CHMI volunteers (n=142). The color intensity represents the strength of correlation. AbC'; antibody-dependent complement fixation activity, OPA; opsonic phagocytosis activity of MSP1$_{FL}$-coupled microsphere beads by monocytes, ADRB; antibody-dependent respiratory burst by neutrophils, IFNγ; Fc-mediated natural killer cell IFNγ production, CD107a; Fc-mediated natural killer cell degranulation.

To assess the possibility of multifunctionality of anti-MSP1$_{FL}$ antibodies, the correlations between Fc-mediated effector functions were measured. I found high and significant

corrections for OPA, ADRB and AbC' (r=0.86-0.92, p<0.0001) but weaker correlations of those functions with Ab-NK (r=0.47-0.59, p<0.0001) (**Fig. 4.15B**). As expected, degranulation and IFNγ production of NK cells were highly correlated (r=0.88, 95% CI 0.84-0.91, p<0.0001) with each other.

4.1.5 Association of anti-MSP1$_{FL}$-specific Fc-mediated effector functions with protection from sporozoite challenge

Next, I determined the association of each MSP1$_{FL}$-specific effector function with the time to treatment post sporozoite challenge as correlates of protection from malaria. First, functions were categorized as 'high' or 'low' based on function-specific thresholds using maximally selected rank statistics with the most significant association with the time to treatment (Musasia et al., 2022; Nkumama et al., 2022; Odera et al., 2021).

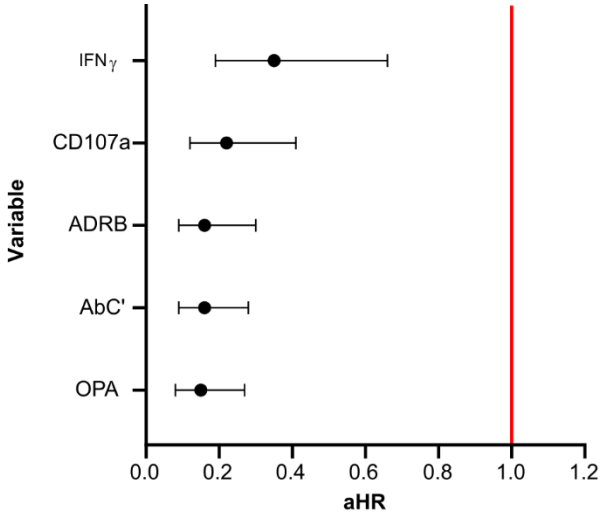

Figure 4.16: Individual MSP1$_{FL}$-specific Fc-mediated effector functions are associated with protection from malaria.
Forest plot showing adjusted hazard ratios (aHR) for MSP1$_{FL}$-specific functional activities ranked from lowest to highest. The aHRs were calculated using the cox regression model comparing time to treatment between high versus low responders based on function-specific thresholds which were determined by using maximally selected rank statistics with the most significant association with the time to treatment while adjusting for confounders (lumefantrine levels and year of study). Error bars indicate 95% confidence intervals and the red line indicates no protection (aHR = 1.0). AbC'; antibody-dependent complement fixation activity, OPA; opsonic phagocytosis activity of MSP1$_{FL}$-coupled microsphere beads by monocytes, ADRB; antibody-dependent respiratory burst by neutrophils, IFNγ; Fc-mediated natural killer cell IFNγ production, CD107a; Fc-mediated natural killer cell degranulation.

Next, cox proportional hazards were adjusted for potential confounders (residual lumefantrine levels and year of study) (Kapulu et al., 2022; Nkumama et al., 2022). Each effector function was highly and significantly associated with protection from sporozoite challenge with aHR estimates ranging between 0.15 to 0.35 (**Fig. 4.16**). Since the confidence intervals of the functions overlapped, no significant differences could be detected between the functions

highlighting that they might contribute equally to a protective immune response against malaria.

4.1.6 Breadth of $MSP1_{FL}$-specific Fc-mediated effector functions

Since I showed that each $MSP1_{FL}$-specific Fc effector function was highly associated with a reduced risk of requiring treatment after CHMI, the combined functional activity (breadth) and its contribution to a protective immune response was determined. To do this the number of functions in the 'high-level' category which were determined previously, were summed up for each study participant to generate individual breadth scores. Although the function breadth was variable across the participants, as shown in **Figure 4.17A**, I found higher breadth scores for non-treated volunteers compared to treated volunteers, with 78% (67/86) versus 29% (16/56) showing a breath score of 5, respectively.

Furthermore, a Kaplan-Meier survival analysis demonstrated a strong distinction in time to treatment post challenge between the different breadth scores. As depicted in **Figure 4.17B**, the level of protection increased stepwise with rising function breadth. To note, only 19% of volunteers with a breadth score of 5 required treatment while 93% of individuals with a breadth score of 0 were treated post CHMI ($p<0.0001$; **Fig. 4.17B**). Moreover, the breadth of function was dependent on antibody titres, with rising anti-$MSP1_{FL}$ IgG levels resulting into higher breadth scores (**Fig. 4.17C**). This highlights the relevance of high anti-$MSP1_{FL}$ antibody levels for protection from malaria.

Together, these results indicate that the breadth of $MSP1_{FL}$-specific functions is a stronger correlate of protection compared to single effector functions.

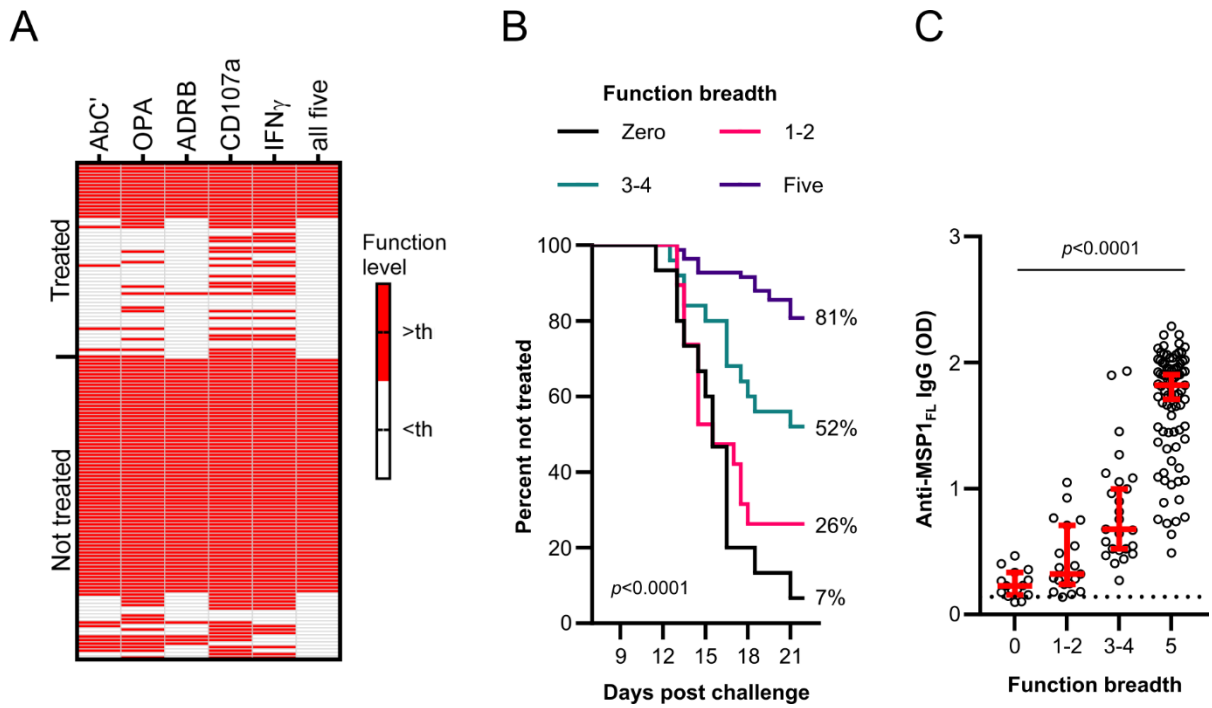

Figure 4.17: Breadth of $MSP1_{FL}$-specific effector functions is a strong predictor of protection from malaria.
(**A**) A heatmap showing the activity levels of all 5 Fc-mediated effector functions in treated (n=56) and non-treated (n=86) volunteers. Responses above a function-specific threshold (th) determined by using maximally selected rank statistics with the most significant association with the time to treatment are shown in red. Each column is a Fc-mediated function while each row is a single volunteer. AbC'; antibody-dependent complement fixation activity, OPA; opsonic phagocytosis activity of $MSP1_{FL}$-coupled microsphere beads by monocytes, ADRB; antibody-dependent respiratory burst by donor neutrophils, IFNγ; Fc-mediated natural killer cell IFNγ production, CD107a; Fc-mediated natural killer cell degranulation. (**B**) Kaplan-Meier plot of volunteers who remained non-treated at specific timepoints over the course of 21 days post challenge. Each line represents a function breadth score starting from 0 (n=15), 1-2 (n=19), 3-4 (n=25) and 5 (n=83). Significant difference between the curves was assessed using Log rank sum test. (**C**) Anti-$MSP1_{FL}$ IgG levels were compared between individuals with different levels of $MSP1_{FL}$-specific breadth of function. Each dot represents antibody reactivity of one sample in two technical replicates. Error bars represent the median optical density (OD) plus 95% confidence intervals. The seropositivity cut-off value was calculated as the optical density (OD) of malaria-naïve plasma samples from German adults (n=5) plus three standard deviations indicated as the dotted line. Statistical differences were calculated using Kruskal-Wallis test followed by Dunn's multiple comparison test.

4.1.7 Antigen-specific Fc-mediated effector functions against merozoite antigens

Our lab has previously identified a list of merozoite antigens that were significantly associated with protection from malaria using the KILchip merozoite protein microarray platform (Nkumama 2021, PhD thesis). This included a known vaccine candidate ($MSP1_{FL}$), known antigens (MSP5, MSP7, MSP11, MSRP4, PTEX150, RAMA and Pf3D7_1136200) as well as novel antigens (Pf3D7_1252300, Pf3D7_1345100, Pf3D7_1401600). All proteins were expressed as 3D7 variants and full-length ectodomains or as the largest predicted extracellular loop in proteins with transmembrane domains (**Tab. 8.2**). Recombinant proteins were tagged

with rat Cd4 domains 3 and 4 tag (CD4 tag) and a hexa-histidine tag for purification. The expression and characterization of those proteins were performed with the help of Sara Kraker and Marie Blickling.

4.1.7.1 Expression and quality control of recombinant antigens

I wanted to compare the levels of functional activities of $MSP1_{FL}$ to other merozoite antigens that were previously identified as targets of NAI (Nkumama 2021, PhD thesis). First, I expressed the proteins in the well-established Expi293 expression system (Invitrogen). Of the antigens listed above, I was able to express sufficient amounts of $MSP1_{FL}$, MSP5, MSP11, MSRP4, PTEX150, Pf3D7_1136200, Pf3D7_1252300, Pf3D7_1345100 and Pf3D7_1401600; however, sufficient quantities of MSP7 and RAMA were not achieved for downstream analysis. The quality and purity of expressed proteins was assessed by SDS gel electrophoresis. As expected, the proteins were pure and showed the correct size. (**Fig. 4.18A**). In agreement with results of the Wright's group, I observed multiple bands for MSP5, Pf3D7_1136200 and PTEX150, possibly due to alternative splicing or posttranslational cleavage of proteins (Crosnier et al., 2013).

Next, I indirectly tested for protein conformation using a monoclonal antibody directed against a conformational epitope within the CD4 tag (Kamuyu et al., 2018). A Gluthathione S-transferase (GST) tag was used as a negative control. As expected, the antibody showed strong reactivity against merozoite proteins while no reactivity was observed against the negative control (**Fig. 4.18B**). $MSP1_{FL}$ showed only little reaction with the anti-CD4 antibody which has been observed previously (Kamuyu et al., 2018), probably due to the size of the protein (218 kDa) and/or masking of the CD4 epitope.

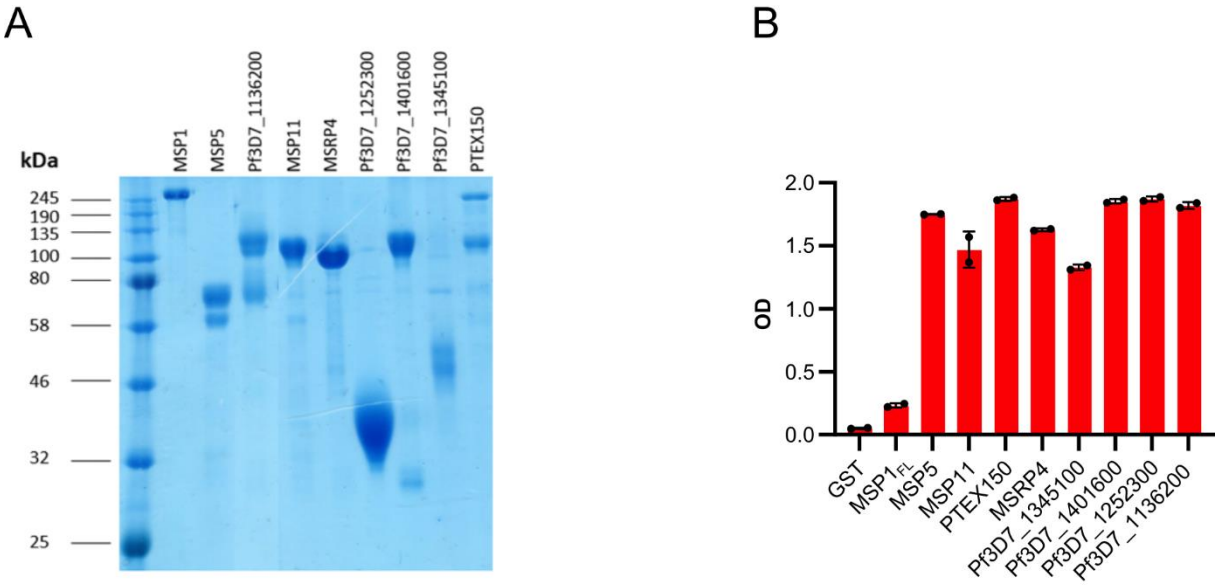

Figure 4.18: Recombinant merozoite proteins have the correct size and react with a monoclonal control antibody.
(**A**) SDS-Page under reducing conditions of merozoite proteins expressed in the Expi293 expression system. Each protein contains a C-terminal rat Cd4 domains 3 and 4 tag (approx. 25kDa). (**B**) The reactivity of the OX68 monoclonal antibody against the rat Cd4 domains 3 and 4 tag was measured by enzyme-linked immunosorbent assay (ELISA) with native recombinant antigens. Recombinant glutathione-S-transferase (GST) without a CD4 tag was used as a negative control. Each data point represents the optical density (OD) measured once with two technical replicates for each antigen. Error bars represent the mean plus standard deviations. Data was produced jointly with Marie Blickling and Sara Kraker.

Immunogenicity of the expressed antigens was validated by standard ELISA using a pool of hyper immune sera (PHIS) from Kenyan adults and a pool of malaria-naïve sera from German adults (GNP). As expected, I observed a dose-dependent response for each antigen with PHIS, while no antibody reactivity was observed with GNP (**Fig. 4.19A, B**). $MSP1_{FL}$ was the most immunogenic antigen showing the strongest responses with PHIS at all concentrations, while for the novel antigens only low reactivity with control sera was detected which has been shown previously (Kamuyu 2017, PhD thesis). Collectively, these results suggest that the proteins are pure, correctly folded and of high quality for immunological characterization.

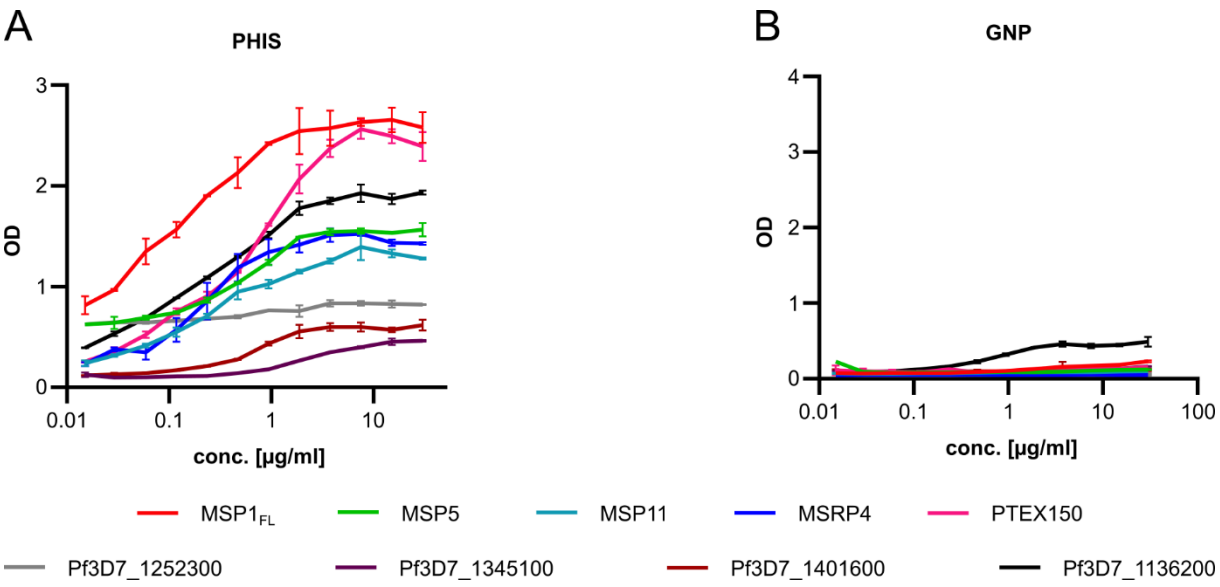

Figure 4.19: Recombinant *P- falciparum* merozoite proteins are immunogenic.
Immunogenicity of recombinant proteins was assessed by enzyme-linked immunosorbent assay (ELISA) at different coating concentrations ranging from 0.01 µg/ml to 30 µg/ml using (**A**) a pool of hyper immune sera from Kenyan adults (PHIS) and (**B**) a pool of plasma from malaria-naïve German adults (GNP). Each data point represents the optical density (OD) at a specific antigen concentration measured once with two technical replicates. Error bars represent the mean plus standard deviations. Data was produced jointly with Marie Blickling and Sara Kraker.

4.1.7.2 Anti-MSP1$_{FL}$ antibodies induce the strongest levels of effector functions compared to other merozoite antigens

Next, I compared the antigens for their ability to induce Fc-mediated effector functions using AbC', ADRB, OPA assays. I selected the top-ten responders for each antigen based on the analysis of KILchip microarray platform (Nkumama 2021, PhD thesis). To note, the selected top responders were all protected from malaria post sporozoite challenge. Next, each antigen was either immobilized on plates or coupled to microsphere beads at previously determined optimal coating concentrations based on the response with PHIS (**Fig. 8.3**).

As shown in **Figure 4.20A**, I observed varying prevalence of antigen-specific functional antibodies ranging from as low as 0% -100%. Interestingly, the prevalence of functional antibodies to the vaccine candidate MSP1$_{FL}$ was 100% for each effector function, while those to the novel antigens Pf3D7_1401600, Pf3D7_1252300, Pf3D7_1345100 were the lowest.

Moreover, MSP1$_{FL}$-antibodies showed the highest median functional activities for AbC' (median OD: 0.94), ADRB (median RLU: 29785) and OPA (median phagocytosis: 32%) (**Fig. 4.20B, Fig. 8.4**). Interestingly, the antigens Pf3D7_1136200 and MSRP4 induced OPA activity similar to MSP1$_{FL}$ (median OPA activity 25.6% and 28.0%, respectively); however, there was a negligible effect on AbC' and ADRB activity for those antigens. This could partially be explained by the level of antigen-specific antibodies in the sera of the volunteers, since OPA

activity requires significantly less antibodies (dilution 1:2000) compared to AbC' and ADRB (dilution 1:10). Together this data showed that $MSP1_{FL}$ was the dominant antigen in inducing Fc-mediated effector functions among the antigens I tested which is corresponding to its abundance and immunogenicity.

A

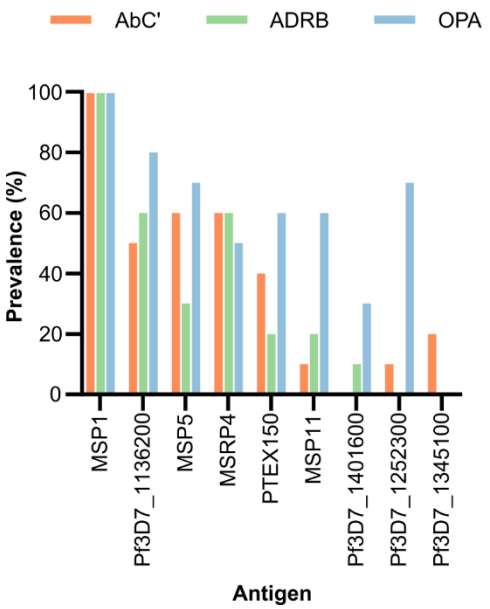

B

Antigen	Functional activity		
	AbC' (OD)	**ADRB** (RLU)	**OPA** (%)
MSP1	0,94	29874,5	32,4
Pf3D7_1136200	0,08	605,0	25,6
MSP5	0,09	1143,5	10,9
MSRP4	0,07	5117,5	28,0
PTEX150	0,10	403,0	5,3
MSP11	0,08	851,3	4,1
Pf3D7_1401600	0,12	363,5	10,1
Pf3D7_1252300	0,09	430,5	6,7
Pf3D7_1345100	0,12	425,3	3,3

Figure 4.20: Anti-$MSP1_{FL}$ antibodies induce the strongest levels of Fc-mediated effector mechanisms compared to other merozoite antigens.
Fc-mediated functional activity of merozoite specific antibodies from antigen-specific top-responders (n=10, respectively) was assessed by AbC'; antibody-dependent complement fixation activity, ADRB; antibody-dependent respiratory burst by neutrophils and OPA; opsonic phagocytosis activity of antigen-coupled microsphere beads by monocytes. Responders that showed the highest antibody reactivity against respective antigens on the KILchip microarray platform were selected for functional assays. (**A**) Prevalence was determined based on the cut-off point for each antigen-specific effector function which was calculated as the mean reactivity plus three standard deviations of non-malaria-exposed sera from German adults (n=5). (**B**) A heatmap showing the median levels of antigen-specific Fc-mediated functional activities for 10 volunteers. Each row represents a merozoite antigen and each column represents a function. The colour intensity represents the strength of functional activity. Data was produced jointly with Marie Blickling and Sara Kraker.

4.2 Immunization with full-length MSP1 induces multifunctional IgG and IgM in malaria-naïve adults

4.2.1 Recombinant full-length MSP1 of SumayaVac1 is correctly folded

4.2.1.1 Recombinant $MSP1_{FL}$ is correctly processed by *P. falciparum* subtilisin-like protease 1

The phase Ia safety and immunogenicity trial with SumayaVac1 ($MSP1_{FL}$ with GLA-SE adjuvant) in malaria-naïve German adults was conducted between April 2017 and December 2018 (EudraCT, No. 2016-002463-3). This trial used full-length MSP1 expressed as heterodimers (p83/p30 and p38/p42) in *E. coli* (**Fig. 8.2**) which was lyophilized and stored in 2ml vials at 4°C (Blank et al., 2020). To ensure that the $MSP1_{FL}$ batch used previously for vaccination of malaria-naïve German adults was still correctly folded, $MSP1_{FL}$ was digested with recombinant subtilisin-like protease 1 (PfSUB1) for 30 min, 1h, 2h or overnight and separated by SDS-Page.

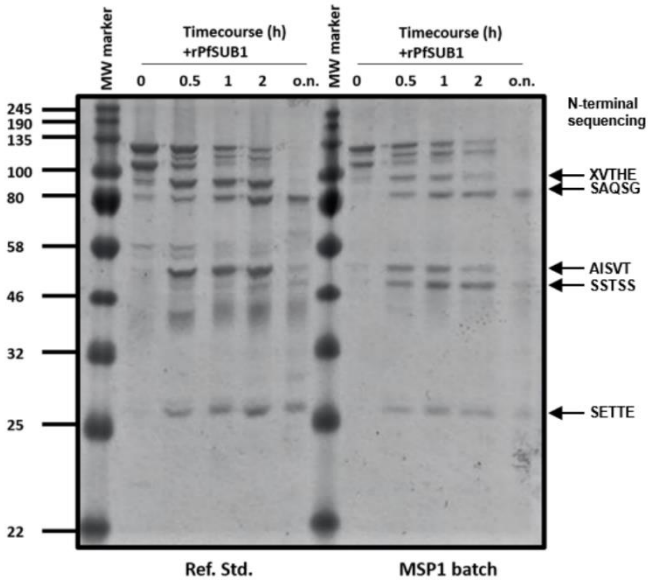

Figure 4.21: $MSP1_{FL}$ is correctly processed by PfSUB1.
SDS-Page under reducing conditions of $MSP1_{FL}$ (reference standard and current batch of use) that was processed with subtilisin-like protease 1 (PfSUB1) for 0 min, 30 min, 1 h, 2 h or overnight. Major processing products are highlighted by arrows with the first 5 residues of their N-terminal amino-acid sequences which were determined by N-terminal sequencing.

In line with previous results, I observed PfSUB1-mediated fragmentation of $MSP1_{FL}$ (disappearance of the two heterodimer bands), resulting into bands corresponding for the p83, p30, p38 and p42 subunits (**Fig. 4.21**). Overnight digestion led to disappearance of some

peptides. Samples were sent to the Proteome factory AG, Berlin for N-terminal sequencing which confirmed the expected cleavage sites (Koussis et al., 2009).

4.2.1.2 Recombinant MSP1$_{FL}$ contains conformational epitopes

Having shown that the MSP1$_{FL}$ batches contained the expected PfSUB1 cleavage sites, I next wanted to assess the conformation of the MSP1$_{FL}$ batch and the reference standard by ELISA using a monoclonal antibody (mAb) directed against a conformational epitope within the p19 region of MSP1 (Kamuyu et al., 2018). I observed a dose-dependent response for the current batch of use and the reference standard (**Fig. 4.22**) showing that both contain the conformational epitope and are likely to be correctly folded. I therefore used the stored MSP1$_{FL}$ batch for subsequent immunological assays.

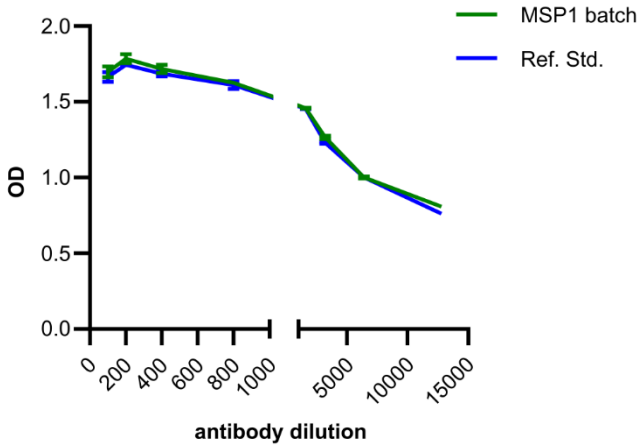

Figure 4.22: MSP1$_{FL}$ contains conformational epitopes.
The reactivity of the monoclonal antibody (mAb) 5.2 against MSP1$_{FL}$ (reference standard and current batch of use) was measured by enzyme-linked immunosorbent assay (ELISA) using different antibody dilutions ranging from 1:100 – 1:12800. Each data point represents the optical density (OD) at a specific antigen concentration measured once with two technical replicates. Error bars represent the mean plus standard deviations.

4.2.2 Similar epitope profile for naturally acquired and vaccine-induced IgG

The linear B cell epitope repertoire of participants of the phase Ia trial has been previously described showing that antibodies target epitopes across the whole molecule (Blank et al., 2020). I wanted to compare the epitope profile of vaccinees with non-treated (protected) PCR-volunteers from the CHMI-SIKA study that I reported above.

Interestingly, I observed similarities between the epitope profile from volunteers who remained parasite free during the CHMI study and participants who received SumayaVac1 (**Fig. 4.23**). Shared epitopes were found for several regions of MSP1, including EEITTK (position 56-61, p83), $(TEE)_2$ (position 747-754, p30) and PPTTPPSPAKT (position 1150-1163, p38) and

PDVTP (position1253-1257, p38); however, since the epitope mapping experiments were conducted independently, the absolute fluorescence intensity between the two sample sets should be interpreted carefully.

This data shows that SumayaVac1 elicits antibodies binding to similar epitopes compared to Kenyan adults who were protected from malaria in the CHMI study.

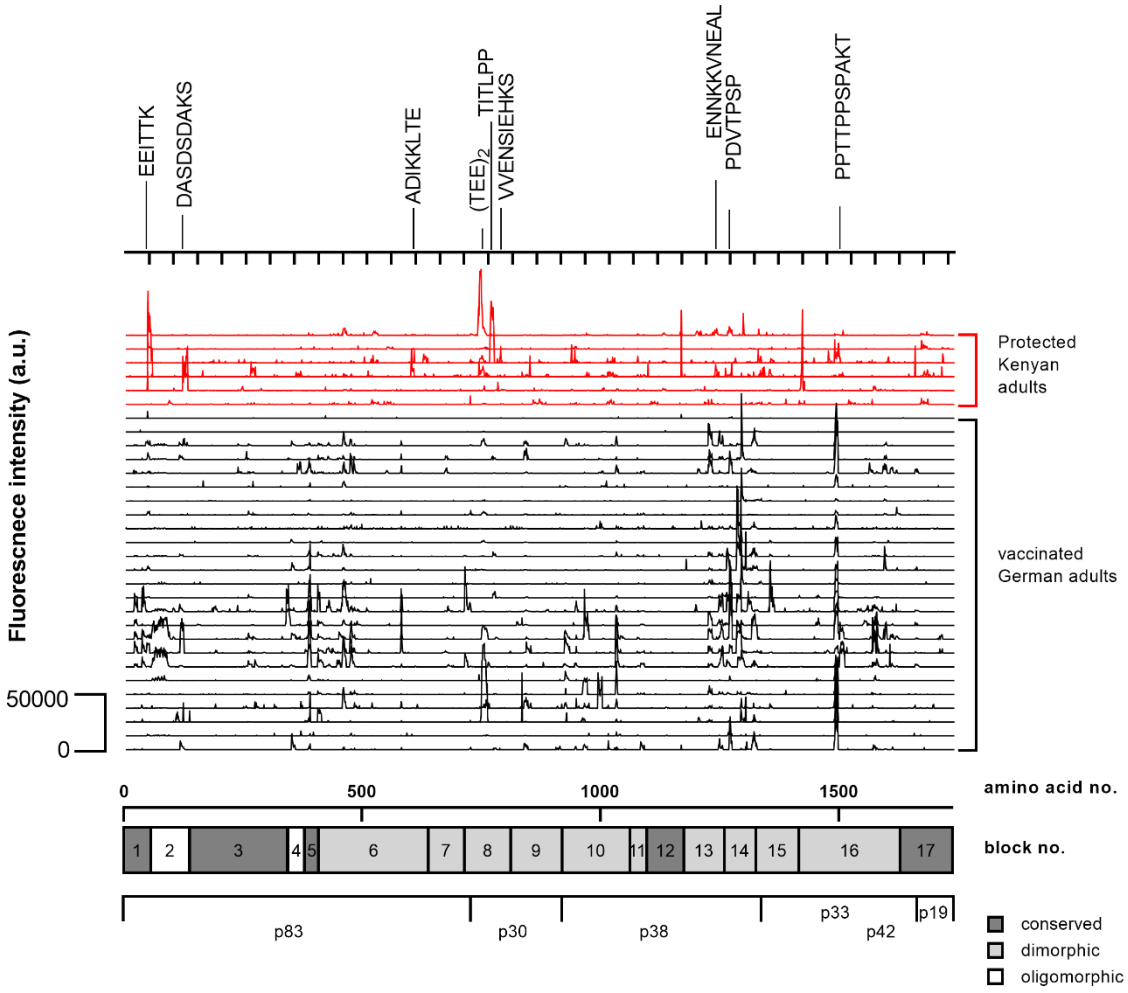

Figure 4.23: Shared epitopes between non-treated CHMI volunteers and malaria-naïve adults immunized with SumayaVac1.
Mapping of linear B cell epitopes was done using two independent peptide protein microarrays. The fluorescence intensity landscapes across the $MSP1_{FL}$ are shown for non-treated PCR- (n=5) highlighted in red and a selection volunteers who were vaccinated with $MSP1_{FL}$ (n=15). Every line represents a sample. Relevant epitopes have been highlighted on top based on signal intensities. For orientation, a graphical representation of the primary structure of MSP1 is shown below the fluorescence intensity landscapes. Epitope mapping data from vaccinees was obtained from Blank at al., 2020.

4.2.3 Immunization with MSP1$_{FL}$ induces several IgG-mediated effector functions

4.2.3.1 Activation of the classical complement cascade

Our group has previously shown that anti-MSP1$_{FL}$ IgG from vaccinees that received 3 immunizations of SumayaVac1 fixed the primary complement factor C1q (Blank et al., 2020). To examine if vaccination with SumayaVac1 also induced opsonizing IgG that could activate the whole classical complement cascade including fixation of C1q, deposition of C3b and formation of C5-C9 (membrane attack complex (MAC)), ELISA-based complement assays were performed with the help of Dr. Richard Thomson and Kristin Fürle.

As shown in **Figure 4.24,** IgG collected at day 85, 4 weeks after the third immunization, resulted not only in significant (p<0.0001) activation of the primary complement factor C1q, as reported by Blank and colleagues (Blank et al., 2020), but also mediated significant deposition of C3b and the formation of MAC (p=0.0002, respectively). This finding shows that vaccine-induced IgG activates the full classical complement pathway.

The use of C1q fixation to determine antibody-dependent complement fixation (AbC') was used for subsequent assays due to its high correlation with the activation of downstream factors.

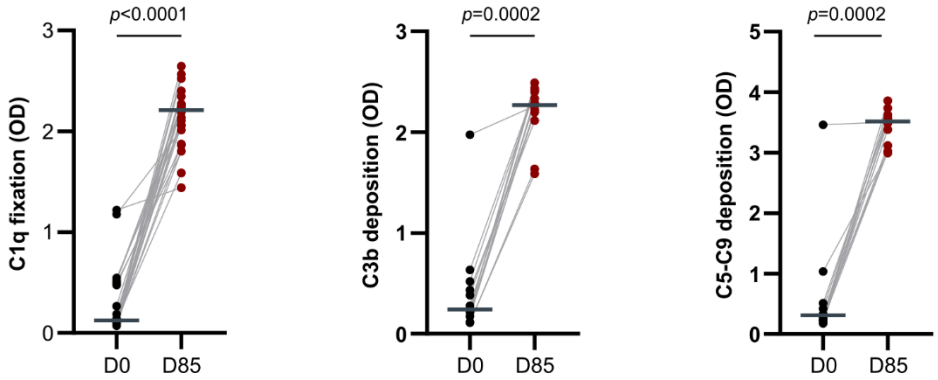

Figure 4.24: Vaccine-induced anti-MSP1$_{FL}$ IgG activate the whole classical complement cascade. Levels of fixation of the complement factors C1q, C3b and C5-C9 (membrane attack complex (MAC)) in a selection of purified IgG samples (n=24 for C1q fixation, n=13 for C3b deposition and C5-C9 formation) collected before (D0) and after the 3rd vaccination (D85). Fixation of complement factors were detected in an ELISA-based format. Each data point represents the optical density (OD) for reactivity of respective complement factors measured once with two technical replicates. Dark grey lines indicate medians. Statistical differences between timepoints were calculated using Wilcoxon matched-pairs signed rank test. Data was produced jointly with Dr. Richard Thomson and Kristin Fürle.

4.2.3.2 Cellular Fc-mediated effector functions

Two independent lines led me to investigate the potential repertoire of effector functions of vaccine-induced anti-MSP1$_{FL}$. First, as described previously, I demonstrated that naturally

acquired anti-$MSP1_{FL}$ antibodies induced a range Fc-mediated effector functions including AbC', OPA of THP1 cells, ADRB and Ab-NK activity (degranulation and IFNγ production) that showed strong and significant association with protection individually and importantly in combination. Second, Blank and colleagues have previously shown that vaccination with SumayaVac1 induced anti-merozoite IgG that promoted the release of reactive oxygen species (ROS) by neutrophil granulocytes (Blank et al., 2020) which indicates the induction of opsonizing antibodies.

To test if vaccine-induced IgG could activate a range of effector cells, I assessed $MSP1_{FL}$-specific functions in vaccinees (n=24) before (D0) and 4 weeks after the third immunization (D85). These assays included OPA of different phagocytes (THP1 cells, or neutrophils), ADRB and Ab-NK activity. To note, to facilitate standardization of reagents and material, the assays were performed with recombinant $MSP1_{FL}$ instead of whole merozoites.

As shown in **Figure 4.25A,** post-immunization IgG induced the whole range of $MSP1_{FL}$-specific Fc-mediated cellular effector functions. I observed statistical differences between the 25µg and the 50µg cohort in regards to OPA of THP1 cells (p=0.0201; **Fig. 4.25B**); however, no statistical differences were observed for the other functions which suggests that IgG induces effector functions independent of the $MSP1_{FL}$ dose.

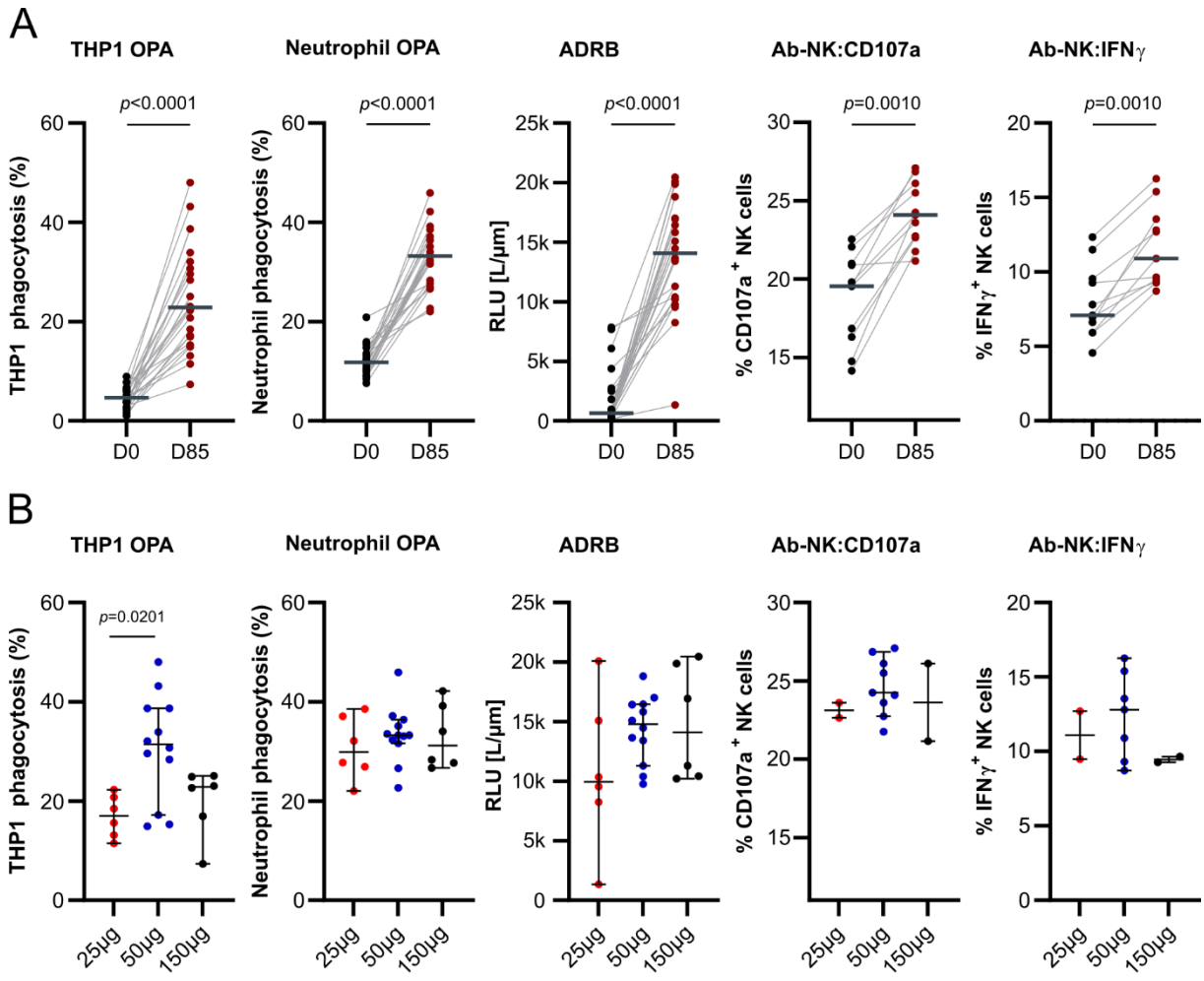

Figure 4.25: Vaccine-induced IgG activates a range of effector cells.
(**A**) Levels of anti-MSP1$_{FL}$ Fc-mediated effector functions of purified IgG samples (n=24; Ab NK, n=11) compared before (D0) and after the 3rd vaccination (D85) (**B**) Levels of anti-MSP1$_{FL}$ Fc-mediated cellular effector functions of post-immunization IgG were compared between the different dose levels (25µg, 50µg, 150µg). Opsonic phagocytosis (OPA) activity of MSP1$_{FL}$-coupled beads by THP1 cells or donor neutrophils was measured by flow cytometry, Antibody-dependent respiratory burst (ADRB) of donor neutrophils was measured by detection of reactive oxygen species (ROS) using chemiluminescence. Ab-NK activity (Ab-NK:CD107a and Ab-NK:IFNγ) by donor NK cells was measured by multiparameter flowcytometry. Each data point represents a specific Fc-function measured once with two technical replicates for one sample. Dark grey lines indicate medians. Error bars represent the median plus 95% confidence intervals. Statistical differences between timepoints were calculated using Wilcoxon matched-pairs signed rank test and for the different dosing groups using Kruskal-Wallis test followed by Dunn's multiple comparisons test.

4.2.3.3 Induction and decay kinetics of Fc-mediated effector functions

I next assessed the induction and decay kinetics of MSP1$_{FL}$-specific IgG-mediated effector functions during the course of the study using samples where all timepoints where available (n=13). Similar to the previously reported IgG titres (Blank et al.,2020), the level of functional activity across all 6 functional assays peaked after the 3rd immunization at day 85 (**Fig. 4.26**) and was not dose-dependent.

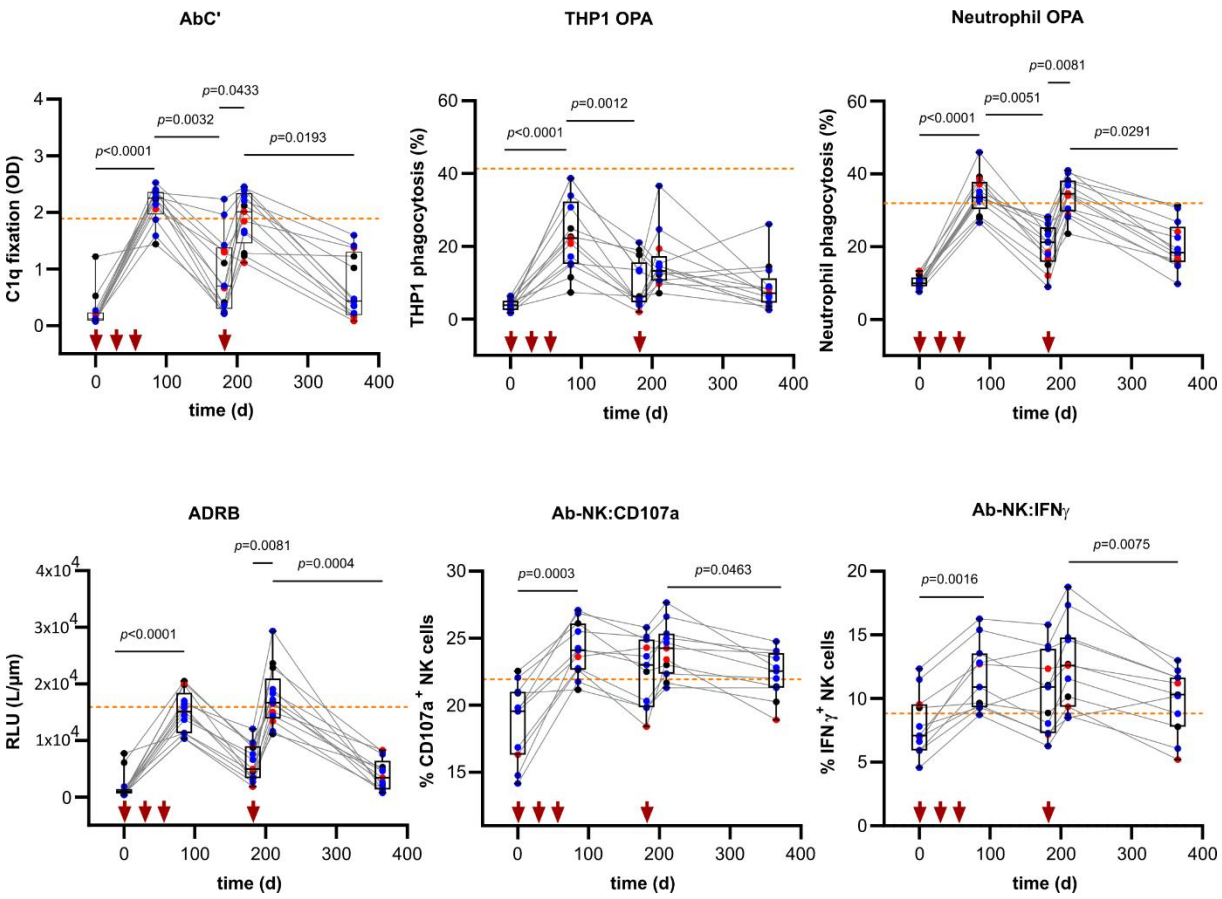

Figure 4.26: Immunization induces functional IgG which is boosted following a 4th dose.
Levels of $MSP1_{FL}$-specific Fc-mediated effector mechanisms of IgG over time. Each data point represents a specific Fc-function measured once with two technical replicates for one sample. Box plots show the median with min/max values. Colours of the dots represent different dose cohorts: red; 25µg (n=3), blue; 50µg (n=7), black; 150µg (n=3). Red arrows indicate the days of immunization (D0, D29, D57, D182). The dashed line indicates reference effector functions of purified IgG from pooled sera from semi-immune individuals from Kisumu, Kenya (NIBSC code 10/198). Statistical differences between timepoints were calculated using Friedman test. CD107a; Fc-mediated natural killer cell degranulation, IFNγ; Fc-mediated natural killer IFNγ production, ADRB; antibody-dependent respiratory burst by donor neutrophils, OPA; opsonic phagocytosis activity of $MSP1_{FL}$-coupled microsphere beads by THP1 cells or donor neutrophils, AbC'; antibody-dependent complement fixation activity.

Moreover, the magnitude of Fc-mediated effector functions from a subset of samples even exceeded the activity levels of IgG from a pool from semi-immune Kenyan adults (AbC'; 77% (n=10), neutrophil OPA; 77% (n=10), ADRB; 46% (n=6), Ab-NK:CD107a; 82% (n=9), Ab-NK:IFNγ; 91% (n=10); however, baseline Ab-NK activity at day 0 was high, for some samples exceeding the activity level of semi-immune Kenyans potentially due to unspecific activation of NK cells. Fc-mediated effector functions declined during the following 4 months but were boosted at day 210, four weeks after a 4th immunization. This boosting of functional activity was statistically significant for AbC' (p=0.0433), neutrophil OPA (p=0.0081) and ADRB (p=0.0081). The level of functional activities significantly declined during the following 6 months (AbC'; p=0.0193, neutrophil OPA; p=0.0291, ADRB; p=0.0004, AbNK:CD107a; p=0.0463 and

Ab-NK:IFNγ; p=0.0075) but stayed above the baseline even 6 months after the last immunization (**Fig. 8.5**)

4.2.3.4 Fc-mediated effector functions are highly correlated with each other and antibody levels

I next wanted to investigate the potential relationship between anti-MSP_{FL} IgG titres and effector functions and as shown in **Figure 4.27A**, I observed strong and positive correlations for IgG and AbC' (r=0.87, 95% CI 0.78-0.92, p<0.0001), THP1 OPA (r=0.80, 95% CI 0.68-0.88, p<0.0001) neutrophil OPA (r=0.91, 95% CI 0.84-0.95, p<0.0001) and ADRB. (r=0.93, 95% CI 0.88-0.96, p<0.0001); however, only moderate correlations (r>0.5) were observed for both Ab-NK readouts. This data highlights that the level of Fc-mediated effector functions is highly dependent on the magnitude of IgG.

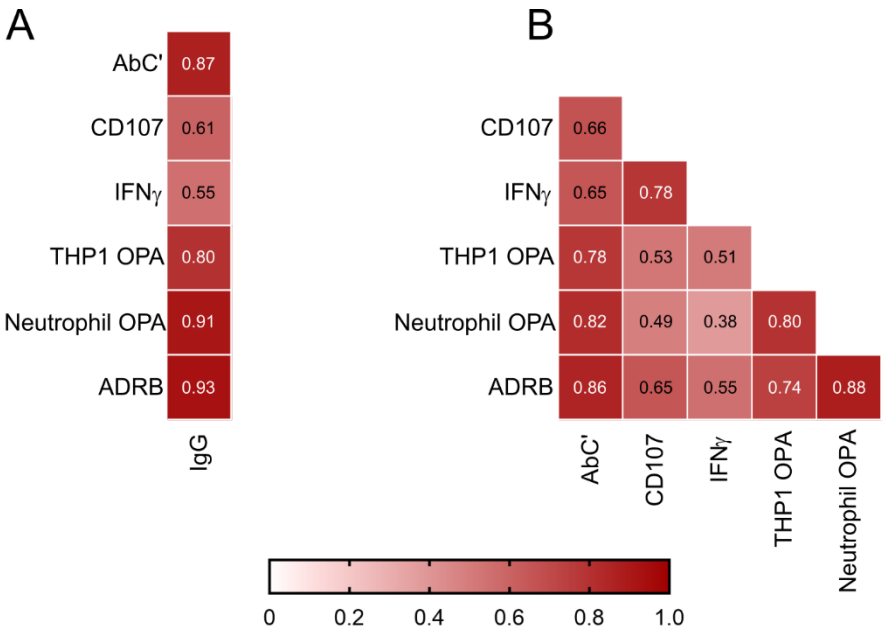

Figure 4.27: Fc-mediated effector mechanisms are highly correlated with IgG titres and with each other.
Heatmaps with correlation matrix showing associations between (**A**) IgG titres and effector functions and (**B**) effector functions with each other. Significant (p<0.0001) spearman rank correlation coefficients for samples (n=13) are highlighted in double digits. The color intensity represents the strength of correlation. AbC'; antibody-dependent complement fixation activity, OPA; opsonic phagocytosis activity of $MSP1_{FL}$-coupled microsphere beads by THP1 cells or neutrophils , ADRB; antibody-dependent respiratory burst by neutrophils, IFNγ; Fc-mediated natural killer IFNγ production, CD107a; Fc-mediated natural killer cell degranulation.

I next investigated the correlations among effector functions and observed high correlations between AbC', THP1 OPA, neutrophil OPA and ADRB (r=0.74-0.88, p<0.0001) while the correlations for the Ab-NK activities were only moderate (r=0.38-0.65, p<0.0001) (**Fig. 4.27B**).

As expected the two readouts of the Ab-NK assay correlated highly with each other (r=0.78, 95% CI 0.65-0.87, p<0.0001).

4.2.4 Anti-MSP1$_{FL}$ antibodies are likely multifunctional

I next wanted to determine the breadth of effector functions of anti-MSP1$_{FL}$ IgG as an indicator of antibody multifunctionality. To do that, effector functions of every study participant 4 weeks after the vaccination were categorized as 'high' or 'low' based on function-specific medians. The Ab-NK was not included in the analysis since only 11 IgG samples were used for that assay due to the limited amount of material. As shown in **Figure 4.28A**, of 19 of 24 vaccinees (79%) showed high functional activity for at least one effector function.

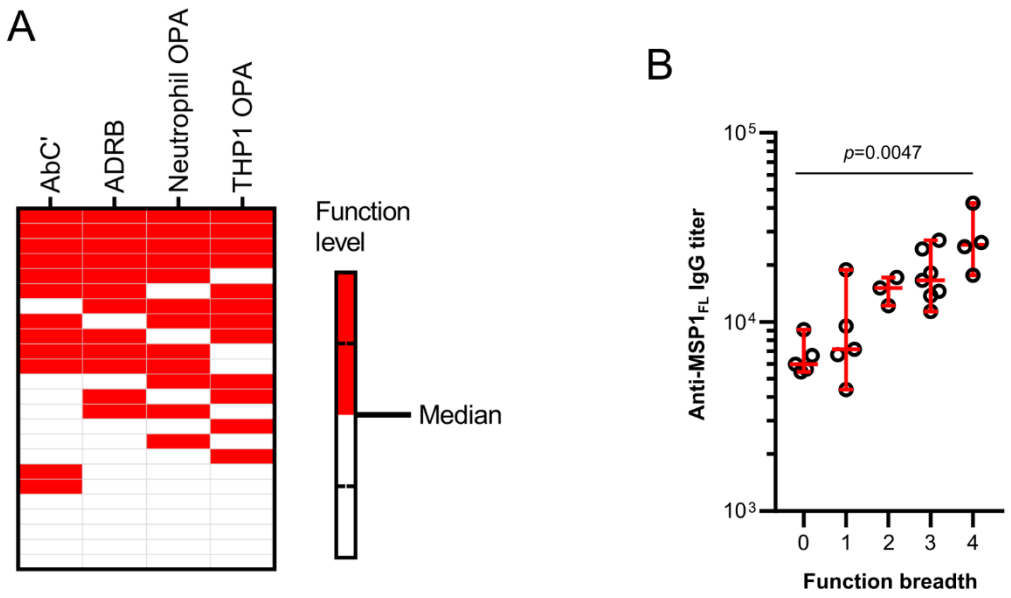

Figure 4.28: Immunization induces IgG with multifunctional activities.
(A) A heatmap showing the activity levels of four Fc-mediated effector functions in vaccinees (n=24) at day 85, four weeks after the last immunization. Responses above a function-specific median are shown in red. Each column is a Fc-mediated function while each row is a single volunteer. AbC'; antibody-dependent complement fixation activity, OPA; opsonic phagocytosis activity of MSP1$_{FL}$-coupled microsphere beads by THP1 cells or neutrophils, ADRB; antibody-dependent respiratory burst by neutrophils. (**B**) Anti-MSP1$_{FL}$ IgG levels were compared between individuals with different levels of MSP1$_{FL}$-specific breadth of function. Each dot represents antibody reactivity of one sample in two technical replicates. Statistical differences were calculated using Kruskal-Wallis test followed by Dunn's multiple comparison test. The IgG titres were obtained from Blank et al., 2020.

Moreover, the breadth of function was dependent on antibody titres (**Fig. 4.28B**), with rising anti-MSP1$_{FL}$ IgG levels resulting into higher breadth scores. These results imply that high titres of anti-MSP$_{FL}$ are necessary for the activation of Fc-mediated effector mechanisms.

4.2.5 N-terminal p83 and C-terminal p42 subunits are major targets of IgG-mediated effector functions

It was previously reported that immunization with SumayaVac1 elicits IgG antibodies that target all MSP1 subunits, particularly the N-terminal p83 and the C-terminal p42 region (Blank et al., 2020). I next wanted to test if those regions are targets of functional antibodies or if Fc-mediated effector functions are directed against specific domains within the MSP1 molecule. Therefore, three representative functional activities (THP1 OPA, ADRB, AbC') against the p83, p30, p38 and p42 subunits of MSP1 were compared between samples collected at day 0 and day 85.

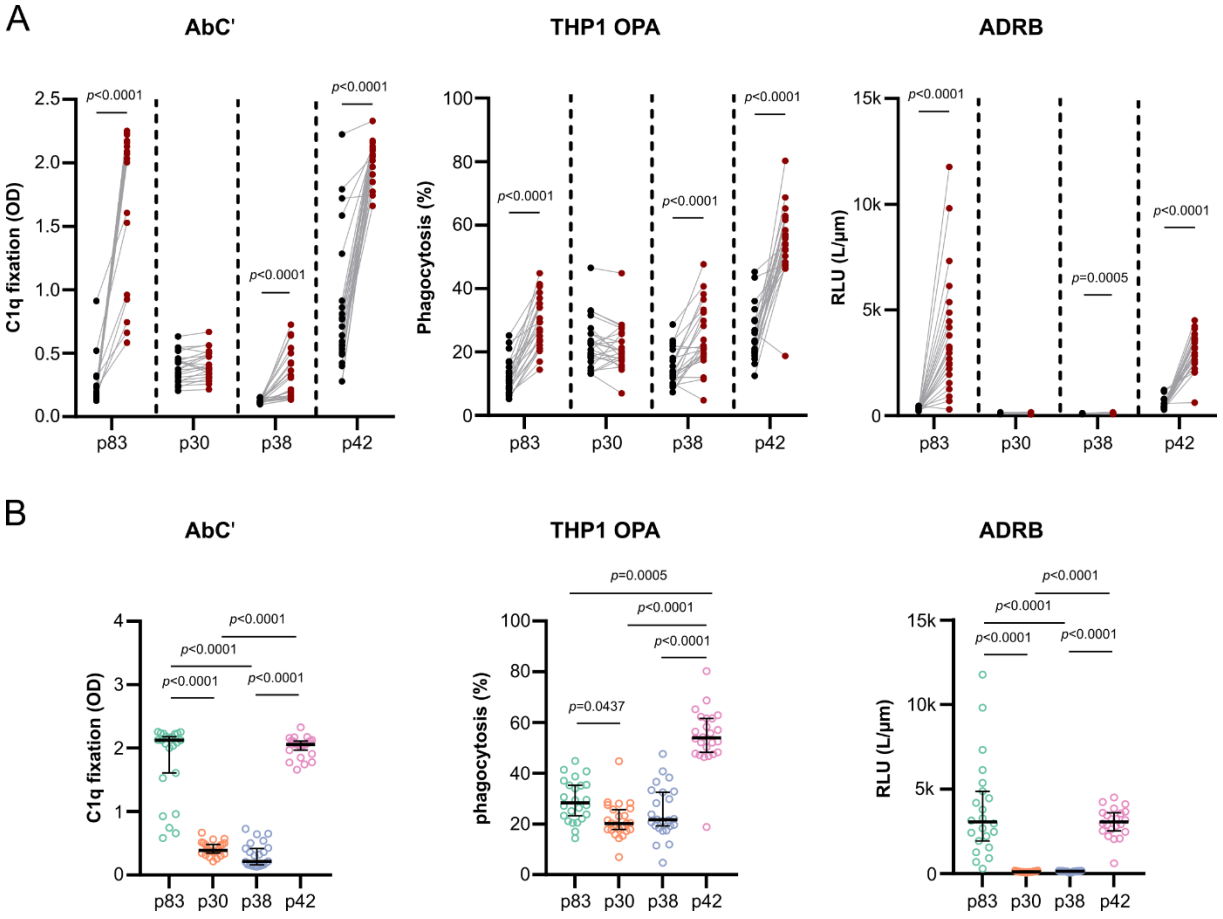

Figure 4.29: Subunits of MSP1 are targets of functional vaccine-induced IgG.
(**A**) Levels of MSP1 subunit-specific effector functions of purified IgG samples (n=23) were compared before (black dots) and after the 3rd vaccination (red dots). (**B**) Levels of effector functions at day 85 were compared between the subunits. Each data point represents a specific Fc-function measured once with two technical replicates for one sample. Error bars represent the median plus 95% confidence intervals. Statistical differences between timepoints were calculated using Wilcoxon matched-pairs signed rank test and for the different subunits using Friedmann test followed by Dunn's multiple comparisons test. ADRB; antibody-dependent respiratory burst by donor neutrophils, OPA; opsonic phagocytosis activity of subunit-coupled microsphere beads by THP1 cells, AbC'; antibody-dependent complement fixation activity.

As shown in **Figure 4.29A**, IgG-mediated AbC', THP1 OPA and ADRB activity against p83, p38 and p42 was significantly (p<0.0001-0.0005) increased upon immunization. Negligible Fc-mediated effector functions were observed for p30. The strongest functional activities were measured for p83 and p42 while the central regions of the molecule did not induce high magnitudes of functions (**Fig. 4.29B**).

The p42 subunit showed the strongest activity for THP1 OPA (p<0.0001-0.0005) compared to the other subunits; however, there were no significant differences between p83 and p42 for the other functions. To note, caution should be taken when comparing the magnitude of responses between the subunits due to potential differences in protein purity and background reactivities as suggested previously. These findings suggest that the net-functional antibody responses against full-length MSP1 are equally driven by the p83 and p42 domain.

4.2.6 Vaccine-induced IgM is multifunctional

4.2.6.1 Activation of Fc-mediated effector functions

It was previously observed that immunization with SumayaVac1 induced IgM at similar kinetics but lower levels to IgG (Blank et al., 2020). Recent findings have strengthened the role of IgM in protective anti-malarial immunity showing that IgM persists over time, is correlated with protection from malaria and inhibits parasite growth in a complement dependent manner (Boyle et al., 2019). This led me to investigate the potential repertoire of IgM-mediated effector functions testing for monocyte OPA, neutrophil OPA, ADRB, Ab-NK activity and complement activation. I used peripheral monocytes isolated from donor PBMCs instead of THP1 cells, since it was previously observed that they can interact with IgM and take up merozoites (Hopp et al., 2021). The purification of IgM was done by Kristin Fürle, Natascha Oßwald and Kalina Chavdarova.

Similarly to IgG, IgM from vaccinees fixed the complement factors C1q and downstream factors including MAC formation (**Fig. 4.30A**). Moreover, I observed that vaccine-induced IgM activated several cellular effector functions including monocyte OPA, neutrophil OPA and both Ab-NK activities (degranulation and IFNγ production) (**Fig. 4.30B**). Interestingly, there was no significant increase in ADRB activity upon full immunization.

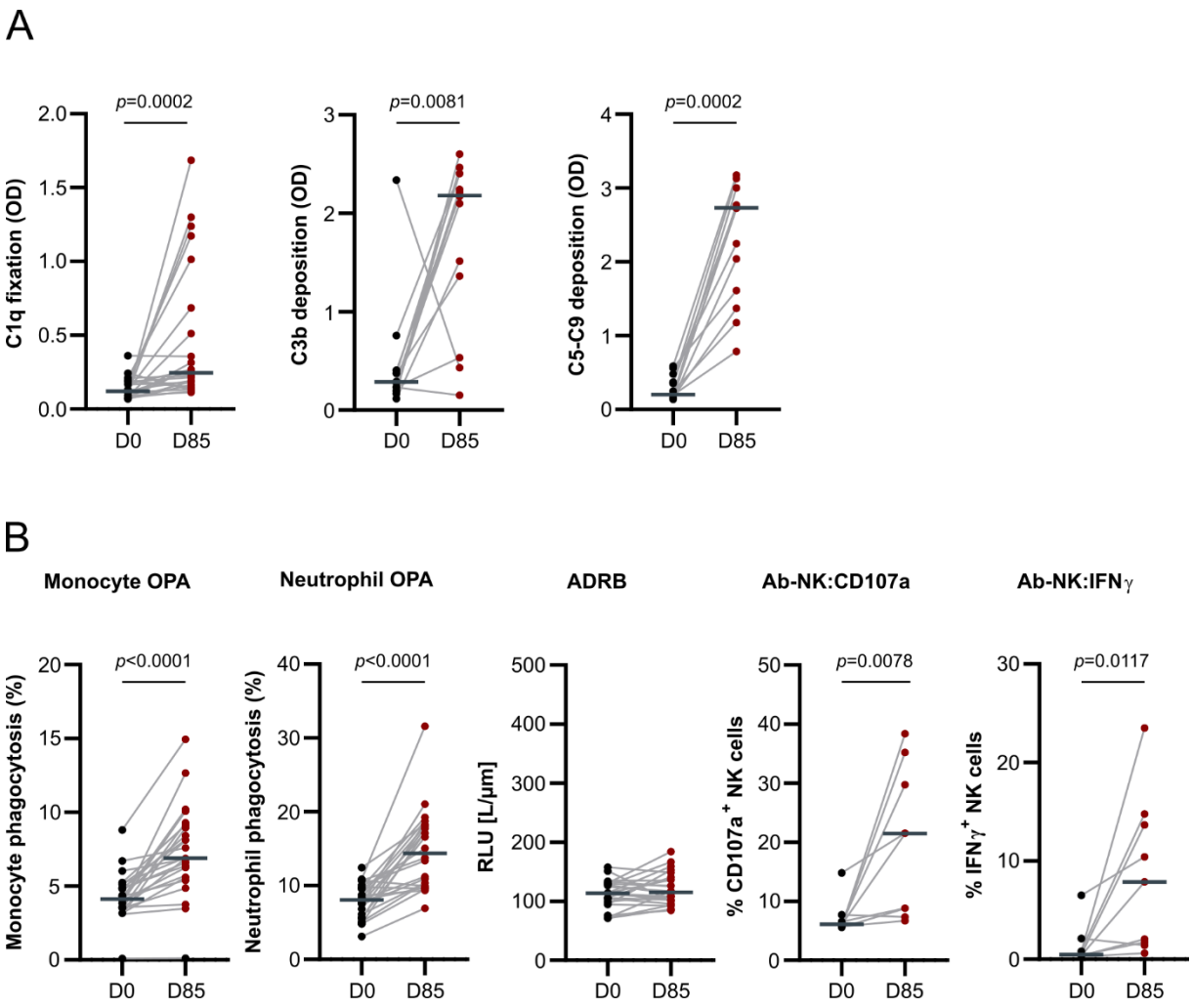

Figure 4.30: Immunization with SumayaVac1 induces IgM antibodies that promote a range of effector mechanisms.
(**A**) Levels of fixation of the complement factors C1q, C3b and C5-C9 (membrane attack complex (MAC)) and (**B**) levels of cellular effector functions of purified IgM samples (n=24 for C1q fixation, n=13 for C3b and C5-C9 deposition) collected before (D0) and after the 3rd vaccination (D85). Each data point represents levels of functions measured once with two technical replicates. Dark grey lines indicate medians. Statistical differences between timepoints were calculated using Wilcoxon matched-pairs signed rank test. CD107a; Fc-mediated natural killer cell degranulation, IFNγ; Fc-mediated natural killer IFNγ production, ADRB; antibody-dependent respiratory burst by donor neutrophils, OPA; opsonic phagocytosis activity of $MSP1_{FL}$-coupled microsphere beads by donor monocytes or donor neutrophils. Data of complement fixation was produced jointly with Dr. Richard Thomson and Kristin Fürle.

4.2.6.1 IgG induces higher levels of Fc-mediated effector functions compared to IgM

I next compared the magnitude of the responses between IgG and IgM collected after the 3rd $MSP1_{FL}$ dose and observed that IgG activated significantly higher (p<0.0001) levels of phagocytosis involving both monocytes and neutrophils as well as AbC' and ADRB compared to IgM (**Fig. 4.31**). No differences in Ab-NK activity were detected. These findings suggest that SumayaVac1 induces higher levels of functional IgG compared to IgM which is in line with the

previously reported titres (Blank et al., 2020). However, these results need to be interpreted carefully due to potential confounders (day to day variation of assays and the different concentrations of IgM and IgG used for these assays).

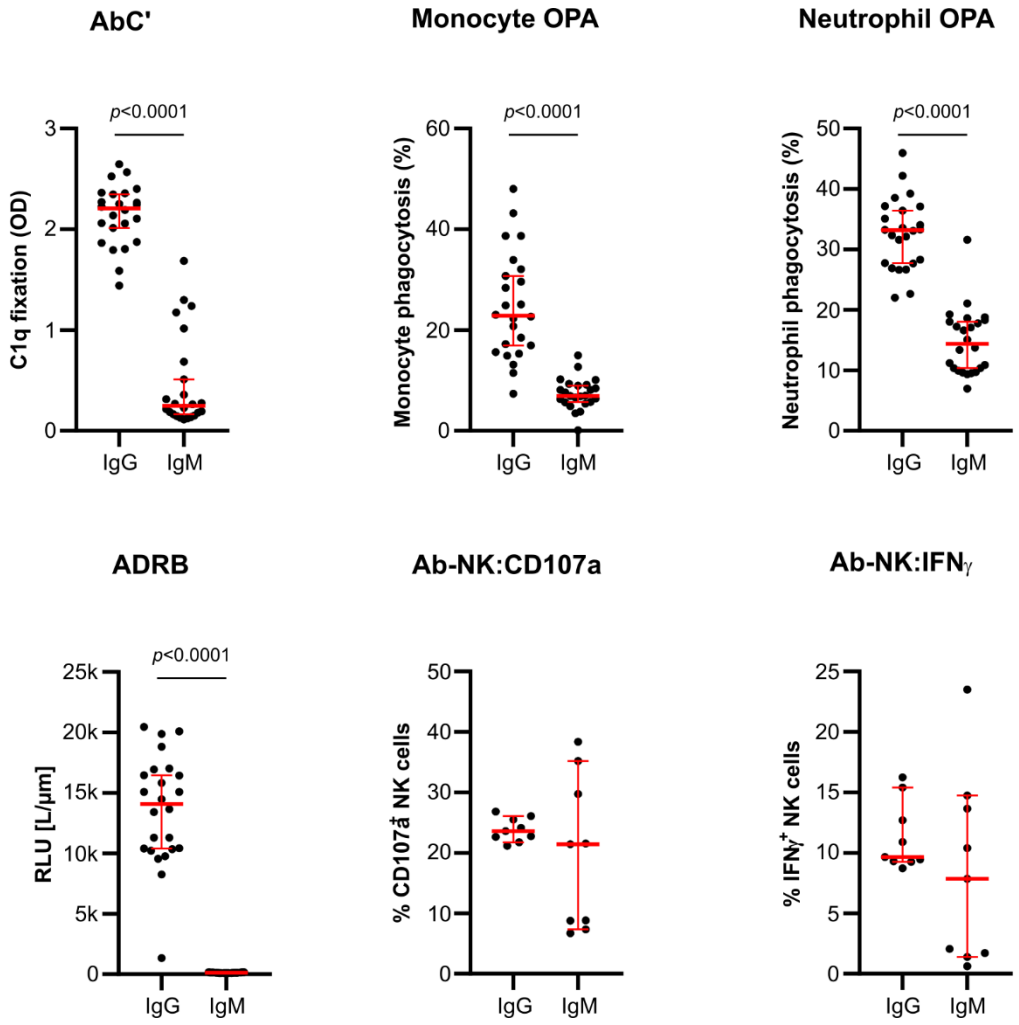

Figure 4.31: IgG induces higher levels of Fc-mediated effector functions compared to IgM. Levels of functional activity was compared between anti-MSP1$_{FL}$ IgG and IgM samples post-immunization (D85). Each data point represents levels of functions measured once with two technical replicates. Statistical differences between antibody isotypes were calculated using Wilcoxon matched-pairs signed rank test. CD107a; Fc-mediated natural killer cell degranulation (n=9), IFNγ; Fc-mediated natural killer IFNγ production (n=9), ADRB; antibody-dependent respiratory burst by donor neutrophils (n=24), OPA; opsonic phagocytosis activity of MSP1$_{FL}$-coupled microsphere beads by donor monocytes or donor neutrophils (n=24).

4.2.6.2 Kinetics of Fc-mediated effector functions

Since I showed that immunization with SumayaVac1 induced several IgM-mediated effector functions involving the complement system and multiple innate immune cells, I wanted to assess the induction and decay kinetics of those activities.

I observed similar dynamics compared to IgG, however, the differences between timepoints following day 85 were insignificant due to the high variations and low level of activity for some samples (**Fig. 4.32**).

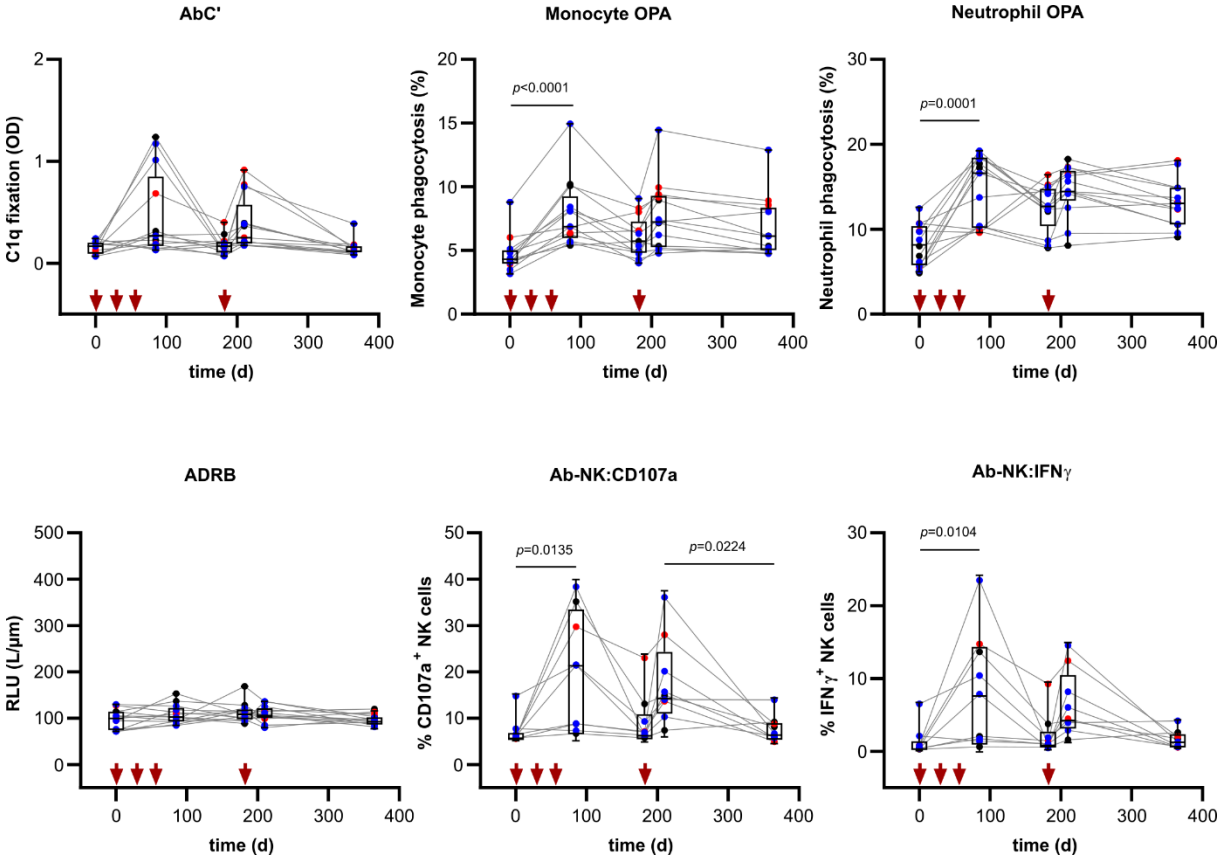

Figure 4.32: Immunization induces functional IgM.
Levels of $MSP1_{FL}$-specific Fc-mediated effector mechanisms of IgM over time. Each data point represents a specific Fc-function measured once with two technical replicates for one sample. Box plots show the median with min/max values. Colours of the dots represent different dose cohorts: red; 25µg (n=3), blue; 50µg (n=7), black; 150µg (n=3). Red arrows indicate the days of immunization (D0, D29, D57, D182). Statistical differences between timepoints were calculated using Friedman test. CD107a; Fc-mediated natural killer cell degranulation, IFNγ; Fc-mediated natural killer IFNγ production, ADRB; antibody-dependent respiratory burst by donor neutrophils, OPA; opsonic phagocytosis activity of $MSP1_{FL}$-coupled microsphere beads by THP1 cells or donor neutrophils, AbC'; antibody-dependent complement fixation activity.

4.2.7 Anti-$MSP1_{FL}$ antibodies do not inhibit parasite growth

Blank et al., have previously shown that vaccine-induced $MSP1_{FL}$ antibodies failed to inhibit parasite growth in a standard growth inhibition assay (GIA) (Blank et al., 2020). Although it was hypothesized that the vaccine failed to induce antibodies directed against specific epitopes associated with GIA activity, other studies suggested that high concentrations of anti-MSP1 antibodies are needed to observe GIA activity of antibodies directed against MSP1 (Jäschke et al., 2017; Woehlbier et al., 2006).

To test if the lack of GIA activity could be the result of low $MSP1_{FL}$ antibody concentrations or interference of non-malarial IgG, I purified $MSP1_{FL}$-specific antibodies (IgG with IgM) from a pool of post-immunization sera from vaccinees (n=24) and from immunized rabbits (n=4) using a previously established protocol (Winter 2022, Bachelor thesis). Anti-$MSP1_{FL}$ antibodies were tested in a standard 1-cylce (48h) GIA at concentrations up to 5mg/ml. I used anti-AMA1 IgG as a positive and pre-immune IgG from the same volunteers as a negative control.

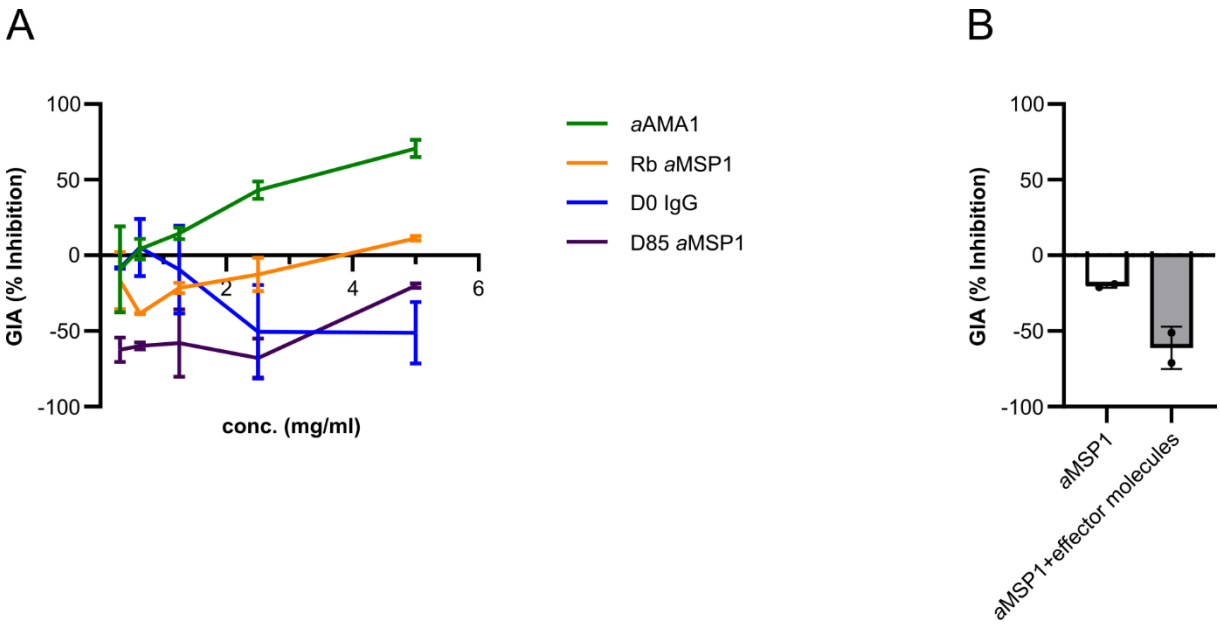

Figure 4.33: Anti-$MSP1_{FL}$ antibodies do not inhibit growth.
(A) Levels of growth inhibition activity of purified antibodies at concentrations ranging from 0.3mg/ml to 5mg/ml in a 1 cycle (48h) growth inhibition assay (GIA). GIA activity was measured by flow cytometry as the percentage growth in relation to parasites without antibodies and white blood cells (WBCs)**.** aAMA1; purified Ig from apical membrane antigen 1 (AMA1) immunized rabbits were used as a positive and pooled IgG from volunteers before immunization (D0 IgG) as negative a negative control, Rb aMSP1; purified $MSP1_{FL}$ antibodies from $MSP1_{FL}$ immunized rabbits, D85 aMSP1; purified $MSP1_{FL}$ antibodies from a pool of vaccinees collected at day 85.(**B**) Levels of growth inhibition activity of purified human anti-$MSP1_{FL}$ antibodies at 5mg/ml with or without effector molecules (WBCs at 1:100 ratio RBCs with normal human serum from malaria-naïve donors). Data points represent mean values in duplicate measurements. Error bars represent standard deviations.

Previously, purified IgG from rabbits vaccinated with $MSP1_{FL}$ have demonstrated strong growth inhibition activity achieving parasite reductions of up to 90% at 10mg/ml total IgG (Blank et al., 2020). However, as shown in **Figure 4.33A**, purified anti-$MSP1_{FL}$ antibodies from rabbits at 5mg/ml only showed 10% inhibition activity while no growth inhibition was observed at lower concentrations. Unfortunately, the rabbit antibodies used by Blank and colleagues were not available and other rabbit sera were used for antibody purification which does not allow direct assay-to-assay comparison. Similarly, no growth inhibition was observed for purified anti-$MSP1_{FL}$ antibodies from study participants. These findings show that anti-$MSP1_{FL}$ antibodies have no direct effect on parasite growth.

We and others have previously shown that the addition of NK cells and complement factors reduce merozoite invasion and parasite growth (Boyle et al., 2015; Odera et al., 2021). To test wether effector cells (monocytes, neutrophils and NK cells) in combination with complement factors have an effect on parasite growth in the presence of anti-$MSP1_{FL}$ antibodies, total white blood cells (WBC) together with human serum collected from malaria-naïve donors as a source of complement factors were co-cultured with parasites and antibodies for 48 hours. Surprisingly the addition of WBC with malaria-naïve serum increased the parasitemia after 1-cycle most likely to the addition of nutrients supplied by extra serum (**Fig. 4.33B**).

That outcome shows that despite vaccine-induced anti-$MSP1_{FL}$ antibodies activate a range of effector functions, these functions do not reduce parasite growth *in-vitro*.

5.0 DISCUSSION

5.1 CHMI-SIKA study

5.1.1 MSP1 as a correlate of protection

For more than 30 years, MSP1 has been studied in the context of naturally acquired immunity (NAI) and as a potential vaccine candidate for *Plasmodium falciparum* malaria. MSP1 takes an essential role in the erythrocytic lifecycle and hence targeting this protein by antibodies has been considered as a key strategy to prevent invasion of red blood cells and thus clinical symptoms of malaria. However, sero-epidemiological studies investigating the role of MSP1 for NAI have not led to a coherent picture, in part due to differences in experimental procedures. A systematic review showed that only antibodies against the conserved C-terminal p19 subunit were associated with a reduced risk of developing symptomatic malaria while there was no evidence of a protective effect for the polymorphic N-terminal MSP1 block 2 (Fowkes et al., 2010).

5.1.2 Quality of antigens

Notably, all human trials and the majority of sero-epidemiological studies focused on C-terminal (p42 or p19) (Egan et al., 1995; Ellis et al., 2010; Malkin et al., 2007; Ogutu et al., 2009; Richards et al., 2013; Stanisic et al., 2009) or N-terminal (MSP1 block 2) subunits (Cavanagh et al., 2001; Cavanagh et al., 2004) rather than the full-length protein and therefore might have missed approximately 80% of the protein and epitopes that could be relevant for a protective immune response. The expression of full-length MSP1 has been shown to be challenging due to its size, however, independent groups managed the successful expression of high quality full-length MSP1 in HEK293 cells (Crosnier et al., 2013) and *E. Coli* (Kauth et al., 2003; Kauth et al., 2006) which enabled me to perform in-depth analysis of full-length MSP1.

5.1.3 Antibody reactivity in semi-immune adults

By using samples from a controlled human malaria infection study with semi-immune Kenyan adults (CHMI-SIKA), I showed that the whole MSP1 molecule is highly immunogenic including the well-studied p42 as well as the less well studied p83 subunit. Moreover, using a linear peptide array did not only confirm the presence of linear B cell epitopes across the whole protein but highlighted that in contrast to volunteers who required treatment post sporozoite

challenge, IgG from non-treated volunteers preferentially targeted conserved or dimorphic epitopes suggesting the presence of acquired strain-transcending antibodies. The high correlation of IgG antibodies between the two main MSP1 variants (MAD20 and K1) furthermore suggested the presence of cross-reactive antibodies. Several studies reported that humoral responses against MSP1 are mostly strain-specific, especially against the polymorphic block 2 region (Cavanagh et al., 1998; Conway et al., 2000). Moreover, vaccinations of *Aotus* monkeys with different variants of the p42 subunit protected only from homologues challenge (Lyon et al., 2008). In contrast, immunization with native $MSP1_{FL}$ purified from lysate of the K1 strain resulted in protection of monkeys from challenge with the heterologous Palo Alto strain (similar to MAD20) (Etlinger et al., 1991). These observations support the view that the use of full-length MSP1 might overcome problems of strain-specific responses due to additional conserved epitopes at the N-terminus.

5.1.4 IgG subclass data

Our results show that the anti-$MSP1_{FL}$ IgG response is dominated by cytophilic IgG3 followed by IgG1 with significantly less magnitudes of IgG2 and IgG4. This is in line with data from several studies involving both the polymorphic N-terminal (MSP1 block 2) and conserved C-terminal (p19) region of MSP1. It is well-established that cytophilic antibodies confer protection from malaria through cell surface Fc gamma receptor ($Fc\gamma R$) engagement on innate effector cells such as monocytes (Hill et al., 2013; Kana et al., 2019; Musasia et al., 2022; Osier et al., 2014a), neutrophils (Joos et al., 2010) or NK cells (Odera et al., 2021), as well as fixing complement (Boyle et al., 2015; Reiling et al., 2019).

5.1.5 Mechanisms in semi-immune adults and correlation with protection

Antibodies against blood stages have been shown to limit parasitemia and protect against clinical symptoms of malaria (Cohen et al., 1961); however, the precise mechanisms behind a protective response are still debated.

The GIA has been considered as the ‘gold-standard’ to evaluate blood stage vaccine candidates including MSP1 (Blackman et al., 1990; Ellis et al., 2010; Malkin et al., 2007; O'Donnell et al., 2001). However, there is an increasing body of evidence showing that the GIA is not a reliable correlate of protection (Dent et al., 2008; Duncan et al., 2012; McCallum et al., 2008; Murungi et al., 2016; Nkumama et al., 2022). Moreover, several vaccine candidates that were prioritized based on GIA activity failed to provide protective efficacy in clinical trials (Duncan et al., 2012; Ogutu et al., 2009; Payne et al., 2016).

Fc-mediated effector functions have been associated with protection from malaria in several independent sero-epidmeological studies (Boyle et al., 2015; Hill et al., 2013; Joos et al., 2010; Odera et al., 2021; Osier et al., 2014a) and emerging data shows that effector functions might be even stronger correlates of protection than neutralization which supports a paradigm shift in the understanding of mechanisms behind naturally acquired immunity (Nkumama et al., 2022; Reiling et al., 2019). Importantly, research from our group suggests that no single mechanism adequately accounts for complete immunity but rather that a combination (breadth) of effector functions is critically important (Nkumama et al., 2022) which implies that vaccine candidates that induce multifunctional responses might surpass protective effects of candidates that induce only single antiparasitic protective mechanisms.

Several independent studies have identified a list of merozoite antigens as targets of opsonizing antibodies that induce Fc-mediated effector functions, including the conserved C-terminal part of MSP1 (p19). Antibodies directed against p19 activated the complement cascade which in turn resulted in complement-mediated invasion inhibition (Boyle et al., 2015) and was associated with protection from malaria (Reiling et al., 2019). My analysis using samples from the CHMI study showed that complement fixing antibodies target the whole MSP1 molecule emphasizing that complement fixation is not restricted to the C-terminus but involves the N-terminal p83 and central p30 and p38 subunits as well.

In another study, naturally acquired antibodies activated opsonic phagocytosis of beads coupled with p19 which correlated with a significantly reduced risk of clinical malaria (Kana et al., 2019). Both the C-terminal p19 as well as the N-terminal p83 subunit have been shown to contribute substantially to an ADRB response against merozoites in independent studies (Jäschke et al., 2017; Joos et al., 2015). Notably, the depletion of antibodies against full-length MSP1 in semi-immune adults from Burkina Faso, resulted in approximately 50% reduction of ADRB activity against merozoites. Together these studies highlight that anti-MSP1 antibodies could contribute to a protective immune response in several independent mechanisms and that the epitopes of opsonizing antibodies are distributed across the whole molecule instead of being restricted towards the C-terminal domain.

Using samples from the CHMI study, I showed for the first time that $MSP1_{FL}$ is a key target of opsonizing antibodies that induce several Fc-mediated effector functions including complement activation, phagocytosis, respiratory burst of neutrophils, degranulation and IFNγ production of NK cells which in turn are strongly correlated with protection from malaria. Furthermore, my analysis showed that the correlations were comparable among effector functions which suggests a similar or equal contribution to protection. Moreover, I observed

high intercorrelations among the effector functions suggesting that antibodies against $MSP1_{FL}$ are multifunctional.

I observed that the breadth of effector functions induced by anti-$MSP1_{FL}$ antibodies was the strongest correlate of protection in line with previous observations from our group using whole merozoites (Nkumama et al., 2022) which suggests that MSP1 could be a major contributor to total Fc-mediated functional activities against merozoites. This was further suggested in my study by showing that $MSP1_{FL}$ consistently induced the strongest level of functional activities (AbC', OPA and ADRB) among merozoite antigens that have previously emerged as important antigens for protection from the analysis of our custom KILchip merozoite microarray platform (Nkumama 2021, PhD thesis). Although other antigens were also targeted by opsonizing functional antibodies such as the vaccine candidate Pf3D7_1136200, the magnitude of effector functions of $MSP1_{FL}$ exceeded all of the other candidates. This suggests that although many antigens are targets of functional antibodies, $MSP1_{FL}$ might be one of the most dominant contributors to such a functional immune response.

5.1.6 Antibody kinetics

I measured the kinetics of anti-$MSP1_{FL}$ antibodies after sporozoite challenge. The antibody levels did not significantly change for non-treated volunteers during follow up; however, I observed a greater magnitude of responses against $MSP1_{FL}$ in non-treated volunteers, especially those with low baseline antibody levels 35 days after challenge. Moreover, the antibody levels reached magnitudes of non-treated CHMI volunteers. The increase in antibody levels upon sporozoite exposure (i.e., boosting) could be an indication for the presence of memory B cells that differentiate and proliferate in antigen secreting B cells (ASC) (Deenick et al., 2013; Good et al., 2009) and several studies have shown that memory B cells can persist independently of the level of circulating antibodies (Hammarlund et al., 2017; Ndungu et al., 2012; Wipasa et al., 2010). The characterization of the properties of anti-$MSP1_{FL}$ specific memory B cells was beyond the scope of this study. For protection from malaria, my study however suggests that high titres of pre-exposure anti-$MSP1_{FL}$ antibodies are necessary. It would be interesting to study potential protective effects of anti-$MSP1_{FL}$ antibodies that were induced upon re-challenge.

5.1.7 The role of IgM in semi-immune adults

I showed that the antibody-mediated response was predominated by IgG; however, anti-$MSP1_{FL}$ IgM was detectable although the volunteers had presumably life-long exposure to malaria parasites. While the role of IgG for a protective anti-malarial response has been known

for more than 60 years (Cohen et al., 1961). IgM has mostly been considered as an early response against malaria re-infection (Krishnamurty et al., 2016) and as a marker of exposure instead of being a true correlate of protection (Orlandi-Pradines et al., 2006). However, recent studies have shown that IgM persists over time and contributes to parasite clearance by fixing complement (Boyle et al., 2019; Zenklusen et al., 2018), neutralization and phagocytosis (Hopp et al., 2021). Although these findings demonstrate that the role of IgM for NAI and vaccine-induced immunity might have been underappreciated, studies on the presence of the IgM receptor (FcµR) distribution among effector cells such as macrophages and NK cells are conflicting (Honjo et al., 2013; Hopp et al., 2021; Kubagawa et al., 2009; Lang et al., 2013; Shima et al., 2010; Uher et al., 1981). partially because of different levels of cell activation and hence expression of FcµR. Due to the limited material, I was not able to measure the repertoire of functional activities for specific isotypes. Although the magnitudes of IgM cannot be directly compared to IgG due to different secondary detection antibodies, I carefully speculate that anti-$MSP1_{FL}$ IgM might play a minor role in NAI to malaria, as the correlations between IgM and total functional activity of serum antibodies was low, similar to the level of IgM compared to IgG.

5.1.8 No protection despite high level of Fc-mediated functions

The majority of volunteers that were treated had the lowest breadth score of functional activities against $MSP1_{FL}$. Not surprisingly though, 19% of volunteers with the highest breadth score required treatment as well. Although MSP1 is the most abundant surface antigen on merozoites based on copy numbers (Gilson et al., 2006), other merozoite antigens have been identified as targets of antibodies (Kana et al., 2019; Osier et al., 2008; Reiling et al., 2019; Richards et al., 2013), including the antigens that I evaluated in this study (Nkumama 2021, PhD thesis). Additionally, it is suggested that combinations of antibody responses against several blood antigens are likely to be even more relevant for a protective anti-malarial response than single antigens (Kana et al., 2019; Odera et al., 2021; Osier et al., 2008; Reiling et al., 2019; Richards et al., 2013). Although antibody responses against CSP from sporozoites have been correlated with protection in several studies (Hamre et al., 2020; Seaton et al., 2021)(Hamre et al., 2020), (Seaton et al., 2021), we were not able to find strong associations with protection of anti-CSP antibodies with time to treatment in this CHMI study (Nkumama 2021, PhD thesis). This suggests that pre-erythrocytic antibodies might play only a minor role in NAI. Notably, antigens of other blood stages such as variant specific surface antigens (VSA) of late blood stages (Kimingi et al., 2022) and EBA175 alongside others found on ring stages (Musasia et al., 2022) have been associated with reduced risk of malaria in the CHMI-SIKA study. As such, antibodies targeting a spectrum of antigens and/or antigens from different

developmental stages might work in synergy to confer even stronger protection. However, combination antigen vaccines, including those with MSP1, failed to high protective efficacies in clinical trials (Genton et al., 2002; Sheehy et al., 2012; Sirima et al., 2016) which implies that better understanding of antigen selection and formulation might be necessary for developing more effective next-generation multi-antigen vaccines.

To the best of my knowledge, I tested the largest set of functional activities of antibodies targeting one single blood stage antigen in a single study. However; other antibody functions that were previously reported to be important for parasite clearance such as neutrophil-mediated phagocytosis (Garcia-Senosiain et al., 2021), antibody-dependent cellular inhibition by monocytes (ADCI) (Tiendrebeogo et al., 2015) or ADCC by γδ T cells (Farrington et al., 2020) were not assessed.

5.2 Phase Ia study with SumayaVac1

5.2.1 MSP1 vaccines

Although immunizations with MSP1 showed partial or complete protection in animal models including mice (Daly and Long, 1995; Tian et al., 1997) and non-human primates (Herrera et al., 1990; Lyon et al., 2008; Perrin et al., 1984), MSP1-based vaccines have yet to demonstrate efficiency in human clinical trials. Notably, all MSP1-based vaccines focused on the C-terminal part, as delineated by p42 and p19 and therefore neglected the majority of the whole protein including conserved epitopes at the N-terminal p83 subunit. Furthermore, most of MSP1-based vaccines were only evaluated for their potential to induce neutralizing antibodies (Chitnis et al., 2015; Ellis et al., 2010; Ellis et al., 2012; Malkin et al., 2007; Ockenhouse et al., 2006).

5.2.2 Lack of GIA activity

Immunization of malaria-naïve adults with the full-length MSP1 vaccine, SumayaVac1, elicited high titres of IgG and IgM; however, similar to previous vaccines, SumayaVac1 failed to induce neutralizing antibodies (Blank et al., 2020). Different explanations for the lack of GIA activity have been raised. First, antibodies elicited by immunization might not target critical epitopes that are involved in MSP1 processing or protein interaction and thus do not inhibit invasion as previously highlighted in other studies (Blackman et al., 1994; Lin et al., 2016). Second, several studies have shown that high anti-MSP1 antibody titres are necessary for growth inhibition (Jäschke et al., 2017; Wilson et al., 2011) most likely due to the abundance of the protein. Although there were differences in the linear B cell epitope repertoire between GIA-inactive

IgG from humans and GIA-active IgG from immunized rabbits (Blank et al., 2020), I explored the second option by purifying anti-MSP1$_{FL}$ antibodies from a pool of sera collected 4 weeks after the 3rd immunization. However, even at high concentrations of purified anti-MSP1$_{FL}$, no significant reduction in parasite growth was observed, even for vaccine-induced rabbit antibodies. Importantly, sera from rabbits that were used in the previous study (Blank et al., 2020) were not available and therefore, no comparisons between the two experiments can be made. Furthermore, since it was shown that SumayaVac1 elicits a broad spectrum of antibodies targeting the whole molecule, antibodies might compete for the binding to neutralizing epitopes. This has been recently shown in competition GIAs using human monoclonal antibodies (hmAb) directed against overlapping conformational epitopes within the p19 subunit (Patel et al., 2022). The functional activity of neutralizing hmAbs was gradually reduced in the presence of interfering non-neutralizing antibodies that bound with high affinity to overlapping epitopes which prevented parasite clearance. Since immunization with SumayaVac1 elicited a broad range of antibodies, with potentially neutralizing and non-neutralizing activity, the lack of GIA activity is not surprising. However, more studies are needed to confirm this.

5.2.3 Fc-mediated functions

Although an MSP1-based protective immune response might include Fab-dependent neutralization, there is an increasing body of evidence that Fc-mediated effector functions are critical for protective anti-malarial responses (Boyle et al., 2015; Garcia-Senosiain et al., 2021; Joos et al., 2010; Musasia et al., 2022; Nkumama et al., 2022; Odera et al., 2021; Osier et al., 2014a). Moreover, I have highlighted previously that full-length MSP1 is a major target of naturally acquired opsonizing antibodies with multifunctional activities that are strongly associated with protection.

Using samples from the recently conducted phase Ia trial, I showed that immunization with SumayaVac1 elicits IgG that interacts with several innate effector cells including neutrophils, monocytes and NK cells resulting in phagocytosis (mediated by monocytes and neutrophils), respiratory burst as well as degranulation and IFNγ expression. Furthermore, post-immunization IgG fixed C1q and the downstream factor C3b of the classical complement cascade resulting in activation of the membrane attack complex.

Remarkably, the magnitude of functional activities was similar to those of semi-immune volunteers from Kenya who had presumably life-long exposure to *Plasmodium falciparum* parasites. Importantly to note, I measured the functional activities against recombinant MSP1$_{FL}$ but not against whole merozoites to avoid variations in merozoite preparations; however, in

previous experiments, post-immunization IgG induced similar levels of ADRB activity against merozoites compared to semi-immune adults (Blank et al., 2020) which underscores the strong contribution of anti-MSP1$_{FL}$ antibodies to total functional activities against whole parasites.

Furthermore, I observed that all anti-MSP1$_{FL}$-mediated effector functions were highly correlated with each other and the IgG titre which underscores the capacity of SumayaVac1 to elicit multifunctional antibodies. This was supported by analysing the breadth of effector functions where I showed that volunteers with high anti-MSP1$_{FL}$ titres post-immunization had higher breadth scores compared to volunteers with lover antibody titres. This further strengthens the view that high antibody levels are needed for detectable and strong multifunctional anti-parasitic responses.

Previous studies have shown that effector functions, including complement or NK cells could significantly reduce invasion of merozoites (Boyle et al., 2015; Odera et al., 2021) which suggests that Fc-mediated effector functions target parasites quickly enough before they invade RBCs. However, the addition of complement did not reduce parasite invasion or growth in previous experiments (Blank et al., 2020). Moreover, the addition of donor white blood cells together with human serum as a source of complement factors did not reduce parasitaemia in the presence of anti-MSP1$_{FL}$ antibodies. The reasons for that observations could only be speculated. The most obvious explanations are difficulties in the experimental set-up, since the starting parasitaemia as well as the ratio of WBC to RBC are critical parameters in this assay.

5.2.4 Subunit-specific functional activity

In contrast to all other MSP1-based vaccines, SumayaVac1 consists of the full-length MSP1 molecule and therefore includes the approximately 80% of epitopes that were neglected in previous clinical trials. I showed that functional antibodies predominantly targeted the C-terminal p42 as well as the N-terminal p83 subunit which contains several conserved regions (block1,3 and 5). This does not only underscore that the whole molecule contributes to a functional anti-parasitic immune response as suggested by previous studies (Jäschke et al., 2017; Woehlbier et al., 2006) but is also of paramount interest for strain-transcending immunity. Vaccination with SumayaVac1 elicited opsonizing antibodies that recognize both main strains (MAD20 and K1) of *Plasmodium falciparum* and induced neutrophil respiratory burst independently of the parasite strain (Blank et al., 2020). These results highlight the potential of SumayaVac1 to induce functional cross-reactive antibodies which have been considered as bottlenecks of vaccine efficacy in malaria endemic regions (Ogutu et al., 2009, Genton et al., 2002).

5.2.5 Antibody properties for Fc receptor interactions

Post translational modifications at the Fc part have been shown to be important for the interaction of IgG with their Fc gamma receptors (FcγR) (Houde et al., 2010). Particularly N-linked glycans at the conserved position 297 (Asn297) located between the CH2/CH3 domains have been shown to modulate antibody interactions with FcγR (Vidarsson et al., 2014). It is well established that lack of core fucose is associated with stronger binding to FcγRIIIa (Ferrara et al., 2011), expressed on NK cells, neutrophils and monocytes resulting in increased ADCC and phagocytosis (Kapur et al., 2014; Shields et al., 2002). Interestingly it was previously shown that naturally acquired IgG to VAR2CSA, a member of the PfEMP1 family, was predominantly afucosylated while vaccination with subunit VAR2CSA resulted in fucosylated IgG (Larsen et al., 2021). Only IgG from semi-immune individuals resulted in NK cell degranulation which was absent for IgG from vaccinees indicating immunomodulatory differences between naturally acquired and vaccine-induced immunity. The identification of the fucosylation status in semi-immune adults and vaccinees was beyond the scope of this study; however, we observed strong functional activities of IgG from $MSP1_{FL}$ vaccinated individuals reaching similar levels of that of semi-immune volunteers which suggests that both antibodies could bind FcγRs with high affinity.

5.2.6 The role of IgM in vaccine-induced immunity

It was previously demonstrated that vaccination with SumayaVac1 induced high IgM titres that similarly to IgG persisted for more than 6 months after the last vaccination (Blank et al., 2020). As previously mentioned, recent studies have highlighted that IgM can contribute to a long lived antiparasitic response by limiting parasite infections due to complement activation or monocyte phagocytosis (Boyle et al., Zenklusen et al., 2018, Hopp et al., 2021). Intrigued by the long-lived IgM titres and its potential role in antimalarial immunity, I performed in-depth characterization of IgM functionality using a range of *in-vitro* functional assays testing for OPA activity of donor monocytes and neutrophils, ADRB as well as Ab-NK activity. Surprisingly, similar to IgG but significantly lower, vaccine-induced IgM was capable of activating monocyte phagocytosis and activation of NK cells resulting in degranulation and IFNγ production. Interestingly, I observed that IgM induced neutrophil phagocytosis but no respiratory burst activity was observed in the ADRB assay. The finding that IgM mediates several anti-parasitic functions is almost expected, yet surprising, since research on the distribution of the IgM Fc-receptor (FcμR) on innate immune cells has led to conflicting results (Honjo et al., 2013; Hopp et al., 2021; Kubagawa et al., 2009; Lang et al., 2013; Shima et al., 2010; Uher et al., 1981). In line with the previously established role of IgM-mediated complement fixation against

merozoites, I observed that vaccine-induced IgM fixed the whole classical complement cascade resulting in formation of the membrane attack complex. This data supports the recent findings that IgM contribute to an antiparasitic immune response by inducing several effector functions. However, although the effector functions mediated by IgG or IgM cannot directly be compared due to differences in antibody concentration, the levels of functional activities were relatively low compared to IgG; therefore, I speculate that vaccine-induced IgG is the predominant inducer of effector functions against $MSP1_{FL}$ which is in line with the results from the CHMI-SIKA study.

6.0 CONCLUSION AND RECOMMENDATIONS

6.1 Summary of findings

To my knowledge I used the most complete characterization of antibody functionality of a malaria blood stage vaccine candidate. I showed that naturally acquired antibodies from semi-immune adults against full-length MSP1 induced a broad spectrum of Fc-mediated effector functions including phagocytosis, complement fixation, respiratory burst, degranulation and IFNγ production that were highly associated with protection from sporozoite challenge. Moreover, IgG and IgM induced by vaccination with the $MSP1_{FL}$-based vaccine, SumayaVac1, activated the same panel of Fc-mediated effector functions reaching similar magnitudes of semi-immune adults from Kenya (**Fig. 6.1**). Both studies highlighted that high titres of anti-$MSP1_{FL}$ are required for high breadth of effector functions which was the strongest correlate of protection in the CHMI study. No Fab-mediated neutralization activity of anti-$MSP1_{FL}$ antibodies was observed.

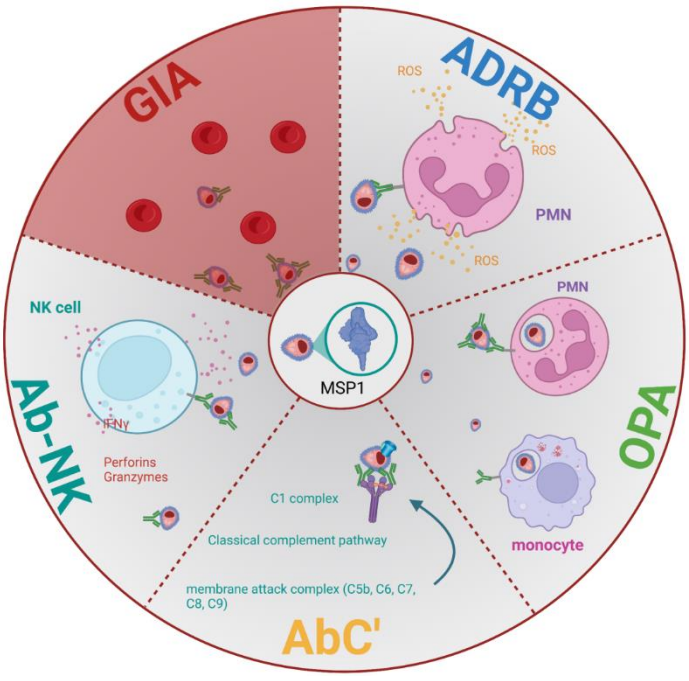

Figure 6.1: Illustration of functional activities of anti-$MSP1_{FL}$ antibodies.
The repertoire of naturally acquired or vaccine-induced anti-$MSP1_{FL}$ was assessed in volunteers from the CHMI study or the phase Ia study with SumayaVAC1.The red slice indicates the absence of GIA activity. AbC‘; antibody-dependent complement fixation activity, OPA; opsonic phagocytosis activity of monocytes or polymorphonuclear cells ADRB; antibody-dependent respiratory burst by polymorpho-nuclear cells, Ab-NK:IFNγ; Fc-mediated natural killer IFNγ production, Ab-NK:CD107a; Fc-mediated natural killer cell degranulation. GIA; growth inhibition assay

Furthermore, I demonstrated that the whole molecule, particularly the N-terminal p83 and the C-terminal p42 subunit are major targets by functional antibodies which supports the development of full-length MSP1-based vaccines.

6.2 Implications of the study

The results from this study will inform that MSP1 is still a relevant antigen for naturally acquired and vaccine-induced immune responses and emphasizes that this protein should be considered as a key target of malaria interventions such as vaccines or monoclonal antibodies.

Furthermore, this study shows that previous clinical trials and sero-epidemoelical studies characterised MSP1 sub optimally by focussing on specific subunits instead of including the whole protein and by neglecting Fc-mediated effector functions.

The outcomes of this study further justify the upcoming phase Ib trial with malaria-exposed volunteers from Tanzania to assess safety, immunogenicity and efficacy of vaccination with SumayaVac1.

6.3 Recommendations

The scope of this study can be extended to inform the development of next-generation MSP1-based vaccines or therapeutics.

I. The functional assays used in this study did not measure direct anti-parasitic effects such as the inhibition of invasion or growth *in vitro*. Optimizing the use of effector cells and complement in a modified growth inhibition or invasion inhibition assay could strengthen the use of Fc-mediated effector functions for the evaluation of next-generation malaria vaccine candidates.

II. The functional *in vitro* assays used effector cells isolated from malaria-naïve healthy adults. Importantly, several polymorphisms of the FcγR showed associations with protection to malaria (Cherif et al., 2016; Shi et al., 2001; Willcocks et al., 2010). Performing functional assays with antibodies and effector cells isolated from the same donor could give more information about the activity of FcγR and its relevance for resistance or susceptibility to malaria.

III. Conformational epitopes of vaccine-induced or naturally acquired anti-$MSP1_{FL}$ antibodies should be investigated for example by use of Hydrogen/Deuterium-

exchange coupled to Mass Spectrometry (HDX-MS) which does not only provide information about the structure of antibody-antigen complexes but also about antibody affinity (Malito et al., 2014; Puchades et al., 2019).

IV. A previous study highlighted that naturally acquired and vaccine-induced antibodies could differ in the fucosylation status of the Fc which affects binding of the FcR and thus the ability to induce effector functions (Larsen et al., 2021). Analysis of the Fc glycosylation of naturally acquired or vaccine-induced $MSP1_{FL}$ antibodies could therefore inform about potential differences between NAI and vaccination.

V. Passive immunization with antibodies showed strong reduction of parasite densities and malaria symptoms (Cohen et al., 1961). Future studies can use samples from the CHMI or phase Ia study to isolate anti-$MSP1_{FL}$ monoclonal antibodies. Antibodies that strongly bind to conserved epitopes could be evaluated for strain-transcending neutralization activity, Fc-mediated functions and protection *in vivo*.

7.0 REFERENCES

Aitken, E.H., S. Mahanty, and S.J. Rogerson. 2020. Antibody effector functions in malaria and other parasitic diseases: a few needles and many haystacks. *Immunology & Cell Biology* 98:264-275.

Akhoon, B.A., K.P. Singh, M. Varshney, S.K. Gupta, Y. Shukla, and S.K. Gupta. 2014. Understanding the Mechanism of Atovaquone Drug Resistance in Plasmodium falciparum Cytochrome b Mutation Y268S Using Computational Methods. *PLOS ONE* 9:e110041.

al-Yaman, F., B. Genton, K.J. Kramer, S.P. Chang, G.S. Hui, M. Baisor, and M.P. Alpers. 1996. Assessment of the role of naturally acquired antibody levels to Plasmodium falciparum merozoite surface protein-1 in protecting Papua New Guinean children from malaria morbidity. *Am J Trop Med Hyg* 54:443-448.

Alam, M.S., B. Ley, M.K. Nima, F.T. Johora, M.E. Hossain, K. Thriemer, S. Auburn, J. Marfurt, R.N. Price, and W.A. Khan. 2017. Molecular analysis demonstrates high prevalence of chloroquine resistance but no evidence of artemisinin resistance in Plasmodium falciparum in the Chittagong Hill Tracts of Bangladesh. *Malaria Journal* 16:335.

Alanine, D.G.W., D. Quinkert, R. Kumarasingha, S. Mehmood, F.R. Donnellan, N.K. Minkah, B. Dadonaite, A. Diouf, F. Galaway, S.E. Silk, A. Jamwal, J.M. Marshall, K. Miura, L. Foquet, S.C. Elias, G.M. Labbé, A.D. Douglas, J. Jin, R.O. Payne, J.J. Illingworth, D.J. Pattinson, D. Pulido, B.G. Williams, W.A. de Jongh, G.J. Wright, S.H.I. Kappe, C.V. Robinson, C.A. Long, B.S. Crabb, P.R. Gilson, M.K. Higgins, and S.J. Draper. 2019. Human Antibodies that Slow Erythrocyte Invasion Potentiate Malaria-Neutralizing Antibodies. *Cell* 178:216-228.e221.

Allison, A.C., and E.M. Eugui. 1983. The role of cell-mediated immune responses in resistance to malaria, with special reference to oxidant stress. *Annu Rev Immunol* 1:361-392.

Amanna, I.J., and M.K. Slifka. 2020. Successful Vaccines. *Curr Top Microbiol Immunol* 428:1-30.

Amino, R., S. Thiberge, S. Blazquez, P. Baldacci, O. Renaud, S. Shorte, and R. Ménard. 2007. Imaging malaria sporozoites in the dermis of the mammalian host. *Nat Protoc* 2:1705-1712.

Angulo, I., and M. Fresno. 2002. Cytokines in the pathogenesis of and protection against malaria. *Clin Diagn Lab Immunol* 9:1145-1152.

Arai, M., O. Billker, H.R. Morris, M. Panico, M. Delcroix, D. Dixon, S.V. Ley, and R.E. Sinden. 2001. Both mosquito-derived xanthurenic acid and a host blood-derived factor regulate gametogenesis of Plasmodium in the midgut of the mosquito. *Mol Biochem Parasitol* 116:17-24.

Arora, G., G.T. Hart, J. Manzella-Lapeira, J.Y.A. Doritchamou, D.L. Narum, L.M. Thomas, J. Brzostowski, S. Rajagopalan, O.K. Doumbo, B. Traore, L.H. Miller, S.K. Pierce, P.E. Duffy, P.D. Crompton, S.A. Desai, and E.O. Long. 2018. NK cells inhibit Plasmodium falciparum growth in red blood cells via antibody-dependent cellular cytotoxicity. *eLife* 7:e36806.

Ashley, E.A., M. Dhorda, R.M. Fairhurst, C. Amaratunga, P. Lim, S. Suon, S. Sreng, J.M. Anderson, S. Mao, B. Sam, C. Sopha, C.M. Chuor, C. Nguon, S. Sovannaroth, S. Pukrittayakamee, P. Jittamala, K. Chotivanich, K. Chutasmit, C. Suchatsoonthorn, R. Runcharoen, T.T. Hien, N.T. Thuy-Nhien, N.V. Thanh, N.H. Phu, Y. Htut, K.-T. Han, K.H. Aye, O.A. Mokuolu, R.R. Olaosebikan, O.O. Folaranmi, M. Mayxay, M. Khanthavong, B. Hongvanthong, P.N. Newton, M.A. Onyamboko, C.I. Fanello, A.K. Tshefu, N. Mishra, N. Valecha, A.P. Phyo, F. Nosten, P. Yi, R. Tripura, S. Borrmann, M. Bashraheil, J. Peshu, M.A. Faiz, A. Ghose, M.A. Hossain, R. Samad, M.R. Rahman, M.M. Hasan, A. Islam, O. Miotto, R. Amato, B. MacInnis, J. Stalker, D.P. Kwiatkowski, Z. Bozdech, A. Jeeyapant, P.Y. Cheah, T. Sakulthaew, J. Chalk, B. Intharabut, K. Silamut, S.J. Lee, B. Vihokhern, C. Kunasol, M. Imwong, J. Tarning, W.J. Taylor, S. Yeung, C.J. Woodrow, J.A. Flegg, D. Das, J. Smith, M. Venkatesan, C.V. Plowe, K. Stepniewska, P.J. Guerin, A.M. Dondorp, N.P. Day, and N.J. White. 2014. Spread of Artemisinin Resistance in Plasmodium falciparum Malaria. *New England Journal of Medicine* 371:411-423.

Ataíde, R., W. Hasang, D.W. Wilson, J.G. Beeson, V. Mwapasa, M.E. Molyneux, S.R. Meshnick, and S.J. Rogerson. 2010. Using an improved phagocytosis assay to evaluate the effect of HIV on specific antibodies to pregnancy-associated malaria. *PLoS One* 5:e10807.

Baba, E., P. Hamade, H. Kivumbi, M. Marasciulo, K. Maxwell, D. Moroso, A. Roca-Feltrer, A. Sanogo, J. Stenstrom Johansson, J. Tibenderana, R. Abdoulaye, P. Coulibaly, E. Hubbard, H. Jah, E.K. Lama, L. Razafindralambo, S. Van Hulle, G. Jagoe, A.-M. Tchouatieu, D. Collins, C. Gilmartin, G. Tetteh, Y. Djibo, F. Ndiaye, M. Kalleh, B. Kandeh, B. Audu, G. Ntadom, A. Kiba, Y. Savodogo, K. Boulotigam, D.A. Sougoudi, T. Guilavogui, M. Keita, D. Kone, H. Jackou, I. Ouba, E. Ouedraogo, H.A. Messan, F. Jah, M.J. Kaira, M.S. Sano, M.C. Traore, N. Ngarnaye, A.Y.C. Elagbaje, C. Halleux, C. Merle, N. Iessa, S. Pal, H. Sefiani, R. Souleymani, I. Laminou, D. Doumagoum, H. Kesseley, M. Coldiron, R. Grais, M. Kana, J.B. Ouedraogo, I. Zongo, T. Eloike, S.J. Ogboi, J. Achan, K. Bojang, S. Ceesay, A. Dicko, A. Djimde, I. Sagara, A. Diallo, J.L. NdDiaye, K.M. Loua, K. Beshir, M. Cairns, Y. Fernandez, S. Lal, R. Mansukhani, J. Muwanguzi, S. Scott, P. Snell, C. Sutherland, R. Tuta, and P. Milligan. 2020. Effectiveness of seasonal malaria chemoprevention at scale in west and central Africa: an observational study. *The Lancet* 396:1829-1840.

Baer, K., M. Roosevelt, A.B. Clarkson, Jr., N. van Rooijen, T. Schnieder, and U. Frevert. 2007. Kupffer cells are obligatory for Plasmodium yoelii sporozoite infection of the liver. *Cell Microbiol* 9:397-412.

Baggish, A.L., and D.R. Hill. 2002. Antiparasitic agent atovaquone. *Antimicrob Agents Chemother* 46:1163-1173.

Baldwin, M.R., X. Li, T. Hanada, S.C. Liu, and A.H. Chishti. 2015. Merozoite surface protein 1 recognition of host glycophorin A mediates malaria parasite invasion of red blood cells. *Blood* 125:2704-2711.

Barry, A., M.C. Behet, I. Nébié, K. Lanke, L. Grignard, A. Ouedraogo, I. Soulama, C. Drakeley, R. Sauerwein, J.M. Bolscher, K.J. Dechering, T. Bousema, A.B. Tiono, and B.P. Gonçalves. 2018. Functional antibodies against Plasmodium falciparum sporozoites are associated with a longer time to qPCR-detected infection among schoolchildren in Burkina Faso. *Wellcome Open Res* 3:159.

Bastos, K.R., R. Barboza, R.M. Elias, L.R. Sardinha, M.G. Grisotto, C.R. Marinho, G.P. Amarante-Mendes, J.M. Alvarez, and M.R. Lima. 2002. Impaired macrophage responses may contribute to exacerbation of blood-stage Plasmodium chabaudi chabaudi malaria in interleukin-12-deficient mice. *J Interferon Cytokine Res* 22:1191-1199.

Beeson, J.G., D.R. Drew, M.J. Boyle, G. Feng, F.J. Fowkes, and J.S. Richards. 2016. Merozoite surface proteins in red blood cell invasion, immunity and vaccines against malaria. *FEMS Microbiol Rev* 40:343-372.

Behet, M.C., L. Foquet, G.-J. van Gemert, E.M. Bijker, P. Meuleman, G. Leroux-Roels, C.C. Hermsen, A. Scholzen, and R.W. Sauerwein. 2014. Sporozoite immunization of human volunteers under chemoprophylaxis induces functional antibodies against pre-erythrocytic stages of Plasmodium falciparum. *Malaria Journal* 13:136.

Behet, M.C., L. Kurtovic, G.J. van Gemert, C.M. Haukes, R. Siebelink-Stoter, W. Graumans, M.G. van de Vegte-Bolmer, A. Scholzen, J.D. Langereis, D.A. Diavatopoulos, J.G. Beeson, and R.W. Sauerwein. 2018. The Complement System Contributes to Functional Antibody-Mediated Responses Induced by Immunization with Plasmodium falciparum Malaria Sporozoites. *Infect Immun* 86:

Behr, C., R. Poupot, M.A. Peyrat, Y. Poquet, P. Constant, P. Dubois, M. Bonneville, and J.J. Fournie. 1996. Plasmodium falciparum stimuli for human gammadelta T cells are related to phosphorylated antigens of mycobacteria. *Infect Immun* 64:2892-2896.

Beier, J.C., J.R. Davis, J.A. Vaughan, B.H. Noden, and M.S. Beier. 1991. Quantitation of Plasmodium falciparum sporozoites transmitted in vitro by experimentally infected Anopheles gambiae and Anopheles stephensi. *Am J Trop Med Hyg* 44:564-570.

Bélard, S., S. Issifou, A.B. Hounkpatin, F. Schaumburg, U.A. Ngoa, M. Esen, R. Fendel, P.M. de Salazar, R.E. Mürbeth, P. Milligan, N. Imbault, E.B. Imoukhuede, M. Theisen, S. Jepsen, R.A. Noor, B. Okech, P.G. Kremsner, and B. Mordmüller. 2011. A randomized controlled phase Ib trial of the malaria vaccine candidate GMZ2 in African children. *PLoS One* 6:e22525.

Belete, T.M. 2020. Recent Progress in the Development of New Antimalarial Drugs with Novel Targets. *Drug Des Devel Ther* 14:3875-3889.

Berhe, S., P. Gerold, M.H. Kedees, A.A. Holder, and R.T. Schwarz. 2000. Plasmodium falciparum: merozoite surface proteins 1 and 2 are not posttranslationally modified by classical N- or O-glycans. *Exp Parasitol* 94:194-197.

Bian, G., Y. Xu, P. Lu, Y. Xie, and Z. Xi. 2010. The endosymbiotic bacterium Wolbachia induces resistance to dengue virus in Aedes aegypti. *PLoS Pathog* 6:e1000833.

Bijker, E.M., S. Borrmann, S.H. Kappe, B. Mordmüller, B.K. Sack, and S.M. Khan. 2015. Novel approaches to whole sporozoite vaccination against malaria. *Vaccine* 33:7462-7468.

Billker, O., A.J. Miller, and R.E. Sinden. 2000. Determination of mosquito bloodmeal pH in situ by ion-selective microelectrode measurement: implications for the regulation of malarial gametogenesis. *Parasitology* 120 (Pt 6):547-551.

Birkenmeyer, L., A.S. Muerhoff, G.J. Dawson, and S.M. Desai. 2010. Isolation and characterization of the MSP1 genes from Plasmodium malariae and Plasmodium ovale. *The American journal of tropical medicine and hygiene* 82:996-1003.

Biswas, S., D. Tomar, and D.N. Rao. 2005. Investigation of the kinetics of histidine-rich protein 2 and of the antibody responses to this antigen, in a group of malaria patients from India. *Ann Trop Med Parasitol* 99:553-562.

Blackman, M.J., and L.H. Bannister. 2001. Apical organelles of Apicomplexa: biology and isolation by subcellular fractionation. *Mol Biochem Parasitol* 117:11-25.

Blackman, M.J., H. Fujioka, W.H.L. Stafford, M. Sajid, B. Clough, S.L. Fleck, M. Aikawa, M. Grainger, and F. Hackett. 1998. A Subtilisin-like Protein in Secretory Organelles of Plasmodium falciparum Merozoites *Journal of Biological Chemistry* 273:23398-23409.

Blackman, M.J., H.G. Heidrich, S. Donachie, J.S. McBride, and A.A. Holder. 1990. A single fragment of a malaria merozoite surface protein remains on the parasite during red cell invasion and is the target of invasion-inhibiting antibodies. *J Exp Med* 172:379-382.

Blackman, M.J., and A.A. Holder. 1992. Secondary processing of the Plasmodium falciparum merozoite surface protein-1 (MSP1) by a calcium-dependent membrane-bound serine protease: shedding of MSP133 as a noncovalently associated complex with other fragments of the MSP1. *Mol Biochem Parasitol* 50:307-315.

Blackman, M.J., T.J. Scott-Finnigan, S. Shai, and A.A. Holder. 1994. Antibodies inhibit the protease-mediated processing of a malaria merozoite surface protein. *J Exp Med* 180:389-393.

Blackman, M.J., H. Whittle, and A.A. Holder. 1991. Processing of the Plasmodium falciparum major merozoite surface protein-1: identification of a 33-kilodalton secondary processing product which is shed prior to erythrocyte invasion. *Mol Biochem Parasitol* 49:35-44.

Blanchette, J., M. Jaramillo, and M. Olivier. 2003. Signalling events involved in interferon-gamma-inducible macrophage nitric oxide generation. *Immunology* 108:513-522.

Blank, A., K. Fürle, A. Jäschke, G. Mikus, M. Lehmann, J. Hüsing, K. Heiss, T. Giese, D. Carter, E. Böhnlein, M. Lanzer, W.E. Haefeli, and H. Bujard. 2020. Immunization with full-length Plasmodium falciparum merozoite surface protein 1 is safe and elicits functional cytophilic antibodies in a randomized first-in-human trial. *NPJ Vaccines* 5:10.

Blasco, B., D. Leroy, and D.A. Fidock. 2017. Antimalarial drug resistance: linking Plasmodium falciparum parasite biology to the clinic. *Nature medicine* 23:917-928.

Bolchoz, L.J., R.A. Budinsky, D.C. McMillan, and D.J. Jollow. 2001. Primaquine-induced hemolytic anemia: formation and hemotoxicity of the arylhydroxylamine metabolite 6-methoxy-8-hydroxylaminoquinoline. *J Pharmacol Exp Ther* 297:509-515.

Bouharoun-Tayoun, H., C. Oeuvray, F. Lunel, and P. Druilhe. 1995. Mechanisms underlying the monocyte-mediated antibody-dependent killing of Plasmodium falciparum asexual blood stages. *J Exp Med* 182:409-418.

Boutlis, C.S., E. Tjitra, H. Maniboey, M.A. Misukonis, J.R. Saunders, S. Suprianto, J.B. Weinberg, and N.M. Anstey. 2003. Nitric oxide production and mononuclear cell nitric oxide synthase activity in malaria-tolerant Papuan adults. *Infection and immunity* 71:3682-3689.

Bowman, N.M., J.J. Juliano, C.J. Snider, O. Kharabora, S.R. Meshnick, J. Vulule, C.C. John, and A.M. Moormann. 2016. Longevity of Genotype-Specific Immune Responses to Plasmodium falciparum Merozoite Surface Protein 1 in Kenyan Children from Regions of Different Malaria Transmission Intensity. *Am J Trop Med Hyg* 95:580-587.

Boyle, M.J., J.A. Chan, I. Handayuni, L. Reiling, G. Feng, A. Hilton, L. Kurtovic, D. Oyong, K.A. Piera, B.E. Barber, T. William, D.P. Eisen, G. Minigo, C. Langer, D.R. Drew, F. de Labastida Rivera, F.H. Amante, T.N. Williams, S. Kinyanjui, K. Marsh, D.L. Doolan, C. Engwerda, F.J.I. Fowkes, M.J. Grigg, I. Mueller, J.S. McCarthy, N.M. Anstey, and J.G. Beeson. 2019. IgM in human immunity to Plasmodium falciparum malaria. *Science Advances* 5:eaax4489.

Boyle, M.J., L. Reiling, G. Feng, C. Langer, F.H. Osier, H. Aspeling-Jones, Y.S. Cheng, J. Stubbs, K.K. Tetteh, D.J. Conway, J.S. McCarthy, I. Muller, K. Marsh, R.F. Anders, and J.G. Beeson. 2015. Human antibodies fix complement to inhibit Plasmodium falciparum invasion of erythrocytes and are associated with protection against malaria. *Immunity* 42:580-590.

Boyle, M.J., J.S. Richards, P.R. Gilson, W. Chai, and J.G. Beeson. 2010. Interactions with heparin-like molecules during erythrocyte invasion by Plasmodium falciparum merozoites. *Blood* 115:4559-4568.

Boyle, M.J., D.W. Wilson, and J.G. Beeson. 2013. New approaches to studying Plasmodium falciparum merozoite invasion and insights into invasion biology. *Int J Parasitol* 43:1-10.

Bozdech, Z., J. Zhu, M.P. Joachimiak, F.E. Cohen, B. Pulliam, and J.L. DeRisi. 2003. Expression profiling of the schizont and trophozoite stages of Plasmodium falciparum with a long-oligonucleotide microarray. *Genome Biol* 4:R9-R9.

Branch, O.H., V. Udhayakumar, A.W. Hightower, A.J. Oloo, W.A. Hawley, B.L. Nahlen, P.B. Bloland, D.C. Kaslow, and A.A. Lal. 1998. A longitudinal investigation of IgG and IgM antibody responses to the merozoite surface protein-1 19-kiloDalton domain of Plasmodium falciparum in pregnant women and infants: associations with febrile illness, parasitemia, and anemia. *Am J Trop Med Hyg* 58:211-219.

Bridgford, J.L., S.C. Xie, S.A. Cobbold, C.F.A. Pasaje, S. Herrmann, T. Yang, D.L. Gillett, L.R. Dick, S.A. Ralph, C. Dogovski, N.J. Spillman, and L. Tilley. 2018. Artemisinin kills malaria parasites by damaging proteins and inhibiting the proteasome. *Nature Communications* 9:3801.

Brownlie, J.C., B.N. Cass, M. Riegler, J.J. Witsenburg, I. Iturbe-Ormaetxe, E.A. McGraw, and S.L. O'Neill. 2009. Evidence for Metabolic Provisioning by a Common Invertebrate Endosymbiont, Wolbachia pipientis, during Periods of Nutritional Stress. *PLOS Pathogens* 5:e1000368.

Bueno, L.L., C.G. Morais, M.V. Lacerda, R.T. Fujiwara, and É.M. Braga. 2012. Interleukin-17 producing T helper cells are increased during natural Plasmodium vivax infection. *Acta Trop* 123:53-57.

Cairns, M., S.J. Ceesay, I. Sagara, I. Zongo, H. Kessely, K. Gamougam, A. Diallo, J.S. Ogboi, D. Moroso, S. Van Hulle, T. Eloike, P. Snell, S. Scott, C. Merle, K. Bojang, J.B. Ouedraogo, A. Dicko, J.-L. Ndiaye, and P. Milligan. 2021. Effectiveness of seasonal malaria chemoprevention (SMC) treatments when SMC is implemented at scale: Case–control studies in 5 countries. *PLOS Medicine* 18:e1003727.

Camarda, G., P. Jirawatcharadech, R.S. Priestley, A. Saif, S. March, M.H.L. Wong, S. Leung, A.B. Miller, D.A. Baker, P. Alano, M.J.I. Paine, S.N. Bhatia, P.M. O'Neill, S.A. Ward, and G.A. Biagini. 2019. Antimalarial activity of primaquine operates via a two-step biochemical relay. *Nature Communications* 10:3226.

Canepa, G.E., A. Molina-Cruz, L. Yenkoidiok-Douti, E. Calvo, A.E. Williams, M. Burkhardt, F. Peng, D. Narum, M.J. Boulanger, J.G. Valenzuela, and C. Barillas-Mury. 2018. Antibody targeting of a specific region of Pfs47 blocks Plasmodium falciparum malaria transmission. *npj Vaccines* 3:26.

Carlton, J.M., J.H. Adams, J.C. Silva, S.L. Bidwell, H. Lorenzi, E. Caler, J. Crabtree, S.V. Angiuoli, E.F. Merino, P. Amedeo, Q. Cheng, R.M. Coulson, B.S. Crabb, H.A. Del Portillo, K. Essien, T.V. Feldblyum, C. Fernandez-Becerra, P.R. Gilson, A.H. Gueye, X. Guo, S. Kang'a, T.W. Kooij, M. Korsinczky, E.V. Meyer, V. Nene, I. Paulsen, O. White, S.A. Ralph, Q. Ren, T.J. Sargeant, S.L. Salzberg, C.J. Stoeckert, S.A. Sullivan, M.M. Yamamoto, S.L. Hoffman, J.R. Wortman, M.J. Gardner, M.R. Galinski, J.W. Barnwell, and C.M. Fraser-Liggett. 2008. Comparative genomics of the neglected human malaria parasite Plasmodium vivax. *Nature* 455:757-763.

Carralot, J.-P., C. Lemmel, S. Stevanovic, and S. Pascolo. 2008. Mass spectrometric identification of an HLA-A*0201 epitope from Plasmodium falciparum MSP-1. *International Immunology* 20:1451-1456.

Castro, M.C. 2017. Malaria Transmission and Prospects for Malaria Eradication: The Role of the Environment. *Cold Spring Harb Perspect Med* 7:a025601.

Cavanagh, D.R., C. Dobaño, I.M. Elhassan, K. Marsh, A. Elhassan, L. Hviid, E.A. Khalil, T.G. Theander, D.E. Arnot, and J.S. McBride. 2001. Differential patterns of human immunoglobulin G subclass responses to distinct regions of a single protein, the merozoite surface protein 1 of Plasmodium falciparum. *Infect Immun* 69:1207-1211.

Cavanagh, D.R., D. Dodoo, L. Hviid, J.A. Kurtzhals, T.G. Theander, B.D. Akanmori, S. Polley, D.J. Conway, K. Koram, and J.S. McBride. 2004. Antibodies to the N-terminal block 2 of Plasmodium falciparum merozoite surface protein 1 are associated with protection against clinical malaria. *Infect Immun* 72:6492-6502.

Cavanagh, D.R., I.M. Elhassan, C. Roper, V.J. Robinson, H. Giha, A.A. Holder, L. Hviid, T.G. Theander, D.E. Arnot, and J.S. McBride. 1998. A longitudinal study of type-specific antibody responses to Plasmodium falciparum merozoite surface protein-1 in an area of unstable malaria in Sudan. *J Immunol* 161:347-359.

Cavanagh, D.R., C.H. Kocken, J.H. White, G.J. Cowan, K. Samuel, M.A. Dubbeld, A. Voorberg-van der Wel, A.W. Thomas, J.S. McBride, and D.E. Arnot. 2014. Antibody responses to a novel Plasmodium falciparum merozoite surface protein vaccine correlate with protection against experimental malaria infection in Aotus monkeys. *PLoS One* 9:e83704.

Chakravarty, S., I.A. Cockburn, S. Kuk, M.G. Overstreet, J.B. Sacci, and F. Zavala. 2007. CD8+ T lymphocytes protective against malaria liver stages are primed in skin-draining lymph nodes. *Nat Med* 13:1035-1041.

Chan, C.L., L. Rénia, and K.S.W. Tan. 2012. A simplified, sensitive phagocytic assay for malaria cultures facilitated by flow cytometry of differentially-stained cell populations. *PloS one* 7:e38523-e38523.

Chan, J.A., M.J. Boyle, K.A. Moore, L. Reiling, Z. Lin, W. Hasang, M. Avril, L. Manning, I. Mueller, M. Laman, T. Davis, J.D. Smith, S.J. Rogerson, J.A. Simpson, F.J.I. Fowkes, and J.G. Beeson. 2019. Antibody Targets on the Surface of Plasmodium falciparum-Infected Erythrocytes That Are Associated With Immunity to Severe Malaria in Young Children. *J Infect Dis* 219:819-828.

Chan, J.A., F.J. Fowkes, and J.G. Beeson. 2014. Surface antigens of Plasmodium falciparum-infected erythrocytes as immune targets and malaria vaccine candidates. *Cell Mol Life Sci* 71:3633-3657.

Chelimo, K., P.B. Embury, P. Odada Sumba, J. Vulule, A.V. Ofulla, C. Long, J.W. Kazura, and A.M. Moormann. 2011. Age-Related Differences in Naturally Acquired T Cell Memory to Plasmodium falciparum Merozoite Surface Protein 1. *PLOS ONE* 6:e24852.

Chelimo, K., P.O. Sumba, J.W. Kazura, A.V. Ofula, and C.C. John. 2003. Interferon-gamma responses to Plasmodium falciparum liver-stage antigen-1 and merozoite-surface protein-1 increase with age in children in a malaria holoendemic area of western Kenya. *Malar J* 2:37.

Cherif, M., D. Amoako-Sakyi, A. Dolo, J.O. Pearson, B. Gyan, D. Obiri-Yeboah, I. Nebie, S.B. Sirima, O. Doumbo, M. Troye-Blomberg, and M. Bakary. 2016. Distribution of FcγR gene polymorphisms among two sympatric populations in Mali: differing allele frequencies, associations with malariometric indices and implications for genetic susceptibility to malaria. *Malar J* 15:29.

Child, M.A., C. Epp, H. Bujard, and M.J. Blackman. 2010. Regulated maturation of malaria merozoite surface protein-1 is essential for parasite growth. *Molecular Microbiology* 78:187-202.

Chiodini, P.L., K. Bowers, P. Jorgensen, J.W. Barnwell, K.K. Grady, J. Luchavez, A.H. Moody, A. Cenizal, and D. Bell. 2007. The heat stability of Plasmodium lactate dehydrogenase-based and histidine-rich protein 2-based malaria rapid diagnostic tests. *Trans R Soc Trop Med Hyg* 101:331-337.

Chitarra, V., I. Holm, G.A. Bentley, S. Pêtres, and S. Longacre. 1999. The Crystal Structure of C-Terminal Merozoite Surface Protein 1 at 1.8 Å Resolution, a Highly Protective Malaria Vaccine Candidate. *Molecular Cell* 3:457-464.

Chitnis, C.E., P. Mukherjee, S. Mehta, S.S. Yazdani, S. Dhawan, A.R. Shakri, R. Bhardwaj, P.K. Gupta, D. Hans, S. Mazumdar, B. Singh, S. Kumar, G. Pandey, V. Parulekar, N. Imbault, P. Shivyogi, G. Godbole, K. Mohan, O. Leroy, K. Singh, and V.S. Chauhan. 2015. Phase I Clinical Trial of a Recombinant Blood Stage Vaccine Candidate for Plasmodium falciparum Malaria Based on MSP1 and EBA175. *PLoS One* 10:e0117820.

Churcher, T.S., N. Lissenden, J.T. Griffin, E. Worrall, and H. Ranson. 2016. The impact of pyrethroid resistance on the efficacy and effectiveness of bednets for malaria control in Africa. *eLife* 5:e16090.

Clark, I.A., and N.H. Hunt. 1983. Evidence for reactive oxygen intermediates causing hemolysis and parasite death in malaria. *Infect Immun* 39:1-6.

Clyde, D.F. 1975. Immunization of man against falciparum and vivax malaria by use of attenuated sporozoites. *Am J Trop Med Hyg* 24:397-401.

Clyde, D.F., H. Most, V.C. McCarthy, and J.P. Vanderberg. 1973. Immunization of man against sporozite-induced falciparum malaria. *Am J Med Sci* 266:169-177.

Cockburn, I.A., R. Amino, R.K. Kelemen, S.C. Kuo, S.-W. Tse, A. Radtke, L. Mac-Daniel, V.V. Ganusov, F. Zavala, and R. Ménard. 2013. In vivo imaging of CD8+ T cell-mediated elimination of malaria liver stages. *Proceedings of the National Academy of Sciences of the United States of America* 110:9090-9095.

Cohen, S., G.I. Mc, and S. Carrington. 1961. Gamma-globulin and acquired immunity to human malaria. *Nature* 192:733-737.

Cohuet, A., C. Harris, V. Robert, and D. Fontenille. 2009. Evolutionary forces on Anopheles : what makes a malaria vector? *Trends in parasitology* 26:130-136.

Coldiron, M.E., L. Von Seidlein, and R.F. Grais. 2017. Seasonal malaria chemoprevention: successes and missed opportunities. *Malaria journal* 16:481-481.

Collins, J.P. 2018. Gene drives in our future: challenges of and opportunities for using a self-sustaining technology in pest and vector management. *BMC Proceedings* 12:9.

Collins, K.A., R. Snaith, M.G. Cottingham, S.C. Gilbert, and A.V.S. Hill. 2017. Enhancing protective immunity to malaria with a highly immunogenic virus-like particle vaccine. *Scientific Reports* 7:46621.

Combe, A., D. Giovannini, T.G. Carvalho, S. Spath, B. Boisson, C. Loussert, S. Thiberge, C. Lacroix, P. Gueirard, and R. Ménard. 2009. Clonal Conditional Mutagenesis in Malaria Parasites. *Cell Host & Microbe* 5:386-396.

Conway, D.J., D.R. Cavanagh, K. Tanabe, C. Roper, Z.S. Mikes, N. Sakihama, K.A. Bojang, A.M. Oduola, P.G. Kremsner, D.E. Arnot, B.M. Greenwood, and J.S. McBride. 2000. A principal target of human immunity to malaria identified by molecular population genetic and immunological analyses. *Nat Med* 6:689-692.

Cooper, J.A., and H. Bujard. 1992. Membrane-associated proteases process Plasmodium falciparum merozoite surface antigen-1 (MSA1) to fragment gp41. *Molecular and Biochemical Parasitology* 56:151-160.

Coulibaly, D., A.K. Kone, K. Traore, A. Niangaly, B. Kouriba, C. Arama, A. Zeguime, A. Dolo, K.E. Lyke, C.V. Plowe, Y. Abebe, G.E. Potter, J.K. Kennedy, S.M. Galbiati, E. Nomicos, G.A. Deye, T.L. Richie, E.R. James, N. Kc, B.K.L. Sim, S.L. Hoffman, O.K. Doumbo, M.A. Thera, and M.B. Laurens. 2022. PfSPZ-CVac malaria vaccine demonstrates safety among malaria-experienced adults: A randomized, controlled phase 1 trial. *eClinicalMedicine* 52:

Cowman, A.F., C.J. Tonkin, W.-H. Tham, and M.T. Duraisingh. 2017. The Molecular Basis of Erythrocyte Invasion by Malaria Parasites. *Cell Host & Microbe* 22:232-245.

Crompton, P.D., M.A. Kayala, B. Traore, K. Kayentao, A. Ongoiba, G.E. Weiss, D.M. Molina, C.R. Burk, M. Waisberg, A. Jasinskas, X. Tan, S. Doumbo, D. Doumtabe, Y. Kone, D.L. Narum, X. Liang, O.K. Doumbo, L.H. Miller, D.L. Doolan, P. Baldi, P.L. Felgner, and S.K. Pierce. 2010. A prospective analysis of the Ab response to Plasmodium falciparum before and after a malaria season by protein microarray. *Proceedings of the National Academy of Sciences of the United States of America* 107:6958-6963.

Crosnier, C., L.Y. Bustamante, S.J. Bartholdson, A.K. Bei, M. Theron, M. Uchikawa, S. Mboup, O. Ndir, D.P. Kwiatkowski, M.T. Duraisingh, J.C. Rayner, and G.J. Wright. 2011. Basigin is a receptor essential for erythrocyte invasion by Plasmodium falciparum. *Nature* 480:534-537.

Crosnier, C., M. Wanaguru, B. McDade, F.H. Osier, K. Marsh, J.C. Rayner, and G.J. Wright. 2013. A library of functional recombinant cell-surface and secreted P. falciparum merozoite proteins. *Mol Cell Proteomics* 12:3976-3986.

D'Ombrain, M.C., L.J. Robinson, D.I. Stanisic, J. Taraika, N. Bernard, P. Michon, I. Mueller, and L. Schofield. 2008. Association of early interferon-gamma production with immunity to clinical malaria: a longitudinal study among Papua New Guinean children. *Clin Infect Dis* 47:1380-1387.

Daly, T.M., and C.A. Long. 1995. Humoral response to a carboxyl-terminal region of the merozoite surface protein-1 plays a predominant role in controlling blood-stage infection in rodent malaria. *J Immunol* 155:236-243.

Dantzler, K.W., S. Ma, P. Ngotho, W.J.R. Stone, D. Tao, S. Rijpma, M. De Niz, S.K. Nilsson Bark, M.M. Jore, T.K. Raaijmakers, A.M. Early, C. Ubaida-Mohien, L. Lemgruber, J.J. Campo, A.A. Teng, T.Q. Le, C.L. Walker, P. Hermand, P. Deterre, D.H. Davies, P. Felgner, I. Morlais, D.F. Wirth, D.E. Neafsey, R.R. Dinglasan, M. Laufer, C. Huttenhower, K. Seydel, T. Taylor, T. Bousema, and M. Marti. 2019. Naturally acquired immunity against immature Plasmodium falciparum gametocytes. *Sci Transl Med* 11:

Das, S., N. Hertrich, A.J. Perrin, C. Withers-Martinez, C.R. Collins, M.L. Jones, J.M. Watermeyer, E.T. Fobes, S.R. Martin, H.R. Saibil, G.J. Wright, M. Treeck, C. Epp, and M.J. Blackman. 2015. Processing of Plasmodium falciparum Merozoite Surface Protein MSP1 Activates a Spectrin-Binding Function Enabling Parasite Egress from RBCs. *Cell Host Microbe* 18:433-444.

Datoo, M.S., H.M. Natama, A. Somé, D. Bellamy, O. Traoré, T. Rouamba, M.C. Tahita, N.F.A. Ido, P. Yameogo, D. Valia, A. Millogo, F. Ouedraogo, R. Soma, S. Sawadogo, F. Sorgho, K. Derra, E. Rouamba, F. Ramos-Lopez, M. Cairns, S. Provstgaard-Morys, J. Aboagye, A. Lawrie, R. Roberts, I. Valéa, H. Sorgho, N. Williams, G. Glenn, L. Fries, J. Reimer, K.J. Ewer, U. Shaligram, A.V.S. Hill, and H. Tinto. 2022. Efficacy and immunogenicity of R21/Matrix-M vaccine against clinical malaria after 2 years' follow-up in children in Burkina Faso: a phase 1/2b randomised controlled trial. *The Lancet Infectious Diseases*

Datoo, M.S., M.H. Natama, A. Somé, O. Traoré, T. Rouamba, D. Bellamy, P. Yameogo, D. Valia, M. Tegneri, F. Ouedraogo, R. Soma, S. Sawadogo, F. Sorgho, K. Derra, E. Rouamba, B. Orindi, F. Ramos Lopez, A. Flaxman, F. Cappuccini, R. Kailath, S. Elias, E. Mukhopadhyay, A. Noe, M. Cairns, A. Lawrie, R. Roberts, I. Valéa, H. Sorgho, N. Williams, G. Glenn, L. Fries, J. Reimer, K.J. Ewer, U. Shaligram, A.V.S. Hill, and H. Tinto. 2021. Efficacy of a low-dose candidate malaria vaccine, R21 in adjuvant Matrix-M, with seasonal administration to children in Burkina Faso: a randomised controlled trial. *The Lancet* 397:1809-1818.

de Korne, C.M., R. van Schuijlenburg, J.C. Sijtsma, H.M. de Bes, E. Baalbergen, S. Azargoshasb, M.N. van Oosterom, M.B.B. McCall, F.W.B. van Leeuwen, and M. Roestenberg. 2022. Sporozoite motility as a quantitative readout for anti-CSP antibody inhibition. *Sci Rep* 12:17194.

Dedeine, F., F. Vavre, F. Fleury, B. Loppin, M.E. Hochberg, and M. Bouletreau. 2001. Removing symbiotic Wolbachia bacteria specifically inhibits oogenesis in a parasitic wasp. *Proc Natl Acad Sci U S A* 98:6247-6252.

Deenick, E.K., D.T. Avery, A. Chan, L.J. Berglund, M.L. Ives, L. Moens, J.L. Stoddard, J. Bustamante, S. Boisson-Dupuis, M. Tsumura, M. Kobayashi, P.D. Arkwright, D. Averbuch, D. Engelhard, J. Roesler, J. Peake, M. Wong, S. Adelstein, S. Choo, J.M. Smart, M.A. French, D.A. Fulcher, M.C. Cook, C. Picard, A. Durandy, C. Klein, S.M. Holland, G. Uzel, J.L. Casanova, C.S. Ma, and S.G. Tangye. 2013. Naive and memory human B cells have distinct requirements for STAT3 activation to differentiate into antibody-secreting plasma cells. *J Exp Med* 210:2739-2753.

Delves, M.J., F. Angrisano, and A.M. Blagborough. 2018. Antimalarial Transmission-Blocking Interventions: Past, Present, and Future. *Trends in Parasitology* 34:735-746.

Dent, A.E., E.S. Bergmann-Leitner, D.W. Wilson, D.J. Tisch, R. Kimmel, J. Vulule, P.O. Sumba, J.G. Beeson, E. Angov, A.M. Moormann, and J.W. Kazura. 2008. Antibody-Mediated Growth Inhibition of Plasmodium falciparum: Relationship to Age and Protection from Parasitemia in Kenyan Children and Adults. *PLOS ONE* 3:e3557.

Dent, A.E., R. Nakajima, L. Liang, E. Baum, A.M. Moormann, P.O. Sumba, J. Vulule, D. Babineau, A. Randall, D.H. Davies, P.L. Felgner, and J.W. Kazura. 2015. Plasmodium falciparum Protein Microarray Antibody Profiles Correlate With Protection From Symptomatic Malaria in Kenya. *The Journal of infectious diseases* 212:1429-1438.

Desai, M., J. Gutman, S.M. Taylor, R.E. Wiegand, C. Khairallah, K. Kayentao, P. Ouma, S.O. Coulibaly, L. Kalilani, K.E. Mace, E. Arinaitwe, D.P. Mathanga, O. Doumbo, K. Otieno, D. Edgar, E. Chaluluka, M. Kamuliwo, V. Ades, J. Skarbinski, Y.P. Shi, P. Magnussen, S. Meshnick, and F.O. Ter Kuile. 2016. Impact of Sulfadoxine-Pyrimethamine Resistance on Effectiveness of Intermittent Preventive Therapy for Malaria in Pregnancy at Clearing Infections and Preventing Low Birth Weight. *Clin Infect Dis* 62:323-333.

Dijkman, P.M., T. Marzluf, Y. Zhang, S.-Y.S. Chang, D. Helm, M. Lanzer, H. Bujard, and M. Kudryashev. 2021. Structure of the merozoite surface protein 1 from Plasmodium falciparum. *Science Advances* 7:eabg0465.

Djimdé, A., O.K. Doumbo, J.F. Cortese, K. Kayentao, S. Doumbo, Y. Diourté, D. Coulibaly, A. Dicko, X.Z. Su, T. Nomura, D.A. Fidock, T.E. Wellems, and C.V. Plowe. 2001. A molecular marker for chloroquine-resistant falciparum malaria. *N Engl J Med* 344:257-263.

Dodoo, D., T.G. Theander, J.A. Kurtzhals, K. Koram, E. Riley, B.D. Akanmori, F.K. Nkrumah, and L. Hviid. 1999. Levels of antibody to conserved parts of Plasmodium falciparum merozoite surface protein 1 in Ghanaian children are not associated with protection from clinical malaria. *Infect Immun* 67:2131-2137.

Dogovski, C., S.C. Xie, G. Burgio, J. Bridgford, S. Mok, J.M. McCaw, K. Chotivanich, S. Kenny, N. Gnädig, J. Straimer, Z. Bozdech, D.A. Fidock, J.A. Simpson, A.M. Dondorp, S. Foote, N. Klonis, and L. Tilley. 2015. Targeting the Cell Stress Response of Plasmodium falciparum to Overcome Artemisinin Resistance. *PLOS Biology* 13:e1002132.

Dondorp, A.M., F. Nosten, P. Yi, D. Das, A.P. Phyo, J. Tarning, K.M. Lwin, F. Ariey, W. Hanpithakpong, S.J. Lee, P. Ringwald, K. Silamut, M. Imwong, K. Chotivanich, P. Lim, T. Herdman, S.S. An, S. Yeung, P. Singhasivanon, N.P.J. Day, N. Lindegardh, D. Socheat, and N.J. White. 2009. Artemisinin Resistance in Plasmodium falciparum Malaria. *New England Journal of Medicine* 361:455-467.

Doolan, D.L., C. Dobaño, and J.K. Baird. 2009. Acquired immunity to malaria. *Clin Microbiol Rev* 22:13-36.

Douglas, A.D., G.C. Baldeviano, J. Jin, K. Miura, A. Diouf, Z.A. Zenonos, J.A. Ventocilla, S.E. Silk, J.M. Marshall, D.G.W. Alanine, C. Wang, N.J. Edwards, K.P. Leiva, L.A. Gomez-Puerta, C.M. Lucas, G.J. Wright, C.A. Long, J.M. Royal, and S.J. Draper. 2019. A defined mechanistic correlate of protection against Plasmodium falciparum malaria in non-human primates. *Nature Communications* 10:1953.

Douglas, A.D., G.C. Baldeviano, C.M. Lucas, L.A. Lugo-Roman, C. Crosnier, S.J. Bartholdson, A. Diouf, K. Miura, L.E. Lambert, J.A. Ventocilla, K.P. Leiva, K.H. Milne, J.J. Illingworth, A.J. Spencer, K.A. Hjerrild, D.G. Alanine, A.V. Turner, J.T. Moorhead, K.A. Edgel, Y. Wu, C.A. Long, G.J. Wright, A.G. Lescano, and S.J. Draper. 2015. A PfRH5-based vaccine is efficacious against heterologous strain blood-stage Plasmodium falciparum infection in aotus monkeys. *Cell Host Microbe* 17:130-139.

Douglas, A.D., A.R. Williams, J.J. Illingworth, G. Kamuyu, S. Biswas, A.L. Goodman, D.H. Wyllie, C. Crosnier, K. Miura, G.J. Wright, C.A. Long, F.H. Osier, K. Marsh, A.V. Turner, A.V. Hill, and S.J. Draper. 2011. The blood-stage malaria antigen PfRH5 is susceptible to vaccine-inducible cross-strain neutralizing antibody. *Nat Commun* 2:601.

Draper, S.J., A.L. Goodman, S. Biswas, E.K. Forbes, A.C. Moore, S.C. Gilbert, and A.V.S. Hill. 2009. Recombinant Viral Vaccines Expressing Merozoite Surface Protein-1 Induce Antibody- and T Cell-Mediated Multistage Protection against Malaria. *Cell Host & Microbe* 5:95-105.

Drew, D.R., R.A. O'Donnell, B.J. Smith, and B.S. Crabb. 2004. A Common Cross-species Function for the Double Epidermal Growth Factor-like Modules of the Highly Divergent Plasmodium Surface Proteins MSP-1 and MSP-8*. *Journal of Biological Chemistry* 279:20147-20153.

Druilhe, P., F. Spertini, D. Soesoe, G. Corradin, P. Mejia, S. Singh, R. Audran, A. Bouzidi, C. Oeuvray, and C. Roussilhon. 2005. A Malaria Vaccine That Elicits in Humans Antibodies Able to Kill Plasmodium falciparum. *PLOS Medicine* 2:e344.

Duffy, P.E., and D.C. Kaslow. 1997. A novel malaria protein, Pfs28, and Pfs25 are genetically linked and synergistic as falciparum malaria transmission-blocking vaccines. *Infection and Immunity* 65:1109-1113.

Duncan, C.J., A.V. Hill, and R.D. Ellis. 2012. Can growth inhibition assays (GIA) predict blood-stage malaria vaccine efficacy? *Hum Vaccin Immunother* 8:706-714.

Dutta, S., J.D. Haynes, J.K. Moch, A. Barbosa, and D.E. Lanar. 2003. Invasion-inhibitory antibodies inhibit proteolytic processing of apical membrane antigen 1 of Plasmodium falciparum merozoites. *Proceedings of the National Academy of Sciences* 100:12295-12300.

Edozien, J.C., H.M. Gilles, and I.O.K. Udeozo. 1962. Adult and chord-blood gamma-globulin and immunity to malaria Nigerians. *The Lancet* 280:951-955.

Egan, A.F., J.A. Chappel, P.A. Burghaus, J.S. Morris, J.S. McBride, A.A. Holder, D.C. Kaslow, and E.M. Riley. 1995. Serum antibodies from malaria-exposed people recognize conserved epitopes formed by the two epidermal growth factor motifs of MSP1(19), the carboxy-terminal fragment of the major merozoite surface protein of Plasmodium falciparum. *Infect Immun* 63:456-466.

Egan, A.F., J. Morris, G. Barnish, S. Allen, B.M. Greenwood, D.C. Kaslow, A.A. Holder, and E.M. Riley. 1996. Clinical immunity to Plasmodium falciparum malaria is associated with serum antibodies to the 19-kDa C-terminal fragment of the merozoite surface antigen, PfMSP-1. *J Infect Dis* 173:765-769.

Ellis, R.D., L.B. Martin, D. Shaffer, C.A. Long, K. Miura, M.P. Fay, D.L. Narum, D. Zhu, G.E. Mullen, S. Mahanty, L.H. Miller, and A.P. Durbin. 2010. Phase 1 trial of the Plasmodium falciparum blood stage vaccine MSP1(42)-C1/Alhydrogel with and without CPG 7909 in malaria naïve adults. *PLoS One* 5:e8787.

Ellis, R.D., Y. Wu, L.B. Martin, D. Shaffer, K. Miura, J. Aebig, A. Orcutt, K. Rausch, D. Zhu, A. Mogensen, M.P. Fay, D.L. Narum, C. Long, L. Miller, and A.P. Durbin. 2012. Phase 1 study in malaria naïve adults of BSAM2/Alhydrogel®+CPG 7909, a blood stage vaccine against P. falciparum malaria. *PLoS One* 7:e46094.

Endeshaw, T., T. Gebre, J. Ngondi, P.M. Graves, E.B. Shargie, Y. Ejigsemahu, B. Ayele, G. Yohannes, T. Teferi, A. Messele, M. Zerihun, A. Genet, A.W. Mosher, P.M. Emerson, and F.O. Richards. 2008. Evaluation of light microscopy and rapid diagnostic test for the detection of malaria under operational field conditions: a household survey in Ethiopia. *Malaria Journal* 7:118.

Epstein, J.E., K.M. Paolino, T.L. Richie, M. Sedegah, A. Singer, A.J. Ruben, S. Chakravarty, A. Stafford, R.C. Ruck, A.G. Eappen, T. Li, P.F. Billingsley, A. Manoj, J.C. Silva, K. Moser, R. Nielsen, D. Tosh, S. Cicatelli, H. Ganeshan, J. Case, D. Padilla, S. Davidson, L. Garver, E. Saverino, T. Murshedkar, A. Gunasekera, P.S. Twomey, S. Reyes, J.E. Moon, E.R. James, N. Kc, M. Li, E. Abot, A. Belmonte, K. Hauns, M. Belmonte, J. Huang, C. Vasquez, S. Remich, M. Carrington, Y. Abebe, A. Tillman, B. Hickey, J. Regules, E. Villasante, B.K.L. Sim, and S.L. Hoffman. 2017. Protection against Plasmodium falciparum malaria by PfSPZ Vaccine. *JCI Insight* 2:e89154.

Esen, M., P.G. Kremsner, R. Schleucher, M. Gässler, E.B. Imoukhuede, N. Imbault, O. Leroy, S. Jepsen, B.W. Knudsen, M. Schumm, J. Knobloch, M. Theisen, and B. Mordmüller. 2009. Safety and immunogenicity of GMZ2 - a MSP3-GLURP fusion protein malaria vaccine candidate. *Vaccine* 27:6862-6868.

Etlinger, H.M., P. Caspers, H. Matile, H.J. Schoenfeld, D. Stueber, and B. Takacs. 1991. Ability of recombinant or native proteins to protect monkeys against heterologous challenge with Plasmodium falciparum. *Infect Immun* 59:3498-3503.

Ewer, K.J., G.A. O'Hara, C.J. Duncan, K.A. Collins, S.H. Sheehy, A. Reyes-Sandoval, A.L. Goodman, N.J. Edwards, S.C. Elias, F.D. Halstead, R.J. Longley, R. Rowland, I.D. Poulton, S.J. Draper, A.M. Blagborough, E. Berrie, S. Moyle, N. Williams, L. Siani, A. Folgori, S. Colloca, R.E. Sinden, A.M. Lawrie, R. Cortese, S.C. Gilbert, A. Nicosia, and A.V. Hill. 2013. Protective CD8+ T-cell immunity to human malaria induced by chimpanzee adenovirus-MVA immunisation. *Nat Commun* 4:2836.

Fairhurst, R.M., and A.M. Dondorp. 2016. Artemisinin-Resistant Plasmodium falciparum Malaria. *Microbiol Spectr* 4:

Färnert, A., K. Wyss, S. Dashti, and P. Naucler. 2015. Duration of residency in a non-endemic area and risk of severe malaria in African immigrants. *Clinical Microbiology and Infection* 21:494-501.

Farrington, L.A., P.C. Callaway, H.M. Vance, K. Baskevitch, E. Lutz, L. Warrier, T.I. McIntyre, R. Budker, P. Jagannathan, F. Nankya, K. Musinguzi, M. Nalubega, E. Sikyomu, K. Naluwu, E. Arinaitwe, G. Dorsey, M.R. Kamya, and M.E. Feeney. 2020. Opsonized antigen activates Vδ2+ T cells via CD16/FCγRIIIa in individuals with chronic malaria exposure. *PLoS Pathog* 16:e1008997.

Faust, C., and A.P. Dobson. 2015. Primate malarias: Diversity, distribution and insights for zoonotic Plasmodium. *One Health* 1:66-75.

Feng, G., M.J. Boyle, N. Cross, J.A. Chan, L. Reiling, F. Osier, D.I. Stanisic, I. Mueller, R.F. Anders, J.S. McCarthy, J.S. Richards, and J.G. Beeson. 2018. Human Immunization With a Polymorphic Malaria Vaccine Candidate Induced Antibodies to Conserved Epitopes That Promote Functional Antibodies to Multiple Parasite Strains. *J Infect Dis* 218:35-43.

Feng, G., L. Kurtovic, P.A. Agius, E.H. Aitken, J. Sacarlal, B.D. Wines, P.M. Hogarth, S.J. Rogerson, F.J.I. Fowkes, C. Dobaño, and J.G. Beeson. 2022. Induction, decay, and determinants of functional antibodies following vaccination with the RTS,S malaria vaccine in young children. *BMC Medicine* 20:289.

Feng, G., B.D. Wines, L. Kurtovic, J.-A. Chan, P. Boeuf, V. Mollard, A. Cozijnsen, D.R. Drew, R.J. Center, D.L. Marshall, S. Chishimba, G.I. McFadden, A.E. Dent, K. Chelimo, M.J. Boyle, J.W. Kazura, P.M. Hogarth, and J.G. Beeson. 2021. Mechanisms and targets of Fcγ-receptor mediated immunity to malaria sporozoites. *Nature Communications* 12:1742.

Ferrara, C., S. Grau, C. Jäger, P. Sondermann, P. Brünker, I. Waldhauer, M. Hennig, A. Ruf, A.C. Rufer, M. Stihle, P. Umaña, and J. Benz. 2011. Unique carbohydrate-carbohydrate interactions are required for high affinity binding between FcgammaRIII and antibodies lacking core fucose. *Proc Natl Acad Sci U S A* 108:12669-12674.

Ferreira, A., L. Schofield, V. Enea, H. Schellekens, P. van der Meide, W.E. Collins, R.S. Nussenzweig, and V. Nussenzweig. 1986. Inhibition of development of exoerythrocytic forms of malaria parasites by gamma-interferon. *Science* 232:881-884.

Fowkes, F.J., J.S. Richards, J.A. Simpson, and J.G. Beeson. 2010. The relationship between anti-merozoite antibodies and incidence of Plasmodium falciparum malaria: A systematic review and meta-analysis. *PLoS Med* 7:e1000218.

Fry, M., and M. Pudney. 1992. Site of action of the antimalarial hydroxynaphthoquinone, 2-[trans-4-(4'-chlorophenyl) cyclohexyl]-3-hydroxy-1,4-naphthoquinone (566C80). *Biochem Pharmacol* 43:1545-1553.

Fullman, N., R. Burstein, S.S. Lim, C. Medlin, and E. Gakidou. 2013. Nets, spray or both? The effectiveness of insecticide-treated nets and indoor residual spraying in reducing malaria morbidity and child mortality in sub-Saharan Africa. *Malaria Journal* 12:62.

Gaillard, T., M. Madamet, F.F. Tsombeng, J. Dormoi, and B. Pradines. 2016. Antibiotics in malaria therapy: which antibiotics except tetracyclines and macrolides may be used against malaria? *Malaria Journal* 15:556.

Galamo, C.D., A. Jafarshad, C. Blanc, and P. Druilhe. 2009. Anti-MSP1 block 2 antibodies are effective at parasite killing in an allele-specific manner by monocyte-mediated antibody-dependent cellular inhibition. *J Infect Dis* 199:1151-1154.

Gantz, V.M., N. Jasinskiene, O. Tatarenkova, A. Fazekas, V.M. Macias, E. Bier, and A.A. James. 2015. Highly efficient Cas9-mediated gene drive for population modification of the malaria vector mosquito Anopheles stephensi. *Proc Natl Acad Sci U S A* 112:E6736-6743.

Garcia-Senosiain, A., I.H. Kana, S. Singh, M.K. Das, M.H. Dziegiel, S. Hertegonne, B. Adu, and M. Theisen. 2021. Neutrophils dominate in opsonic phagocytosis of P. falciparum blood-stage merozoites and protect against febrile malaria. *Commun Biol* 4:984.

Garcia-Senosiain, A., I.H. Kana, S.K. Singh, B.K. Chourasia, M.K. Das, D. Dodoo, S. Singh, B. Adu, and M. Theisen. 2020. Peripheral Merozoite Surface Proteins Are Targets of Naturally Acquired Immunity against Malaria in both India and Ghana. *Infect Immun* 88:

Gardner, M.J., N. Hall, E. Fung, O. White, M. Berriman, R.W. Hyman, J.M. Carlton, A. Pain, K.E. Nelson, S. Bowman, I.T. Paulsen, K. James, J.A. Eisen, K. Rutherford, S.L. Salzberg, A. Craig, S. Kyes, M.S. Chan, V. Nene, S.J. Shallom, B. Suh, J. Peterson, S. Angiuoli, M. Pertea, J. Allen, J. Selengut, D. Haft, M.W. Mather, A.B. Vaidya, D.M. Martin, A.H. Fairlamb, M.J. Fraunholz, D.S. Roos, S.A. Ralph, G.I. McFadden, L.M. Cummings, G.M. Subramanian, C. Mungall, J.C. Venter, D.J. Carucci, S.L. Hoffman, C. Newbold, R.W. Davis, C.M. Fraser, and B. Barrell. 2002. Genome sequence of the human malaria parasite Plasmodium falciparum. *Nature* 419:498-511.

Garg, S., S. Agarwal, S. Dabral, N. Kumar, S. Sehrawat, and S. Singh. 2015. Visualization and quantification of Plasmodium falciparum intraerythrocytic merozoites. *Syst Synth Biol* 9:23-26.

Gaudinski, M.R., N.M. Berkowitz, A.H. Idris, E.E. Coates, L.A. Holman, F. Mendoza, I.J. Gordon, S.H. Plummer, O. Trofymenko, Z. Hu, A. Campos Chagas, S. O'Connell, M. Basappa, N. Douek, S.R. Narpala, C.R. Barry, A.T. Widge, R. Hicks, S.F. Awan, R.L. Wu, S. Hickman, D. Wycuff, J.A. Stein, C. Case, B.P. Evans, K. Carlton, J.G. Gall, S. Vazquez, B. Flach, G.L. Chen, J.R. Francica, B.J. Flynn, N.K. Kisalu, E.V. Capparelli, A. McDermott, J.R. Mascola, J.E. Ledgerwood, and R.A. Seder. 2021. A Monoclonal Antibody for Malaria Prevention. *New England Journal of Medicine* 385:803-814.

Genton, B., F. Al-Yaman, R. Anders, A. Saul, G. Brown, D. Pye, D.O. Irving, W.R. Briggs, A. Mai, M. Ginny, T. Adiguma, L. Rare, A. Giddy, R. Reber-Liske, D. Stuerchler, and M.P. Alpers. 2000. Safety and immunogenicity of a three-component blood-stage malaria vaccine in adults living in an endemic area of Papua New Guinea. *Vaccine* 18:2504-2511.

Genton, B., I. Betuela, I. Felger, F. Al-Yaman, R.F. Anders, A. Saul, L. Rare, M. Baisor, K. Lorry, G.V. Brown, D. Pye, D.O. Irving, T.A. Smith, H.P. Beck, and M.P. Alpers. 2002. A recombinant blood-stage malaria vaccine reduces Plasmodium falciparum density and exerts selective pressure on parasite populations in a phase 1-2b trial in Papua New Guinea. *J Infect Dis* 185:820-827.

Gerald, N., B. Mahajan, and S. Kumar. 2011. Mitosis in the human malaria parasite Plasmodium falciparum. *Eukaryot Cell* 10:474-482.

Ghumra, A., P. Khunrae, R. Ataide, A. Raza, S.J. Rogerson, M.K. Higgins, and J.A. Rowe. 2011. Immunisation with recombinant PfEMP1 domains elicits functional rosette-inhibiting and phagocytosis-inducing antibodies to Plasmodium falciparum. *PloS one* 6:e16414-e16414.

Gillies, M., and B. De Meillon. 1968. The Anophelinae of Africa south of the Sahara, vol. 54. *Johannesburg: The South African Institute for Medical Research*

Gilson, P.R., and B.S. Crabb. 2009. Morphology and kinetics of the three distinct phases of red blood cell invasion by Plasmodium falciparum merozoites. *Int J Parasitol* 39:91-96.

Gilson, P.R., T. Nebl, D. Vukcevic, R.L. Moritz, T. Sargeant, T.P. Speed, L. Schofield, and B.S. Crabb. 2006. Identification and stoichiometry of glycosylphosphatidylinositol-anchored membrane proteins of the human malaria parasite Plasmodium falciparum. *Mol Cell Proteomics* 5:1286-1299.

Gleave, K., N. Lissenden, M. Chaplin, L. Choi, and H. Ranson. 2021. Piperonyl butoxide (PBO) combined with pyrethroids in insecticide-treated nets to prevent malaria in Africa. *Cochrane Database Syst Rev* 5:Cd012776.

Goel, V.K., X. Li, H. Chen, S.C. Liu, A.H. Chishti, and S.S. Oh. 2003. Band 3 is a host receptor binding merozoite surface protein 1 during the Plasmodium falciparum invasion of erythrocytes. *Proc Natl Acad Sci U S A* 100:5164-5169.

Golenser, J., M. Kamyl, A. Tsafack, E. Marva, A. Cohen, N. Kitrossky, and M. Chevion. 1992. Correlation between destruction of malarial parasites by polymorphonuclear leucocytes and oxidative stress. *Free Radic Res Commun* 17:249-262.

Gomes, F.M., B.L. Hixson, M.D.W. Tyner, J.L. Ramirez, G.E. Canepa, T.L. Alves e Silva, A. Molina-Cruz, M. Keita, F. Kane, B. Traoré, N. Sogoba, and C. Barillas-Mury. 2017. Effect of naturally occurring Wolbachia in Anopheles gambiae s.l. mosquitoes from Mali on Plasmodium falciparum malaria transmission. *Proceedings of the National Academy of Sciences* 114:12566-12571.

Good, K.L., D.T. Avery, and S.G. Tangye. 2009. Resting human memory B cells are intrinsically programmed for enhanced survival and responsiveness to diverse stimuli compared to naive B cells. *J Immunol* 182:890-901.

Goodman, C.D., J.E. Siregar, V. Mollard, J. Vega-Rodríguez, D. Syafruddin, H. Matsuoka, M. Matsuzaki, T. Toyama, A. Sturm, A. Cozijnsen, M. Jacobs-Lorena, K. Kita, S. Marzuki, and G.I. McFadden. 2016. Parasites resistant to the antimalarial atovaquone fail to transmit by mosquitoes. *Science* 352:349-353.

Gosling, R.D., L. Okell, J. Mosha, and D. Chandramohan. 2011. The role of antimalarial treatment in the elimination of malaria. *Clin Microbiol Infect* 17:1617-1623.

Goswami, D., W. Betz, N.K. Locham, C. Parthiban, C. Brager, C. Schäfer, N. Camargo, T. Nguyen, S.Y. Kennedy, S.C. Murphy, A.M. Vaughan, and S.H. Kappe. 2020. A replication-competent late liver stage-attenuated human malaria parasite. *JCI Insight* 5:

Grandesso, F., C. Nabasumba, D. Nyehangane, A.L. Page, M. Bastard, M. De Smet, Y. Boum, and J.F. Etard. 2016. Performance and time to become negative after treatment of three malaria rapid diagnostic tests in low and high malaria transmission settings. *Malar J* 15:496.

Green, T.J., M. Morhardt, R.G. Brackett, and R.L. Jacobs. 1981. Serum inhibition of merozoite dispersal from Plasmodium falciparum schizonts: indicator of immune status. *Infect Immun* 31:1203-1208.

Griffin, J.T., M. Cairns, A.C. Ghani, C. Roper, D. Schellenberg, I. Carneiro, R.D. Newman, M.P. Grobusch, B. Greenwood, D. Chandramohan, and R.D. Gosling. 2010. Protective efficacy of intermittent preventive treatment of malaria in infants (IPTi) using sulfadoxine-pyrimethamine and parasite resistance. *PLoS One* 5:e12618.

Guenot, M., S. Loizon, J. Howard, G. Costa, D.A. Baker, S.Y. Mohabeer, M. Troye-Blomberg, J.F. Moreau, J. Déchanet-Merville, O. Mercereau-Puijalon, M. Mamani-Matsuda, and C. Behr. 2015. Phosphoantigen Burst upon Plasmodium falciparum Schizont Rupture Can Distantly Activate Vγ9Vδ2 T Cells. *Infect Immun* 83:3816-3824.

Guevara Patiño, J.A., A.A. Holder, J.S. McBride, and M.J. Blackman. 1997. Antibodies that inhibit malaria merozoite surface protein-1 processing and erythrocyte invasion are blocked by naturally acquired human antibodies. *The Journal of experimental medicine* 186:1689-1699.

Haldar, K., S. Bhattacharjee, and I. Safeukui. 2018. Drug resistance in Plasmodium. *Nat Rev Microbiol* 16:156-170.

Hamel, M.J., P. Otieno, N. Bayoh, S. Kariuki, V. Were, D. Marwanga, K.F. Laserson, J. Williamson, L. Slutsker, and J. Gimnig. 2011. The combination of indoor residual spraying and insecticide-treated nets provides added protection against malaria compared with insecticide-treated nets alone. *Am J Trop Med Hyg* 85:1080-1086.

Hammarlund, E., A. Thomas, I.J. Amanna, L.A. Holden, O.D. Slayden, B. Park, L. Gao, and M.K. Slifka. 2017. Plasma cell survival in the absence of B cell memory. *Nature Communications* 8:1781.

Hammond, A., R. Galizi, K. Kyrou, A. Simoni, C. Siniscalchi, D. Katsanos, M. Gribble, D. Baker, E. Marois, S. Russell, A. Burt, N. Windbichler, A. Crisanti, and T. Nolan. 2016. A CRISPR-Cas9 gene drive system targeting female reproduction in the malaria mosquito vector Anopheles gambiae. *Nature Biotechnology* 34:78-83.

Hammond, A.M., K. Kyrou, M. Bruttini, A. North, R. Galizi, X. Karlsson, N. Kranjc, F.M. Carpi, R. D'Aurizio, A. Crisanti, and T. Nolan. 2017. The creation and selection of mutations resistant to a gene drive over multiple generations in the malaria mosquito. *PLOS Genetics* 13:e1007039.

Hamre, K.E.S., B.N. Ondigo, J.S. Hodges, S. Dutta, M. Theisen, G. Ayodo, and C.C. John. 2020. Antibody Correlates of Protection from Clinical Plasmodium falciparum Malaria in an Area of Low and Unstable Malaria Transmission. *The American journal of tropical medicine and hygiene* 103:2174-2182.

Harbach, R.E. 2004. The classification of genus Anopheles (Diptera: Culicidae): a working hypothesis of phylogenetic relationships. *Bulletin of Entomological Research* 94:537-553.

Harris, K.S., J.L. Casey, A.M. Coley, R. Masciantonio, J.K. Sabo, D.W. Keizer, E.F. Lee, A. McMahon, R.S. Norton, R.F. Anders, and M. Foley. 2005. Binding hot spot for invasion inhibitory molecules on Plasmodium falciparum apical membrane antigen 1. *Infection and immunity* 73:6981-6989.

Hawking, F., M.E. Wilson, and K. Gammage. 1971. Evidence for cyclic development and short-lived maturity in the gametocytes of Plasmodium falciparum. *Trans R Soc Trop Med Hyg* 65:549-559.

Hay, S.I., M.E. Sinka, R.M. Okara, C.W. Kabaria, P.M. Mbithi, C.C. Tago, D. Benz, P.W. Gething, R.E. Howes, A.P. Patil, W.H. Temperley, M.J. Bangs, T. Chareonviriyaphap, I.R.F. Elyazar, R.E. Harbach, J. Hemingway, S. Manguin, C.M. Mbogo, Y. Rubio-Palis, and H.C.J. Godfray. 2010. Developing Global Maps of the Dominant Anopheles Vectors of Human Malaria. *PLOS Medicine* 7:e1000209.

Healer, J., A. Graszynski, and E. Riley. 1999. Phagocytosis does not play a major role in naturally acquired transmission-blocking immunity to Plasmodium falciparum malaria. *Infect Immun* 67:2334-2339.

Healy, S.A., C. Anderson, B.J. Swihart, A. Mwakingwe, E.E. Gabriel, H. Decederfelt, C.V. Hobbs, K.M. Rausch, D. Zhu, O. Muratova, R. Herrera, P.V. Scaria, N.J. MacDonald, L.E. Lambert, I. Zaidi, C.H. Coelho, J.P. Renn, Y. Wu, D.L. Narum, and P.E. Duffy. 2021. Pfs230 yields higher malaria transmission-blocking vaccine activity than Pfs25 in humans but not mice. *J Clin Invest* 131:

Herrera, S., M.A. Herrera, B.L. Perlaza, Y. Burki, P. Caspers, H. Döbeli, D. Rotmann, and U. Certa. 1990. Immunization of Aotus monkeys with Plasmodium falciparum blood-stage recombinant proteins. *Proceedings of the National Academy of Sciences* 87:4017-4021.

Hertig, M., and S.B. Wolbach. 1924. Studies on Rickettsia-Like Micro-Organisms in Insects. *J Med Res* 44:329-374.327.

Hilgenboecker, K., P. Hammerstein, P. Schlattmann, A. Telschow, and J.H. Werren. 2008. How many species are infected with Wolbachia?--A statistical analysis of current data. *FEMS Microbiol Lett* 281:215-220.

Hill, D.L., E.M. Eriksson, C.S. Li Wai Suen, C.Y. Chiu, V. Ryg-Cornejo, L.J. Robinson, P.M. Siba, I. Mueller, D.S. Hansen, and L. Schofield. 2013. Opsonising antibodies to P. falciparum merozoites associated with immunity to clinical malaria. *PLoS One* 8:e74627.

Hirunpetcharat, C., J.H. Tian, D.C. Kaslow, N. van Rooijen, S. Kumar, J.A. Berzofsky, L.H. Miller, and M.F. Good. 1997. Complete protective immunity induced in mice by immunization with the 19-kilodalton carboxyl-terminal fragment of the merozoite surface protein-1 (MSP1[19]) of Plasmodium yoelii expressed in Saccharomyces cerevisiae: correlation of protection with antigen-specific antibody titer, but not with effector CD4+ T cells. *J Immunol* 159:3400-3411.

Ho, M., P. Tongtawe, J. Kriangkum, T. Wimonwattrawatee, K. Pattanapanyasat, L. Bryant, J. Shafiq, P. Suntharsamai, S. Looareesuwan, H.K. Webster, and J.F. Elliott. 1994. Polyclonal expansion of peripheral gamma delta T cells in human Plasmodium falciparum malaria. *Infect Immun* 62:855-862.

Hodder, A.N., P.E. Czabotar, A.D. Uboldi, O.B. Clarke, C.S. Lin, J. Healer, B.J. Smith, and A.F. Cowman. 2012. Insights into Duffy binding-like domains through the crystal structure and function of the merozoite surface protein MSPDBL2 from Plasmodium falciparum. *J Biol Chem* 287:32922-32939.

Hoffman, S.L., P.F. Billingsley, E. James, A. Richman, M. Loyevsky, T. Li, S. Chakravarty, A. Gunasekera, R. Chattopadhyay, M. Li, R. Stafford, A. Ahumada, J.E. Epstein, M. Sedegah, S. Reyes, T.L. Richie, K.E. Lyke, R. Edelman, M.B. Laurens, C.V. Plowe, and B.K. Sim. 2010. Development of a metabolically active, non-replicating sporozoite vaccine to prevent Plasmodium falciparum malaria. *Hum Vaccin* 6:97-106.

Holder, A.A., and R.R. Freeman. 1981. Immunization against blood-stage rodent malaria using purified parasite antigens. *Nature* 294:361-364.

Holder, A.A., J.S. Sandhu, Y. Hillman, L.S. Davey, S.C. Nicholls, H. Cooper, and M.J. Lockyer. 1987. Processing of the precursor to the major merozoite surface antigens of Plasmodium falciparum. *Parasitology* 94 (Pt 2):199-208.

Honjo, K., Y. Kubagawa, and H. Kubagawa. 2013. Is Toso/IgM Fc receptor (FcμR) expressed by innate immune cells? *Proc Natl Acad Sci U S A* 110:E2540-2541.

Hopp, C.S., P. Sekar, A. Diouf, K. Miura, K. Boswell, J. Skinner, C.M. Tipton, M.E. Peterson, M.J. Chambers, S. Andrews, J. Lu, J. Tan, S. Li, S. Doumbo, K. Kayentao, A. Ongoiba, B. Traore, S. Portugal, P.D. Sun, C. Long, R.A. Koup, E.O. Long, A.B. McDermott, and P.D. Crompton. 2021. Plasmodium falciparum-specific IgM B cells dominate in children, expand with malaria, and produce functional IgM. *J Exp Med* 218:

Horowitz, A., K.C. Newman, J.H. Evans, D.S. Korbel, D.M. Davis, and E.M. Riley. 2010. Cross-talk between T cells and NK cells generates rapid effector responses to Plasmodium falciparum-infected erythrocytes. *J Immunol* 184:6043-6052.

Houde, D., Y. Peng, S.A. Berkowitz, and J.R. Engen. 2010. Post-translational modifications differentially affect IgG1 conformation and receptor binding. *Molecular & cellular proteomics : MCP* 9:1716-1728.

Howell, S.A., I. Well, S.L. Fleck, C. Kettleborough, C.R. Collins, and M.J. Blackman. 2003. A single malaria merozoite serine protease mediates shedding of multiple surface proteins by juxtamembrane cleavage. *J Biol Chem* 278:23890-23898.

Hughes, G.L., R. Koga, P. Xue, T. Fukatsu, and J.L. Rasgon. 2011. Wolbachia infections are virulent and inhibit the human malaria parasite Plasmodium falciparum in Anopheles gambiae. *PLoS Pathog* 7:e1002043.

Hyde, J.E. 1990. The dihydrofolate reductase-thymidylate synthetase gene in the drug resistance of malaria parasites. *Pharmacol Ther* 48:45-59.

Hyde, J.E. 2005. Exploring the folate pathway in Plasmodium falciparum. *Acta Trop* 94:191-206.

Imai, T., J. Shen, B. Chou, X. Duan, L. Tu, K. Tetsutani, C. Moriya, H. Ishida, S. Hamano, C. Shimokawa, H. Hisaeda, and K. Himeno. 2010. Involvement of CD8+ T cells in protective immunity against murine blood-stage infection with Plasmodium yoelii 17XL strain. *Eur J Immunol* 40:1053-1061.

Imkeller, K., S.W. Scally, A. Bosch, G.P. Martí, G. Costa, G. Triller, R. Murugan, V. Renna, H. Jumaa, P.G. Kremsner, B.K.L. Sim, S.L. Hoffman, B. Mordmüller, E.A. Levashina, J.P. Julien, and H. Wardemann. 2018. Antihomotypic affinity maturation improves human B cell responses against a repetitive epitope. *Science* 360:1358-1362.

Ishizuka, A.S., K.E. Lyke, A. DeZure, A.A. Berry, T.L. Richie, F.H. Mendoza, M.E. Enama, I.J. Gordon, L.J. Chang, U.N. Sarwar, K.L. Zephir, L.A. Holman, E.R. James, P.F. Billingsley, A. Gunasekera, S. Chakravarty, A. Manoj, M. Li, A.J. Ruben, T. Li, A.G. Eappen, R.E. Stafford, C.N. K, T. Murshedkar, H. DeCederfelt, S.H. Plummer, C.S. Hendel, L. Novik, P.J. Costner, J.G. Saunders, M.B. Laurens, C.V. Plowe, B. Flynn, W.R. Whalen, J.P. Todd, J. Noor, S. Rao, K. Sierra-Davidson, G.M. Lynn, J.E. Epstein, M.A. Kemp, G.A. Fahle, S.A. Mikolajczak, M. Fishbaugher, B.K. Sack, S.H. Kappe, S.A. Davidson, L.S. Garver, N.K. Björkström, M.C. Nason, B.S. Graham, M. Roederer, B.K. Sim, S.L. Hoffman, J.E. Ledgerwood, and R.A. Seder. 2016. Protection against malaria at 1 year and immune correlates following PfSPZ vaccination. *Nat Med* 22:614-623.

Jagannathan, P., F. Lutwama, M.J. Boyle, F. Nankya, L.A. Farrington, T.I. McIntyre, K. Bowen, K. Naluwu, M. Nalubega, K. Musinguzi, E. Sikyomu, R. Budker, A. Katureebe, J. Rek, B. Greenhouse, G. Dorsey, M.R. Kamya, and M.E. Feeney. 2017. Vδ2+ T cell response to malaria correlates with protection from infection but is attenuated with repeated exposure. *Scientific reports* 7:11487-11487.

Jaramillo, M., D.C. Gowda, D. Radzioch, and M. Olivier. 2003. Hemozoin increases IFN-gamma-inducible macrophage nitric oxide generation through extracellular signal-regulated kinase- and NF-kappa B-dependent pathways. *J Immunol* 171:4243-4253.

Jäschke, A. (2017). Analysis of the human response against the Merozoite Surface Protein (MSP)- from Plasmodium falciparum - a malaria vaccine candidate. PhD thesis. heidelberg university.1

Jäschke, A., B. Coulibaly, E.J. Remarque, H. Bujard, and C. Epp. 2017. Merozoite Surface Protein 1 from Plasmodium falciparum Is a Major Target of Opsonizing Antibodies in Individuals with Acquired Immunity against Malaria. *Clin Vaccine Immunol* 24:

Jepsen, M.P.G., P.S. Jogdand, S.K. Singh, M. Esen, M. Christiansen, S. Issifou, A.B. Hounkpatin, U. Ateba-Ngoa, P.G. Kremsner, M.H. Dziegiel, S. Olesen-Larsen, S. Jepsen, B. Mordmüller, and M. Theisen. 2013. The Malaria Vaccine Candidate GMZ2 Elicits Functional Antibodies in Individuals From Malaria Endemic and Non-Endemic Areas. *The Journal of Infectious Diseases* 208:479-488.

Jeyaprakash, A., and M.A. Hoy. 2000. Long PCR improves Wolbachia DNA amplification: wsp sequences found in 76% of sixty-three arthropod species. *Insect Mol Biol* 9:393-405.

Joos, C., L. Marrama, H.E. Polson, S. Corre, A.M. Diatta, B. Diouf, J.F. Trape, A. Tall, S. Longacre, and R. Perraut. 2010. Clinical protection from falciparum malaria correlates with neutrophil respiratory bursts induced by merozoites opsonized with human serum antibodies. *PLoS One* 5:e9871.

Joos, C., M.L. Varela, B. Mbengue, A. Mansourou, L. Marrama, C. Sokhna, A. Tall, J.F. Trape, A. Touré, O. Mercereau-Puijalon, and R. Perraut. 2015. Antibodies to Plasmodium falciparum merozoite surface protein-1p19 malaria vaccine candidate induce antibody-dependent respiratory burst in human neutrophils. *Malar J* 14:409.

Julien, J.P., and H. Wardemann. 2019. Antibodies against Plasmodium falciparum malaria at the molecular level. *Nat Rev Immunol* 19:761-775.

Kaiser, K., K. Matuschewski, N. Camargo, J. Ross, and S.H. Kappe. 2004. Differential transcriptome profiling identifies Plasmodium genes encoding pre-erythrocytic stage-specific proteins. *Mol Microbiol* 51:1221-1232.

Kamuyu, G. (2017) Identifying the Merozoite Targets of Protective Immunity to Plasmodium flaciparum Malaria. PhD thesis. Open University.

Kamuyu, G., J. Tuju, R. Kimathi, K. Mwai, J. Mburu, N. Kibinge, M. Chong Kwan, S. Hawkings, R. Yaa, E. Chepsat, J.M. Njunge, T. Chege, F. Guleid, M. Rosenkranz, C.K. Kariuki, R. Frank, S.M. Kinyanjui, L.M. Murungi, P. Bejon, A. Färnert, K.K.A. Tetteh, J.G. Beeson, D.J. Conway, K. Marsh, J.C. Rayner, and F.H.A. Osier. 2018. KILchip v1.0: A Novel Plasmodium falciparum Merozoite Protein Microarray to Facilitate Malaria Vaccine Candidate Prioritization. *Front Immunol* 9:2866.

Kana, I.H., S.K. Singh, A. Garcia-Senosiain, D. Dodoo, S. Singh, B. Adu, and M. Theisen. 2019. Breadth of Functional Antibodies Is Associated With Plasmodium falciparum Merozoite Phagocytosis and Protection Against Febrile Malaria. *J Infect Dis* 220:275-284.

Kapelski, S., T. Klockenbring, R. Fischer, S. Barth, and R. Fendel. 2014. Assessment of the neutrophilic antibody-dependent respiratory burst (ADRB) response to Plasmodium falciparum. *J Leukoc Biol* 96:1131-1142.

Kapulu, M.C., D.F. Da, K. Miura, Y. Li, A.M. Blagborough, T.S. Churcher, D. Nikolaeva, A.R. Williams, A.L. Goodman, I. Sangare, A.V. Turner, M.G. Cottingham, A. Nicosia, U. Straschil, T. Tsuboi, S.C. Gilbert, C.A. Long, R.E. Sinden, S.J. Draper, A.V. Hill, A. Cohuet, and S. Biswas. 2015. Comparative assessment of transmission-blocking vaccine candidates against Plasmodium falciparum. *Sci Rep* 5:11193.

Kapulu, M.C., D. Kimani, P. Njuguna, M. Hamaluba, E. Otieno, R. Kimathi, J. Tuju, B.K.L. Sim, A.I. Abdi, Y. Abebe, P. Bejon, P.F. Billingsley, P.C. Bull, Z. de Laurent, S.L. Hoffman, E.R. James, S. Kariuki, S. Kinyanjui, C. Kivisi, J. Makale, K. Marsh, K.S. Mohammed, M. Mosobo, J. Musembi, J. Musyoki, M. Muthui, J. Mwacharo, K. Mwai, J.M. Ngoi, O. Ngoto, I. Nkumama, F. Ndungu, D. Odera, B. Ogutu, F. Olewe, D. Omuoyo, J. Ong'echa, F. Osier, T.L. Richie, J. Shangala, J. Wambua, T.N. Williams, and C.-S.S. Team. 2022. Controlled human malaria infection (CHMI) outcomes in Kenyan adults is associated with prior history of malaria exposure and anti-schizont antibody response. *BMC Infectious Diseases* 22:86.

Kapulu, M.C., P. Njuguna, and M.M. Hamaluba. 2018. Controlled Human Malaria Infection in Semi-Immune Kenyan Adults (CHMI-SIKA): a study protocol to investigate in vivo Plasmodium falciparum malaria parasite growth in the context of pre-existing immunity. *Wellcome Open Res* 3:155.

Kapur, R., I. Kustiawan, A. Vestrheim, C.A. Koeleman, R. Visser, H.K. Einarsdottir, L. Porcelijn, D. Jackson, B. Kumpel, A.M. Deelder, D. Blank, B. Skogen, M.K. Killie, T.E. Michaelsen, M. de Haas, T. Rispens, C.E. van der Schoot, M. Wuhrer, and G. Vidarsson. 2014. A prominent lack of IgG1-Fc fucosylation of platelet alloantibodies in pregnancy. *Blood* 123:471-480.

Kassim, O.O., K.A. Ako-Anai, S.E. Torimiro, G.P. Hollowell, V.C. Okoye, and S.K. Martin. 2000. Inhibitory factors in breastmilk, maternal and infant sera against in vitro growth of Plasmodium falciparum malaria parasite. *J Trop Pediatr* 46:92-96.

Kauth, C.W., C. Epp, H. Bujard, and R. Lutz. 2003. The merozoite surface protein 1 complex of human malaria parasite Plasmodium falciparum: interactions and arrangements of subunits. *J Biol Chem* 278:22257-22264.

Kauth, C.W., U. Woehlbier, M. Kern, Z. Mekonnen, R. Lutz, N. Mücke, J. Langowski, and H. Bujard. 2006. Interactions between merozoite surface proteins 1, 6, and 7 of the malaria parasite Plasmodium falciparum. *J Biol Chem* 281:31517-31527.

Keitel, W.A., K.E. Kester, R.L. Atmar, A.C. White, N.H. Bond, C.A. Holland, U. Krzych, D.R. Palmer, A. Egan, C. Diggs, W.R. Ballou, B.F. Hall, and D. Kaslow. 1999. Phase I trial of two recombinant vaccines containing the 19kd carboxy terminal fragment of Plasmodium falciparum merozoite surface protein 1 (msp-1(19)) and T helper epitopes of tetanus toxoid. *Vaccine* 18:531-539.

Khusmith, S., and P. Druilhe. 1982. Specific arming of monocytes by cytophilic IgG promotes Plasmodium falciparum merozoite ingestion. *Transactions of The Royal Society of Tropical Medicine and Hygiene* 76:423-424.

Khusmith, S., P. Druilhe, and M. Gentilini. 1982. Enhanced Plasmodium falciparum merozoite phagocytosis by monocytes from immune individuals. *Infect Immun* 35:874-879.

Kiemde, F., M.D.A. Bonko, M.C. Tahita, P. Lompo, T. Rouamba, H. Tinto, M.B. van Hensbroek, P.F. Mens, and H. Schallig. 2017. Accuracy of a Plasmodium falciparum specific histidine-rich protein 2 rapid diagnostic test in the context of the presence of non-malaria fevers, prior anti-malarial use and seasonal malaria transmission. *Malar J* 16:294.

Kimingi, H.W., A.W. Kinyua, N.A. Achieng, K.M. Wambui, S. Mwangi, R. Nguti, C.A. Kivisi, A.T.R. Jensen, P. Bejon, M.C. Kapulu, A.I. Abdi, and S.M. Kinyanjui. 2022. Breadth of Antibodies to Plasmodium falciparum Variant Surface Antigens Is Associated With Immunity in a Controlled Human Malaria Infection Study. *Front Immunol* 13:894770.

Kisalu, N.K., A.H. Idris, C. Weidle, Y. Flores-Garcia, B.J. Flynn, B.K. Sack, S. Murphy, A. Schön, E. Freire, J.R. Francica, A.B. Miller, J. Gregory, S. March, H.-X. Liao, B.F. Haynes, K. Wiehe, A.M. Trama, K.O. Saunders, M.A. Gladden, A. Monroe, M. Bonsignori, M. Kanekiyo, A.K. Wheatley, A.B. McDermott, S.K. Farney, G.-Y. Chuang, B. Zhang, N. Kc, S. Chakravarty, P.D. Kwong, P. Sinnis, S.N. Bhatia, S.H.I. Kappe, B.K.L. Sim, S.L. Hoffman, F. Zavala, M. Pancera, and R.A. Seder. 2018. A human monoclonal antibody prevents malaria infection by targeting a new site of vulnerability on the parasite. *Nature medicine* 24:408-416.

Kleinschmidt, I., C. Schwabe, M. Shiva, J.L. Segura, V. Sima, S.J. Mabunda, and M. Coleman. 2009. Combining indoor residual spraying and insecticide-treated net interventions. *Am J Trop Med Hyg* 81:519-524.

Koita, O.A., O.K. Doumbo, A. Ouattara, L.K. Tall, A. Konaré, M. Diakité, M. Diallo, I. Sagara, G.L. Masinde, S.N. Doumbo, A. Dolo, A. Tounkara, I. Traoré, and D.J. Krogstad. 2012. False-negative rapid diagnostic tests for malaria and deletion of the histidine-rich repeat region of the hrp2 gene. *Am J Trop Med Hyg* 86:194-198.

Koussis, K., C. Withers-Martinez, S. Yeoh, M. Child, F. Hackett, E. Knuepfer, L. Juliano, U. Woehlbier, H. Bujard, and M.J. Blackman. 2009. A multifunctional serine protease primes the malaria parasite for red blood cell invasion. *Embo j* 28:725-735.

Kozycki, C.T., N. Umulisa, S. Rulisa, E.I. Mwikarago, J.P. Musabyimana, J.P. Habimana, C. Karema, and D.J. Krogstad. 2017. False-negative malaria rapid diagnostic tests in Rwanda: impact of Plasmodium falciparum isolates lacking hrp2 and declining malaria transmission. *Malar J* 16:123.

Kraemer, S.M., and J.D. Smith. 2006. A family affair: var genes, PfEMP1 binding, and malaria disease. *Curr Opin Microbiol* 9:374-380.

Krishnamurty, A.T., C.D. Thouvenel, S. Portugal, G.J. Keitany, K.S. Kim, A. Holder, P.D. Crompton, D.J. Rawlings, and M. Pepper. 2016. Somatically Hypermutated Plasmodium-Specific IgM(+) Memory B Cells Are Rapid, Plastic, Early Responders upon Malaria Rechallenge. *Immunity* 45:402-414.

Kubagawa, H., S. Oka, Y. Kubagawa, I. Torii, E. Takayama, D.W. Kang, G.L. Gartland, L.F. Bertoli, H. Mori, H. Takatsu, T. Kitamura, H. Ohno, and J.Y. Wang. 2009. Identity of the elusive IgM Fc receptor (FcmuR) in humans. *J Exp Med* 206:2779-2793.

Kumar, S., A. Yadava, D.B. Keister, J.H. Tian, M. Ohl, K.A. Perdue-Greenfield, L.H. Miller, and D.C. Kaslow. 1995. Immunogenicity and In Vivo Efficacy of Recombinant Plasmodium falciparum Merozoite Surface Protein-1 in Aotus Monkeys. *Molecular Medicine* 1:325-332.

Kumaratilake, L.M., and A. Ferrante. 2000. Opsonization and phagocytosis of Plasmodium falciparum merozoites measured by flow cytometry. *Clin Diagn Lab Immunol* 7:9-13.

Kurtovic, L., M.C. Behet, G. Feng, L. Reiling, K. Chelimo, A.E. Dent, I. Mueller, J.W. Kazura, R.W. Sauerwein, F.J.I. Fowkes, and J.G. Beeson. 2018. Human antibodies activate complement against Plasmodium falciparum sporozoites, and are associated with protection against malaria in children. *BMC Med* 16:61.

Kurtzhals, J.A., V. Adabayeri, B.Q. Goka, B.D. Akanmori, J.O. Oliver-Commey, F.K. Nkrumah, C. Behr, and L. Hviid. 1998. Low plasma concentrations of interleukin 10 in severe malarial anaemia compared with cerebral and uncomplicated malaria. *Lancet* 351:1768-1772.

Kurup, S.P., N.S. Butler, and J.T. Harty. 2019. T cell-mediated immunity to malaria. *Nature Reviews Immunology* 19:457-471.

Kyabayinze, D.J., J.K. Tibenderana, G.W. Odong, J.B. Rwakimari, and H. Counihan. 2008. Operational accuracy and comparative persistent antigenicity of HRP2 rapid diagnostic tests for Plasmodium falciparum malaria in a hyperendemic region of Uganda. *Malaria Journal* 7:221.

Kyrou, K., A.M. Hammond, R. Galizi, N. Kranjc, A. Burt, A.K. Beaghton, T. Nolan, and A. Crisanti. 2018. A CRISPR-Cas9 gene drive targeting doublesex causes complete population suppression in caged Anopheles gambiae mosquitoes. *Nat Biotechnol* 36:1062-1066.

Lang, K.S., P.A. Lang, A. Meryk, A.A. Pandyra, L.-M. Boucher, V.I. Pozdeev, M.W. Tusche, J.R. Göthert, J. Haight, A. Wakeham, A.J. You-Ten, D.R. McIlwain, K. Merches, V. Khairnar, M. Recher, G.P. Nolan, Y. Hitoshi, P. Funkner, A.A. Navarini, A. Verschoor, N. Shaabani, N. Honke, L.Z. Penn, P.S. Ohashi, D. Häussinger, K.-H. Lee, and T.W. Mak. 2013. Involvement of Toso in activation of monocytes, macrophages, and granulocytes. *Proceedings of the National Academy of Sciences* 110:2593-2598.

Langhorne, J., F.M. Ndungu, A.M. Sponaas, and K. Marsh. 2008. Immunity to malaria: more questions than answers. *Nat Immunol* 9:725-732.

Larsen, M.D., M. Lopez-Perez, E.K. Dickson, P. Ampomah, N. Tuikue Ndam, J. Nouta, C.A.M. Koeleman, A.L.H. Ederveen, B. Mordmüller, A. Salanti, M.A. Nielsen, A. Massougbodji, C.E. van der Schoot, M.F. Ofori, M. Wuhrer, L. Hviid, and G. Vidarsson. 2021. Afucosylated Plasmodium falciparum-specific IgG is induced by infection but not by subunit vaccination. *Nature Communications* 12:5838.

Laurens, M.B., B. Kouriba, E. Bergmann-Leitner, E. Angov, D. Coulibaly, I. Diarra, M. Daou, A. Niangaly, W.C. Blackwelder, Y. Wu, J. Cohen, W.R. Ballou, J. Vekemans, D.E. Lanar, S. Dutta, C. Diggs, L. Soisson, D.G. Heppner, O.K. Doumbo, C.V. Plowe, and M.A. Thera. 2017. Strain-specific Plasmodium falciparum growth inhibition among Malian children immunized with a blood-stage malaria vaccine. *PLoS One* 12:e0173294.

Lausen, B., and M. Schumacher. 1992. Maximally Selected Rank Statistics. *Biometrics* 48:73-85.

Lengeler, C. 2004. Insecticide-treated bed nets and curtains for preventing malaria. *Cochrane Database Syst Rev* Cd000363.

Li, X., H. Chen, T.H. Oo, T.M. Daly, L.W. Bergman, S.C. Liu, A.H. Chishti, and S.S. Oh. 2004. A co-ligand complex anchors Plasmodium falciparum merozoites to the erythrocyte invasion receptor band 3. *J Biol Chem* 279:5765-5771.

Lin, C.S., A.D. Uboldi, C. Epp, H. Bujard, T. Tsuboi, P.E. Czabotar, and A.F. Cowman. 2016. Multiple Plasmodium falciparum Merozoite Surface Protein 1 Complexes Mediate Merozoite Binding to Human Erythrocytes. *The Journal of biological chemistry* 291:7703-7715.

Lin, C.S., A.D. Uboldi, D. Marapana, P.E. Czabotar, C. Epp, H. Bujard, N.L. Taylor, M.A. Perugini, A.N. Hodder, and A.F. Cowman. 2014. The Merozoite Surface Protein 1 Complex Is a Platform for Binding to Human Erythrocytes by Plasmodium falciparum*. *Journal of Biological Chemistry* 289:25655-25669.

Lingelbach, K., and K.A. Joiner. 1998. The parasitophorous vacuole membrane surrounding Plasmodium and Toxoplasma: an unusual compartment in infected cells. *J Cell Sci* 111 (Pt 11):1467-1475.

Lobo, N.F., N.L. Achee, J. Greico, and F.H. Collins. 2018. Modern Vector Control. *Cold Spring Harb Perspect Med* 8:a025643.

Luty, A.J., D.J. Perkins, B. Lell, R. Schmidt-Ott, L.G. Lehman, D. Luckner, B. Greve, P. Matousek, K. Herbich, D. Schmid, J.B. Weinberg, and P.G. Kremsner. 2000. Low interleukin-12 activity in severe Plasmodium falciparum malaria. *Infect Immun* 68:3909-3915.

Lyon, J.A., E. Angov, M.P. Fay, J.S. Sullivan, A.S. Girourd, S.J. Robinson, E.S. Bergmann-Leitner, E.H. Duncan, C.A. Darko, W.E. Collins, C.A. Long, and J.W. Barnwell. 2008. Protection induced by Plasmodium falciparum MSP1(42) is strain-specific, antigen and adjuvant dependent, and correlates with antibody responses. *PLoS One* 3:e2830.

Maier, A.G., M.T. Duraisingh, J.C. Reeder, S.S. Patel, J.W. Kazura, P.A. Zimmerman, and A.F. Cowman. 2003. Plasmodium falciparum erythrocyte invasion through glycophorin C and selection for Gerbich negativity in human populations. *Nat Med* 9:87-92.

Malito, E., M. Biancucci, A. Faleri, I. Ferlenghi, M. Scarselli, G. Maruggi, P. Lo Surdo, D. Veggi, A. Liguori, L. Santini, I. Bertoldi, R. Petracca, S. Marchi, G. Romagnoli, E. Cartocci, I. Vercellino, S. Savino, G. Spraggon, N. Norais, M. Pizza, R. Rappuoli, V. Masignani, and M.J. Bottomley. 2014. Structure of the meningococcal vaccine antigen NadA and epitope mapping of a bactericidal antibody. *Proceedings of the National Academy of Sciences* 111:17128-17133.

Malkin, E., C.A. Long, A.W. Stowers, L. Zou, S. Singh, N.J. MacDonald, D.L. Narum, A.P. Miles, A.C. Orcutt, O. Muratova, S.E. Moretz, H. Zhou, A. Diouf, M. Fay, E. Tierney, P. Leese, S. Mahanty, L.H. Miller, A. Saul, and L.B. Martin. 2007. Phase 1 study of two merozoite surface protein 1 (MSP1(42)) vaccines for Plasmodium falciparum malaria. *PLoS Clin Trials* 2:e12.

Marques-da-Silva, C., K. Peissig, and S.P. Kurup. 2020. Pre-Erythrocytic Vaccines against Malaria. *Vaccines* 8:400.

Marsh, K., and S. Kinyanjui. 2006. Immune effector mechanisms in malaria. *Parasite Immunology* 28:51-60.

Martin, J.L., F.W. Mosha, E. Lukole, M. Rowland, J. Todd, J.D. Charlwood, J.F. Mosha, and N. Protopopoff. 2021. Personal protection with PBO-pyrethroid synergist-treated nets after 2 years of household use against pyrethroid-resistant Anopheles in Tanzania. *Parasites & Vectors* 14:150.

Mbengue, A., S. Bhattacharjee, T. Pandharkar, H. Liu, G. Estiu, R.V. Stahelin, S.S. Rizk, D.L. Njimoh, Y. Ryan, K. Chotivanich, C. Nguon, M. Ghorbal, J.-J. Lopez-Rubio, M. Pfrender, S. Emrich, N. Mohandas, A.M. Dondorp, O. Wiest, and K. Haldar. 2015. A molecular mechanism of artemisinin resistance in Plasmodium falciparum malaria. *Nature* 520:683-687.

McBride, J.S., and H.-G. Heidrich. 1987. Fragments of the polymorphic Mr 185 000 glycoprotein from the surface of isolated Plasmodium falciparum merozoites form an antigenic complex. *Molecular and Biochemical Parasitology* 23:71-84.

McCallum, F.J., K.E.M. Persson, C.K. Mugyenyi, F.J.I. Fowkes, J.A. Simpson, J.S. Richards, T.N. Williams, K. Marsh, and J.G. Beeson. 2008. Acquisition of Growth-Inhibitory Antibodies against Blood-Stage Plasmodium falciparum. *PLOS ONE* 3:e3571.

McCarthy, J.S., J. Marjason, S. Elliott, P. Fahey, G. Bang, E. Malkin, E. Tierney, H. Aked-Hurditch, C. Adda, N. Cross, J.S. Richards, F.J. Fowkes, M.J. Boyle, C. Long, P. Druilhe, J.G. Beeson, and R.F. Anders. 2011. A phase 1 trial of MSP2-C1, a blood-stage malaria vaccine containing 2 isoforms of MSP2 formulated with Montanide® ISA 720. *PLoS One* 6:e24413.

McLeod, B., M.T. Mabrouk, K. Miura, R. Ravichandran, S. Kephart, S. Hailemariam, T.P. Pham, A. Semesi, I. Kucharska, P. Kundu, W.-C. Huang, M. Johnson, A. Blackstone, D. Pettie, M. Murphy, J.C. Kraft, E.M. Leaf, Y. Jiao, M. van de Vegte-Bolmer, G.-J. van Gemert, J. Ramjith, C.R. King, R.S. MacGill, Y. Wu, K.K. Lee, M.M. Jore, N.P. King, J.F. Lovell, and J.-P. Julien. 2022. Vaccination with a structure-based stabilized version of malarial antigen Pfs48/45 elicits ultra-potent transmission-blocking antibody responses. *Immunity* 55:1680-1692.e1688.

Medica, D.L., and P. Sinnis. 2005. Quantitative dynamics of Plasmodium yoelii sporozoite transmission by infected anopheline mosquitoes. *Infect Immun* 73:4363-4369.

Medicines for Malaria Venture. (2021). Annual report 2021.

Mellouk, S., R.K. Maheshwari, A. Rhodes-Feuillette, R.L. Beaudoin, N. Berbiguier, H. Matile, F. Miltgen, I. Landau, S. Pied, and J.P. Chigot. 1987. Inhibitory activity of interferons and interleukin 1 on the development of Plasmodium falciparum in human hepatocyte cultures. *The Journal of Immunology* 139:4192-4195.

Menon, V., M.C. Kapulu, I. Taylor, K. Jewell, Y. Li, F. Hill, C.A. Long, K. Miura, and S. Biswas. 2018. Assessment of Antibodies Induced by Multivalent Transmission-Blocking Malaria Vaccines. *Frontiers in immunology* 8:1998-1998.

Mensah, V.A., A. Gueye, M. Ndiaye, N.J. Edwards, D. Wright, N.A. Anagnostou, M. Syll, A. Ndaw, A. Abiola, C. Bliss, J.-F. Gomis, I. Petersen, C. Ogwang, T. Dieye, N.K. Viebig, A.M. Lawrie, R. Roberts, A. Nicosia, B. Faye, O. Gaye, O. Leroy, E.B. Imoukhuede, K.J. Ewer, P. Bejon, A.V.S. Hill, B. Cisse, and M. group. 2016. Safety, Immunogenicity and Efficacy of Prime-Boost Vaccination with ChAd63 and MVA Encoding ME-TRAP against Plasmodium falciparum Infection in Adults in Senegal. *PloS one* 11:e0167951-e0167951.

Merle, N.S., S.E. Church, V. Fremeaux-Bacchi, and L.T. Roumenina. 2015. Complement System Part I – Molecular Mechanisms of Activation and Regulation. *Frontiers in Immunology* 6:

Miller, L.H., D.I. Baruch, K. Marsh, and O.K. Doumbo. 2002. The pathogenic basis of malaria. *Nature* 415:673-679.

Miura, K., H. Zhou, S.E. Moretz, A. Diouf, M.A. Thera, A. Dolo, O. Doumbo, E. Malkin, D. Diemert, L.H. Miller, G.E. Mullen, and C.A. Long. 2008. Comparison of biological activity of human anti-apical membrane antigen-1 antibodies induced by natural infection and vaccination. *J Immunol* 181:8776-8783.

Moormann, A.M., P.O. Sumba, K. Chelimo, H. Fang, D.J. Tisch, A.E. Dent, C.C. John, C.A. Long, J. Vulule, and J.W. Kazura. 2013. Humoral and Cellular Immunity to Plasmodium falciparum Merozoite Surface Protein 1 and Protection From Infection With Blood-Stage Parasites. *The Journal of Infectious Diseases* 208:149-158.

Morassin, B., R. Fabre, A. Berry, and J.F. Magnaval. 2002. One year's experience with the polymerase chain reaction as a routine method for the diagnosis of imported malaria. *Am J Trop Med Hyg* 66:503-508.

Mordmüller, B., Z. Sulyok, M. Sulyok, Z. Molnar, A. Lalremruata, C.L. Calle, P.G. Bayon, M. Esen, M. Gmeiner, J. Held, H.-L. Heimann, T.G. Woldearegai, J. Ibáñez, J. Flügge, R. Fendel, A. Kreidenweiss, N. Kc, T. Murshedkar, S. Chakravarty, P. Riyahi, P.F. Billingsley, L.W.P. Church, T.L. Richie, B.K.L. Sim, S.L. Hoffman, and P.G. Kremsner. 2022. A PfSPZ vaccine immunization regimen equally protective against homologous and heterologous controlled human malaria infection. *npj Vaccines* 7:100.

Mordmüller, B., G. Surat, H. Lagler, S. Chakravarty, A.S. Ishizuka, A. Lalremruata, M. Gmeiner, J.J. Campo, M. Esen, A.J. Ruben, J. Held, C.L. Calle, J.B. Mengue, T. Gebru, J. Ibáñez, M. Sulyok, E.R. James, P.F. Billingsley, K.C. Natasha, A. Manoj, T. Murshedkar, A. Gunasekera, A.G. Eappen, T. Li, R.E. Stafford, M. Li, P.L. Felgner, R.A. Seder, T.L. Richie, B.K. Sim, S.L. Hoffman, and P.G. Kremsner. 2017. Sterile protection against human malaria by chemoattenuated PfSPZ vaccine. *Nature* 542:445-449.

Mordmüller, B., K. Szywon, B. Greutelaers, M. Esen, L. Mewono, C. Treut, R.E. Mürbeth, R. Chilengi, R. Noor, W.L. Kilama, E.B. Imoukhuede, N. Imbault, O. Leroy, M. Theisen, S. Jepsen, P. Milligan, R. Fendel, P.G. Kremsner, and S. Issifou. 2010. Safety and immunogenicity of the malaria vaccine candidate GMZ2 in malaria-exposed, adult individuals from Lambaréné, Gabon. *Vaccine* 28:6698-6703.

Moreira, L.A., I. Iturbe-Ormaetxe, J.A. Jeffery, G. Lu, A.T. Pyke, L.M. Hedges, B.C. Rocha, S. Hall-Mendelin, A. Day, M. Riegler, L.E. Hugo, K.N. Johnson, B.H. Kay, E.A. McGraw, A.F. van den Hurk, P.A. Ryan, and S.L. O'Neill. 2009. A Wolbachia symbiont in Aedes aegypti limits infection with dengue, Chikungunya, and Plasmodium. *Cell* 139:1268-1278.

Morgan, W.D., B. Birdsall, T.A. Frenkiel, M.G. Gradwell, P.A. Burghaus, S.E. Syed, C. Uthaipibull, A.A. Holder, and J. Feeney. 1999. Solution structure of an EGF module pair from the Plasmodium falciparum merozoite surface protein 1. *J Mol Biol* 289:113-122.

Mota, M.M., G. Pradel, J.P. Vanderberg, J.C. Hafalla, U. Frevert, R.S. Nussenzweig, V. Nussenzweig, and A. Rodríguez. 2001. Migration of Plasmodium sporozoites through cells before infection. *Science* 291:141-144.

Muniz-Junqueira, M.I., L.L. dos Santos-Neto, and C.E. Tosta. 2001. Influence of tumor necrosis factor-alpha on the ability of monocytes and lymphocytes to destroy intraerythrocytic Plasmodium falciparum in vitro. *Cell Immunol* 208:73-79.

Murphy, S.C., A.M. Vaughan, J.G. Kublin, M. Fishbauger, A.M. Seilie, K.P. Cruz, T. Mankowski, M. Firat, S. Magee, W. Betz, H. Kain, N. Camargo, M.T. Haile, J. Armstrong, E. Fritzen, N. Hertoghs, S. Kumar, D.N. Sather, L.F. Pinder, G.A. Deye, S. Galbiati, C. Geber, J. Butts, L.A. Jackson, and S.H.I. Kappe. 2022. A genetically engineered Plasmodium falciparum parasite vaccine provides protection from controlled human malaria infection. *Science Translational Medicine* 14:eabn9709.

Murungi, L.M., K. Sondén, D. Llewellyn, J. Rono, F. Guleid, A.R. Williams, E. Ogada, A. Thairu, A. Färnert, K. Marsh, S.J. Draper, and F.H.A. Osier. 2016. Targets and Mechanisms Associated with Protection from Severe Plasmodium falciparum Malaria in Kenyan Children. *Infect Immun* 84:950-963.

Murungi, L.M., K. Sondén, D. Odera, L.B. Oduor, F. Guleid, I.N. Nkumama, M. Otiende, D.T. Kangoye, G. Fegan, A. Färnert, K. Marsh, and F.H.A. Osier. 2017. Cord blood IgG and the risk of severe Plasmodium falciparum malaria in the first year of life. *International Journal for Parasitology* 47:153-162.

Musasia, F.K., I.N. Nkumama, R. Frank, V. Kipkemboi, M. Schneider, K. Mwai, D.O. Odera, M. Rosenkranz, K. Fürle, D. Kimani, J. Tuju, P. Njuguna, M. Hamaluba, M.C. Kapulu, H. Wardemann, and F.H.A. Osier. 2022. Phagocytosis of Plasmodium falciparum ring-stage parasites predicts protection against malaria. *Nat Commun* 13:4098.

Mwai, L., E. Ochong, A. Abdirahman, S.M. Kiara, S. Ward, G. Kokwaro, P. Sasi, K. Marsh, S. Borrmann, M. Mackinnon, and A. Nzila. 2009. Chloroquine resistance before and after its withdrawal in Kenya. *Malaria journal* 8:106-106.

Mwakingwe-Omari, A., S.A. Healy, J. Lane, D.M. Cook, S. Kalhori, C. Wyatt, A. Kolluri, O. Marte-Salcedo, A. Imeru, M. Nason, L.K. Ding, H. Decederfelt, J. Duan, J. Neal, J. Raiten, G. Lee, J.C.C. Hume, J.E. Jeon, I. Ikpeama, N. Kc, S. Chakravarty, T. Murshedkar, L.W.P. Church, A. Manoj, A. Gunasekera, C. Anderson, S.C. Murphy, S. March, S.N. Bhatia, E.R. James, P.F. Billingsley, B.K.L. Sim, T.L. Richie, I. Zaidi, S.L. Hoffman, and P.E. Duffy. 2021. Two chemoattenuated PfSPZ malaria vaccines induce sterile hepatic immunity. *Nature* 595:289-294.

Mwaniki, M.K., A.W. Talbert, F.N. Mturi, J.A. Berkley, P. Kager, K. Marsh, and C.R. Newton. 2010. Congenital and neonatal malaria in a rural Kenyan district hospital: An eight-year analysis. *Malaria Journal* 9:313.

Ndungu, F.M., A. Olotu, J. Mwacharo, M. Nyonda, J. Apfeld, L.K. Mramba, G.W. Fegan, P. Bejon, and K. Marsh. 2012. Memory B cells are a more reliable archive for historical antimalarial responses than plasma antibodies in no-longer exposed children. *Proc Natl Acad Sci U S A* 109:8247-8252.

Nebie, I., A. Diarra, A. Ouedraogo, I. Soulama, E.C. Bougouma, A.B. Tiono, A.T. Konate, R. Chilengi, M. Theisen, D. Dodoo, E. Remarque, S. Bosomprah, P. Milligan, and S.B. Sirima. 2008. Humoral responses to Plasmodium falciparum blood-stage antigens and association with incidence of clinical malaria in children living in an area of seasonal malaria transmission in Burkina Faso, West Africa. *Infect Immun* 76:759-766.

Ngongang-Yipmo, E.S., M. Tchouakui, B.D. Menze, L.M.J. Mugenzi, F. Njiokou, and C.S. Wondji. 2022. Reduced performance of community bednets against pyrethroid-resistant Anopheles funestus and Anopheles gambiae, major malaria vectors in Cameroon. *Parasites & Vectors* 15:230.

Nilsson, S.K., L.M. Childs, C. Buckee, and M. Marti. 2015. Targeting Human Transmission Biology for Malaria Elimination. *PLOS Pathogens* 11:e1004871.

Nkumama, N. (2021). Characterisation of the mechanism of action and target antigens of naturally acquired antibodies against Plasmodium falciparum malaria. PhD thesis. Heidelberg University.

Nkumama, I.N., D. Odera, F. Musasia, K. Mwai, L. Nyamako, L. Murungi, J. Tuju, K. Furle, M. Rosenkranz, R. Kimathi, P. Njuguna, M. Hamaluba, M.C. Kapulu, R. Frank, and F. Osier. 2022. Breadth of Fc-mediated effector function delineates grades of clinical immunity following human malaria challenge. *bioRxiv* 2022.2010.2011.511755.

Nosten, F., and N.J. White. 2007. Artemisinin-based combination treatment of falciparum malaria. *Am J Trop Med Hyg* 77:181-192.

O'Donnell, R.A., T.F. de Koning-Ward, R.A. Burt, M. Bockarie, J.C. Reeder, A.F. Cowman, and B.S. Crabb. 2001. Antibodies against merozoite surface protein (MSP)-1(19) are a major component of the invasion-inhibitory response in individuals immune to malaria. *J Exp Med* 193:1403-1412.

Obiero, J.M., J.J. Campo, A. Scholzen, A. Randall, E.M. Bijker, M. Roestenberg, C.C. Hermsen, A. Teng, A. Jain, D.H. Davies, R.W. Sauerwein, and P.L. Felgner. 2019. Antibody Biomarkers Associated with Sterile Protection Induced by Controlled Human Malaria Infection under Chloroquine Prophylaxis. *mSphere* 4:

Ochomo, E.O., J.E. Gimnig, A. Bhattarai, A.M. Samuels, S. Kariuki, G. Okello, B. Abong'o, E.A. Ouma, J. Kosgei, S. Munga, K. Njagi, W. Odongo, F. Liu, J.P. Grieco, and N.L. Achee. 2022. Evaluation of the protective efficacy of a spatial repellent to reduce malaria incidence in children in western Kenya compared to placebo: study protocol for a cluster-randomized double-blinded control trial (the AEGIS program). *Trials* 23:260.

Ockenhouse, C.F., E. Angov, K.E. Kester, C. Diggs, L. Soisson, J.F. Cummings, A.V. Stewart, D.R. Palmer, B. Mahajan, U. Krzych, N. Tornieporth, M. Delchambre, M. Vanhandenhove, O. Ofori-Anyinam, J. Cohen, J.A. Lyon, and D.G. Heppner. 2006. Phase I safety and immunogenicity trial of FMP1/AS02A, a Plasmodium falciparum MSP-1 asexual blood stage vaccine. *Vaccine* 24:3009-3017.

Odera, D.O., J. Tuju, K. Mwai, I.N. Nkumama, K. Fürle, T. Chege, R. Kimathi, S. Diel, F.K. Musasia, M. Rosenkranz, P. Njuguna, M. Hamaluba, M.C. Kapulu, R. Frank, and F.H.A. Osier. 2021. Antibodies targeting merozoites induce natural killer cell degranulation and interferon gamma secretion and are associated with immunity against malaria. *medRxiv* 2021.2012.2014.21267763.

Ogutu, B.R., O.J. Apollo, D. McKinney, W. Okoth, J. Siangla, F. Dubovsky, K. Tucker, J.N. Waitumbi, C. Diggs, J. Wittes, E. Malkin, A. Leach, L.A. Soisson, J.B. Milman, L. Otieno, C.A. Holland, M. Polhemus, S.A. Remich, C.F. Ockenhouse, J. Cohen, W.R. Ballou, S.K. Martin, E. Angov, V.A. Stewart, J.A. Lyon, D.G. Heppner, and M.R. Withers. 2009. Blood stage malaria vaccine eliciting high antigen-specific antibody concentrations confers no protection to young children in Western Kenya. *PLoS One* 4:e4708.

Ohrt, C., Purnomo, M.A. Sutamihardja, D. Tang, and K.C. Kain. 2002. Impact of microscopy error on estimates of protective efficacy in malaria-prevention trials. *J Infect Dis* 186:540-546.

Okech, B.A., P.H. Corran, J. Todd, A. Joynson-Hicks, C. Uthaipibull, T.G. Egwang, A.A. Holder, and E.M. Riley. 2004. Fine specificity of serum antibodies to Plasmodium falciparum merozoite surface protein, PfMSP-1(19), predicts protection from malaria infection and high-density parasitemia. *Infect Immun* 72:1557-1567.

Olsen, R.W., G. Ecklu-Mensah, A. Bengtsson, M.F. Ofori, J.P.A. Lusingu, F.C. Castberg, L. Hviid, Y. Adams, and A.T.R. Jensen. 2018. Natural and Vaccine-Induced Acquisition of Cross-Reactive IgG-Inhibiting ICAM-1-Specific Binding of a Plasmodium falciparum PfEMP1 Subtype Associated Specifically with Cerebral Malaria. *Infect Immun* 86:

Ord, R.L., M. Rodriguez, T. Yamasaki, S. Takeo, T. Tsuboi, and C.A. Lobo. 2012. Targeting Sialic Acid Dependent and Independent Pathways of Invasion in Plasmodium falciparum. *PLOS ONE* 7:e30251.

Orlandi-Pradines, E., K. Penhoat, C. Durand, C. Pons, C. Bay, B. Pradines, T. Fusai, R. Josse, P. Dubrous, J.B. Meynard, J.P. Durand, R. Migliani, J.P. Boutin, P. Druilhe, and C. Rogier. 2006. Antibody responses to several malaria pre-erythrocytic antigens as a marker of malaria exposure among travelers. *Am J Trop Med Hyg* 74:979-985.

Osier, F.H., G. Fegan, S.D. Polley, L. Murungi, F. Verra, K.K. Tetteh, B. Lowe, T. Mwangi, P.C. Bull, A.W. Thomas, D.R. Cavanagh, J.S. McBride, D.E. Lanar, M.J. Mackinnon, D.J. Conway, and K. Marsh. 2008. Breadth and magnitude of antibody responses to multiple Plasmodium falciparum merozoite antigens are associated with protection from clinical malaria. *Infect Immun* 76:2240-2248.

Osier, F.H., G. Feng, M.J. Boyle, C. Langer, J. Zhou, J.S. Richards, F.J. McCallum, L. Reiling, A. Jaworowski, R.F. Anders, K. Marsh, and J.G. Beeson. 2014a. Opsonic phagocytosis of Plasmodium falciparum merozoites: mechanism in human immunity and a correlate of protection against malaria. *BMC Med* 12:108.

Osier, F.H., M.J. Mackinnon, C. Crosnier, G. Fegan, G. Kamuyu, M. Wanaguru, E. Ogada, B. McDade, J.C. Rayner, G.J. Wright, and K. Marsh. 2014b. New antigens for a multicomponent blood-stage malaria vaccine. *Sci Transl Med* 6:247ra102.

Othoro, C., A.A. Lal, B. Nahlen, D. Koech, A.S.S. Orago, and V. Udhayakumar. 1999. A Low Interleukin-10 Tumor Necrosis Factor-α Ratio Is Associated with Malaria Anemia in Children Residing in a Holoendemic Malaria Region in Western Kenya. *The Journal of Infectious Diseases* 179:279-282.

Oyen, D., J.L. Torres, U. Wille-Reece, C.F. Ockenhouse, D. Emerling, J. Glanville, W. Volkmuth, Y. Flores-Garcia, F. Zavala, A.B. Ward, C.R. King, and I.A. Wilson. 2017. Structural basis for antibody recognition of the NANP repeats in Plasmodium falciparum circumsporozoite protein. *Proc Natl Acad Sci U S A* 114:E10438-e10445.

Partnership, R.C.T. 2015. Efficacy and safety of RTS,S/AS01 malaria vaccine with or without a booster dose in infants and children in Africa: final results of a phase 3, individually randomised, controlled trial. *Lancet* 386:31-45.

Patel, P.N., T.H. Dickey, C.S. Hopp, A. Diouf, W.K. Tang, C.A. Long, K. Miura, P.D. Crompton, and N.H. Tolia. 2022. Neutralizing and interfering human antibodies define the structural and mechanistic basis for antigenic diversion. *Nature Communications* 13:5888.

Payne, D. 1988. Use and limitations of light microscopy for diagnosing malaria at the primary health care level. *Bull World Health Organ* 66:621-626.

Payne, R.O., K.H. Milne, S.C. Elias, N.J. Edwards, A.D. Douglas, R.E. Brown, S.E. Silk, S. Biswas, K. Miura, R. Roberts, T.W. Rampling, N. Venkatraman, S.H. Hodgson, G.M. Labbé, F.D. Halstead, I.D. Poulton, F.L. Nugent, H. de Graaf, P. Sukhtankar, N.C. Williams, C.F. Ockenhouse, A.K. Kathcart, A.N. Qabar, N.C. Waters, L.A. Soisson, A.J. Birkett, G.S. Cooke, S.N. Faust, C. Woods, K. Ivinson, J.S. McCarthy, C.L. Diggs, J. Vekemans, C.A. Long, A.V. Hill, A.M. Lawrie, S. Dutta, and S.J. Draper. 2016. Demonstration of the Blood-Stage Plasmodium falciparum Controlled Human Malaria Infection Model to Assess Efficacy of the P. falciparum Apical Membrane Antigen 1 Vaccine, FMP2.1/AS01. *J Infect Dis* 213:1743-1751.

Payne, R.O., S.E. Silk, S.C. Elias, K. Miura, A. Diouf, F. Galaway, H. de Graaf, N.J. Brendish, I.D. Poulton, O.J. Griffiths, N.J. Edwards, J. Jin, G.M. Labbé, D.G. Alanine, L. Siani, S. Di Marco, R. Roberts, N. Green, E. Berrie, A.S. Ishizuka, C.M. Nielsen, M. Bardelli, F.D. Partey, M.F. Ofori, L. Barfod, J. Wambua, L.M. Murungi, F.H. Osier, S. Biswas, J.S. McCarthy, A.M. Minassian, R. Ashfield, N.K. Viebig, F.L. Nugent, A.D. Douglas, J. Vekemans, G.J. Wright, S.N. Faust, A.V. Hill, C.A. Long, A.M. Lawrie, and S.J. Draper. 2017. Human vaccination against RH5 induces neutralizing antimalarial antibodies that inhibit RH5 invasion complex interactions. *JCI Insight* 2:

Perez-Mazliah, D., and J. Langhorne. 2014. CD4 T-cell subsets in malaria: TH1/TH2 revisited. *Front Immunol* 5:671.

Perraut, R., C. Joos, C. Sokhna, H.E.J. Polson, J.-F. Trape, A. Tall, L. Marrama, O. Mercereau-Puijalon, V. Richard, and S. Longacre. 2014. Association of Antibody Responses to the Conserved Plasmodium falciparum Merozoite Surface Protein 5 with Protection against Clinical Malaria. *PLOS ONE* 9:e101737.

Perraut, R., L. Marrama, B. Diouf, C. Sokhna, A. Tall, P. Nabeth, J.F. Trape, S. Longacre, and O. Mercereau-Puijalon. 2005. Antibodies to the conserved C-terminal domain of the Plasmodium falciparum merozoite surface protein 1 and to the merozoite extract and their relationship with in vitro inhibitory antibodies and protection against clinical malaria in a Senegalese village. *J Infect Dis* 191:264-271.

Perrin, L.H., B. Merkli, M. Loche, C. Chizzolini, J. Smart, and R. Richle. 1984. Antimalarial immunity in Saimiri monkeys. Immunization with surface components of asexual blood stages. *J Exp Med* 160:441-451.

Peterson, D.S., W.K. Milhous, and T.E. Wellems. 1990. Molecular basis of differential resistance to cycloguanil and pyrimethamine in Plasmodium falciparum malaria. *Proc Natl Acad Sci U S A* 87:3018-3022.

Peterson, D.S., D. Walliker, and T.E. Wellems. 1988. Evidence that a point mutation in dihydrofolate reductase-thymidylate synthase confers resistance to pyrimethamine in falciparum malaria. *Proc Natl Acad Sci U S A* 85:9114-9118.

Pizarro, J.C., V. Chitarra, D. Verger, I. Holm, S. Pêtres, S. Dartevelle, F. Nato, S. Longacre, and G.A. Bentley. 2003. Crystal structure of a Fab complex formed with PfMSP1-19, the C-terminal fragment of merozoite surface protein 1 from Plasmodium falciparum: a malaria vaccine candidate. *J Mol Biol* 328:1091-1103.

Polley, S.D., K.K. Tetteh, D.R. Cavanagh, R.J. Pearce, J.M. Lloyd, K.A. Bojang, D.M. Okenu, B.M. Greenwood, J.S. McBride, and D.J. Conway. 2003. Repeat sequences in block 2 of Plasmodium falciparum merozoite surface protein 1 are targets of antibodies associated with protection from malaria. *Infect Immun* 71:1833-1842.

Proietti, C., L. Krause, A. Trieu, D. Dodoo, B. Gyan, K.A. Koram, W.O. Rogers, T.L. Richie, P.D. Crompton, P.L. Felgner, and D.L. Doolan. 2020. Immune Signature Against Plasmodium falciparum Antigens Predicts Clinical Immunity in Distinct Malaria Endemic Communities. *Mol Cell Proteomics* 19:101-113.

Puchades, C., B. Kűkrer, O. Diefenbach, E. Sneekes-Vriese, J. Juraszek, W. Koudstaal, and A. Apetri. 2019. Epitope mapping of diverse influenza Hemagglutinin drug candidates using HDX-MS. *Scientific Reports* 9:4735.

Quintana, M.d.P., D. Angeletti, K. Moll, Q. Chen, and M. Wahlgren. 2016. Phagocytosis-inducing antibodies to Plasmodium falciparum upon immunization with a recombinant PfEMP1 NTS-DBL1α domain. *Malaria Journal* 15:416.

Raj, D.K., C.P. Nixon, C.E. Nixon, J.D. Dvorin, C.G. DiPetrillo, S. Pond-Tor, H.-W. Wu, G. Jolly, L. Pischel, A. Lu, I.C. Michelow, L. Cheng, S. Conteh, E.A. McDonald, S. Absalon, S.E. Holte, J.F. Friedman, M. Fried, P.E. Duffy, and J.D. Kurtis. 2014. Antibodies to PfSEA-1 block parasite egress from RBCs and protect against malaria infection. *Science (New York, N.Y.)* 344:871-877.

Raja, A.I., Y. Cai, J.M. Reiman, P. Groves, S. Chakravarty, V. McPhun, D.L. Doolan, I. Cockburn, S.L. Hoffman, D.I. Stanisic, and M.F. Good. 2016. Chemically Attenuated Blood-Stage Plasmodium yoelii Parasites Induce Long-Lived and Strain-Transcending Protection. *Infect Immun* 84:2274-2288.

Ratsimbasoa, A., L. Fanazava, R. Radrianjafy, J. Ramilijaona, H. Rafanomezantsoa, and D. Ménard. 2008. Evaluation of two new immunochromatographic assays for diagnosis of malaria. *Am J Trop Med Hyg* 79:670-672.

Read, D., A.H. Lensen, S. Begarnie, S. Haley, A. Raza, and R. Carter. 1994. Transmission-blocking antibodies against multiple, non-variant target epitopes of the Plasmodium falciparum gamete surface antigen Pfs230 are all complement-fixing. *Parasite Immunol* 16:511-519.

Reece, W.H.H., M. Pinder, P.K. Gothard, P. Milligan, K. Bojang, T. Doherty, M. Plebanski, P. Akinwunmi, S. Everaere, K.R. Watkins, G. Voss, N. Tornieporth, A. Alloueche, B.M. Greenwood, K.E. Kester, K.P.W.J. McAdam, J. Cohen, and A.V.S. Hill. 2004. A CD4+ T-cell immune response to a conserved epitope in the circumsporozoite protein correlates with protection from natural Plasmodium falciparum infection and disease. *Nature Medicine* 10:406-410.

Reiling, L., M.J. Boyle, M.T. White, D.W. Wilson, G. Feng, R. Weaver, D.H. Opi, K.E.M. Persson, J.S. Richards, P.M. Siba, F.J.I. Fowkes, E. Takashima, T. Tsuboi, I. Mueller, and J.G. Beeson. 2019. Targets of complement-fixing antibodies in protective immunity against malaria in children. *Nature Communications* 10:610.

Rénia, L., I.T. Ling, M. Marussig, F. Miltgen, A.A. Holder, and D. Mazier. 1997. Immunization with a recombinant C-terminal fragment of Plasmodium yoelii merozoite surface protein 1 protects mice against homologous but not heterologous P. yoelii sporozoite challenge. *Infect Immun* 65:4419-4423.

Richards, J.S., T.U. Arumugam, L. Reiling, J. Healer, A.N. Hodder, F.J.I. Fowkes, N. Cross, C. Langer, S. Takeo, A.D. Uboldi, J.K. Thompson, P.R. Gilson, R.L. Coppel, P.M. Siba, C.L. King, M. Torii, C.E. Chitnis, D.L. Narum, I. Mueller, B.S. Crabb, A.F. Cowman, T. Tsuboi, and J.G. Beeson. 2013. Identification and Prioritization of Merozoite Antigens as Targets of Protective Human Immunity to Plasmodium falciparum Malaria for Vaccine and Biomarker Development. *The Journal of Immunology* 191:795-809.

Riglar, D.T., D. Richard, D.W. Wilson, M.J. Boyle, C. Dekiwadia, L. Turnbull, F. Angrisano, D.S. Marapana, K.L. Rogers, C.B. Whitchurch, J.G. Beeson, A.F. Cowman, S.A. Ralph, and J. Baum. 2011. Super-Resolution Dissection of Coordinated Events during Malaria Parasite Invasion of the Human Erythrocyte. *Cell Host & Microbe* 9:9-20.

Riley, E.M., G.E. Wagner, B.D. Akanmori, and K.A. Koram. 2001. Do maternally acquired antibodies protect infants from malaria infection? *Parasite Immunol* 23:51-59.

Roestenberg, M., J. Walk, S.C. van der Boor, M.C.C. Langenberg, M.A. Hoogerwerf, J.J. Janse, M. Manurung, X.Z. Yap, A.F. García, J.P.R. Koopman, P. Meij, E. Wessels, K. Teelen, Y.M. van Waardenburg, M. van de Vegte-Bolmer, G.J. van Gemert, L.G. Visser, A. van der Ven, Q. de Mast, K.C. Natasha, Y. Abebe, T. Murshedkar, P.F. Billingsley, T.L. Richie, B.K.L. Sim, C.J. Janse, S.L. Hoffman, S.M. Khan, and R.W. Sauerwein. 2020. A double-blind, placebo-controlled phase 1/2a trial of the genetically attenuated malaria vaccine PfSPZ-GA1. *Sci Transl Med* 12:

Rosenberg, R., and J. Rungsiwongse. 1991. The number of sporozoites produced by individual malaria oocysts. *Am J Trop Med Hyg* 45:574-577.

Rosenkranz , M. (2019). Characterisation of antibody-mediated immune effector mechanisms against Plasmodium falciparum merozoite antigens MSP2, PfPAT and PHISTb. Master thesis. Heidelberg University

Rosenkranz, M., I.N. Nkumama, S. Kraker, M. Blickling, K. Mwai, D. Odera, J. Tuju, K. Fürle, R. Frank, E. Chepsat, M.C. Kapulu, and F.H.A. Osier. 2022. Full-length merozoite surface protein 1 of Plasmodium falciparum is a major target of protective immunity following controlled human malaria infections. *medRxiv* 2022.2010.2012.22280947.

Roussilhon, C., M. Agrapart, J.-J. Ballet, and A. Bensussan. 1990. T Lymphocytes Bearing the γδ T Cell Receptor in Patients with Acute Plasmodium falciparum Malaria. *The Journal of Infectious Diseases* 162:283-285.

Sabchareon, A., T. Burnouf, D. Ouattara, P. Attanath, H. Bouharoun-Tayoun, P. Chantavanich, C. Foucault, T. Chongsuphajaisiddhi, and P. Druilhe. 1991. Parasitologic and clinical human response to immunoglobulin administration in falciparum malaria. *Am J Trop Med Hyg* 45:297-308.

Sagara, I., S.A. Healy, M.H. Assadou, E.E. Gabriel, M. Kone, K. Sissoko, I. Tembine, M.A. Guindo, M. Doucoure, K. Niaré, A. Dolo, K.M. Rausch, D.L. Narum, D.L. Jones, N.J. MacDonald, D. Zhu, R. Mohan, O. Muratova, I. Baber, M.B. Coulibaly, M.P. Fay, C. Anderson, Y. Wu, S.F. Traore, O.K. Doumbo, and P.E. Duffy. 2018. Safety and immunogenicity of Pfs25H-EPA/Alhydrogel, a transmission-blocking vaccine against Plasmodium falciparum: a randomised, double-blind, comparator-controlled, dose-escalation study in healthy Malian adults. *Lancet Infect Dis* 18:969-982.

Sanders, P.R., G.T. Cantin, D.C. Greenbaum, P.R. Gilson, T. Nebl, R.L. Moritz, J.R. Yates, 3rd, A.N. Hodder, and B.S. Crabb. 2007. Identification of protein complexes in detergent-resistant membranes of Plasmodium falciparum schizonts. *Mol Biochem Parasitol* 154:148-157.

Sandquist, I., and J. Kolls. 2018. Update on regulation and effector functions of Th17 cells. *F1000Res* 7:205-205.

Saul, A., G. Lawrence, A. Smillie, C.M. Rzepczyk, C. Reed, D. Taylor, K. Anderson, A. Stowers, R. Kemp, A. Allworth, R.F. Anders, G.V. Brown, D. Pye, P. Schoofs, D.O. Irving, S.L. Dyer, G.C. Woodrow, W.R. Briggs, R. Reber, and D. Stürchler. 1999. Human phase I vaccine trials of 3 recombinant asexual stage malaria antigens with Montanide ISA720 adjuvant. *Vaccine* 17:3145-3159.

Seaton, K.E., R.L. Spreng, M. Abraha, M. Reichartz, M. Rojas, F. Feely, R.H.C. Huntwork, S. Dutta, S.V. Mudrak, S.M. Alam, S. Gregory, E. Jongert, M. Coccia, F. Ulloa-Montoya, U. Wille-Reece, G.D. Tomaras, and S.M. Dennison. 2021. Subclass and avidity of circumsporozoite protein specific antibodies associate with protection status against malaria infection. *npj Vaccines* 6:110.

Seder, R.A., L.-J. Chang, M.E. Enama, K.L. Zephir, U.N. Sarwar, I.J. Gordon, L.A. Holman, E.R. James, P.F. Billingsley, A. Gunasekera, A. Richman, S. Chakravarty, A. Manoj, S. Velmurugan, M. Li, A.J. Ruben, T. Li, A.G. Eappen, R.E. Stafford, S.H. Plummer, C.S. Hendel, L. Novik, P.J.M. Costner, F.H. Mendoza, J.G. Saunders, M.C. Nason, J.H. Richardson, J. Murphy, S.A. Davidson, T.L. Richie, M. Sedegah, A. Sutamihardja, G.A. Fahle, K.E. Lyke, M.B. Laurens, M. Roederer, K. Tewari, J.E. Epstein, B.K.L. Sim, J.E. Ledgerwood, B.S. Graham, S.L. Hoffman, C. DiGiovanni, P. Williams, N. Luongo, J. Mitchell, M.B. Florez, B. Larkin, N. Berkowitz, B. Wilson, T. Clarke, O. Vasilenko, G. Yamshchikov, S. Sitar, L. Stanford, I. Pittman, R.T. Bailer, J. Casazza, H. Decederfelt, J. Starling, E.C. Williams, A. Lau, S. Antonara, J. Brocious, M. Kemp, J. Inglese, P. Dranchak, E.N. Abot, S. Reyes, H. Ganeshan, M. Belmonte, J. Huang, A. Belmonte, J. Komisar, Y. Abebe, Y. Getachew, A. Patil, S. Matheny, K. Nelson, J. Overby, V. Pich, Y. Wen, R. Fan, E. Fomumbod, A. Awe, C. Chakiath, M. King, M.S. Orozco, T. Murshedkar, D. Padilla, B. Jiang, L. Gao, N. KC, R. Xu, M. Adams, C. Plowe, H. Loblein, P.Z. Renehan, M. Kunchai, and L. Diep. 2013. Protection Against Malaria by Intravenous Immunization with a Nonreplicating Sporozoite Vaccine. *Science* 341:1359-1365.

Seguin, M.C., F.W. Klotz, I. Schneider, J.P. Weir, M. Goodbary, M. Slayter, J.J. Raney, J.U. Aniagolu, and S.J. Green. 1994. Induction of nitric oxide synthase protects against malaria in mice exposed to irradiated Plasmodium berghei infected mosquitoes: involvement of interferon gamma and CD8+ T cells. *J Exp Med* 180:353-358.

Sehgal, V.M., W.A. Siddjiqui, and M.P. Alpers. 1989. A seroepidemiological study to evaluate the role of passive maternal immunity to malaria in infants. *Trans R Soc Trop Med Hyg* 83 Suppl:105-106.

Shaw, W.R., P. Marcenac, L.M. Childs, C.O. Buckee, F. Baldini, S.P. Sawadogo, R.K. Dabiré, A. Diabaté, and F. Catteruccia. 2016. Wolbachia infections in natural Anopheles populations affect egg laying and negatively correlate with Plasmodium development. *Nature Communications* 7:11772.

Sheehy, S.H., C.J. Duncan, S.C. Elias, P. Choudhary, S. Biswas, F.D. Halstead, K.A. Collins, N.J. Edwards, A.D. Douglas, N.A. Anagnostou, K.J. Ewer, T. Havelock, T. Mahungu, C.M. Bliss, K. Miura, I.D. Poulton, P.J. Lillie, R.D. Antrobus, E. Berrie, S. Moyle, K. Gantlett, S. Colloca, R. Cortese, C.A. Long, R.E. Sinden, S.C. Gilbert, A.M. Lawrie, T. Doherty, S.N. Faust, A. Nicosia, A.V. Hill, and S.J. Draper. 2012. ChAd63-MVA-vectored blood-stage malaria vaccines targeting MSP1 and AMA1: assessment of efficacy against mosquito bite challenge in humans. *Mol Ther* 20:2355-2368.

Sheehy, S.H., C.J. Duncan, S.C. Elias, K.A. Collins, K.J. Ewer, A.J. Spencer, A.R. Williams, F.D. Halstead, S.E. Moretz, K. Miura, C. Epp, M.D. Dicks, I.D. Poulton, A.M. Lawrie, E. Berrie, S. Moyle, C.A. Long, S. Colloca, R. Cortese, S.C. Gilbert, A. Nicosia, A.V. Hill, and S.J. Draper. 2011. Phase Ia clinical evaluation of the Plasmodium falciparum blood-stage antigen MSP1 in ChAd63 and MVA vaccine vectors. *Mol Ther* 19:2269-2276.

Shi, Y.P., B.L. Nahlen, S. Kariuki, K.B. Urdahl, P.D. McElroy, J.M. Roberts, and A.A. Lal. 2001. Fcgamma receptor IIa (CD32) polymorphism is associated with protection of infants against high-density Plasmodium falciparum infection. VII. Asembo Bay Cohort Project. *J Infect Dis* 184:107-111.

Shields, R.L., J. Lai, R. Keck, L.Y. O'Connell, K. Hong, Y.G. Meng, S.H. Weikert, and L.G. Presta. 2002. Lack of fucose on human IgG1 N-linked oligosaccharide improves binding to human Fcgamma RIII and antibody-dependent cellular toxicity. *J Biol Chem* 277:26733-26740.

Shima, H., H. Takatsu, S. Fukuda, M. Ohmae, K. Hase, H. Kubagawa, J.Y. Wang, and H. Ohno. 2010. Identification of TOSO/FAIM3 as an Fc receptor for IgM. *Int Immunol* 22:149-156.

Shimoda, K., J. van Deursen, M.Y. Sangster, S.R. Sarawar, R.T. Carson, R.A. Tripp, C. Chu, F.W. Quelle, T. Nosaka, D.A. Vignali, P.C. Doherty, G. Grosveld, W.E. Paul, and J.N. Ihle. 1996. Lack of IL-4-induced Th2 response and IgE class switching in mice with disrupted Stat6 gene. *Nature* 380:630-633.

Sibley, C.H., J.E. Hyde, P.F. Sims, C.V. Plowe, J.G. Kublin, E.K. Mberu, A.F. Cowman, P.A. Winstanley, W.M. Watkins, and A.M. Nzila. 2001. Pyrimethamine-sulfadoxine resistance in Plasmodium falciparum: what next? *Trends Parasitol* 17:582-588.

Siddiqui, W.A., L.Q. Tam, K.J. Kramer, G.S. Hui, S.E. Case, K.M. Yamaga, S.P. Chang, E.B. Chan, and S.C. Kan. 1987. Merozoite surface coat precursor protein completely protects Aotus monkeys against Plasmodium falciparum malaria. *Proc Natl Acad Sci U S A* 84:3014-3018.

Sidjanski, S., and J.P. Vanderberg. 1997. Delayed migration of Plasmodium sporozoites from the mosquito bite site to the blood. *Am J Trop Med Hyg* 57:426-429.

Silvino, A.C.R., G.L. Costa, F.C.F.d. Araújo, D.B. Ascher, D.E.V. Pires, C.J.F. Fontes, L.H. Carvalho, C.F.A.d. Brito, and T.N. Sousa. 2016. Variation in Human Cytochrome P-450 Drug-Metabolism Genes: A Gateway to the Understanding of Plasmodium vivax Relapses. *PLOS ONE* 11:e0160172.

Simister, N.E. 2003. Placental transport of immunoglobulin G. *Vaccine* 21:3365-3369.

Sinden, R.E., and N.A. Croll. 1975. Cytology and Kinetics of microgametogenesis and fertilization in Plasmodium yoelii nigeriensis. *Parasitology* 70:53-65.

Sirima, S.B., S. Cousens, and P. Druilhe. 2011. Protection against malaria by MSP3 candidate vaccine. *N Engl J Med* 365:1062-1064.

Sirima, S.B., C. Durier, L. Kara, S. Houard, A. Gansane, P. Loulergue, M. Bahuaud, N. Benhamouda, I. Nebié, B. Faber, E. Remarque, and O. Launay. 2017. Safety and immunogenicity of a recombinant Plasmodium falciparum AMA1-DiCo malaria vaccine adjuvanted with GLA-SE or Alhydrogel® in European and African adults: A phase 1a/1b, randomized, double-blind multi-centre trial. *Vaccine* 35:6218-6227.

Sirima, S.B., B. Mordmüller, P. Milligan, U.A. Ngoa, F. Kironde, F. Atuguba, A.B. Tiono, S. Issifou, M. Kaddumukasa, O. Bangre, C. Flach, M. Christiansen, P. Bang, R. Chilengi, S. Jepsen, P.G. Kremsner, and M. Theisen. 2016. A phase 2b randomized, controlled trial of the efficacy of the GMZ2 malaria vaccine in African children. *Vaccine* 34:4536-4542.

Sissoko, M.S., S.A. Healy, A. Katile, F. Omaswa, I. Zaidi, E.E. Gabriel, B. Kamate, Y. Samake, M.A. Guindo, A. Dolo, A. Niangaly, K. Niaré, A. Zeguime, K. Sissoko, H. Diallo, I. Thera, K. Ding, M.P. Fay, E.M. O'Connell, T.B. Nutman, S. Wong-Madden, T. Murshedkar, A.J. Ruben, M. Li, Y. Abebe, A. Manoj, A. Gunasekera, S. Chakravarty, B.K.L. Sim, P.F. Billingsley, E.R. James, M. Walther, T.L. Richie, S.L. Hoffman, O. Doumbo, and P.E. Duffy. 2017. Safety and efficacy of PfSPZ Vaccine against Plasmodium falciparum via direct venous inoculation in healthy malaria-exposed adults in Mali: a randomised, double-blind phase 1 trial. *Lancet Infect Dis* 17:498-509.

Snow, R.W., B. Nahlen, A. Palmer, C.A. Donnelly, S. Gupta, and K. Marsh. 1998. Risk of Severe Malaria among African Infants: Direct Evidence of Clinical Protection during Early Infancy. *The Journal of Infectious Diseases* 177:819-822.

Stafford, W.H.L., M.J. Blackman, A. Harris, S. Shai, M. Grainger, and A.A. Holder. 1994. N-terminal amino acid sequence of the Plasmodium falciparum merozoite surface protein-1 polypeptides. *Molecular and Biochemical Parasitology* 66:157-160.

Stanisic, D.I., J. Fink, J. Mayer, S. Coghill, L. Gore, X.Q. Liu, I. El-Deeb, I.B. Rodriguez, J. Powell, N.M. Willemsen, S.L. De, M.F. Ho, S.L. Hoffman, J. Gerrard, and M.F. Good. 2018. Vaccination with chemically attenuated Plasmodium falciparum asexual blood-stage parasites induces parasite-specific cellular immune responses in malaria-naïve volunteers: a pilot study. *BMC Med* 16:184.

Stanisic, D.I., J.S. Richards, F.J. McCallum, P. Michon, C.L. King, S. Schoepflin, P.R. Gilson, V.J. Murphy, R.F. Anders, I. Mueller, and J.G. Beeson. 2009. Immunoglobulin G subclass-specific responses against Plasmodium falciparum merozoite antigens are associated with control of parasitemia and protection from symptomatic illness. *Infect Immun* 77:1165-1174.

Stone, W.J.R., J.J. Campo, A.L. Ouédraogo, L. Meerstein-Kessel, I. Morlais, D. Da, A. Cohuet, S. Nsango, C.J. Sutherland, M. van de Vegte-Bolmer, R. Siebelink-Stoter, G.-J. van Gemert, W. Graumans, K. Lanke, A.D. Shandling, J.V. Pablo, A.A. Teng, S. Jones, R.M. de Jong, A. Fabra-García, J. Bradley, W. Roeffen, E. Lasonder, G. Gremo, E. Schwarzer, C.J. Janse, S.K. Singh, M. Theisen, P. Felgner, M. Marti, C. Drakeley, R. Sauerwein, T. Bousema, and M.M. Jore. 2018. Unravelling the immune signature of Plasmodium falciparum transmission-reducing immunity. *Nature Communications* 9:558.

Stoute, J.A., J. Gombe, M.R. Withers, J. Siangla, D. McKinney, M. Onyango, J.F. Cummings, J. Milman, K. Tucker, L. Soisson, V.A. Stewart, J.A. Lyon, E. Angov, A. Leach, J. Cohen, K.E. Kester, C.F. Ockenhouse, C.A. Holland, C.L. Diggs, J. Wittes, and D.G. Heppner, Jr. 2007. Phase 1 randomized double-blind safety and immunogenicity trial of Plasmodium falciparum malaria merozoite surface protein FMP1 vaccine, adjuvanted with AS02A, in adults in western Kenya. *Vaccine* 25:176-184.

Sturm, A., R. Amino, C. van de Sand, T. Regen, S. Retzlaff, A. Rennenberg, A. Krueger, J.M. Pollok, R. Menard, and V.T. Heussler. 2006. Manipulation of host hepatocytes by the malaria parasite for delivery into liver sinusoids. *Science* 313:1287-1290.

Su, Z., and M.M. Stevenson. 2000. Central role of endogenous gamma interferon in protective immunity against blood-stage Plasmodium chabaudi AS infection. *Infect Immun* 68:4399-4406.

Swan, H., L. Sloan, A. Muyombwe, P. Chavalitshewinkoon-Petmitr, S. Krudsood, W. Leowattana, P. Wilairatana, S. Looareesuwan, and J. Rosenblatt. 2005. Evaluation of a real-time polymerase chain reaction assay for the diagnosis of malaria in patients from Thailand. *Am J Trop Med Hyg* 73:850-854.

Syafruddin, D., P.B.S. Asih, I.E. Rozi, D.H. Permana, A.P. Nur Hidayati, L. Syahrani, S. Zubaidah, D. Sidik, M.J. Bangs, C. Bøgh, F. Liu, E.C. Eugenio, J. Hendrickson, T. Burton, J.K. Baird, F. Collins, J.P. Grieco, N.F. Lobo, and N.L. Achee. 2020. Efficacy of a Spatial Repellent for Control of Malaria in Indonesia: A Cluster-Randomized Controlled Trial. *Am J Trop Med Hyg* 103:344-358.

Szarfman, A., J.A. Lyon, D. Walliker, I. Quakyi, R.J. Howard, S. Sun, W.R. Ballou, K. Esser, W.T. London, R.A. Wirtz, and et al. 1988. Mature liver stages of cloned Plasmodium falciparum share epitopes with proteins from sporozoites and asexual blood stages. *Parasite Immunol* 10:339-351.

Talaat, K.R., R.D. Ellis, J. Hurd, A. Hentrich, E. Gabriel, N.A. Hynes, K.M. Rausch, D. Zhu, O. Muratova, R. Herrera, C. Anderson, D. Jones, J. Aebig, S. Brockley, N.J. MacDonald, X. Wang, M.P. Fay, S.A. Healy, A.P. Durbin, D.L. Narum, Y. Wu, and P.E. Duffy. 2016. Safety and Immunogenicity of Pfs25-EPA/Alhydrogel®, a Transmission Blocking Vaccine against Plasmodium falciparum: An Open Label Study in Malaria Naïve Adults. *PLoS One* 11:e0163144.

Tanabe, K., M. Mackay, M. Goman, and J.G. Scaife. 1987. Allelic dimorphism in a surface antigen gene of the malaria parasite Plasmodium falciparum. *J Mol Biol* 195:273-287.

Tangena, J.-A.A., C.M.J. Hendriks, M. Devine, M. Tammaro, A.E. Trett, I. Williams, A.J. DePina, A. Sisay, R. Herizo, H.T. Kafy, E. Chizema, A. Were, J. Rozier, M. Coleman, and C.L. Moyes. 2020. Indoor residual spraying for malaria control in sub-Saharan Africa 1997 to 2017: an adjusted retrospective analysis. *Malaria Journal* 19:150.

Tarun, A.S., K. Baer, R.F. Dumpit, S. Gray, N. Lejarcegui, U. Frevert, and S.H. Kappe. 2006. Quantitative isolation and in vivo imaging of malaria parasite liver stages. *Int J Parasitol* 36:1283-1293.

Tarun, A.S., X. Peng, R.F. Dumpit, Y. Ogata, H. Silva-Rivera, N. Camargo, T.M. Daly, L.W. Bergman, and S.H.I. Kappe. 2008. A combined transcriptome and proteome survey of malaria parasite liver stages. *Proceedings of the National Academy of Sciences* 105:305-310.

Tham, W.H., D.W. Wilson, S. Lopaticki, C.Q. Schmidt, P.B. Tetteh-Quarcoo, P.N. Barlow, D. Richard, J.E. Corbin, J.G. Beeson, and A.F. Cowman. 2010. Complement receptor 1 is the host erythrocyte receptor for Plasmodium falciparum PfRh4 invasion ligand. *Proc Natl Acad Sci U S A* 107:17327-17332.

Thera, M.A., O.K. Doumbo, D. Coulibaly, D.A. Diallo, I. Sagara, A. Dicko, D.J. Diemert, D.G. Heppner, Jr., V.A. Stewart, E. Angov, L. Soisson, A. Leach, K. Tucker, K.E. Lyke, C.V. Plowe, and F.M.P.W.G. for the Mali. 2006. Safety and Allele-Specific Immunogenicity of a Malaria Vaccine in Malian Adults: Results of a Phase I Randomized Trial. *PLOS Clinical Trials* 1:e34.

Thera, M.A., O.K. Doumbo, D. Coulibaly, M.B. Laurens, A. Ouattara, A.K. Kone, A.B. Guindo, K. Traore, I. Traore, B. Kouriba, D.A. Diallo, I. Diarra, M. Daou, A. Dolo, Y. Tolo, M.S. Sissoko, A. Niangaly, M. Sissoko, S. Takala-Harrison, K.E. Lyke, Y. Wu, W.C. Blackwelder, O. Godeaux, J. Vekemans, M.C. Dubois, W.R. Ballou, J. Cohen, D. Thompson, T. Dube, L. Soisson, C.L. Diggs, B. House, D.E. Lanar, S. Dutta, D.G. Heppner, Jr., and C.V. Plowe. 2011. A field trial to assess a blood-stage malaria vaccine. *N Engl J Med* 365:1004-1013.

Thomas, D., H. Tazerouni, K.G.S. Sundararaj, and J.C. Cooper. 2016. Therapeutic failure of primaquine and need for new medicines in radical cure of Plasmodium vivax. *Acta Trop* 160:35-38.

Tian, J.H., S. Kumar, D.C. Kaslow, and L.H. Miller. 1997. Comparison of protection induced by immunization with recombinant proteins from different regions of merozoite surface protein 1 of Plasmodium yoelii. *Infect Immun* 65:3032-3036.

Tiendrebeogo, R.W., B. Adu, S.K. Singh, M.H. Dziegiel, I. Nébié, S.B. Sirima, M. Christiansen, D. Dodoo, and M. Theisen. 2015. Antibody-Dependent Cellular Inhibition Is Associated With Reduced Risk Against Febrile Malaria in a Longitudinal Cohort Study Involving Ghanaian Children. *Open Forum Infect Dis* 2:ofv044.

Tilley, L., J. Straimer, N.F. Gnädig, S.A. Ralph, and D.A. Fidock. 2016. Artemisinin Action and Resistance in Plasmodium falciparum. *Trends Parasitol* 32:682-696.

Tiono, A.B., I. Nébié, N. Anagnostou, A.S. Coulibaly, G. Bowyer, E. Lam, E.C. Bougouma, A. Ouedraogo, J.B.B. Yaro, A. Barry, R. Roberts, T. Rampling, C. Bliss, S. Hodgson, A. Lawrie, A. Ouedraogo, E.B. Imoukhuede, K.J. Ewer, N.K. Viebig, A. Diarra, O. Leroy, P. Bejon, A.V.S. Hill, and S.B. Sirima. 2018. First field efficacy trial of the ChAd63 MVA ME-TRAP vectored malaria vaccine candidate in 5-17 months old infants and children. *PLOS ONE* 13:e0208328.

Tonkin, M.L., M. Roques, M.H. Lamarque, M. Pugnière, D. Douguet, J. Crawford, M. Lebrun, and M.J. Boulanger. 2011. Host Cell Invasion by Apicomplexan Parasites: Insights from the Co-Structure of AMA1 with a RON2 Peptide. *Science* 333:463-467.

Trampuz, A., M. Jereb, I. Muzlovic, and R.M. Prabhu. 2003. Clinical review: Severe malaria. *Crit Care* 7:315-323.

Trape, J.F., A. Tall, N. Diagne, O. Ndiath, A.B. Ly, J. Faye, F. Dieye-Ba, C. Roucher, C. Bouganali, A. Badiane, F.D. Sarr, C. Mazenot, A. Touré-Baldé, D. Raoult, P. Druilhe, O. Mercereau-Puijalon, C. Rogier, and C. Sokhna. 2011. Malaria morbidity and pyrethroid resistance after the introduction of insecticide-treated bednets and artemisinin-based combination therapies: a longitudinal study. *Lancet Infect Dis* 11:925-932.

Triller, G., S.W. Scally, G. Costa, M. Pissarev, C. Kreschel, A. Bosch, E. Marois, B.K. Sack, R. Murugan, A.M. Salman, C.J. Janse, S.M. Khan, S.H.I. Kappe, A.A. Adegnika, B. Mordmüller, E.A. Levashina, J.P. Julien, and H. Wardemann. 2017. Natural Parasite Exposure Induces Protective Human Anti-Malarial Antibodies. *Immunity* 47:1197-1209.e1110.

Troye-Blomberg, M., E.M. Riley, L. Kabilan, M. Holmberg, H. Perlmann, U. Andersson, C.H. Heusser, and P. Perlmann. 1990. Production by activated human T cells of interleukin 4 but not interferon-gamma is associated with elevated levels of serum antibodies to activating malaria antigens. *Proc Natl Acad Sci U S A* 87:5484-5488.

Tun, K.M., M. Imwong, K.M. Lwin, A.A. Win, T.M. Hlaing, T. Hlaing, K. Lin, M.P. Kyaw, K. Plewes, M.A. Faiz, M. Dhorda, P.Y. Cheah, S. Pukrittayakamee, E.A. Ashley, T.J.C. Anderson, S. Nair, M. McDew-White, J.A. Flegg, E.P.M. Grist, P. Guerin, R.J. Maude, F. Smithuis, A.M. Dondorp, N.P.J. Day, F. Nosten, N.J. White, and C.J. Woodrow. 2015. Spread of artemisinin-resistant Plasmodium falciparum in Myanmar: a cross-sectional survey of the K13 molecular marker. *The Lancet Infectious Diseases* 15:415-421.

Turner, L., T. Lavstsen, B.P. Mmbando, C.W. Wang, P.A. Magistrado, L.S. Vestergaard, D.S. Ishengoma, D.T.R. Minja, J.P. Lusingu, and T.G. Theander. 2015. IgG antibodies to endothelial protein C receptor-binding cysteine-rich interdomain region domains of Plasmodium falciparum erythrocyte membrane protein 1 are acquired early in life in individuals exposed to malaria. *Infection and immunity* 83:3096-3103.

Uher, F., I. Dobronyi, and J. Gergel. 1981. IgM-Fc receptor-mediated phagocytosis of rat macrophages. *Immunology* 42:419-425.

van Schaijk, B.C., I.H. Ploemen, T. Annoura, M.W. Vos, L. Foquet, G.J. van Gemert, S. Chevalley-Maurel, M. van de Vegte-Bolmer, M. Sajid, J.F. Franetich, A. Lorthiois, G. Leroux-Roels, P. Meuleman, C.C. Hermsen, D. Mazier, S.L. Hoffman, C.J. Janse, S.M. Khan, and R.W. Sauerwein. 2014. A genetically attenuated malaria vaccine candidate based on P. falciparum b9/slarp gene-deficient sporozoites. *Elife* 3:

VanBuskirk, K.M., M.T. O'Neill, P. De La Vega, A.G. Maier, U. Krzych, J. Williams, M.G. Dowler, J.B. Sacci, Jr., N. Kangwanrangsan, T. Tsuboi, N.M. Kneteman, D.G. Heppner, Jr., B.A. Murdock, S.A. Mikolajczak, A.S. Aly, A.F. Cowman, and S.H. Kappe. 2009. Preerythrocytic, live-attenuated Plasmodium falciparum vaccine candidates by design. *Proc Natl Acad Sci U S A* 106:13004-13009.

Vanderberg, J.P., and U. Frevert. 2004. Intravital microscopy demonstrating antibody-mediated immobilisation of Plasmodium berghei sporozoites injected into skin by mosquitoes. *Int J Parasitol* 34:991-996.

Vidarsson, G., G. Dekkers, and T. Rispens. 2014. IgG subclasses and allotypes: from structure to effector functions. *Front Immunol* 5:520.

Volz, Jennifer C., A. Yap, X. Sisquella, Jenn K. Thompson, Nicholas T.Y. Lim, Lachlan W. Whitehead, L. Chen, M. Lampe, W.-H. Tham, D. Wilson, T. Nebl, D. Marapana, T. Triglia, W. Wong, Kelly L. Rogers, and Alan F. Cowman. 2016. Essential Role of the PfRh5/PfRipr/CyRPA Complex during Plasmodium falciparum Invasion of Erythrocytes. *Cell Host & Microbe* 20:60-71.

von der Weid, T., M. Kopf, G. Köhler, and J. Langhorne. 1994. The immune response to Plasmodium chabaudi malaria in interleukin-4-deficient mice. *Eur J Immunol* 24:2285-2293.

Wagner, G., K. Koram, D. McGuinness, S. Bennett, F. Nkrumah, and E. Riley. 1998. High incidence of asymptomatic malara infections in a birth cohort of children less than one year of age in Ghana, detected by multicopy gene polymerase chain reaction. *Am J Trop Med Hyg* 59:115-123.

Wang, L.T., L.S. Pereira, Y. Flores-Garcia, J. O'Connor, B.J. Flynn, A. Schön, N.K. Hurlburt, M. Dillon, A.S.P. Yang, A. Fabra-García, A.H. Idris, B.T. Mayer, M.W. Gerber, R. Gottardo, R.D. Mason, N. Cavett, R.B. Ballard, N.K. Kisalu, A. Molina-Cruz, J. Nelson, R. Vistein, C. Barillas-Mury, R. Amino, D. Baker, N.P. King, R.W. Sauerwein, M. Pancera, I.A. Cockburn, F. Zavala, J.R. Francica, and R.A. Seder. 2020. A Potent Anti-Malarial Human Monoclonal Antibody Targets Circumsporozoite Protein Minor Repeats and Neutralizes Sporozoites in the Liver. *Immunity* 53:733-744.e738.

Webster, R., S. Sekuloski, A. Odedra, S. Woolley, H. Jennings, F. Amante, K.R. Trenholme, J. Healer, A.F. Cowman, E.M. Eriksson, P. Sathe, J. Penington, A.J. Blanch, M.W.A. Dixon, L. Tilley, M.F. Duffy, A. Craig, J. Storm, J.-A. Chan, K. Evans, A.T. Papenfuss, L. Schofield, P. Griffin, B.E. Barber, D. Andrew, M.J. Boyle, F. de Labastida Rivera, C. Engwerda, and J.S. McCarthy. 2021. Safety, infectivity and immunogenicity of a genetically attenuated blood-stage malaria vaccine. *BMC Medicine* 19:293.

Weiss, G.E., P.R. Gilson, T. Taechalertpaisarn, W.-H. Tham, N.W.M. de Jong, K.L. Harvey, F.J.I. Fowkes, P.N. Barlow, J.C. Rayner, G.J. Wright, A.F. Cowman, and B.S. Crabb. 2015. Revealing the Sequence and Resulting Cellular Morphology of Receptor-Ligand Interactions during Plasmodium falciparum Invasion of Erythrocytes. *PLOS Pathogens* 11:e1004670.

White, N.J. 2004. Antimalarial drug resistance. *J Clin Invest* 113:1084-1092.

World Health Organization. (2012). WHO policy recommendation: seasonal malaria chemoprevention (SMC) for plasmodium falciparum malaria control in highly seasonal transmission areas of the Sahel sub-region in Africa.

World Health Organisation. (2015). Global technical strategy for malaria 2016-2030.

World Health Organisation. (2020). World malaria report 2020.

World Health Organisation. (2021). World malaria report 2021.

World Health Organisation. (2022). Malaria vaccine: WHO position paper-March 2022: p:60-80.

Wickramarachchi, T., A.L. Cabrera, D. Sinha, S. Dhawan, T. Chandran, Y.S. Devi, M. Kono, T. Spielmann, T.W. Gilberger, V.S. Chauhan, and A. Mohmmed. 2009. A novel Plasmodium falciparum erythrocyte binding protein associated with the merozoite surface, PfDBLMSP. *Int J Parasitol* 39:763-773.

Willcocks, L.C., E.J. Carr, H.A. Niederer, T.F. Rayner, T.N. Williams, W. Yang, J.A. Scott, B.C. Urban, N. Peshu, T.J. Vyse, Y.L. Lau, P.A. Lyons, and K.G. Smith. 2010. A defunctioning polymorphism in FCGR2B is associated with protection against malaria but susceptibility to systemic lupus erythematosus. *Proc Natl Acad Sci U S A* 107:7881-7885.

Wilson, D.W., F.J. Fowkes, P.R. Gilson, S.R. Elliott, L. Tavul, P. Michon, E. Dabod, P.M. Siba, I. Mueller, B.S. Crabb, and J.G. Beeson. 2011. Quantifying the importance of MSP1-19 as a target of growth-inhibitory and protective antibodies against Plasmodium falciparum in humans. *PLoS One* 6:e27705.

Winter, M. (2022). Exploring the growth inhibition activity of vaccine induced full-length Merozoite Surface Protein 1 antibodies. Bachelor thesis. Heidelberg University.

Wipasa, J., C. Suphavilai, L.C. Okell, J. Cook, P.H. Corran, K. Thaikla, W. Liewsaree, E.M. Riley, and J.C.R. Hafalla. 2010. Long-lived antibody and B Cell memory responses to the human malaria parasites, Plasmodium falciparum and Plasmodium vivax. *PLoS pathogens* 6:e1000770-e1000770.

Withers, M.R., D. McKinney, B.R. Ogutu, J.N. Waitumbi, J.B. Milman, O.J. Apollo, O.G. Allen, K. Tucker, L.A. Soisson, C. Diggs, A. Leach, J. Wittes, F. Dubovsky, V.A. Stewart, S.A. Remich, J. Cohen, W.R. Ballou, C.A. Holland, J.A. Lyon, E. Angov, J.A. Stoute, S.K. Martin, and D.G. Heppner, Jr. 2006. Safety and reactogenicity of an MSP-1 malaria vaccine candidate: a randomized phase Ib dose-escalation trial in Kenyan children. *PLoS Clin Trials* 1:e32.

Woehlbier, U., C. Epp, C.W. Kauth, R. Lutz, C.A. Long, B. Coulibaly, B. Kouyaté, M. Arevalo-Herrera, S. Herrera, and H. Bujard. 2006. Analysis of antibodies directed against merozoite surface protein 1 of the human malaria parasite Plasmodium falciparum. *Infect Immun* 74:1313-1322.

Wolf, A.-S., S. Sherratt, and E.M. Riley. 2017. NK Cells: Uncertain Allies against Malaria. *Frontiers in Immunology* 8:

Wu, R.L., A.H. Idris, N.M. Berkowitz, M. Happe, M.R. Gaudinski, C. Buettner, L. Strom, S.F. Awan, L.A. Holman, F. Mendoza, I.J. Gordon, Z. Hu, A. Campos Chagas, L.T. Wang, L. Da Silva Pereira, J.R. Francica, N.K. Kisalu, B.J. Flynn, W. Shi, W.P. Kong, S. O'Connell, S.H. Plummer, A. Beck, A. McDermott, S.R. Narpala, L. Serebryannyy, M. Castro, R. Silva, M. Imam, I. Pittman, S.P. Hickman, A.J. McDougal, A.E. Lukoskie, J.R. Murphy, J.G. Gall, K. Carlton, P. Morgan, E. Seo, J.A. Stein, S. Vazquez, S. Telscher, E.V. Capparelli, E.E. Coates, J.R. Mascola, J.E. Ledgerwood, L.K. Dropulic, and R.A. Seder. 2022. Low-Dose Subcutaneous or Intravenous Monoclonal Antibody to Prevent Malaria. *N Engl J Med* 387:397-407.

Wu, Y., R.D. Ellis, D. Shaffer, E. Fontes, E.M. Malkin, S. Mahanty, M.P. Fay, D. Narum, K. Rausch, A.P. Miles, J. Aebig, A. Orcutt, O. Muratova, G. Song, L. Lambert, D. Zhu, K. Miura, C. Long, A. Saul, L.H. Miller, and A.P. Durbin. 2008. Phase 1 Trial of Malaria Transmission Blocking Vaccine Candidates Pfs25 and Pvs25 Formulated with Montanide ISA 51. *PLOS ONE* 3:e2636.

Xie, S.C., C. Dogovski, E. Hanssen, F. Chiu, T. Yang, M.P. Crespo, C. Stafford, S. Batinovic, S. Teguh, S. Charman, N. Klonis, and L. Tilley. 2016. Haemoglobin degradation underpins the sensitivity of early ring stage Plasmodium falciparum to artemisinins. *J Cell Sci* 129:406-416.

Yeoh, S., R.A. O'Donnell, K. Koussis, A.R. Dluzewski, K.H. Ansell, S.A. Osborne, F. Hackett, C. Withers-Martinez, G.H. Mitchell, L.H. Bannister, J.S. Bryans, C.A. Kettleborough, and M.J. Blackman. 2007. Subcellular Discharge of a Serine Protease Mediates Release of Invasive Malaria Parasites from Host Erythrocytes. *Cell* 131:1072-1083.

Zenklusen, I., S. Jongo, S. Abdulla, K. Ramadhani, B.K. Lee Sim, H. Cardamone, E.L. Flannery, T. Nguyen, M. Fishbaugher, R.W.J. Steel, W. Betz, N. Carmago, S. Mikolajczak, S.H.I. Kappe, S.L. Hoffman, B.K. Sack, and C. Daubenberger. 2018. Immunization of Malaria-Preexposed Volunteers With PfSPZ Vaccine Elicits Long-Lived IgM Invasion-Inhibitory and Complement-Fixing Antibodies. *J Infect Dis* 217:1569-1578.

8.0 APPENDICES

VTHESYQELVKKLEALEDAVLTGYSLFQKEKMVLNEEEITTKGASAQSGASAQSGASAQSGASAQSGASAQ
SGASAQSGTSGPSGPSGTSPSSRSNTLPRSNTASGASPPADASDSDAKSYADLKHRVRNYLFTIKELKYPE
LFDLTNHMLTLCDNIHGFKYLIDGYEEINELLYKLNFYFDLLRAKLNDVCANDYCQIPFNLKIRANELDVLKKLV
FGYRKPLDNIKDNVGKMEDYIKKNKATIANINELIEGSKKTIDQNKNADNEEGKKKLYQAQYDLSIYNKQLEEA
HNLISVLEKRIDTLKKNENIKKLLDKINEIKNPPPANSGNTPNTLLDKNKKIEEHEEKIKEIAKTIKFNIDSLFTDPL
ELEYYLREKNKKVDVTPKSQDPTKSVQIPKVPYPNGIVYPLPLTDIHNSLAADNDKNSYGDLMNPHTKEKINE
KIITDNKERKIFINNIKKKIDLEEKNINHAKEQNKKLLEDYEKSKKDYEELLEKFYEMKFNNNFNKDVVDKIFSAR
YTYNVEKQRYNNKFSSSNNAVYNVQKLKKALSYLEDYSLRKGISEKDFNHYYTLKTGLEADIKKLTEEIKSSE
NKILEKNFKGLTHSANGALEVSDIVKLQVQKVLLIKKIEDLRKIELFLKNAQLKDSIHVPNIYKPQNKPEPYYLIVL
KKEVDKLKEFIPKVKDMLKKEQAVLSSITQPLVAASETTEDGGHSTHTLSQSGETEVTEETEETEETVGHTTT
VTITLPPTQPSPPKEVKVVENSIEHKSNDNSQALTKTVYLKKLDEFLTKSYICHKYILVSNSAMDQKLLEVYNL
APEEENELKSCDPLDLLFNIQNNIPAMYSLYDSMNNDLQHLFFELYQKEMIYYLHKLKEENHIKKLLEEQKQIT
GTSSTSSPGNTAVNTAQSATHSNSQNQQSNAASTNTQNGVAVSSGPAVVEESHDPLTVLSISNDLKGIVSLL
NLGNKAKVPNPLTISTTEMEKFYENILKNNDAYFNDDIKQFVKSNSKVITGLTETQKNALN DEIKKLKDTLQLSF
DLYNKYKLKLDRLFNKKKELGQDKMQIKKLTLLKEQLESKLNSLNNPHNVLQNFAVFFNKKKEAEIAETENTL
ENTKILLKHYKGLVKYYNGESSPLKTLSEVSIQTEDNYANLEKFRVLSKIDGKLNDNLHLGKKKLSFLSSGLHH
LITELKEVIKNKNYAGNSPSENNKKVNEALKSYENFLPEAKVTTVVTPPQPDVTPSPLSVRVSGSSGSTKEET
QIPTSGSLLTELQQVVQLQNYDEEDDSLVVLPIFGESEDNDEYLDQVVTGEAISVTMDNILSGFENEYDVIYLK
PLAGVYRSLKKQIEKNIFTFNLNLNDILNSRLKKRKYFLDVLESDLMQFKHISSNEYIIEDSFKLLNSEQKNTLLK
SYKYIKESVENDIKFAQEGISYYEKVLAKYKDDLESIKKVIKEEKEKFPSSPPTTPPSPAKTDEQKKESKFLPFL
TNIETLYNNLVNKIDDYLINLKAKINDCNVEKDEAHVKITKLSDLKAIDDKID LFKNPYDFEAIKKLINDDTKKDML
GKLLSTGLVQNFPNTIISKLIEGKFQDMLNIAQHQCVKKQCPENSGCFRHLDEREECKCLLNYKQEGDKCVE
NPNPTCNENNGGCDADATCTEEDSGSSRKKITCECTKPDSYPLFDGIFCSSSG

Figure 8.1: Protein sequence of recombinant $MSP1_{FL}$ used for CHMI study.
$MSP1_{FL}$ sequence was codon optimized for expression in HEK293 cells. Predicted N-glycosylation sites were mutated: Serine123, Threonine262, Threonine491, Serine557, Serine628, Serine823, Threonine835, Threonine920, Serine940, Threonine986, Threonine1012, Serine1110, Threonine1217, Serine1609 to Alanine residues. The signal peptide and GPI anchor are removed.

MVTHESYQELVKKLEALEDAVLTGYSLFQKEKMVLNEEEITTKGASAQSGASAQSGASAQGASAQSGASAQS
GASAQSGTSGPSGPSGTSPSSRSNTLPRSNTSSGASPPADASDSDAKSYADLKHRVRNYLFTIKELKYPELF
DLTNHMLTLCDNIHGFKYLIDGYEEINELLYKLNFYFDLLRAKLNDVCANDYCQIPFNLKIRANELDVLKKLVFGY
RKPLDNIKDNVGKMEDYIKKNKTTIANINELIEGSKKTIDQNKNADNEEGKKKLYQAQYDLSIYNKQLEEAHNLIS
VLEKRIDTLKKNENIKKLLDKINEIKNPPPANSGNTPNTLLDKNKKIEEHEEKIKEIAKTIKFNIDSLFTDPLELEYYL
REKNKKVDVTPKSQDPTKSVQIPKVPYPNGIVYPLPLTDIHNSLAADNDKNSYGDLMNPHTKEKINEKIITDNKE
RKIFINNIKKKIDLEEKNINHTKEQNKKLLEDYEKSKKDYEELLEKFYEMKFNNNFNKDVVDKIFSARYTYNVEK
QRYNNKFSSSNNSVYNVQKLKKALSYLEDYSLRKGISEKDFNHYYTLKTGLEADIKKLTEEIKSSENKILEKNFK
GLTHSANGSLEVSDIVKLQVQKVLLIKKIEDLRKIELFLKNAQLKDSIHVPNIYKPQNKPEPYYLIVLKKEVDKLKE
FIPKVKDMLKKEQAVLSSITQPLVAASETTEDGGHSTHTLSQSGETEVTEETEETEETVGHTTTVTITLPPTQP
SPPKEVKVVNSIEHKSNDNSQALTKTVYLKKLDEFLTKSYICHKYLVSNSSMDQKLLEVYNLTPEEENELKSCD
PLDLLFNIQNNIPAMYSLYDSMNNDLQHLFFELYQKEM IYYLHKLKEENHIKKLLEEQKQITGTMSSTSSPGNTT
VNTAQSATHSNSQNQQSNASSTNTQNGVAVSSGPAVVEESHDPLTVLSISNDLKGIVSLLNLGNKTKVPNPLT
ISTTEMEKFYENILKNNDTYFNDDIKQFVKSNSKVITGLTETQKNALNDEIKKLKDTLQLSFDLYNKYKLKLDRLF
NKKKELGQDKMQIKKLTLLKEQLESKLNSLNNPHNVLQNFSVFFNKKKEAEIAETENTLENTKILLKHYKGLVKY
YNGESSPLKTLSEVSIQTEDNYANLEKFRVLSKIDGKLNDNLHLGKKKLSFLSSGLHHLITELKEVIKNKNYTGN
SPSENNKKVNEALKSYENFLPEAKVTTVVTPPQPDVTPSPLSVRVSGSSGSTKEETQIPTSGSLLTELQQVVQ
LQNYDEEDDSLVVLPIFGESEDNDEYLDQVVTGEAISVTMDNILSGFENEYDVIYLKPLAGVYRSLKKQIEKNIF
TFNLNLNDILNSRLKKRKYFLDVLESDLMQFKHISSNEYIIEDSFKLLNSEQKNTLLKSYKYIKESVENDIKFAQE
GISYYEKVLAKYKDDLESIKKVIKEEKEKFPSSPPTTPPSPAKTDEQKKESKFLPFLTNIETLYNNLVNKIDDYLIN
LKAKINDCNVEKDEAHVKITKLSDLKAIDDKIDLFKNPYDFEAIKKLINDDTKKDMLGKLLSTGLVQNFPNTIISKLI
EGKFQDMLNISQHQCVKKQCPENSGCFRHLDEREECKCLLNYKQEGDKCVENPNPTCNENNGGCDADATC
TEEDSGSSRKKITCECTKPDSYPLFDGIFCSSSN

Figure 8.2: Protein sequence of recombinant MSP1$_{FL}$ used for vaccination.
MSP1 is expressed in two halves (p83/p30 and p38/p42). The p83 subunit is highlighted in light grey, the p30 subunit is highlighted in white, the p38 subunit is highlighted in dark grey, the p33 subunit is highlighted in red and the p19 subunit is highlighted in yellow. The signal peptide and GPI anchor are removed.

Table 8.1: Significantly different epitopes between treated and non-treated volunteers.

peptide	Subunit	Nature of origin	statistic	p.adj	signif[a]
VTHESYQELVKKLEA	83	conserved	141.5	0.0247	*
FQKEKMVLNEEEITT	83	conserved	270	0.0306	*
KMVLNEEEITTKGAS	83	conserved	253	0.032	*
MVLNEEEITTKGASA	83	conserved	293	0.00147	**
LNEEEITTKGASAQS	83	conserved	253	0.032	*
KGASAQSGASAQSGA	83	oligomorphic	160	0.0402	*
ASAQSGASAQSGASA	83	oligomorphic	3739.5	0.00172	**
SGASAQSGASAQSGA	83	oligomorphic	1541	0.0482	*
QSGASAQSGTSGPSG	83	oligomorphic	261	0.0314	*
GTSPSSRSNTLPRSN	83	oligomorphic	250	0.0198	*
TSSGASPPADASDSD	83	oligomorphic	280.5	0.0178	*
GASPPADASDSDAKS	83	oligomorphic	258.5	0.0247	*
ASPPADASDSDAKSY	83	oligomorphic	288	0.0123	*
SPPADASDSDAKSYA	83	oligomorphic	306.5	0.00218	**
PADASDSDAKSYADL	83	oligomorphic	270.5	0.043	*
ADASDSDAKSYADLK	83	oligomorphic	274	0.0196	*
DASDSDAKSYADLKH	83	oligomorphic	277	0.0234	*
NYLFTIKELKYPELF	83	conserved	271	0.0252	*
LFTIKELKYPELFDL	83	conserved	276	0.0188	*
GFKYLIDGYEEINEL	83	conserved	289	0.0127	*
FKYLIDGYEEINELL	83	conserved	270	0.0445	*
KYLIDGYEEINELLY	83	conserved	290	0.0144	*
YLIDGYEEINELLYK	83	conserved	261.5	0.0418	*
GYEEINELLYKLNFY	83	conserved	278	0.0159	*
NDVCANDYCQIPFNL	83	conserved	272	0.014	*
CQIPFNLKIRANELD	83	conserved	251	0.0392	*
DNVGKMEDYIKKNKT	83	conserved	240	0.0402	*
EGSKKTIDQNKNADN	83	conserved	250	0.0198	*
LKKNENIKKLLDKIN	83	conserved	260	0.0408	*
PANSGNTPNTLLDKN	83	oligomorphic	258.5	0.0247	*
EHEEKIKEIAKTIKF	83	oligomorphic	265	0.0218	*
FNIDSLFTDPLELEY	83	conserved	288	0.0144	*
IDSLFTDPLELEYYL	83	conserved	294.5	0.0104	*
DSLFTDPLELEYYLR	83	conserved	277	0.027	*
FTDPLELEYYLREKN	83	conserved	310	0.00189	**
PTKSVQIPKVPYPNG	83	dimorphic	118	0.0112	*
KSVQIPKVPYPNGIV	83	dimorphic	136.5	0.0147	*
LTDIHNSLAADNDKN	83	dimorphic	261	0.0493	*
FINNIKKKIDLEEKN	83	dimorphic	263.5	0.0147	*
LLEDYEKSKKDYEEL	83	dimorphic	258	0.0481	*
NVEKQRYNNKFSSSN	83	dimorphic	251	0.0392	*
QRYNNKFSSSNNSVY	83	dimorphic	288	0.00855	**
SEKDFNHYYTLKTGL	83	dimorphic	160	0.0402	*
EADIKKLTEEIKSSE	83	dimorphic	266	0.049	*
ADIKKLTEEIKSSEN	83	dimorphic	268.5	0.0233	*

peptide	Subunit	Nature of origin	statistic	p.adj	signif[a]
AASETTEDGGHSTHT	30	dimorphic	271	0.0154	*
SQSGETEVTEETEET	30	dimorphic	279	0.0259	*
QSGETEVTEETEETE	30	dimorphic	273	0.0413	*
SGETEVTEETEETEE	30	dimorphic	295	0.00781	**
GETEVTEETEETEET	30	dimorphic	283	0.0232	*
ETEVTEETEETEETV	30	dimorphic	284	0.0228	*
TEVTEETEETEETVG	30	dimorphic	287	0.0181	*
EVTEETEETEETVGH	30	dimorphic	272.5	0.0484	*
KVVENSIEHKSNDNS	30	dimorphic	250	0.0198	*
TKTVYLKKLDEFLTK	30	dimorphic	160	0.0402	*
SMDQKLLEVYNLTPE	30	dimorphic	127.5	0.0133	*
QKLLEVYNLTPEEEN	30	dimorphic	260	0.00958	**
KLLEVYNLTPEEENE	30	dimorphic	267.5	0.0472	*
LLEVYNLTPEEENEL	30	dimorphic	289	0.00965	**
LEVYNLTPEEENELK	30	dimorphic	266	0.0198	*
YSLYDSMNNDLQHLF	30	dimorphic	273	0.00732	**
LYDSMNNDLQHLFFE	30	dimorphic	273.5	0.0383	*
DLQHLFFELYQKEMI	30	dimorphic	270	0.0273	*
GNTTVNTAQSATHSN	38	dimorphic	260	0.00958	**
TVNTAQSATHSNSQN	38	dimorphic	258	0.0408	*
NTAQSATHSNSQNQQ	38	dimorphic	273	0.00732	**
AQSATHSNSQNQQSN	38	dimorphic	262	0.0345	*
QSATHSNSQNQQSNA	38	dimorphic	240	0.0402	*
SATHSNSQNQQSNAS	38	dimorphic	240	0.0402	*
HSNSQNQQSNASSTN	38	dimorphic	252	0.0354	*
SQNQQSNASSTNTQN	38	dimorphic	262	0.0287	*
STNTQNGVAVSSGPA	38	dimorphic	160	0.0402	*
KVPNPLTISTTEMEK	38	dimorphic	250	0.0432	*
VPNPLTISTTEMEKF	38	dimorphic	273.5	0.0348	*
PNPLTISTTEMEKFY	38	dimorphic	279	0.0271	*
LTISTTEMEKFYENI	38	dimorphic	273	0.00732	**
YENILKNNDTYFNDD	38	dimorphic	293.5	0.0114	*
ILKNNDTYFNDDIKQ	38	dimorphic	253	0.032	*
DTYFNDDIKQFVKSN	38	dimorphic	240	0.0402	*
TYFNDDIKQFVKSNS	38	dimorphic	250	0.0198	*
FVKSNSKVITGLTET	38	dimorphic	240	0.0402	*
TGLTETQKNALNDEI	38	dimorphic	259	0.0443	*
KKKELGQDKMQIKKL	38	dimorphic	275	0.0384	*
SVFFNKKKEAEIAET	38	conserved	274	0.0295	*
VFFNKKKEAEIAETE	38	conserved	282.5	0.02	*
FFNKKKEAEIAETEN	38	conserved	263	0.0472	*
FNKKKEAEIAETENT	38	conserved	285	0.0111	*
NKKKEAEIAETENTL	38	conserved	282.5	0.00922	**
KKEAEIAETENTLEN	38	conserved	300	0.00279	**
KEAEIAETENTLENT	38	conserved	317	4.63E-04	***
SIQTEDNYANLEKFR	38	dimorphic	252	0.0354	*
KFRVLSKIDGKLNDN	38	dimorphic	240	0.0402	*
GLHHLITELKEVIKN	38	dimorphic	270	0.00453	**
VIKNKNYTGNSPSEN	38	dimorphic	294	0.00131	**
EAKVTTVVTPPQPDV	38	dimorphic	240	0.0402	*

peptide	Subunit	Nature of origin	statistic	p.adj	signif[a]
VVTPPQPDVTPSPLS	38	dimorphic	286	0.00782	**
TELQQVVQLQNYDEE	38	dimorphic	134	0.0333	*
IFGESEDNDEYLDQV	38	dimorphic	277	0.0253	*
GESEDNDEYLDQVVT	38	dimorphic	272.5	0.0279	*
DNDEYLDQVVTGEAI	38	dimorphic	276.5	0.0244	*
MDNILSGFENEYDVI	33	dimorphic	300	0.00617	**
NILSGFENEYDVIYL	33	dimorphic	275	0.0417	*
LKKRKYFLDVLESDL	33	dimorphic	240	0.0402	*
RKYFLDVLESDLMQF	33	dimorphic	289.5	0.00838	**
SDLMQFKHISSNEYI	33	dimorphic	262.5	0.0164	*
FKHISSNEYIIEDSF	33	dimorphic	297	0.00373	**
AIDDKIDLFKNPYDF	33	dimorphic	280	0.0298	*
PYDFEAIKKLINDDT	33	dimorphic	260.5	0.0202	*
IISKLIEGKFQDMLN	33	dimorphic	240	0.0402	*
KCLLNYKQEGDKCVE	33	conserved	160	0.0402	*
LNYKQEGDKCVENPN	33	conserved	256	0.0401	*
GDKCVENPNPTCNEN	19	conserved	270	0.0367	*
DKCVENPNPTCNENN	19	conserved	276	0.0165	*
KCVENPNPTCNENNG	19	conserved	270.5	0.0195	*
VENPNPTCNENNGGC	19	conserved	290	0.00886	**
ENPNPTCNENNGGCD	19	conserved	291	0.0119	*
NPNPTCNENNGGCDA	19	conserved	290	0.00886	**
PNPTCNENNGGCDAD	19	conserved	282	0.0208	*
NPTCNENNGGCDADA	19	conserved	280	0.0169	*
PTCNENNGGCDADAT	19	conserved	284	0.0121	*
TCNENNGGCDADATC	19	conserved	272	0.0232	*
CNENNGGCDADATCT	19	conserved	267.5	0.0254	*
NENNGGCDADATCTE	19	conserved	280	0.0252	*
ENNGGCDADATCTEE	19	conserved	284	0.021	*
NNGGCDADATCTEED	19	conserved	272	0.0425	*
NGGCDADATCTEEDS	19	conserved	271.5	0.044	*
DADATCTEEDSGSSR	19	conserved	296	0.0041	**
TCTEEDSGSSRKKIT	19	conserved	263.5	0.0355	*
ECTKPDSYPLFDGIF	19	conserved	299	0.00481	**
CTKPDSYPLFDGIFC	19	conserved	268	0.0203	*

[a] significant difference in anti-MSP1 peptide IgG responses between randomly selected treated (n=20) and non-treated (n=20) volunteers were calculated using Wilcoxon matched-pairs signed rank test. P-values were adjusted for multiple testing using Hommel's method. Peptides that are stronger recognized by non-treated volunteers compared to treated volunteers are highlighted in blue. Peptides that are stronger recognized by treated volunteers compared to non-treated volunteers are highlighted in brown.

Table 8.2: List of recombinant merozoite antigens used in this study.

P.f. merozoite proteins	Expression system	Region expressed	Allele	References	Expression levels
MSP1	Mammalian	Full-length ectodomain	3D7	Crosnier et al, 2013	intermediate expressor
MSP11	Mammalian	Full-length ectodomain	3D7	Crosnier et al, 2013	intermediate expressor
MSP5	Mammalian	Full-length ectodomain	3D7	Crosnier et al, 2013	high expressor
MSRP4	Mammalian	Full-length ectodomain	3D7	Zenonos et al, 2014	high expressor
PF3D7_1136200	Mammalian	Full-length ectodomain	3D7	Crosnier et al, 2013	intermediate expressor
PF3D7_1252300	Mammalian	largest predicted extracellular loop	3D7	Kamuyu 2017, PhD Thesis	high expressor
PF3D7_1345100	Mammalian	Full-length ectodomain	3D7	Kamuyu 2017, PhD Thesis	high expressor
PF3D7_1401600	Mammalian	largest predicted extracellular loop	3D7	Kamuyu 2017, PhD Thesis	high expressor
PTEX150	Mammalian	Full-length ectodomain	3D7	Crosnier et al, 2013	intermediate expressor

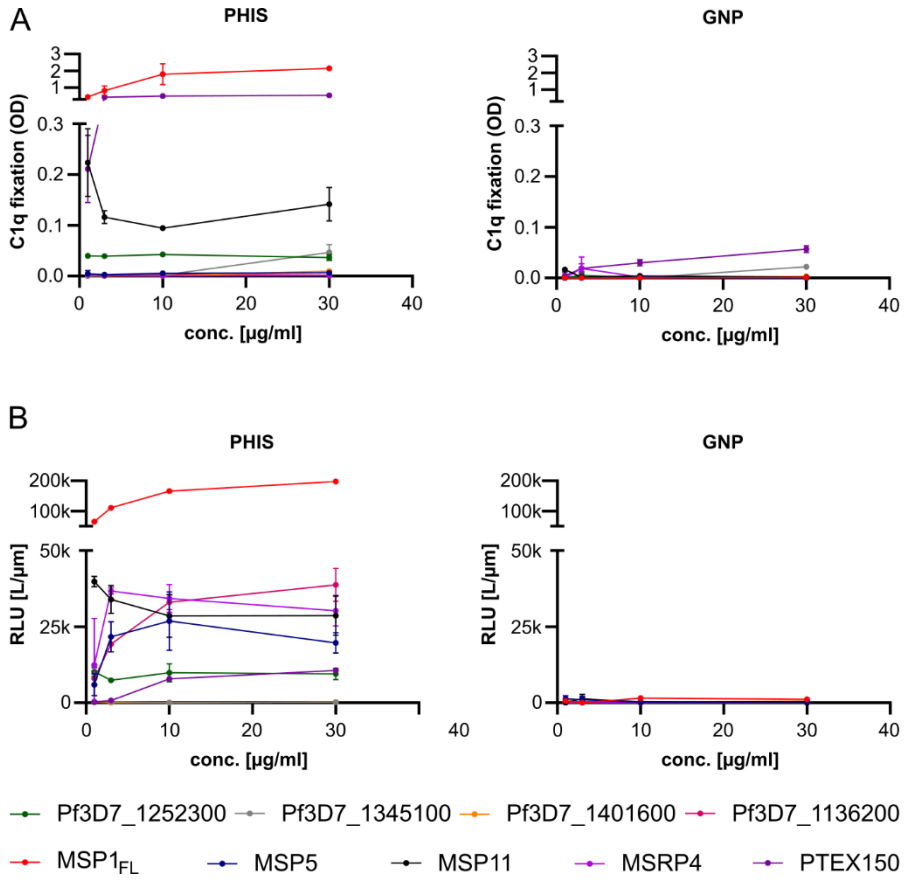

Figure 8.3: Optimization of coating concentrations of recombinant merozoite proteins for antigen-specific functional assays.
Recombinant antigens were tested for (**A**) complement fixation (AbC') and (**B**) ADRB activity using a pool of hyper immune sera from Kenyan adults (PHIS) or a pool of malaria-naïve sera from German adults (GNP). Merozoite proteins were coated at concentrations ranging from 0.01µg/ml to 30µg/ml. Dots represent means of technical replicates and error bars standard deviations.

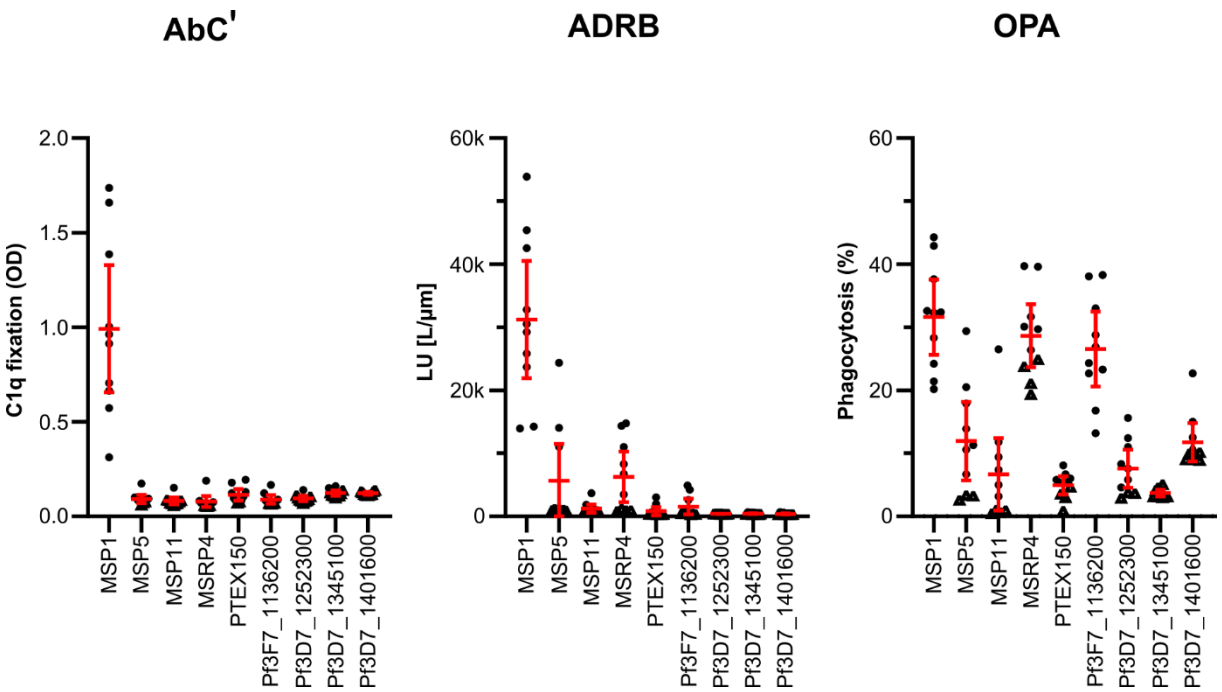

Figure 8.4: Fc-mediated effector functions for anti-MSP1$_{FL}$ antibodies are higher compared to other merozoite antigens.
Fc-mediated functional activities (AbC', ADRB and OPA) for each merozoite antigen was assessed by using top responders (n=10) that showed the highest reactivity for respective antigens using KILchip (Nkumama 2021, PhD thesis). Dots represent means of duplicate measurements above and triangles below the seropositivity cut-off which was calculated for each antigen and function as the reactivity of malaria-naïve plasma samples (n=4) plus three standard deviations. Error bars represent the median plus 95% confidence intervals.

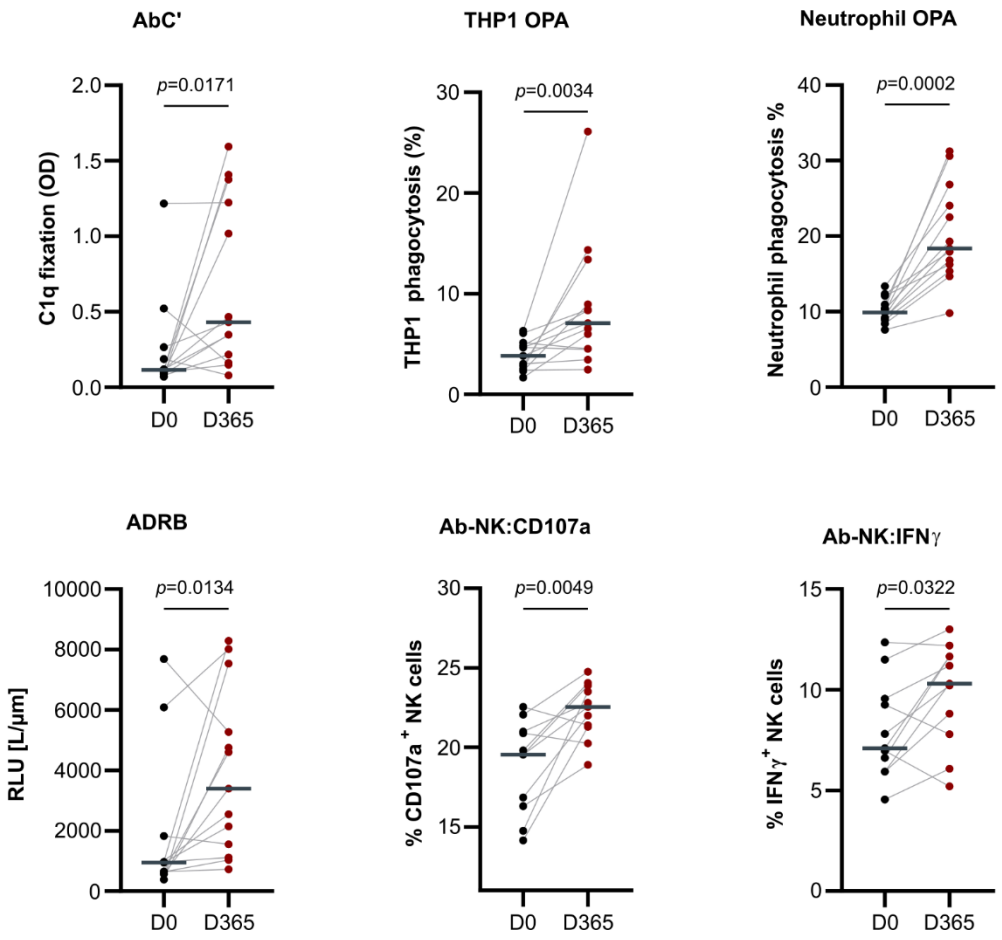

Figure 8.5: Vaccine-induced IgG remains over baseline levels.
(**A**) Levels of anti-MSP1$_{FL}$ Fc-mediated effector functions of purified IgG samples were compared before (D0) and 6 months after the last vaccination (D365). Opsonic phagocytosis (OPA) activity of MSP1$_{FL}$-coupled beads by THP1 cells or donor neutrophils was measured by flow cytometry, Antibody-dependent respiratory burst (ADRB) of donor neutrophils was measured by detection of reactive oxygen species (ROS) using chemiluminescence. Ab-NK activity (Ab-NK:CD107a and Ab-NK:IFNγ) by donor NK cells was measured by multiparameter flowcytometry. Each data point represents a specific Fc-function measured once with two technical replicates for one sample. Dark grey lines indicate medians. Statistical differences between timepoints were calculated using Wilcoxon matched-pairs signed rank test.